Thermoresponsive Magnetic Colloidal Gels for *In vitro* Cell Expansion

Shwana A. Braim, MSc

Thesis submitted to The University of Nottingham
for the degree of Doctor of Philosophy

May 2016

Abstract

Recent studies and clinical trials have shown the potential of cell-based therapies for the treatment of a number of diseases and organ/ tissue damages. However, limited availability of some therapeutically important cells (i.e. adult stem cells) still remain as main challenges in the development of tissue engineering through to the clinic. Healthy cells are required in large numbers to form a tissue-engineered construct and primary cells must therefore be expanded *in vitro* for both scientific and clinical applications.

Various strategies have been developed to expand cells *in vitro* with increasing emphasis on 3D matrices because it can provide microenvironments which more closely mimic *in vivo* systems. In this way the inherent difficulties associated with 2D culture such as loss of phenotype could be overcome. Moreover, 3D matrices provide higher surface areas to support expansion of larger cell numbers compared to monolayer culture. Although each 3D method has certain advantages, there is no single technique that can be used to produce material assemblies that address all the fundamental problems linked to 3D cell seeding (penetration into the scaffold), passaging (use of enzymes), and harvesting (cell yield).

Recently, thermally reversibly-associating particles have been studied for the growth and support of multiple cell types and for delivery of therapeutic cells. But coupling of thermoresponsive properties to magnetic microspheres would enhance the 3D culture and expansion of

multiple cell types, and facilitate rapid recovery of the expanded cell population by simple magnetic separation. In this study, it was proposed that the thermoresponsive properties would allow simple cell seeding at temperatures below the LCST of polymer stabiliser when the suspension is flowing and upon heating to above the LCST cells would be encapsulated and cultured within the particle gels (every cells surrounded by a number of particles, as the size of the particles are much smaller than the cells). The magnetic responsive property would allow efficient and scaffold free cell recovery after expansion without the need for using trypsin or enzymatic treatment.

The 'switchable' component of reversibly associating colloidal microparticles were prepared via two different strategies. In the first strategy, thermoresponsive PDEGMA was physically adsorbed onto the surface of PS microspheres, whereas, in the second strategy, PDEGMA was chemically grafted from functionalised PCMS microspheres via SI-ATRP. The most simple method i.e. physical adsorption is rapid and can be adapted to many microparticle surfaces but has the drawback of possible desorption of polymer chains during extended use. The chemical grafting method i.e. the formation of covalent bonds between the polymer corona and the microparticle core provides robust and well defined materials but is more complex and time-consuming. In both cases, particle aggregation in their suspensions occurred on increasing the temperature to above the LCST of PDEGMA, but could be reversed by cooling the suspensions back to below the LCST. This confirmed the presence of the thermoresponsive polymer on the surface of the microspheres using both methods (adsorption and grafting). Rheological

measurements demonstrated that the viscoelasticity of the prepared particle gels can be tuned, enabling these gels to have the mechanical properties that should facilitate their applications as 3D cell scaffolds for *in vitro* expansion of cells.

Cell culture studies showed that these microparticle based scaffolds can support expansion of clinically relevant cell types (human MSC) and allowed efficient cell recovery after proliferation without the need for using trypsin or enzymatic treatment.

Overall, those results suggest that the designed scaffolds had great potential for 3D *in vitro* cell expansion. The new developed materials have excellent biocompatibility, allow simple and rapid cell seeding and cell recovery after expansion, and possess mechanical strength and stability to support cell growth and proliferation. The materials developed and studied in this thesis may represent a significant contribution to the fields of biomaterials, tissue engineering, 3D cell culture and even bio-separation.

Declaration

I declare that this thesis is the result of my own work which has been mainly undertaken during my period of registration for the degree of Doctor of Philosophy at the University of Nottingham.

Acknowledgement

I would like to express gratitude to my supervisors Professor Cameron Alexander and Professor Kevin Shakesheff for the inspiration, guidance, time and support they offered with all aspects of the practical and written work undertaken during my 3 year PhD. Their encouragement and belief in my abilities contributed greatly to the success of this study. It has been and will always be my privilege to walk this journey under their supervision.

I would also like to thank Associate Professor Dr. Felicity Rose for being my internal assessor. Her feedback and recommendations were invaluable in the development of a logically structured scientific investigation and the resultant interpretation.

I would also like to thank Professor Brian Saunders, University of Manchester for his help and input over the period of this project.

I would also like to thank Mrs Christine Grainger-Boultby, Mr Paul Cooling, Mrs Julia Crouch, and Mrs Teresa Marshall for technical support during my PhD.

I am deeply appreciative of the help I received from my colleagues in the Tissue engineering and Drug delivery groups, especially Omar, Aram, Mahmood, and Giovanna who were willing to provide help and advice in the lab whenever I needed. Many thanks must go to Gemma for my training on cell culture. Many thanks must also go to my close friend Abdulhamid.

I would like to say a special thanks to the most important person in my life – my wife Kawthar, whose support, patient, motivation, inspiration

and love has provided the energy necessary for me to undertake and complete this PhD program.

Lastly, I would like to acknowledge the financial support from the Engineering and Physical Sciences Research Council (EPSRC) and Ministry of Higher Education and scientific research/ Kurdistan regional government throughout my PhD study at the University of Nottingham.

Publications and Presentations

The work presented in this thesis has given rise to the following publications and presentations.

Publications in peer-reviewed journals

The following publication has contributed to this PhD thesis:

S. A. Braim, K. M. Shakesheff, B. R. Saunders and C. Alexander, Thermoresponsive Magnetic Colloidal Gels via Surface-Initiated Polymerisation from Functional Microparticles, ***J. Mater. Chem. B***, 2016,**4**, 962-972. **DOI:** 10.1039/C5TB01739D

Conference Abstracts

The following abstract has been accepted for presentation and going to publish as conference paper at the Tissue Engineering and Regenerative Medicine International Society Conference (TERMIS-EU 2016) in Uppsala, Sweden (28 June-1 July 2016):

S. A. Braim, K. M. Shakesheff, B. R. Saunders and C. Alexander, Thermoresponsive Magnetic Colloidal Gels via Surface-Initiated Polymerisation from Functional Microparticles.

Table of Contents

Abstract……..I

Declaration……..III

Acknowledgements……..IV

Publications and presentations……..VI

Table of contents……..VII

List of figures……..XIII

List of tables……..XVIII

Abbreviations……..XIX

Abstract I

Declaration IV

Acknowledgement V

Publications and Presentations VII

1. Introduction 1

1.1. Tissue engineering and regenerative medicine 1

1.2. *In vitro* cell culture models for tissue engineering applications 4

1.2.1. Monolayer cell culture system 4

1.2.2. Three dimensional (3D) cell culture systems 5

1.3. Polymeric scaffolds in tissue engineering 8

1.4. Temperature responsive polymers in tissue engineering 12

1.5. Particulate suspensions and colloidal gels 20

1.5.1. Colloidal stabilisation methods 20

1.5.2. Colloidal aggregation and gel formation 24

1.6. Magnetic bioseparation based on magnetite nanoparticles 26

1.7. Thesis aims and objectives 29

2. General materials and methods 32

2.1. Materials 32
2.1.1. General Chemicals 32
2.1.2. Cell culture reagents 32
2.2. Methods 33
2.2.1. Scanning Electron Microscopy (SEM) 33
2.2.2. ATR- FTIR characterization 33
2.2.3. Rheometry characterizations 34
2.2.3.i. Strain sweep 34
2.2.3.ii. Temperature sweep 34
2.2.3.iii. Frequency sweep 35
2.2.4. Water contact angle (WCA) 35
2.2.5. Thermogravimetric analyses (TGA) 35
2.2.6. ^{1}H NMR spectroscopy 35
2.2.7. Gel permeation chromatography (GPC) 36
2.2.8. General procedure for synthesis of magnetite nanoparticles 36
2.2.9. Synthesis of linear thermoresponsive 'control' polymer 37

3. Synthesis and characterisation of thermoresponsive magnetic PS/ PDEGMA colloidal suspensions/ gels via physical adsorption of polymer stabiliser onto microspheres 38

3.1. Introduction 38
3.2. Aims and Objectives 41
3.3. Materials and Methods 42
3.3.1. Synthesis of polystyrene microspheres 42
3.3.2. Preparation of magnetic PS microspheres 43
3.3.3. Preparation of thermoresponsive suspensions 43
3.3.4. Electronic Microscopy characterizations 44
3.3.5. ^{1}H NMR spectroscopy 44
3.3.6. ATR- FTIR characterization 44
3.3.7. SQUID Magnetometer 44
3.3.8. Gel permeation chromatography (GPC) 45
3.3.9. Measurement of cloud point temperatures of thermoresponsive polymers 45

3.3.10. Tube Inversion test 45
3.3.11. Rheometry characterization 46
3.4. Results and discussion 46
3.4.1. Synthesis and characterisations of polystyrene microspheres 47
3.4.2. Synthesis and characterization of magnetite nanoparticles 53
3.4.3. Loading magnetite nanoparticles to the microspheres 56
3.4.4. Synthesis and characterization of PDEGMA linear polymer 59
3.4.5. Colloidal gel evaluations 63
3.4.6. Rheological studies 68
3.5. Conclusion 77
4. Synthesis and characterisation of thermoresponsive magnetic PCMS-PDEGMA colloidal suspensions/ gels via surface-initiated polymerization from functional microspheres 78
4.1. Introduction 78
4.2. Aims and Objectives 81
4.3. Materials and Methods 82
4.3.1. Synthesis of poly(chloromethylstyrene) microspheres 82
4.3.2. Preparation of magnetic PCMS-PDEGMA microspheres 83
4.3.3. Surface initiated atomic transfer radical polymerization (SI-ATRP) for grafting of PDEGMA on PCMS microspheres. 84
4.3.4. Preparation of thermoresponsive suspensions 84
4.3.5. Electronic Microscopy characterizations 85
4.3.6. ATR- FTIR characterization 85
4.3.7. Time-of-Flight Secondary Ion Mass Spectrometry (ToF-SIMS) 85
4.3.8. X-Ray Photoelectron Spectroscopy 85
4.3.9. Temperature dependent turbidity measurement 86
4.3.10. Tube Inversion test 86
4.3.11. Rheometry characterizations 86
4.4. Results and discussion 86
4.4.1. Microscopy analysis 89
4.4.2. Surface characterisation 92
4.4.3. Thermal analysis 96
4.4.4. Colloidal gel evaluations 101

4.4.5. Rheological studies 102
4.5. Conclusions 108
5. Study of the applicability of synthesised thermoresponsive magnetic colloidal gels for *in vitro* cell expansion 109
5.1. Introduction 109
5.2. Aims and objectives 111
5.3. Materials and Methods 112
5.3.1. Material sterilisation 112
5.3.2. Cell culture and maintenance 112
5.3.3. Cell culture on top of particle gels 113
5.3.4. Cell encapsulation and three dimensional cell cultures within the Colloidal Gels 114
5.3.5. Trypsin-free cell recovery via magnetic cell separation and cell passages 115
5.3.6. Cell count and viability assessment for routine 2D cell culture 115
5.3.7. Statistical analysis 116
5.3.8. Live/Dead cell viability assay 116
5.3.9. Confocal microscopy cell imaging 116
5.3.10. Fluorescence microscopy 117
5.4. Results and discussion 117
5.4.1. Evaluation of cell compatibility on the top of colloidal gels 118
5.4.2. Application of thermoresponsive magnetic colloidal gels to 3D cell culture 123
5.4.3. Cell recovery and passaging via Magnetic particle separation 129
5.5. Conclusions 134
6. Conclusions and future work 135

List of figures

FIGURE 1.1: SCHEMATIC DIAGRAM SHOWS TISSUE ENGINEERING PRINCIPLES. (A) CELLS ISOLATED FROM DONOR (AUTOLOGOUS OR ALLOGENEIC). (B) CELLS ARE EXPANDED *IN VITRO*. (C) EXPANDED CELLS ADDED TO SCAFFOLD TO SUPPORT CELL GROWTH IN THE PRESENCE OF SPECIFIC GROWTH FACTORS AND MECHANICAL STIMULI. (D) RECREATES A FUNCTIONAL MICROENVIRONMENT THAT STIMULATES TISSUE ORGANIZATION INTO AN ENGINEERED GRAFT, WHICH IS THEN TRANSPLANTED INTO A PATIENT (SERBO AND GERECHT, 2013)..... 2

FIGURE 1.2: COMPARISON OF NATURAL CELL AND TISSUE MORPHOLOGY CULTURED ON 2D AND 3D SUBSTRATES. NATURAL TISSUES AND CELLS HAVE DISTINCT 3D ORGANIZED MORPHOLOGICAL FEATURES: HISTOLOGICAL IMAGES OF (A) BONE (D) LIVER, AND (G) SCANNING ELECTRON MICROSCOPE IMAGE OF THE THYMUS. WHEN TISSUE CELLS ARE CULTURED ON 2D SUBSTRATE, THEY SHOW A SIMILAR MORPHOLOGICAL PATTERN (STRETCHED). OPTICAL MICROSCOPE IMAGES OF (B) OSTEOBLASTS, (E) HEPATOCYTES, AND (H) CO-CULTURE OF LYMPHOCYTES AND STROMAL CELLS. CELLULAR MORPHOLOGY BECOMES CLOSER TO THAT OF NATURAL TISSUE WHEN CULTURED ON 3D MATRICES; DIFFERENT APPEARANCE OF (C) OSTEOBLASTS, (F) HEPATOCYTES, AND (I) MONONUCLEAR CELLS IN A 3D MATRIX (LEE ET AL., 2008). 7

FIGURE 1.3: DIFFERENT POLYMERIC SCAFFOLD FORMS FOR TISSUE ENGINEERING: (A) 3-D POROUS MATRIX, (B) A THERMOSENSITIVE SOL–GEL TRANSITION HYDROGEL, (C) A NANO FIBROUS MATRIX, AND (D) POROUS MICROSPHERE (CHUNG AND PARK, 2007). 10

FIGURE 1.4: (A) SCHEMATIC SHOWS THE POLYMER CHAIN CONFORMATION (COIL – GLOBULE) BELOW AND ABOVE LCST. (B) DEMONSTRATION OF THE PHASE TRANSITION ASSOCIATED WITH THE LCST (LEFT) AND UCST (RIGHT) (PHILLIPS AND GIBSON, 2015)..... 15

FIGURE 1.5: CHEMICAL STRUCTURE OF PNIPAM 16

FIGURE 1.6: MOLECULAR STRUCTURES OF VARIOUS OLIGO(ETHYLENE GLYCOL) METHACRYLATES. HYDROPHOBIC AND HYDROPHILIC MOLECULAR REGIONS ARE INDICATED IN RED AND BLUE, RESPECTIVELY (LUTZ, 2008). 17

FIGURE 1.7: COLLOIDAL STABILIZATION METHODS IN AQUEOUS SOLUTION. (A) STERIC STABILIZATION, (B) ELECTROSTATIC STABILIZATION (C) ELECTROSTERIC STABILIZATION: (D) DEPLETION STABILIZATION. 23

FIGURE 1.8: BASIC PRINCIPLE OF DIRECT MAGNETIC SEPARATION (POSITIVE ISOLATION). 29

FIGURE 3.1: SCHEMATIC TO SHOW FORMATION OF REVERSIBLY GELLING MAGNETIC MICROSPHERES THROUGH PHYSICAL ADSORPTION OF THERMORESPONSIVE POLYMER. 47

FIGURE 3.2: SCANNING ELECTRON MICROGRAPHS AT LOW AND HIGH MAGNIFICATION OF PS MICROSPHERES THAT SHOWS (A) SMOOTH SPHERICAL SHAPES (1.5 μM) AND THEN PARTICLE MORPHOLOGY CHANGES TO (B) 'CHICKPEA'-LIKE AT 2.5 μM AND (C) 'CAULIFLOWER'-LIKE AT 3.3 μM. SCALE BARS 5 μM. 51

FIGURE 3.3: (A) REACTION OF STYRENE AND DIVINYLBENZENE TO PRODUCE LIGHTLY CROSSLINKED POLYSTYRENE MICROSPHERES. (B) ATR-FTIR SPECTRUM OF PS MICROSPHERES. (C) TGA THERMOGRAM OF POLYSTYRENE MICROSPHERES SHOWS ONE STEP WEIGHT LOSS, THUS CONFIRMING THE PURITY OF THE PARTICLES. (D) WCA OF PS PARTICLE FILM INDICATING HYDROPHOBIC SURFACE. 52

FIGURE 3.4: (A) TEM IMAGES OF MAGNETITE NANOPARTICLES PREPARED BY A MODIFIED CHEMICAL CO-PRECIPITATION METHOD, SHOWING INDIVIDUAL PARTICLES WITH AVERAGE DIAMETERS OF ~10 NM, SCALE BAR 100 NM. (B) PHOTOGRAPHIC IMAGES OF SUSPENDED MAGNETITE NANOPARTICLES, IN THE ABSENCE AND PRESENCE OF MAGNET. THE STRONG MAGNETIC RESPONSE CAN BE SEEN BY THE SOLUTION BECOMING CLEAR UPON APPLICATION OF THE MAGNETIC FIELD, WHILE UPON REMOVAL OF THE FIELD THE PARTICLES WERE EASILY REDISPERSED BY GENTLY SHAKING THE VIAL. 54

FIGURE 3.5: (A) ATR-FTIR SPECTRUM OF SODIUM OLEATE STABILISED MAGNETITE NANOPARTICLES, SHOWING PEAKS FOR ALIPHATIC HYDROCARBON CORRESPONDING TO THE OLEATE, CONFIRMING PARTICLE SURFACE COVERAGE BY STABILISER. (B) TGA THERMOGRAM OF STABILISED MAGNETITE NANOPARTICLES, SHOWS 50% WEIGH LOSS DURING HEATING FROM 20-800 °C, CORRESPONDING TO THE DECOMPOSITION OF OLEATE STABILISER THAT COVERED MAGNETITE NANOPARTICLES. 55

FIGURE 3.6: (A) SCHEMATIC OF THE PREPARATION OF MAGNETIC POLYSTYRENE MICROSPHERES THROUGH LOADING MAGNETITE INTO PS MICROSPHERES. (B) SEM IMAGES OF MAGNETIC POLYSTYRENE MICROSPHERES AT LOW AND HIGH MAGNIFICATIONS. SCALE BARS ARE 10 μM 57

FIGURE 3.7: (A) TEMPERATURE DEPENDENCE OF THE MAGNETIZATION FOR MAGNETIC POLYSTYRENE MICROSPHERES; ZERO FIELD COOLING SHOWS A BLOCKING TEMPERATURE TYPICAL OF PARAMAGNETIC BEHAVIOUR. (B) PHOTOGRAPHS OF AN AQUEOUS DISPERSION OF MAGNETIC POLYSTYRENE MICROSPHERES IN THE ABSENCE AND PRESENCE OF MAGNET. IT WAS OBSERVED THAT THE PARTICLES WERE STRONGLY ATTRACTED BY EXTERNAL MAGNETIC FIELD AND EASILY RE-DISPERSED BY REMOVING THIS MAGNETIC FIELD AND GENTLE SHAKING. 58

FIGURE 3.8: SYNTHESIS OF THERMORESPONSIVE POLYMER (PDEGMA-DDT) BY CONVENTIONAL FREE RADICAL POLYMERIZATION..... 59

FIGURE 3.9: NMR SPECTRUM OF PREPARED PDEGMA WHICH WAS USED IN THE ADSORPTION ISOTHERM STUDIES. THE ABSENCE OF MONOMER PEAKS (THE RANGE BETWEEN 5.5 AND 6.5) CONFIRMS THE COMPLETE REMOVAL OF MONOMER. 60

FIGURE 3.10: (A) ABSORBANCE AS A FUNCTION OF TEMPERATURE FOR 1 % W/V PDEGMA SOLUTIONS IN DEIONIZED WATER, MEASURED BY UV-VISIBLE SPECTROSCOPY. LCST BEHAVIOUR OBSERVED AT 24 °C. ABSORBANCE OF THE SAMPLES WAS MEASURED AT A WAVELENGTH OF 550 NM. (B) TGA THERMOGRAM SHOWS ONE STEP OF DECOMPOSITION FOR PDEGMA POLYMER, INDICATING THE HIGH PURITY OF RESULTS. 62

FIGURE 3.11: (A) IMAGES OF TUBE INVERSION TEST OF SUSPENSION CONTAIN 25% OF PARTICLES AND 4% OF PDEGMA. (B) GEL–FLUID PHASE DIAGRAM FOR PS / PDEGMA SUSPENSIONS AT 37 °C, AS DETERMINED BY THE TUBE INVERSION ASSAY..... 67

FIGURE 3.12: TEMPERATURE SWEEP TESTS SHOW VARIATION OF G′ WITH TEMPERATURE FOR MPS/PDEGMA OR MPS PARTICULATE SUSPENSIONS AT (A) DIFFERENT PDEGMA CONCENTRATIONS AND CONSTANT MPS PARTICLE CONCENTRATIONS OF 25%;(B) DIFFERENT PARTICLE CONCENTRATIONS AND PDEGMA CONCENTRATION OF 4%. FOR ALL EXPERIMENTS THE SWEEP FREQUENCY WAS 1 RAD SEC^{-1} AND STRAIN 0.05% WERE USED. 71

FIGURE 3.13: (A) TEMPERATURE SWEEP TEST SHOWS THE VARIATION OF TAN Δ WITH INCREASE OF TEMPERATURE (B) MULTIPLE HEATING-COOLING CYCLES OF A SUSPENSION CONTAINING 15% MPS PARTICLES AND 4% PDEGMA WHICH SHOWS TEMPERATURE DRIVEN FLUID-GEL-FLUID BEHAVIOUR THROUGH VARIATION OF G′ VALUES UPON HEATING AND COOLING..... 72

FIGURE 3.14: STRAIN SWEEP TESTS SHOW THE VARIATION OF (A) G′ AND (B) TAN Δ WITH STRAIN% FOR DIFFERENT MPS PARTICLE CONCENTRATIONS (SAME AMOUNT OF PDEGMA 4%), MEASURED AT FREQUENCY 1 RAD SEC^{-1} AND 37°C 74

FIGURE 3.15: FREQUENCY SWEEP TESTS SHOW VARIATION OF (A) G′ AND (B) TAN Δ WITH FREQUENCY FOR DIFFERENT CONCENTRATION OF MPS PARTICLE SUSPENSION (SAME AMOUNT OF PDEGMA 4%); STRAIN 0.05% AND TEMPERATURE 37 °C WERE USED DURING MEASUREMENTS. 76

FIGURE 4.1: SCHEMATIC DIAGRAM SHOWS SYNTHESIS OF THERMORESPONSIVE MAGNETIC MICROSPHERES. 88

FIGURE 4.2: REPRESENTATIVE SCANNING ELECTRON MICROGRAPHS AT LOW (A) AND HIGH (B) MAGNIFICATION OF PCMS MICROPARTICLES THAT SHOWS SMOOTH SPHERICAL SHAPE AND PCMS-PDEGMA MICROPARTICLES PRODUCED

WITH DIFFERENT INITIATOR: MONOMER LOADING DURING GRAFTING REACTION (1:50, 1:100, AND 1:150). AFTER GRAFTING, THE PARTICLE DIAMETER AND SURFACE ROUGHNESS INCREASED IN LINE WITH MONOMER CONCENTRATION DURING THE SURFACE ATRP REACTION. 90

FIGURE 4.3: REPRESENTATIVE TRANSMISSION ELECTRON MICROGRAPHS AT LOW (A) AND HIGH (B) MAGNIFICATION OF THE SAME SAMPLES. IMAGES DEMONSTRATE THAT THE GRAFTED PDEGMA REGIONS ON AND IN THE SURFACE OF MICROPARTICLES, OBSERVED AS DIFFUSE REGIONS BECAUSE THE BRUSH LAYER WAS LIKELY TO BE LESS COMPACT COMPARED TO THE CORE PCMS..... 91

FIGURE 4.4: ATR-FTIR SPECTRA OF (A) PCMS AND (B) PCMS- PDEGMA MICROSPHERES (2.1 μM) WHICH HAVE BEEN PREPARED FROM 1:150 INITIATOR;MONOMER RATIO. 94

FIGURE 4.5: XPS SURVEY SPECTRA OF (A) PCMS AND (B) PCMS- PDEGMA MICROSPHERES (2.1 μM) WHICH HAVE BEEN PREPARED FROM 1:150 INITIATOR;MONOMER RATIO. (C) AND (D) ARE HIGH RESOLUTION CARBON SPECTRA OF PCMS AND PCMS- PDEGMA (2.1 μM), RESPECTIVELY. THE LATTER SPECTRA SHOW AN INCREASE IN THE PROPORTION OF METHOXY GROUPS CORRESPONDING TO PDEGMA AFTER GRAFTING. DATA ANALYSES AND CURVE FITTING WERE CARRIED OUT USING CASAXPS SOFTWARE (VERSION 2.3.16) (CASA SOFTWARE LTD, TEIGNMOUTH, UNITED KINGDOM). FOR HIGH RESOLUTION CARBON SPECTRA ALL SCANS WERE CHARGE CORRECTED TO C 1S AT 284 EV. 95

FIGURE 4.6: TOF-SIMS MASS SPECTRA OF Cl^- AND CH_3O^- PRESENT ON THE SURFACE OF PCMS AND PCMS- PDEGMA (WITH DIFFERENT INITIATOR: MONOMER RATIO DURING GRAFTING REACTIONS). THE SPECTRA WERE OBTAINED IN THE NEGATIVE ION MODE. 96

FIGURE 4.7: TGA THERMOGRAM SHOWING THE DECOMPOSITION OF PCMS MICROPARTICLES, MAGNETIC PCMS-PDEGMA MICROSPHERES (15% MAGNETITE WAS LOADED), AND LINEAR PDEGMA WITH TEMPERATURE..... 97

FIGURE 4.8: TEMPERATURE DEPENDENT TURBIDITY MEASUREMENTS, SHOWING THE VARIATION OF ABSORBANCE AS TEMPERATURE INCREASE OF DILUTE SUSPENSIONS OF PCMS- PDEGMA AND PCMS MICROSPHERES. ABSORBANCES OF THE SAMPLES WERE MEASURED AT A WAVELENGTH OF 550 NM. 99

FIGURE 4.9: TEM IMAGES OF (A) MAGNETITE NANOPARTICLES PREPARED BY A CO-PRECIPITATION METHOD, SHOWING INDIVIDUAL PARTICLES WITH AVERAGE DIAMETERS OF ~10 NM. (B) MAGNETIC LOADED MICROSPHERE SHOWING THE DISTRIBUTION OF MAGNETITE NANOPARTICLES WITHIN THE MICROSPHERE. (C) PHOTOGRAPHIC IMAGES OF AN AQUEOUS SUSPENSION OF MAGNETIC MAGNETOTHERMALLY RESPONSIVE MICROSPHERES (MAGNETIC PDEGMA-G-

PCMS). It was observed that the particles were strongly attracted by an external magnetic field and easily re-dispersed by removing this magnetic field and with gentle shaking. 100

Figure 4.10: Images of tube inversion tests for different concentrations of particles. In (a) and (b) are shown PCMS-PDEGMA in cell culture medium and distilled water, respectively. In (c) magnetic PCMS-PDEGMA microparticles are shown in cell culture medium. Glass vial capacity 7 mL (Height 4.2 cm, Diameter 2 cm). 102

Figure 4.11: (a) and (b) Temperature ramp test showing variation of G′ and tan Δ with temperature for magnetic PCMS-PDEGMA (filled marks) and magnetic PCMS particles (open marks) at different particle concentration, frequency 1 rad sec^{-1} and strain 0.05% were used. In (c) temperature sweep test shows reversible gelation and flow, and increased G′ values upon heating and reduced G′ upon cooling. In (d) is depicted multiple heating-cooling cycles of a suspension containing 30% particles which shows temperature driven Fluid-Gel-Fluid behaviour 104

Figure 4.12: (a) and (b) strain sweep tests show the variation of G′ and tan Δ with strain% for different magnetic PCMS-PDEGMA particle concentration, measured at frequency 1 rad sec^{-1} and 37°C . In (c) and (d) frequency sweep tests show variation of G′ and tan Δ with frequency for different concentration of magnetic PCMS-PDEGMA particle suspension; strain 0.05% and temperature 37 °C were used during measurements 107

Figure 5.1: (a) 3T3 and (b) MSCs cell number standard curve determined using the PrestoBlue assay, cells were harvested from conventional 2D T75 culture flasks and counted using a haemocytometer and Trypan Blue dye exclusion. Serial dilutions were made to give appropriate cell, seeding numbers. n= 9 (nine measurmentswere performed at each time point). 117

Figure 5.2: Proliferation of 3T3 cells cultured on the (a) colloidal gels and (b) tissue culture plates over 6 days, respectively. Cell numbers were measured by the PrestoBlue viability assay on day 1, 3 and 6. Error bars are ± standard deviations. (**** represent P value < 0.0001). n= 9 (nine measurmentswere performed at each time point). 121

Figure 5.3: Fluorescence microscopy images of RFP-3T3 cells cultured over 6 days. (a) (b) (c) and (d) cells cultured on PCMS- PDEGMA magnetic colloidal gels on day 0, 1, 3 and 6, respectively. (e)(f)(g) and (h) cells cultured on tissue culture plate on day 0, 1, 3 and 6, respectively. *Scale bars - 100 μm*... 122

FIGURE 5.4: SCHEMATIC REPRESENTATION OF THE SYNTHESIS AND APPLICATION OF THERMOREVERSIBLE PCMS-PDEGMA PARTICLE GEL AS 3D SCAFFOLDS FOR *IN VITRO* CELL EXPANSION. REVERSIBLE THERMOGELLING BEHAVIOUR ALLOWS EASY CELL SEEDING AND ENCAPSULATION AND THE MAGNETIC CORE ALLOWS CELL HARVESTING AFTER EXPANSION. 123

FIGURE 5.6: PROLIFERATION OF 3T3 CELLS CULTURED (A) WITHIN COLLOIDAL GEL AND (B) IN TISSUE CULTURE FLASK. (C) AND (D) SHOW PROLIFERATION OF MSCS CULTURED WITHIN THE PARTICLE GELS AND IN TISSUE CULTURE FLASKS, RESPECTIVELY. CELL NUMBERS WERE MEASURED BY THE PRESTOBLUE VIABILITY ASSAY ON DAY 1, 3 AND 6 FOR 3T3 CELLS AND ON DAY 1, 5 AND 10 FOR MSCS. ERROR BARS ARE ± STANDARD DEVIATIONS. (**** REPRESENT P VALUE < 0.0001). N= 9 (NINE MEASURMENTSWERE PERFORMED AT EACH TIME POINT). 126

FIGURE 5.7: *FLUORESCENCE MICROSCOPY IMAGES OF RFP-3T3 CELLS IN 3D SCAFFOLD ON DAY 0, 1, 3, AND 6 POST-SEEDING. SCALE BARS - 100 µM.* 127

FIGURE 5.8: CONFOCAL MICROSCOPY IMAGES OF RFP-3T3 CELLS IN 3D SCAFFOLD ON DAY 0, 3, AND 6 POST-SEEDING. IMAGES WERE TAKEN AT LOW (10X) AND HIGH (40X) MAGNIFICATION FOR THE SAME SAMPLES. SCALE BARS - 100 µM. 128

FIGURE 5.9: *CONFOCAL MICROSCOPIC IMAGES REPRESENT LIVE/DEAD ASSAY OF MSC GROWN WITHIN THE COLLOIDAL GEL SCAFFOLD AT (A) 5 DAY AND (B) 10 DAY. GREEN DENOTES CELLS STAINING POSITIVE FOR CALCEIN AM (LIVE) AND RED SHOWS STAINING WITH ETHIDIUM HOMODIMER (DEAD). SCALE BARS - 100 µM* 129

FIGURE 5.10: *(A) AND (B) THE EFFICIENCY OF THE RECOVERY OF PROLIFERATED 3T3 AND MSC WITHIN THE COLLOIDAL GEL BY MAGNETIC SEPARATION, RESPECTIVELY. THE BLACK REGION REPRESENT THE NUMBER OF UNRECOVERED CELLS, AFTER PERFORMED MAGNETIC SEPARATION. (C) AND (D) ARE 3T3 AND MSC CELL PROLIFERATION WITHIN THE COLLOIDAL GEL OVER TIME, RESPECTIVELY. STRAIGHT LINES REPRESENT CONTINUOUS CELL PROLIFERATION WITHOUT PASSAGE AND DASHED LINES REPRESENT CELL PROLIFERATION WHEN PASSAGED TWO TIMES (ON DAY 3 AND 6 FOR 3T3 AND ON DAY 5 AD 10 FOR MSC).* ERROR BARS ARE ± STANDARD DEVIATIONS. N= 9 (NINE MEASURMENTSWERE PERFORMED AT EACH TIME POINT). 131

FIGURE 5.11: *(A) PHOTOGRAPHIC IMAGES OF AQUEOUS SUSPENSION OF MAGNETIC AND THERMALLY RESPONSIVE MICROSPHERES (MAGNETIC PCMS-PDEGMA). IT IS OBSERVED THAT THE PARTICLES ARE STRONGLY ATTRACTED BY EXTERNAL MAGNETIC FIELD AND EASILY RE-DISPERSED BY REMOVING THIS MAGNETIC FIELD AND GENTLE SHAKING. IN (B) IMAGES SHOW MAGNETIC SEPARATIONS OVER THREE SEPARATION CYCLES.* 132

FIGURE 5.12: *REPRESENTATIVE LIGHT MICROSCOPY IMAGES OF 3T3 CELLS RECOVERED FROM THE CELL/PARTICLES MIXTURE AFTER SUCCESSIVE MAGNETIC SEPARATION PROCESS. THE RECOVERED CELLS WERE THEN CULTURED IN TCP FOR 3 HOURS, THEN IMAGED. (A) WITHOUT PERFORMING MAGNETIC SEPARATION, MANY MAGNETIC PARTICLES CAN BE SEEN, (B) AFTER PERFORMING FIRST CYCLE SEPARATION, LESS PARTICLE ARE REMAINING, (C) AFTER PERFORMING TWO SUSBSEQUENT MAGNETIC SEPARATION STEPS, FEW PARTICLE REMAINING WITH THE CELLS, AND (D) AFTER THREE SUSBSEQUENT MAGNETIC SEPARATION STEPS, NO FURTHER PARTICLES REMAN WITH THE CELLS. SCALE BAR 100µM* 133

List of tables

TABLE 3.1: EXPERIMENTAL CONDITIONS AND RESULTS FOR DISPERSION POLYMERISATION OF STYRENE AND DVB TO PRODUCE PS MICROSPHERES. DIFFERENT RATIOS OF STABILISER : MONOMER COMPOSITION WERE USED. 49

TABLE 3.2: TUBE INVERSION TEST RESULTS OF PS/ PDEGMA PARTICULATE SUSPENSIONS IN DEIONISED WATER AND/ OR DMEM. THE RESULTS SHOW THE REVERSIBLE GELATION (+) AND FLOW (-) OF SUSPENSIONS AT 37°C FOR DIFFERENT PARTICLE AND PDEGMA CONCENTRATIONS. SUSPENSIONS MADE WITH EITHER WATER OR DMEM MEDIUM WERE COMPARED AND NO DIFFERENCE WAS FOUND. 66

TABLE 4.1: TUBE INVERSION TEST RESULTS OF PARTICULATE SUSPENSIONS AT DIFFERENT PARTICLE CONCENTRATIONS IN DDW AND/ OR DMEM. 101

List of abbrevations

%w/v	%weight per volume
2D	Two-dimensional
3D	Three-dimensional
AIBN	Azo-isobutrilinitrile
ATRP	Atomic Transfer Radical Polymerisation
ATR-FTIR	Attenuated total reflectance Fourier transform infrared
CV	Coefficient of variation
DMEM	Dulbecco's modified Eagles medium
DNA	Deoxyribonucleic acid
D_n	The number average diameter
EDTA	Ethylene diamine tetraacetic acid
ECM	Extracellular matrix
FBS	Fetal bovine serum
FDA	Food and drug administartion
FRP	Free radical polymerisation
G'	Storage (elastic) modulus
G''	Loss (viscous) modulus
GPC	Gel permeation chromatography
HBSS	Hank's balanced salt solution
^{1}H NMR	Proton nuclear magnetic resonance
kDa	Kilo Daltons
LCST	Lower Critical Solution Temperature
LVE	Linear viscoelastic region
MIONP	Magnetic iron oxide nanoparticles

Mn	Number average molecular weight
Mw	Weight average molecular weight
MPS	Magnetic polystyrene
MSCs	Mesenchymal stem cells
PBS	Phosphate buffered saline
PCMS	Poly(chloromethylstyrene)
PDEGMA	Poly (Di(ethylene glycol) methyl ether methacrylate)
PEG	Poly(ethylene glycol)
PEGMA	poly(ethylene glycol) methacylate
PEO/PEG	poly(ethylene oxide)/poly(ethylene glycol)
PEGMA246-EE	poly(ethylene glycol) methacrylate ethyl ether (Mn=246)
PEGMA475-ME	poly(ethylene glycol) methacrylate methyl ether (Mn=475)
PLGA	Poly (lactic-co-glycolic) acid
PolyNIPAm	poly(N-isopropylacrylamide)
PS	Polystyrene
PVP	Pol(yvinylpyrrolidone)
RAFT	Reversible addition fragmentation transfer reaction
RM	Regenerative medicine
SD	Standard deviation
SI	Surface-initiated
SEM	Scanning electron microscopy / Standard error of the mean
TCP	Tissue culture plastic
TE	Tissue engineering
TEM	Transmission Electron Microscopy

TGA	Thermo- gravimetric analysis
ToF-SIMS	Time-of-Flight Secondary Ion Mass Spectrometry
UCST	Upper critical solution temperature
XPS	X-Ray Photoelectron Spectroscopy

1. Introduction

1.1. Tissue engineering and regenerative medicine

Tissue and organ damage is a serious clinical issue which accounts for millions of health problems worldwide every year. Despite continuous development, current surgical transplantation strategies for treating organ failure retain some limitations such as shortage of donor organs, difficulty to control cell functions after transplantation, and undesirable immunological response (Tabata, 2001, Zhang and Kohn, 2012). During the last three decades tissue engineering (TE) and regenerative medicine (RM) have become a focus for scientists aiming to construct biological substitutes to regenerate or replace diseased or damaged tissues or organs (Berthiaume et al., 2011). These strategies avoid complicated surgical interference and allow different cell manipulations before injection to restore the functions of tissues or organs (Hou et al., 2004, Melero-Martin et al., 2007). Accordingly, such procedures may become a promising alternative to traditional homologous organ transplantation. Also, these strategies may offer solutions for clinical problems which are currently untreatable by drug therapy such as spinal cord injury and liver failure (Langer, 2009). Tissue engineering, has been defined by Langer and Vacanti as: "An interdisciplinary field that applies the principles of engineering and life sciences toward the development of biological substitutes that restore, maintain or improve tissue function or a whole organ" (Langer and Vacanti, 1993).

Cells, scaffolds and growth factors are the main required components for tissue engineering. These are necessary to achieve neo-tissue

construction and restoration. Figure 1.1 shows the principles of tissue engineering. Cells can be obtained either from the patient (autologous) or from a donor (allogeneic), and then they can be expanded *in vitro* to achieve sufficient cell numbers. Various primary cells and stem cells have been explored by tissue engineers to define the best cell source for constructing a particular tissue (Polak and Bishop, 2006).

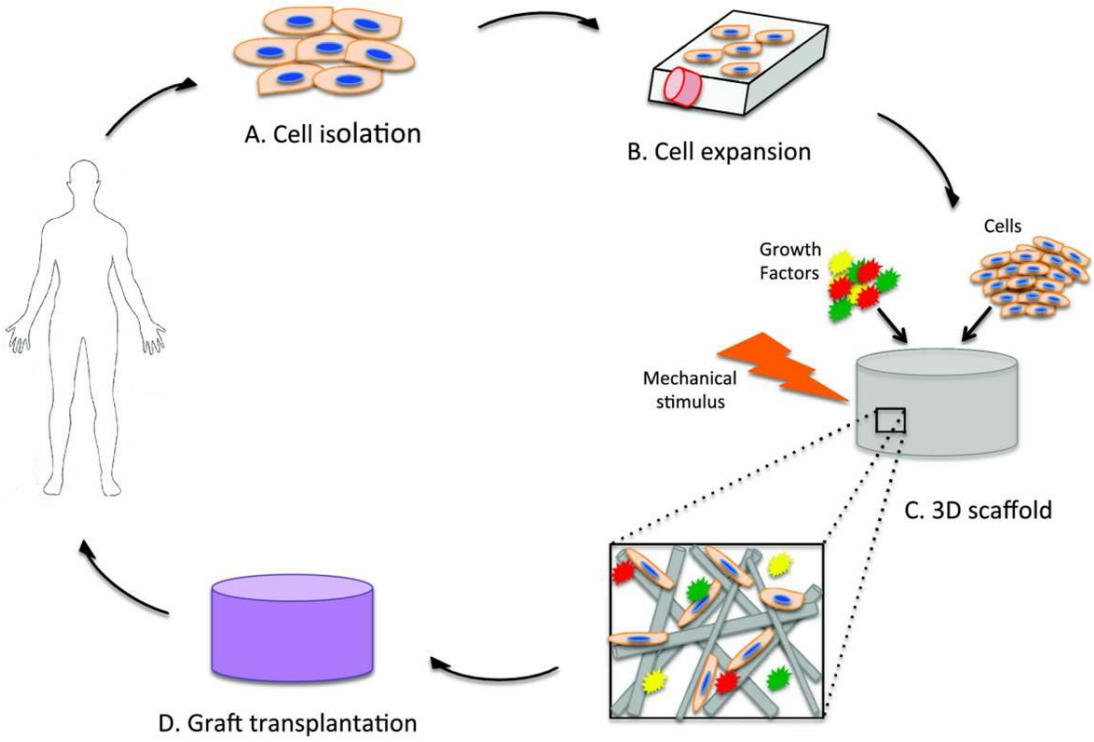


Figure 1.1: Schematic diagram shows tissue engineering principles. (A) Cells isolated from donor (autologous or allogeneic). (B) Cells are expanded *in vitro*. (C) Expanded cells added to scaffold to support cell growth in the presence of specific growth factors and mechanical stimuli. (D) Recreates a functional microenvironment that stimulates tissue organization into an engineered graft, which is then transplanted into a patient (Serbo and Gerecht, 2013).

An adult stem cell is an undifferentiated cell found in various tissue niches throughout the body, including bone marrow, kidney, pancreas, skeletal muscle, adipose tissue, brain, and liver (Chen and Tuan, 2008, Nombela-Arrieta et al., 2011). For example, mesenchymal stem cells (MSCs) have the ability to differentiate into mesoderm, ectoderm and

endoderm cell lineages (Uccelli et al., 2008). Commercialised human MSCs are now available and there are attempts to industrialize these cells for medical therapy. The use of autologous MSCs obtained from the same patient receiving the implanatation can reduce the risk of immunological rejection problems and need for a second surgical step. Therefore, they are considered good candidates for cell transplantation and regenerative medicine. The capability to expand these cells *in vitro* with the maintenance of their full biological properties is the key requirement for tissue engineering and regenerative medicine (Ng et al., 2014). The expanded cells can be seeded onto three dimensional scaffolds that provide a biomechanical environment to form a tissue engineered construct which can be used for *in vitro* research or as implants (Shimizu et al., 2007). The implanted tissue engineered construct has to be able to survive, restore normal function, and integrate with the surrounding tissue. Accordingly, suitable growth factors which can regulate cell functions are necessary to promote tissue regeneration (Lee et al., 2011).

The challenges facing tissue engineers working on stem cells are to optimise cell isolation, proliferation and differentiation, besides the design of scaffolds and/or delivery systems that promote the coordinated growth of three-dimensional tissues. To maximise their chances of success, with regards to scaffold design, tissue engineers attempt to replicate as far as possible the natural microenvironment in which the cell/tissue would normally grow and function within the body (Polak and Bishop, 2006). The strategies attempted to reproduce the natural cell microenvironment include the controlled delivery of growth factors, three

dimensionality, bio-functionalisation of synthetic materials, and controlling the scaffold elasticity in addition to the development of cell co-culture protocols (Lutolf and Blau, 2009).

Researchers have attempted to grow skin and cartilage (Eaglstein and Falanga, 1998), bone and cartilage(Boyan et al., 1999), liver (Mayer et al., 2000), heart valves and arteries (Sodian et al., 1999), bladder (Oberpenning et al., 1999), pancreas (Tziampazis and Sambanis, 1995), nerves (Mohammad et al., 2000), corneas (Germain et al., 1999), and various other soft tissues (DiEdwardo et al., 1999).

Despite the tremendous advancement in tissue engineering, there are many challenges. Research into the large scale production of these tissue or organs or improvement of the cell culture environment is still necessary.

1.2. *In vitro* cell culture models for tissue engineering applications

1.2.1. Monolayer cell culture system

The majority of cell culture studies have been performed on monolayer surfaces (e.g. tissue culture flasks, micro well plates and petri dishes) due to ease of preparation, convenience, good cell viability and biocompatibility (Kim, 2005). These monolayer cell culture systems have have improved our understanding of basic cell biology (Lee et al., 2008, Jaiswal et al., 1997), tissue morphogenesis (Schnaper et al., 1993) and the dynamic relationship between cell function and interactions with the cellular environment (Tibbitt and Anseth, 2009).

However, two-dimensional (2D) cell cultures systems do not closely mimic the *in vivo* environment. These cultures overlook the dimensionality and microenvironmental signalling, cell-cell interactions are limited and cell functions may change (Huh et al., 2011). Cells cultured in 2D are often elongated, unnatural in shape, with less capacity to grow and to behave as they would *in vivo*. Furthermore, altered cell metabolism and reduced functionality may result from dramatic adaptation by surviving cells cultured on 2D rigid substrate due to the lack of the unique extracellular matrix (ECM) environment of each cell type. (Zhang, 2004, Abbott, 2003, Cukierman et al., 2001). Therefore, two dimensional culture substrates are likely to misrepresent findings to some degree by forcing cells to adjust to an artificial flat, rigid surface (Lee et al., 2008). Therefore, traditional monolayer cell culture methods might not be sufficient for new challenges in tissue regeneration, pharmaceutical assays, cell biology and biochemistry.

Recently, tissue engineers have begun to develop new three dimensional cell culturing systems to overcome the limitations and challenges inherent with 2D cell culture (Tibbitt and Anseth, 2009, Zhang et al., 2005a). Various recent studies have emphasised the importance of 3D culture environments, especially with regards to stem cells (Lutolf and Blau, 2009).

1.2.2. Three dimensional (3D) cell culture systems

In 3D cell cultures, cell morphology and function are much closer to those of cells grown *in vivo* (Lee et al., 2008, Nisbet et al., 2007) (Levenberg et al., 2003). Also, three dimensional cell cultures are important for phenotype presentation, cell proliferation and cell migration

(Guillame-Gentil et al., 2010). Moreover, the three dimensional microenvironment influences the diffusion and adhesion of the key proteins, growth factors, and enzymes which ensure cell viability and which influence function (Griffith and Swartz, 2006). These 3D environments are crucial for the engineering of tissue models for drug testing or further biological studies and the generation of tissue substitutes (Fischbach et al., 2007, Griffith and Swartz, 2006, McGuigan and Sefton, 2006, Albrecht et al., 2006, Khademhosseini and Langer, 2007, Yang et al., 2009, Lutolf and Hubbell, 2005b).

One of the challenges in the use of human mesenchymal stem cells (hMSC) in tissue engineering is the availability of *in vitro* conditions which retain the cells' native characteristics and improve their capability to treat diseased and damaged organs or tissues (Derubeis and Cancedda, 2004). Three-dimensional (3D) cell-biology methods possess fundamental advantages over traditional culture techniques for providing insight into the native characteristics of cells. Figure 1.2 shows Comparison of natural cell and tissue morphology cultured on 2D and 3D substrates.

3D culture can be performed either by using scaffolds to support cell growth, for example hydrogels, inert matrix and other materials such as fibres, or by scaffold-free techniques such as low adhesion plates, micropatterned surfaces, hanging drops, suspension using methyl cellulose, rolling vessels or by magnetic levitation. The choice of experimental model system, the goals of experiment, and the number of samples are key factors in determining which 3D model system is the most preferable for use (Haycock, 2011).

All three dimensional cell culture systems produce a microenvironments which better mimics *in vivo* compared to monolayer methods. However, there are some limitations with most existing 3D methods such as scalability, reproducibility, sensitivity, and compatibility with high-throughput screening (HTS) instruments in the drug development process.

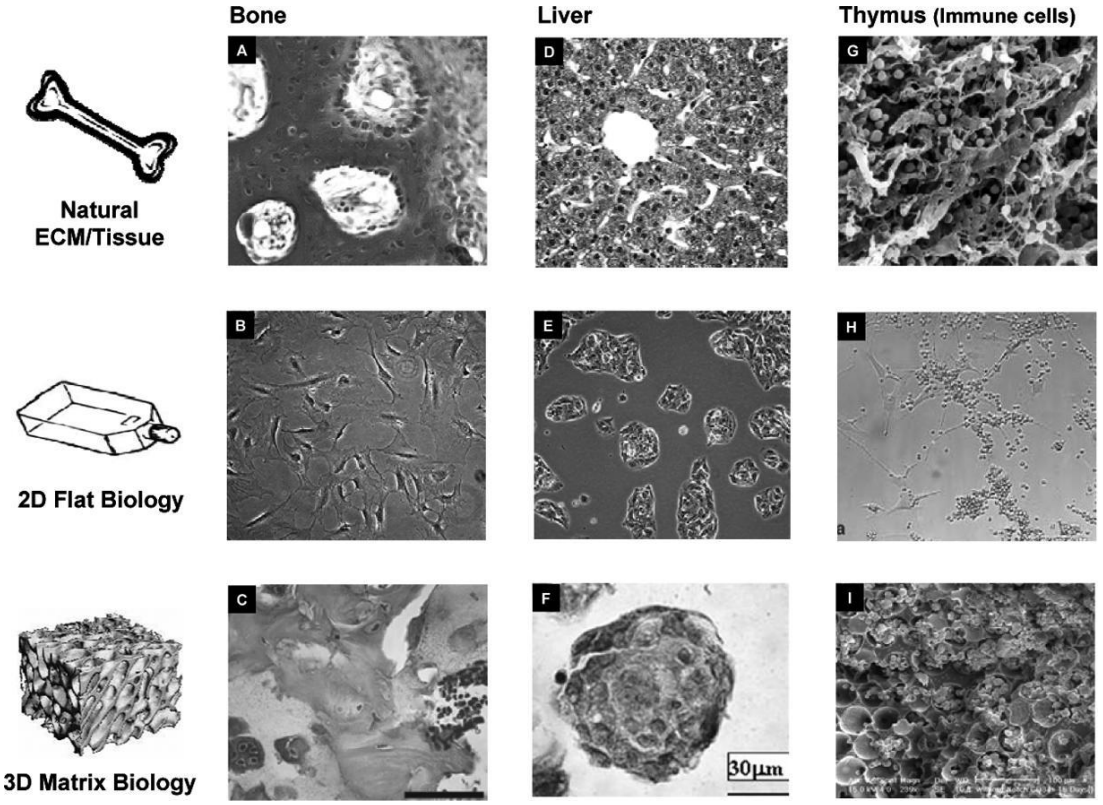


Figure 1.2: Comparison of natural cell and tissue morphology cultured on 2D and 3D substrates. Natural tissues and cells have distinct 3D organized morphological features: histological images of (A) bone (D) liver, and (G) scanning electron microscope image of the thymus. When tissue cells are cultured on 2D substrate, they show a similar morphological pattern (stretched). Optical microscope images of (B) osteoblasts, (E) hepatocytes, and (H) co-culture of lymphocytes and stromal cells. Cellular morphology becomes closer to that of natural tissue when cultured on 3D matrices; different appearance of (C) osteoblasts, (F) hepatocytes, and (I) mononuclear cells in a 3D matrix (Lee et al., 2008).

1.3. Polymeric scaffolds in tissue engineering

Three dimensional cell culture scaffolds consist of porous substrates that support cell growth, differentiation and organization (Lee et al., 2008). The roles of the scaffold is to provide the supporting architecture for the cells to guide tissue formation into the desired shape, while allowing transportation of nutrients and growth factors to promote tissue growth (Langer and Vacanti, 1993, Spector, 2006, Dhandayuthapani et al., 2011b). Design of scaffolds is the most investigated area of biomaterial research and one of the most important subjects in TE and RM (Dhandayuthapani et al., 2011b, Armentano et al., 2010). One of the most critical issues in TE is the design of scaffolds with specific biological, mechanical, and physical properties (Vasita and Katti, 2006). Therefore, there are many efforts to design different scaffolds with different surface morphology, porosity and mechanical characteristics (Guillame-Gentil et al., 2010).

Polymers are widely regarded as the most attractive and useful biomaterials for scaffold fabrication (Ji et al., 2006) due to their desirable and configurable chemical, mechanical and physical properties. Many kinds of biocompatible polymers have been prepared for scaffold fabrication (Wang et al., 2011), including fibres, (Dhandayuthapani et al., 2011a), microspheres (Dhandayuthapani et al., 2011b), hydrogels (Sasaki et al., 2010, Macaya and Spector, 2012, Burdick, 2012, Amini and Nair, 2012), solid foams (Chung and Park, 2007) and many more.

Figure 1.3 shows different polymeric scaffold forms for tissue engineering.

Soft materials engineering and fabrication processes allows the design of 3D matrices with complex functionalities such as the ability to release potent bioactive molecules (e.g. growth factors, DNA, or drugs) in a sustained manner to facilitate tissue regeneration (Hench and Polak, 2002, Langer and Tirrell, 2004, Salvay and Shea, 2006, Chung and Park, 2007) to promote cell adhesion (Lutolf and Hubbell, 2005b), and as a cell delivery carrier (Hoffman, 2002, Drury and Mooney, 2003, Chung and Park, 2007).

The scaffold fabrication technique is influenced by the surface and bulk properties of the polymer and the required proposed functionality of the scaffold (Dhandayuthapani et al., 2011b). Different scaffold fabrication methodologies/techniques can utilise several synthetic and natural polymers, each technique has its inherent merits and demerits, such techniques including solvent casting, particulate leaching, gas foaming, phase separation, electrospinning, fibre mesh formation, self-assembly, and freeze drying (Ifkovits and Burdick, 2007).

3D scaffolds can be applied either for clinical or *in vitro* 3D modelling approaches. The first applications mainly including of tissue engineering or regenerative medicine, with the purpose of functional replacement within the body (Langer and Vacanti, 1993, Vacanti and Langer, 1999). Therefore, these material has to be biodegradable and metabolized in the body without causing serious systemic or immunogenic problems (Griffith and Naughton, 2002).

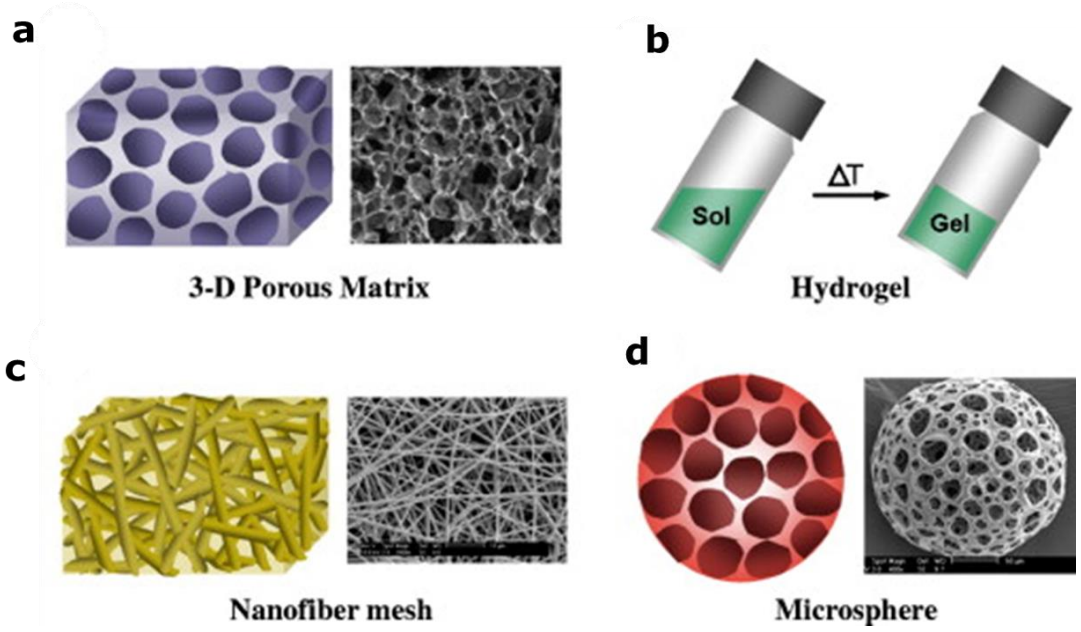


Figure 1.3: Different polymeric scaffold forms for tissue engineering: (a) 3-D porous matrix, (B) a thermosensitive sol–gel transition hydrogel, (C) a Nano fibrous matrix, and (D) porous microsphere (Chung and Park, 2007).

Polymeric biomaterials used as scaffolds can be classified into natural and synthetic biomaterials (Dhandayuthapani et al., 2011b). Natural polymers include proteins (collagen, fibrinogen, silk, elastin, gelatine, and keratin,), polysaccharides (cellulose, amylose, dextran, chitin, and glycosaminoglycans), or polynucleotides (DNA, RNA) (Dhandayuthapani et al., 2011b). Naturally derived polymers have the potential advantage of biological recognition, excellent biocompatibility and high cell viability. However, natural materials also have some disadvantages, such as limited physical and mechanical properties, immunogenicity and pathogen transfer (Ratner and Bryant, 2004), supply/availability and complexities associated with cost, processing and purification (Armentano et al., 2010). Synthetic polymeric scaffolds are more favoured due to possessing some superior properties such as susceptibility to modification, controlled degradation, easy processability

(Peter et al., 1998), adaptable chemistries, reproducibility and elimination of infection transmission risk (Dhandayuthapani et al., 2011b). Their processability allow polymers to be fabricated into highly porous 3-dimensional scaffolds, fibres, sheets, blocks and microspheres (Reinout, 2008). There are also possibilities to modify the physico-mechanical properties of these polymers to match the intended application by controlling their molecular weight, molecular weight distribution, composition and molecular architecture (Jagur-Grodzinski, 2006). However, scaffolds made from some synthetic polymers can be limited by a lack of bio-functionality and relatively high hydrophobicity which impact on the ability of cells to adhere to them (Lutolf and Hubbell, 2005a). Various methods have been utilised to fabricate synthetic polymeric scaffolds including solvent casting, particulate leaching, phase separation, and electrospinning (Dhandayuthapani et al., 2011b, Mikos et al., 1994, Nam et al., 2000, Ma et al., 2005, Lutolf and Hubbell, 2005b, Chung and Park, 2007). Biodegradable polyesters are the most widely used of the synthetic polymers in tissue engineering. They are approved by the Food and Drug Administration (FDA) for human use and they can be easily processed into porous scaffolds. Poly(glycolic acid) (PGA), poly(lactic acid) (PLA) and their copolymer poly(lactic-co-glycolic acid) (PLGA) have been extensively applied in bone and cartilage repair.

The combination of the synthetic and natural polymers, appears to be a promising strategy for TE, both in terms of structural/mechanical and biological properties (Borzacchiello et al., 2011). Composite scaffolds are most likely to overcome the above mentioned drawbacks of natural and synthetic scaffolds. The essential requirements of the biomaterials that

can be used for scaffold design are favourable mechanical properties (Armentano et al., 2010), suitable surface chemistry for cell attachment and proliferation (Hutmacher, 2000, Ifkovits and Burdick, 2007), wettability, and sometimes biodegradability (Jagur-Grodzinski, 2006, Lee et al., 2008). Despite continuous developments in scaffold design, significant issues and restrictions continue to exist such as reproducibility of the microstructure and properties of the fabricated scaffolds, cost, and scalability to scale-up fabrication processes. These challenges bring the need for developing alternative biomaterials and fabrication methods.

1.4. Temperature responsive polymers in tissue engineering

Thermoresponsive polymers that have the ability to respond to a change in temperature are of interest for many biomedical applications (Ward and Georgiou, 2011, Gil and Hudson, 2004). This response may be in the form of alternation between hydrophobic and hydrophilic states, precipitation, gelation, and reversible adsorption onto a surface. Such properties can be harnessed in applications ranging from producing thermos swithcable surfaces, biosensors, drug delivery and tissue engineering (Stuart et al., 2010), and selective bioseparation (Galaev and Mattiasson, 1999, Hoffman and Stayton, 2004, Lutz, 2006)**.**

In tissue engineering, thermoresponsive polymers are mainly used either as injectable gels to encapsulate cells in 3D structures in the body (Ward and Georgiou, 2010) or as substrates that support cell growth and proliferation (Kumashiro et al., 2010, Reed et al., 2010, Nitschke et al., 2007).

Many natural and synthetic thermoresponsive polymers have been prepared for tissue engineering applications. Considerable research has been directed toward endowing natural products, alone or in combination with synthetic polymers, with enhanced mechanical properties and altered phase transition temperatures, usually Lower Critical Solution Temperatures (LCST)s under physiological conditions. Natural polymers such as methylcellulose, chitosan and xyloglucan exhibit thermosensitivity and biocompatibility. Methylcellulose is a derivative of the naturally occurring polysaccharide cellulose and becomes hydrophobic and water-insoluble at 60-80 °C. However considerable extra functionalisation is necessary to reduce the phase transition temperature to be useful for tissue engineering applications (Li et al., 2002, Takahashi et al., 2001, Tate et al., 2001). Chitosan is another naturally derived polymer that has a number of advantages for tissue-engineering applications, such as biocompatibility, biodegradation, antimicrobial activity, and haemostasis. However, it lacks intrinsic thermosensitive properties; thus, other thermosensitive materials need to be introduced into chitosan to make it applicable for thermosensitive hydrogels (Prabaharan and Mano, 2006, Jiang et al., 2008). Xyloglucan, obtained from tamarind seed, is a biocompatible and biodegradable polysaccharide consisting of glucopyranosyl, xylopyranose, and galactose. It is known to show thermosensitive gelation at approximately 20 ^{o}C (Shirakawa et al., 1998, Miyazaki et al., 1998, Nisbet et al., 2006) Xyloglucan-based thermosensitive hydrogels have recently been evaluated as possible cell and drug delivery vehicles (Nisbet et al., 2010).

Thermoresponsive synthetic polymers can be divided into two main types; polymers that possessing a lower critical solution temperature (LCST) (Jonas et al., 2007, Ishida and Biggs, 2010) and polymers that possess an upper critical solution temperature (UCST) (Cheng et al., 2008). LCST and UCST are the respective critical temperature points below and above which the polymer and solvent are completely miscible. Above an LCST, chain solvation cannot compete with interchain interactions, resulting in a collapse (reduction of swelling) of the polymer conformation. Above a UCST, the opposite phenomenon occurs and chains open up. (Krishnamoorthy et al., 2014). It is noteworthy that "LCST is an entropically driven effect while UCST is an enthalpically driven effect" (Ward and Georgiou, 2011). The characteristic of polymer chain conformation in both types are shown in figure 1.4.

The reasons for the entropic dominance of the LCST can be understood by free energy from the Gibbs equation $\Delta G = \Delta H - T\Delta S$ (G: Gibbs free energy, H: enthalpy and S: entropy). The water is less ordered and has higher entropy when the polymer is not in solution, so the enthalpic contribution of the water becomes less than the entropic gain of the system as a whole, making hydration unfavourable and leading to polymer chain dehydration and the formation of precipitates or physical gels (Dimitrov et al., 2007, Schild, 1992). Synthetic polymers with LCST behaviour are the most widely used in tissue engineering. A solution of polymers with LCST becomes clear below this temperature because polymer is dissolved, however it becomes cloudy above this temperature due to the aggregation of polymer (sometimes LCST is referred to as cloud temperature, although the two are not the same).

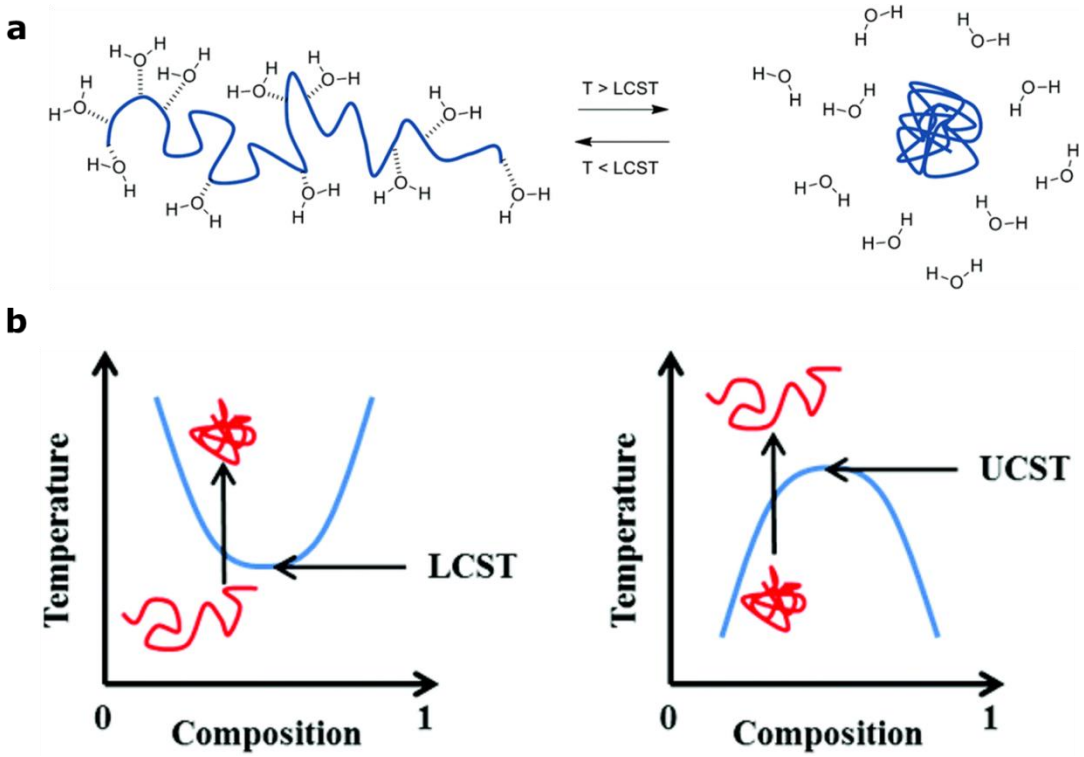


Figure 1.4: (a) Schematic shows the polymer chain conformation (coil – globule) below and above LCST. (b) Demonstration of the phase transition associated with the LCST (left) and UCST (right) (Phillips and Gibson, 2015).

Among thermosensitive polymers with LCST, poly(N-isopropylmethacrylamide) (polyNIPAm) is the most used polymer (Tauer et al., 2009) and shows a sharp coil-to-globule transition in water at 32 °C (Schild, 1992, Feil et al., 1993, Zhang et al., 2001, Stile and Healy, 2002). PolyNIPAm-based materials have been used as surface modifiers for cell-sheet tissue engineering to provide an enzyme and shear free cell harvesting system. Surfaces coated with this polymer promote cell attachment and growth at 37 °C when the polymer is chain-collapsed and hydrophobic. However by lowering the temperature to below the LCST of polymer allows cell detachment because of chain extension and hydration of the polymer brush layer (Yamato et al., 2001, Shimizu et al., 2003, Tang et al., 2014, Matsuda et al., 2007). PolyNIPAM polymers

have also been used as injectable hydrogel scaffolds in tissue engineering (Na et al., 2006, Vernon et al., 1999), as controlled drug and gene delivery systems, and as new forms of chromatographic matrices for the separation of bioactive compounds (Hoffman, 2013). Despite the above roles and interest that polyNIPAM have in biomedicine, there remain concerns about polymer biocompatibility. This polymer has secondary amide groups (figure 1.5) which may be involved in cooperative hydrogen-bonding interactions with proteins present on the cell. These groups can induce cellular cytotoxicity when switched from hydrophilic to hydrophobic state at its LCST (Vihola et al., 2005).

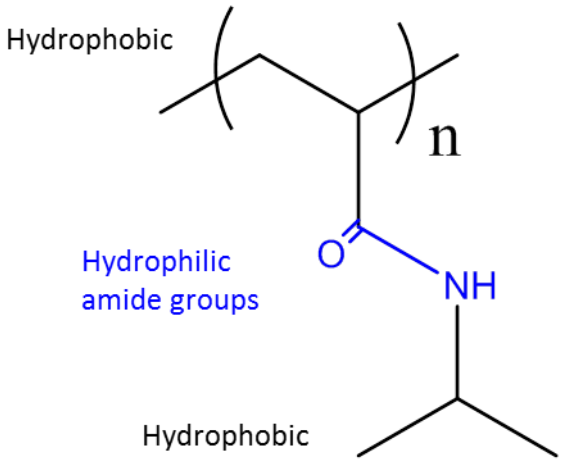


Figure 1.5: Chemical Structure of PNIPAm

Thermoresponsive polyethylene glycol methacrylate (PEGMA) derivatives have been suggested as alternatives to polyNIPAM (Lutz et al., 2006). The side-chain PEGMA polymers are composed of up to 85% in weight of PEG and are therefore water soluble and biocompatible (Ederle et al., 2010). Their LCST in water and their hydrophilicity was found to increase with the length of the polyethylene glycol side chain (figure 1.6). Lutz *et al* showed that the copolymerization of different EGMA macromonomers

with different chain-lengths can result in thermosensitive copolymers with a tuneable LCST (Lutz et al., 2006). For instance, di(ethylene glycol) methacrylate (DEGMA, Mn=188 g/mol) and oligo(ethylene glycol) methacrylate (OEGMA, Mn = 475 g/mol) exhibit LCST values between 26 and 90 °C, which can be precisely adjusted by varying the comonomer composition. For example, copolymers that contain 5, 8, or 10% of OEGMA units per chain exhibit an LCST of 32, 37, or 39 °C in pure water, respectively. These PDEGMA polymers are very promising for biomedical applications since they are principally composed of biocompatible oligo(ethylene glycol) segments which is an uncharged, water-soluble, nontoxic, and nonimmunogenic polymer (Lutz et al., 2006). Recently, PEGMA copolymers have been widely used in tissue engineering (Wischerhoff et al., 2008a, Al Ghanami et al., 2010).

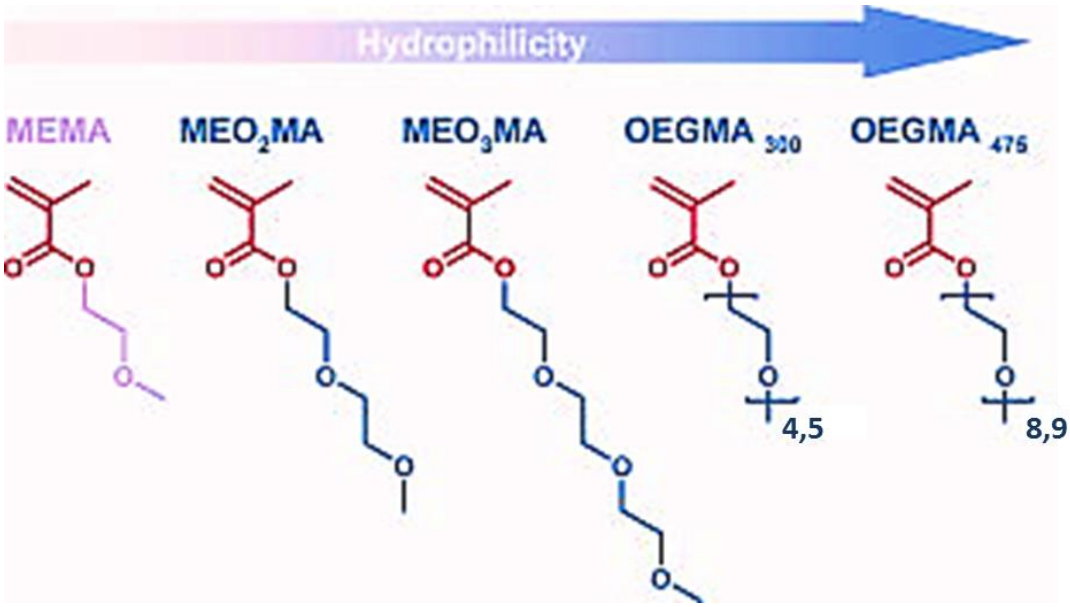


Figure 1.6: Molecular structures of various oligo(ethylene glycol) methacrylates. Hydrophobic and hydrophilic molecular regions are indicated in red and blue, respectively (Lutz, 2008).

Triblock copolymers of poly (ethylene oxide)-poly (propylene oxide)-poly (ethylene oxide) (PEO–PPO–PEO), also known as Pluronic or Poloxamers can form reversible gels. Gelation temperature depends on polymer composition, with Poloxamer 407 (Pluronic F-127) forming gels at 37°C in solutions containing 20wt% or more of polymer (Gutowska et al., 2001). Pluronics have been applied in tissue engineering applications (Alexandridis et al., 1997), in drug and gene delivery systems (Kabanov et al., 2002), for the inhibition of tissue adhesion (Steinleitner et al., 1991, Ahmed et al., 2001), and in burn wound dressings (Schmolka, 1972, Nalbandian et al., 1987), exploiting their thermosensitivity and low cell and protein adhesion (Kim et al., 2011). The main limitation that faces the widespread application of Pluronics in tissue engineering is their limited mechanical integrity and stability, with rapid dilution and dissolution at physiological conditions, just within few hours (He et al., 2008).

Another group of synthetic thermoresponsive polymers are block copolymers of PEG with polyester (Jeong et al., 1999, Jeong et al., 1997). Examples include triblock copolymers of PLGA-PEG-PLGA and PEG-PLGA-PEG which both exhibit thermoreversible gelation properties. The sol-to-gel transition temperature of these triblock copolymers in aqueous solution could be controlled over the temperature range from 15°C to 45°C by changing some parameters such as change the ratio of lactic acid/glycolic acid (LA/ GA) and the length of PLGA or PEG chains (Jeong and Gutowska, 2002). PEG-PLGA-PEG has been used as a dressing and a stem cell scaffold for diabetic wounds, and was found to significantly enhance healing (Lee et al., 2007). Low molecular weight

PLGA-PEG-PLGA (1500–1000–1500) has been commercialised under the trade name ReGel which can be used as a drug delivery depot (Zentner et al., 2001, Elstad and Fowers, 2009). Block copolymers of PEG and other biodegradable aliphatic polyesters (e.g. poly(ε-caprolactone) have also shown thermoreversible (sol–gel) transition in aqueous solutions which supported adipose derived stem cell myogenic differentiation for muscle regeneration (Kim et al., 2010).

Thermoresponsive peptides have also been used in tissue engineering. Engineered elastin-like polypeptides (ELPs) are a class of artificial repetitive polypeptides which are deemed biocompatible, biodegradable, and non-immunogenic (Nettles et al., 2010). ELPs have been extensively investigated as drug delivery systems and for applications as matrices in tissue engineering including cartilage and intervertebral disks, vascular grafts, ocular, and liver as well as cell-sheet engineering (Nettles et al., 2010). However, these polymers have limited mechanical strength when the temperature is elevated.

Suitably substituted poly(organophosphazene)s can show sol-gel transition behaviour in response to a change in temperature. The LCST (25-98 °C) and degradation rate of poly(organophosphazene) can be modulated by altering the ratio of methoxy polyethylene and amino acid ester chains (Lee et al., 1999, Lee et al., 2002). Research has been undertaken to develop poly (organophosphazene)-based thermosensitive hydrogels by modulating the LCST, degradation rate, and biocompatibility (Lee and Song, 2004). This polymer has been used for the controlled delivery of human growth hormone and albumin (Park et al., 2010a, Park et al., 2010b, Kim et al., 2011)

1.5. Particulate suspensions and colloidal gels

Particulate colloidal suspension systems consist of a dispersed phase of particles of size ranges between a few nanometres and a few micrometres, and a continuous liquid phase (Qin and Zaman, 2003, Mewis et al., 1989, Genovese, 2012). For these particulate suspension systems, surface interactions dominate the stability of suspensions through various interaction forces that contribute to the particle interaction potential (Tadros, 1996). Colloidal interactions can be divided into attractive forces and repulsive forces. Attractive forces include van der Waals, hydrophobic, electrostatic attractive, depletion, and bridging, while repulsive forces include hydration, steric, electrostatic repulsive, and structural (Zhou et al., 2001).

1.5.1. Colloidal stabilisation methods

The stability of colloids is controlled by the interparticle interaction in the suspension; these interactions can be either attractive or repulsive. When attractive forces control the interactions, the particles will adhere with each other and finally aggregation occurs, whilst when repulsion forces controls the interactions, the particles remain apart from each other and the suspension remain in a liquid state. Van der Waals attraction forces, which are present between particles of similar properties, are the primary source of attraction between colloidal particles. In a suspension when repulsive forces are sufficiently strong to counteract the van der Waals attractions, particles remained in stabilised state. The magnitude of interparticle force is influenced by the particle radius and the distance between particles (Genovese, 2012). A long range repulsion between the similar particles is necessary to impart stability because strong long-

range attractive forces are always present between these particles. The provided repulsion has to be at least strong enough to counteract the attractive force. As demonstrated in figure 1.7, particle stabilisation can be obtained by providing an electrical double layer (electrostatic stabilization) or by attaching a polymeric stabiliser onto the particles surfaces (steric stabilization) or by addition of free polymer in the suspension (depletion stabilization). Combination of the first two stabilization mechanisms leads to electrosteric stabilization (Liu et al., 2014).

In electrostatic stabilisation, the electrical double layer (EDL) results from arrangement of charges present on the particle surface in electrolyte charged particles. This EDL produces long-range repulsive forces between the neighbour particles. The strength of this repulsion is influenced by the concentration of electrolyte and ionic strength (Genovese, 2012).

Steric stabilisation, through the presence of a polymer brush stabiliser on the surface of particles is an effective and a robust technique to provide colloidal stabilisation (Crowl and Malati, 1966, Smith and Bruce, 1979, Wong et al., 1988, Croucher et al., 1985, Napper, 1977). The stabilised polymers can be attached onto the surface of particles either by physical adsorption or grafting techniques (Das et al., 2002, Guo et al., 1999, Guo and Ballauff, 2001, Guo and Ballauff, 2000). The stabilizing moieties in the polymer has to produce repulsive forces which are able to keep the particles at a distance from each other and balance the van der Waals force (Napper, 1983). Amphiphilic molecules which contain both lyophilic and lyophobic groups are most effective to impart

steric stabilisation and have been extensively used for this purpose (Miano et al., 1992a, Miano et al., 1992b, Ito et al., 1986, Dawkins et al., 1994, Choi and Krieger, 1986, Dawkins et al., 1986). The lyophobic backbone allows the polymer to be strongly adsorbed to the particle, while the lyophilic side chain extends into the dispersion medium (Corner and Gerrard, 1982). Many amphiphilic polymers have been synthesized for use as steric stabilizers and the effects of polymer components on suspension properties have been stidied (Bonaccorsi et al., 1993, Garti et al., 1993, Cardenasvalera et al., 1995, Wesslen and Wesslen, 1989). Chemical grafting produces more effective stabilization compared to physical adsorption due to the lack of possible desorption of stabiliser in grafting under changing environment. Purely steric stabilization of particles can be obtained by chemically bonding amphiphilic polymers to the particle (Fox et al., 1987). However, a limited number of functional polymers and functional particles are available to produce this brush and the grafting process is a complex reaction (Bromley, 1986, Ottewill and Satgurunathan, 1988, Prestidge and Tadros, 1988, Liang et al., 1992). The polymer molecular weight and side chain length have been found to influence the subsequent dispersion stabilization properties.

Steric stabilization is mostly more desirable than electrostatic stabilization because it doesn't require the to control of ion concentration (Fritz et al., 2002). Therefore, both aqueous and nonaqueous dispersion media can be used, the reversibility of flocculation and freeze-thaw stability results and this allows steric stabilizers to be in a more concentrated stable dispersion. In steric stabilization a less thick layer is

needed and a higher particle density is permitted to provide effective stabilization (Araki et al., 2001).

Electrosteric stabilization can be obtained by polyelectrolyte polymer brushes. In this system, both electrostatic stabilisation and steric stabilisation are imparted by the polymer on the particle surfaces. The stabilisation is influenced by the amount of polymer stabiliser, ionic strength, pH, and dielectric properties of the solvent (Ortega-Vinuesa and Bastos-Gonzalez, 2001, Ortega-Vinuesa et al., 1998, Molina-Bolivar and Ortega-Vinuesa, 1999, Fritz et al., 2002).

Depletion stabilization is further imparted by free polymer in the solution. This stabilization can be combined with steric and/or electrostatic stabilization. The combination of depletion and steric stabilization is very common when high concentrations of free polymer are present in the suspension medium (Feigin and Napper, 1980, Kim et al., 2015).

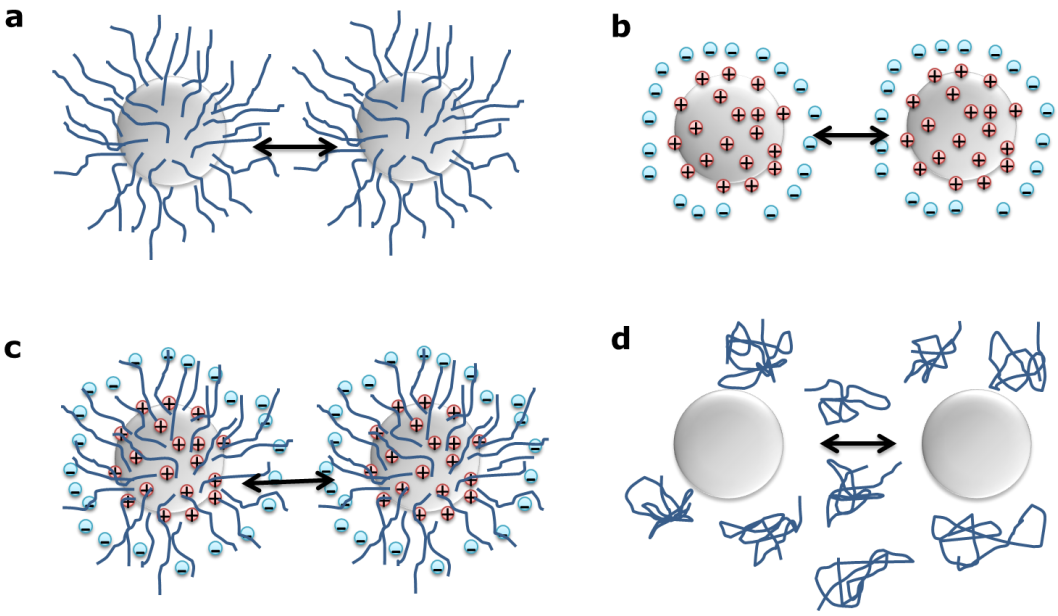


Figure 1.7: colloidal stabilization methods in aqueous solution. (a) steric stabilization, (b) electrostatic stabilization (c) electrosteric stabilization: (d) depletion stabilization.

1.5.2. Colloidal aggregation and gel formation

The ability to control interparticle interactions through the prudent variation of certain solution conditions can lead to innovative biomedical applications (Franks, 2005). Aggregation of suspended particles destabilises the system. If the particle concentration and strength of attraction between the particles are sufficiently high, the aggregating particles can form a percolating space-filling three dimensional network, leading to gelation. The obtained gels constitute a unique class of materials termed colloidal or particle gels (Gibaud et al., 2010).

Generally, particle aggregation can be induced by changes in the particle interaction potential, as a result of changes in characteristics of the stabilising polymer, pH, or ionic strength. In electrostatically stabilised suspensions, neutralisation of the surface charge abolishes the repulsive forces, leading to particle aggregation (Fritz et al., 2002). In sterically stabilised suspensions, the stabilisation fails when the solvent quality for the stabilising moieties deteriorates leading to particle flocculation. This can occur on addition of a non-solvent or by changing the temperature to near the LCST when the polymer becomes insoluble in the solvent; this is referred to as incipient flocculation (Al Ghanami et al., 2010). In both cases, gels are obtained if the particle concentration and strength of interaction are sufficiently high. Gelation tends to be irreversible in electrostatically stabilised systems, while it is reversible in sterically stabilised systems when the continuous phase become a good solvent quality for the stabilising moieties (Franks et al., 2004).

The change in temperature can be used to induce thermoreversible particle aggregation and gel formation if a temperature sensitive polymer is used (Franks, 2005). A stable suspension can be made with an appropriate quantity of a temperature sensitive free polymer in its soluble state (below LCST of polymer). Changing the temperature to that at which the polymer becomes insoluble (above its LCST) makes the polymer adsorb on the particles and aggregate with other polymer molecules, particle aggregation will rapidly follow. If the temperature is altered back to the temperature at which the polymer is soluble, repulsion is re-established. Thermoresponsive dispersions which are enable the formation of gels when heated are attracting increased research attention (Alava and Saunders, 2004, Alava and Saunders, 2006, Saunders et al., 2007, Alava and Saunders, 2005, Liu et al., 2009a, Liu et al., 2008, Liu et al., 2009b, Liu et al., 2009c, Liu et al., 2010, Dickinson, 2000, Durand et al., 2002, Fraylich et al., 2010b, Choi et al., 2006, Vihola et al., 2007b, Elaissari, 2006a). Several kinds of amphiphilic polymers with controlled design have been prepared to provide thermoresponsive triggered gelation to emulsions (Alava and Saunders, 2004, Koh and Saunders, 2005, Alava and Saunders, 2005), latexes (Alava and Saunders, 2005) and inorganic particle dispersions (Uhrich et al., 1999). Particle gels tend to be more brittle and exhibit structure breakdown at lower strains compared to macromolecular gels (Dickinson, 1995). The application of mouldable colloidal gels towards regenerating tissues has been used in tissue engineering (Xie et al., 2006, Dellinger et al., 2007, Lee et al., 2005, Wang et al., 2008, Pek et al., 2008).

1.6. Magnetic bioseparation based on magnetite nanoparticles

Magnetic iron oxide nanoparticles (MIONP) are amongst the most studied magnetic particles for biomedical applications (Kaaki et al., 2012) due to a combination of favourable superparamagnetic properties, biocompatibility, biodegradability, and surface functionality (Stephen et al., 2011, Stanciu et al., 2009, Mascolo et al., 2013). Paramagnetic materials (e.g. magnetite nanoparticles) are more biocompatible compared to ferromagnetic materials (e.g. cobalt and nickel nanoparticles) because ferromagnetic materials are oversensitive to oxidation (Akbarzadeh et al., 2012). Magnetite nanoparticles have a strong magnetic response in the presence of an external field but no magnetic memory in the absence of field (Faraji et al., 2010). The magnetite can be synthesized by several methods, including chemical co-precipitation (Wang et al., 2012a, Mascolo et al., 2013), laser pyrolysis (Wan et al., 2007), and thermal decomposition (Guardia et al., 2011, Robinson et al., 2007).

Recently, the use of magnetic particles in biotechnology and biomedicine applications has dramatically increased for *in vitro* and *in vivo* use. *In vitro*, magnetic nanoparticles have been mainly used in diagnostic and separation/labelling of biomolecules (e.g. such as protein, cell, DNA/RNA, microorganism) while *in vivo* they have been investigated for therapeutic (drug delivery and hyperthermia) and diagnostic applications (magnetic resonance imaging) (Ma and Liu, 2007). 'Combination' nanoparticles have been prepared for both MRI and drug delivery together (Kedziorek and Kraitchman, 2010, Hu et al., 2012, Kievit and Zhang, 2011), and

even for all of these applications (drug delivery, hyperthermia and MRI) combined (Yallapu et al., 2011).

For biomedical applications, MIONP must be coated with biocompatible polymers to prevent aggregation. The most common stabilizing and surface coating materials are PEG (Hao et al., 2010), oleic acid (Hofmann et al., 2010), silica (Prijic et al., 2010), sodium oleate (Kim et al., 2001), folic acid (Kaaki et al., 2012) and chitosan (Gregorio-Jauregui et al., 2012, Osuna et al., 2012). Both core size (initial size of magnetic nanoparticles) and hydrodynamic size (final size of coated magnetic particle) are important for biomedical applications.

Magnetic microspheres have certain advantages over magnetic nanoparticles such as higher magnetophoretic mobility (due to higher magnetic content), higher drug loading capacity, and they can be designed for greater retention time in the body and potential for controlled release (Filipcsei, 2008).

Magnetic separation is a promising technology, successfully used in lab-scale and industrial small-scale applications, particularly for analytics and diagnostics (Kappler et al., 2008). Commercially available magnetic particles that are suited for bioseparation can be obtained from a variety of companies. Mostly, the matrices are based on polystyrene, silica, porous glass, cellulose, and agarose (Berensmeier, 2006).

Magnetic polystyrene (MPS) microspheres are the most used for bioseparation. They have been commercialised in various size ranges, and can be prepared by three major strategies including in situ synthesis, direct mixing, and embedding (Yuan and Williams, 2007, Yu and Yang, 2010). There are some required properties of MPS microspheres for

biomedical application such as stability under working environment (no iron leakage), biocompatibility, superparamagnetic behaviour and high magnetization value, and a narrow size distribution (Hai et al., 2009).

Many published works report the synthesis of micrometre-sized polymer beads containing magnetic particles and the applicability of these beads for bioseparation has been reported (Peng et al., 2004, Stanciu et al., 2009). Magnetic polymer microspheres have been widely used for isolation and purification of proteins, antibodies, nucleic acid and enzymes or for immunomagnetic cell separation (Karumanchi et al., 2002). The immunomagnetic cell separation includs tagging or labelling the desired cells with a magnetic marker and then separating magnetically labelled cells from unlabelled cells (figure 1.8). Separation can be done in a batch or continuous process, depending on the specific application. One challenge in magnetic separation is nonspecific binding of magnetic nano/micro particles to non-targeted cells (Chalmers et al., 2010).

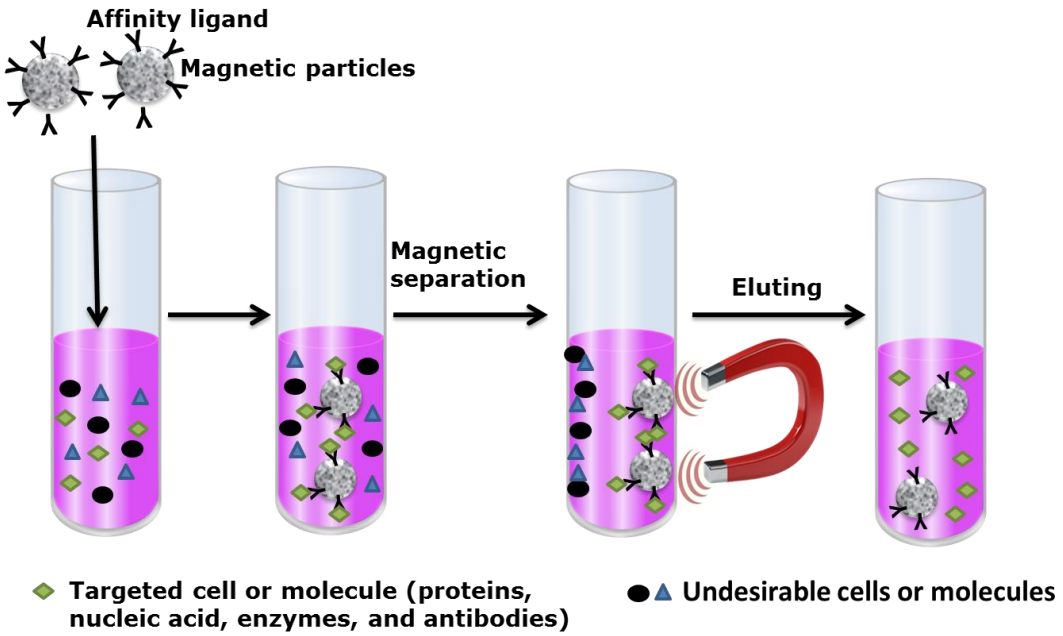


Figure 1.8: Basic principle of direct magnetic separation (positive isolation).

1.7. Thesis aims and objectives

A variety of techniques have been developed to fabricate 3D scaffolds for proliferation of therapeutically important cells *in vitro*. Although each technique has definite advantages, none of the methods to date have been able to solve all the essential challenges linked to cell seeding, passaging, and harvesting. The fundamental requirements of an ideal scaffold for *in vitro* expansion are simplicity of the cell seeding system, mechanical strength and stability to support cell proliferation, and efficient and maximum cell recovery after expansion. Cell harvesting remains the main technical challenge for most 3D cell culture methods. The use of proteolytic enzymes such as trypsin to detach cells from support materials during passaging or after cell expansion may affect the long term quality of cells (Umegaki et al., 2004, Garg et al., 2014, Steinber.Ms et al., 1973, Huang et al., 2010). Accordingly, there is a

necessity for new biomaterials that would be able to support expansion of clinically relevant cell types and allow easy recovery of the cells after proliferation.

The overall aim of the work described in this thesis was to develop a new 3D scaffold suitable to expand therapeutically important cells *in vitro* and to allow efficient and enzyme free cell harvesting. To achieve this aim, the following hypotheses were proposed:

A cell support material was proposed which would have the properties of high cell attachment under one set of conditions and rapid detachment of cells under another set of conditions. The underlying hypothesis for this was that thermoresponsive polymers, which bind water and solubilise reversibly dependent on temperature, could provide a surface which would exhibit varying affinity for a range of cell types. The second hypothesis centred on whether magnetioc nanoparticles could be encapsulated within microparticles which had thermoresponsiove surfaces, such that a dual magnetic/thermal process might be used to control cell attachment and allow separation of particles away from cells. Accordingly, the overall objective was to evaluate if thermo and magnetic responsive colloidal gels could be prepared which would be suitable for growth and support of cells, and also allow efficient and enzyme free cell harvesting once sufficient populations of cells had grown on the supports. More specific aims were that the 'switchable' components of the reversibly associating colloidal microparticles would be generated by attaching thermoresponsive poly(polyethyleneglycolmethacrylate)s to the particle surfaces either by physical adsorption (chapter 3) or chemical

grafting (chapter 4). The subsequent cell work to evaluate the overall success of these procedures is given in subsequent chapters.

We also aimed to assess 'practical' hypotheses, i.e. whether it was possible to make these responsive microparticles in ways that might allow simple translation to a commercial product. Therefore the sub-hypotheses were that the most simple method i.e. physical adsorption of polymers to micripartiles would be rapid and might be adapted to many microparticle surfaces, but might also suffer from the drawback of possible desorption of polymer chains during extended use. The second sub-aim was to test if a chemical grafting method i.e. the formation of covalent bonds between the polymer corona and the microparticle core, could provide robust and well-defined materials without being too complex and time-consuming.

2. General materials and methods

The materials and methods used for the experimental work throughout the thesis are described in this chapter. More detailed experimental procedures are given in the relevant chapters that follow

2.1. Materials

2.1.1. General Chemicals

2,2-Azobisisobutyronitrile (AIBN) was recrystallized from methanol, 1-dodecanethiol, ferric chloride hexahydrate ($FeCl_3.6H_2O$), ferrous chloride tetrahydrate ($FeCl_2.4H_2O$), sodium oleate, and diethylene glycol methyl ether methacrylate (DEGMA, Mw =188) were purchased from Sigma-Aldrich Company Ltd. UK and used as received. Ethanol, chloroform, 2-butanone, hexane and all other solvents were of analytical grade and used as received. Water was purified by distillation followed by deionization using ion exchange resins.

2.1.2. Cell culture reagents

Complete Medium which consisted of Dulbecco's Modified Eagle Medium (DMEM) supplemented with 10% foetal bovine serum (FBS), 1% antibiotic/antimycotic solution (contains 10,000 units/mL of penicillin, 10,000 µg/mL of streptomycin, and 25 µg/mL of amphotericin B), 1% L-glutamine (2 mM) and 1% non-essential amino acids (Sigma-Aldrich, UK), was supplied by Invitrogen, UK. Trypsin, phosphate buffered saline (PBS), and industrial methylated spirits (IMS) were purchased from Fisher Scientific UK.

2.2. Methods

2.2.1. Scanning Electron Microscopy (SEM)

SEM was used to measure the average size, particle size distribution and surface morphology of microparticles. Samples were prepared by spreading a suspension of particles on an aluminium stub coated with carbon tape. The samples were dried and then coated with a thin layer of gold (Blazer SCD030 Sputter coater, Blazer Union Ltd, Liechtenstein) for 180 second. The samples were viewed using a JEOL 6060V scanning electron microscope at 30 kV program (JEOL Ltd., Welwyn Garden City, Hertfordshire, UK). Particle size measurements were performed using associated Smile View program the associated Smile View program (JEOL Ltd., Welwyn Garden City, Hertfordshire, UK). The number average diameter (D_n), standard deviation (SD) and coefficient of variation CV (%) were calculated by measuring at least 100 particles from different areas of three images of the sample Transmission Electron Microscopy (TEM)

The morphologies and sizes of synthesized particles were examined by using transmission electron microscopy (TEM - FEI Tecnai) at an acceleration voltage of 100 kV. Samples were prepared by placing drops of diluted particle suspensions in water on the surface of a copper mesh grid, and then drying the particles in air at room temperature prior to examination.

2.2.2. ATR- FTIR characterization

FTIR spectra of the poly(chloromethyl styrene) PCMS and surface-grafted particles were recorded in the range of 4000-400 cm^{-1} on a BioRad FTS

6000 FTIR Spectrometer, equipped with an attenuated total reflectance (ATR) accessory providing an analysis of the sample surface. Particle powders were loaded directly onto the ATR surface for analysis: DTGS optics at 5 kHz and 4 cm^{-1} resolution were used.

2.2.3. Rheometry characterizations

The rheological measurements were performed using an Anton Paar Physica Rheometer, equipped with parallel plate geometry (25 mm diameter) and the gap distance between two plates was set as 0.5 mm. Rheoplus Software (Version: 3.6x) was used for analysing data.

2.2.3.i. Strain sweep

Strain sweep tests were performed by using a fresh aliquot of sample. The sample was left in between the plates for 5 min at 37°C before running the strain sweep test. Strain sweeps were carried out between 0.01% and 100% strain at an angular frequency of 1 rad s^{-1} and at a temperature of 37°C.

2.2.3.ii. Temperature sweep

Temperature ramp experiments were recorded at 0.05% strain at a frequency of 1 rad s^{-1} with a heating rate of 1°C/min from 10°C to 40°C. Before running the experiment, the lower plate and the upper parallel plate 25 mm (PP25) were left in contact for 5 min at 10°C. Afterwards, 300 µl of sample was applied on the lower plate. The sample was equilibrated at the desired temperature (10°C) for 4 min before starting the run. The tests were all performed using fresh aliquots of sample.

2.2.3.iii. Frequency sweep

Frequency Sweeps were performed at 37°C between 0.1 and 100 rad s^{-1} at a strain value of 0.05%. Before running the experiment, the PP25 and the lower plate were left in contact at 37°C for 5 min. Then, 300 µl of sample was applied on the lower plate. The sample was equilibrated at the 37°C for 5 min before starting the run.

2.2.4. Water contact angle (WCA)

Discs were prepared from particles (PS, PCMS, and PDEGMA-PCMS) by compressing the particles under pressure (10 kbar) for 3 minutes, following the same common protocol as KBr pellet making procedure for FT-IR characterizations. The static water contact angle of the particles discs was measured by using CAM 200 Optical Contact Angle Meter (KSV instruments LTD, Finland). A drop (~5 µl) of water was gently placed on to the surface of discs using a micro-syringe. Three repeated measuements were made for each sample.

2.2.5. Thermogravimetric analyses (TGA)

TGA analyses were carried out with a TGA Q5000 Thermogravimetric Analyzer (TA instruments, USA). All analyses were performed with a 5 mg sample in aluminium pans under a dynamic nitrogen atmosphere between 20 and 900 °C. The experiments were run at a scanning rate of 20 K/min.

2.2.6. ^{1}H NMR spectroscopy

A Bruker 400 spectrometer at 399.8 MHz (^{1}H) was used to record ^{1}H NMR spectra in $CDCl_3$. The chemical shifts were reported in ppm relative to tetramethylsilane (TMS).

2.2.7. Gel permeation chromatography (GPC)

Gel permeation chromatography using an instrument (PL-50 Polymer Labs, UK) fitted with a refractive index (RI) detector was used to determine the weight average molecular weight (M_w), number average molecular weight (M_n), and polydispersity (Đ) of the synthesized PDEGMA. The columns (30 cm PLgel Mixed-C, two in series) were eluted with chloroform and calibrated with polystyrene standards (Polymer Labs, UK). The sample was dissolved in chloroform for chromatography and was filtered (0.2 μm filter) before injection. The calibration and analyses were performed at 40°C and at a flow rate of 1mL/min.

2.2.8. General procedure for synthesis of magnetite nanoparticles

Magnetite (Fe_3O_4) nanoparticles were obtained by a chemical co-precipitation method as described elsewhere (Maity and Agrawal, 2007, Mascolo et al., 2013) with some modifications. $FeCl_3 \cdot 6H_2O$ (3.65 g, 13.5 mmol) and $FeCl_2 \cdot 4H_2O$ (1.34 g, 6.75 mmol) were dissolved in water (10 mL) which had been deoxygenated by bubbling with nitrogen gas. The temperature of the solution was elevated to 80 °C and heating continued for 0.5 h. To this solution, 12.5 mL of 25% ammonia solution was added at 80 °C with continuous stirring. After 30 min sodium oleate (1.5 g, 5 mmol) was added to stabilise the resultant magnetite nanoparticles. The solution was cooled to room temp and the precipitate was isolated by magnetic separation (decantation) and washed several times with distilled water. The sizes and morphologies of the obtained nanoparticles were determined by transmission electron microscopy.

2.2.9. Synthesis of linear thermoresponsive 'control' polymer

Poly(diethyleneglycolmethacrylate) (PDEGMA) was prepared by conventional free radical polymerisation in accordance with previous protocols (Saeed et al., 2015). Diethyleneglycolmethacrylate (11 g, 59 mmol) was weighed into a round bottom flask and 1-dodecanethiol (0.08 g, 0.4 mmol) and 20 mL of 2-butanone were added. AIBN (0.07 g, 0.4 mmol) was added and the mixture was degassed with nitrogen for 25 minutes. The solution temperature was elevated to 70 °C and polymerization was performed at that temperature for 1 h. The reaction was then stopped by cooling the reaction vessel to 0 °C and opening the contents to air. The polymer was precipitated and excess monomers were removed by cycles of precipitation of polymer from 2-butanone into hexane (polymer solution to hexane 1:10). Polymer properties (M_w, M_n), and polydispersity (Đ) were determined by GPC compared to polystyrene standards: M_w = 50.3 kDa,, M_n= 28 kDa, Đ = 1.8. NMR data matched those of prior preparations of this material (Saeed et al., 2015).

^{1}H NMR ($CDCl_3$) δ: 0.7-1.2 ppm (-CH3 of methacrylate), 1.65-2.1 ppm (-CH2- of methacrylate), 3.4 ppm (-OCH3), 3.5-3.8 ppm (-OCH2-CH2-), 4.2 ppm (-CH2 protons of the PEG next to the -OC=O group).

3. Synthesis and characterisation of thermoresponsive magnetic PS/ PDEGMA colloidal suspensions/ gels via physical adsorption of polymer stabiliser onto microspheres

3.1. Introduction

Concentrated particulate dispersions or suspensions have been widely used in applications ranging from ceramics, paints, printing inks and cosmetics through to pharmaceutical formulations (Tadros, 2011). These dispersions or suspensions can be considered as biphasic systems where the particles or droplets are dispersed in a continuous fluid. In particulate suspensions the nature of interparticle interactions determines the microstructure of the system and its rheological properties. According to interparticle interactions, particulate suspensions can be classified into hard-spheres, stabilized particles, or aggregates. Hard sphere microstructures result when inert, rigid spherical particles are suspended at low shear rate, and no interparticle forces are present in this system except infinite particle-particle repulsion at contact. Stabilized colloidal suspensions occur when long range repulsions between particles are able to keep particles separated from each other (Genovese, 2012). The mean sizes of particles in stabilized colloidal systems range usually from the nanometre scale to several micrometres (Qin and Zaman, 2003). Flocculated or aggregated suspensions result when attractive forces between particles are dominant, causing the formation of fractal clusters (Genovese, 2012). These clusters are not interconnected at low particle concentrations and the suspension remains in the fluid or in a weakly

elastic state with no yield stress (Channell and Zukoski, 1997). However, at high particle concentrations in suspension (i.e. above the gelation concentration) these clusters are further interconnected into a network and form a space filling particulate gel (Quemada and Berli, 2002). Dependent on the strength of the attractive forces between particles in the suspension, this may lead to the formation of reversible weak gels (flocculation) or irreversible strong gels (coagulation), respectively (Genovese, 2012, Dickinson, 2000, Fritz et al., 2002, Rueb and Zukoski, 1998, Rueb and Zukoski, 1992, Zaccarelli, 2007).

The magnitude of interparticle forces and the dynamic rheology properties are in proportional change with the volume fraction of particles and size of the particles (Tadros, 2011). For particles in the size range from submicrons up to 10 μm, the combination of hydrodynamic forces and interparticle forces determine the flow behaviour of a suspension made from these particles (Qin and Zaman, 2003, Russel, 1980). In particulate suspensions the overall viscosity of suspensions is influenced by the properties of the fluid and the particles too. The suspension viscosity and overall interparticle governing forces are also proportional to the viscosity of the continuous (liquid) phase; for example, for very viscous liquids the interparticle interaction forces might be negligibly small compared to the solution phase viscous forces (Genovese, 2012). Moreover, external driving forces such as shear are able to play a role in determining the structural and rheological properties of the suspension/gel (Brady and Vicic, 1995).

Particle aggregation is particularly interesting from a materials point of view as it can lead to gelation in concentrated suspensions. The

properties of concentrated suspensions and their tendency to form aggregates or remain stabilized can be controlled by variation of the interparticle interactions (Tadros, 1996). The most effective way to overcome the flocculation resulting from van der Waals attraction is by steric stabilization. For example by forming a brush-like amphiphilic block copolymer on the particles' surfaces either through physical adsorption or chemical grafting (Zhou et al., 2001). In sterically stabilized dispersions, flocculation can still occur when the stabilizing chains become poorly solvated. Suspension aggregation in sterically stabilised systems can thus be induced by decreasing the solvency of the dispersion medium for the stabilising moieties, a phenomenon referred to as incipient flocculation (Tadros, 1996). One way of achieving this in aqueous systems is by altering the temperature and / or pressure to reduce the solvent power of water to the stabilising moieties. Spontaneous re-dispersion occurs on making the dispersion medium a better solvent for the stabilising chains (Napper, 1970). Based on the above, aqueous suspensions can be prepared where a thermoresponsive polymer is used to address the issue of stability by acting as a steric stabilizer, while at the same time offering a way to control the properties of the suspension by acting as a temperature-induced flocculent. This can accordingly yield suspensions that can be reversibly transformed into particle gels with a temperature stimulus.

Polymer brushes are assemblies of polymer chains which are attached by one end to a surface (Boyes et al., 2004). Polymer brushes which have LCST properties and thus exhibit different solubility properties above and below this temperature are promising for a number of applications and

have been extensively investigated as chemical switches and gates (Zhao and Brittain, 2000). In a good solvent, these types of polymer chains extend to maximize contact with solvent molecules. However, in poor solvent conditions these chains collapse to avoid contact with solvent (Zhao and Brittain, 2000). The history of using polymer brushes as steric stabilisers of particles can be traced back to the 1950s, when polymers were first reported as an effective way to prevent particle flocculation (Mackor, 1951, Mackor and Vanderwaals, 1952, Clayfiel.Ej and Lumb, 1966). Attachment of polymer chains on colloidal particle surfaces in the presence of a good solvent produces repulsion forces between particles, which resist overlap and consequently invoke colloidal stabilization (Zhao and Brittain, 2000).

3.2. Aims and Objectives

The aim of the work described in this chapter was the synthesis of thermo and magnetic responsive colloidal gels via physical adsorption of thermoresponsive polymer onto the surface of magnetic microsphere. To achieve this aim, the following hypotheses were proposed:

Monodisperse polystyrene microspheres with the size range between 1-5 μm can be prepared via dispersion polymerisation.

These microspheres can be magnetized by loading magnetite nanoparticles via swelling/deswelling techynique.

If successeful, thermoreversible magnertic colloidal suspensions/gels can be prepared via mixing different percentages of magnetic polystyrene particles (MPS) with different concentrations of PDEGMA (Pre-

synthesised by conventional free radical polymerization) in cell culture medium (DMEM).

3.3. Materials and Methods

Styrene and divinylbenzene (DVB) were washed three times with sodium hydroxide (5% w/w) to remove inhibitors then washed with distilled water until the washings were neutral and stored in a refrigerator until use. 2,2-Azobisisobutyronitrile (AIBN) and polyvinylpyrrolidone (PVP K-30, Mw=40 000) were used as initiator and stabilizer, respectively. Ferric chloride hexahydrate ($FeCl_3.6H_2O$), ferrous chloride tetrahydrate ($FeCl_2.4H_2O$), sodium oleate, and the macromeres, di(ethylene glycol) methyl ether methacrylate (DEGMA, Mw =188) were purchased from Sigma-Aldrich. Hexane, ethanol, chloroform, and all other solvents were of analytical grade and used as received. Water was of HPLC grade.

3.3.1. Synthesis of polystyrene microspheres

Polystyrene microspheres were synthesized by dispersion polymerization in a sealed round-bottom flask. The flask was equipped with a magnetic stirrer and a reflux condenser. Next, ethanol (160 g), water (18 g) , and polyvinylpyrrolidone (PVP) (3 g) were added and stirred until the polymer completely dissolved. Then, styrene (10 g ,96 mmoles) and DVB (0.5 g, 3.9 mmoles) were added onto the above solution. The final mixture was degassed with nitrogen for 30 minutes and the temperature was increased to 74ºC. At this temperature AIBN (0.4 g, 2.4 mmoles) was addedandthe polymerization allowed to continue for 24 hours at 120 rpm. The obtained polystyrene microspheres were separated by

centrifugation (3000x g for 10 minutes) and repeatedly washed by re-suspension and centrifugation steps with distilled water. The resulting microspheres were dried in a freeze dryer. The percentage of yield were calculated by dividing the weight of polymer were obtained after freeze drying on the total weight of monomers were used.

3.3.2. Preparation of magnetic PS microspheres

Magnetic polymer microspheres were prepared by a swelling and solvent evaporation process. Polymer microspheres (1.0 g) were swollen by immersion in chloroform, and then dispersed magnetic nanoparticles (150 mg) in chloroform were added to the above suspension. The used magnetite nanoparticles had been prepared previously by chemical co-precipitations, details described in chapter 2 and section 2.2.6. The final mixture was shaken for 24 hours to allow the magnetite nanoparticles to enter the swollen polymer microspheres. After this time, the temperature of the solution was increased and the chloroform was evaporated slowly under reduced pressure, enabling the magnetite nanoparticles to be retained inside the microspheres. The resulting magnetite-impregnated microspheres were precipitated by addition of petroleum ether and separated by centrifugation (2000x g for 5 minutes). The final microparticles were washed with ethanol then with distilled water before being lyophilised.

3.3.3. Preparation of thermoresponsive suspensions

All suspensions studied were obtained by mixing different concentrations (% w/v) of PS microspheres (10%, 15%, 20%, 25% and 30%) with PDEGMA polymer (1%, 2%, 3% and 4%) dissolved in cell culture

medium (DMEM) or in distilled water. The suspensions were subjected to frequent vortex mixing for 1 minute each time and cooling to 0 °C in an ice bath.

3.3.4. Electronic Microscopy characterizations

Scanning electron microscopy (SEM) and transmission electron microscopy (TEM) characterizations were performed. The details of SEM and TEM procedures have been described in chapter two sections 2.2.1 and 2.2.2, respectively. Microparticle size measurements were made from three repeatable batches and these measurements were performed three times for each batch.

3.3.5. ^{1}H NMR spectroscopy

A Bruker 400 spectrometer at 399.8 MHz (^{1}H) was used to record ^{1}H NMR spectra in $CDCl_3$. The chemical shifts were reported in ppm relative to tetramethylsilane (TMS).

3.3.6. ATR- FTIR characterization

The details of ATR-FTIR characterization procedure has been provided in chapter two, section 2.2.3.

3.3.7. SQUID Magnetometer

The magnetic properties of the magnetic polymer microspheres were tested by using a Superconducting Quantum Interference Device (SQUID) magnetometer (Quantum design, mpms xl) at a temperature range from 5 to 320 K under different applied magnetic fields.

3.3.8. Gel permeation chromatography (GPC)

Gel permeation chromatography using an instrument (PL-50 Polymer Labs, UK) fitted with a refractive index (RI) detector was used to determine the weight average molecular weight (M_w), number average molecular weight (M_n), and polydispersity (Đ) of the synthesized PDEGMA. The columns (30 cm PLgel Mixed-C, two in series) were eluted with chloroform and calibrated with polystyrene standards (Polymer Labs, UK). The sample was dissolved in chloroform for chromatography and was filtered (0.2 μm filter) before injection. The calibration and analyses were performed at 40°C and at a flow rate of 1mL/min.

3.3.9. Measurement of cloud point temperatures of thermoresponsive polymers

A Beckman Coulter DU 800 UV-vis spectrophotometer with a thermostat was used for measuring the cloud point temperature of dilute solution of PDEGMA over a temperature range of 10–40 °C. The temperature was controlled and measured using a Peltier plate heating system (Beckman) and was increased at a rate of 1 °C min^{-1}. Absorbances of the samples were measured at a wavelength of 550 nm.

3.3.10. Tube Inversion test

Typically 1 mL of aqueous PDEGMA/PS suspension was added to a 5 mL glass vial. The sample was adjusted to the desired temperature (37 °C) for 2 minutes in a thermostat water bath. The mobility of the dispersions was assessed by inverting the vial. If the suspension had not flowed after 10 seconds it was considered to be gelled.

3.3.11. Rheometry characterization

The details of rheometry characterization procedures have been provided in chapter 2, section 2.2.4.

3.4. Results and discussion

Magnetothermally responsive PS/PDEGMA suspensions/gels were prepared through physical adsorption of PDEGMA on PS microspheres. These microspheres were chosen as a core substrate because polystyrene surfaces have been widely used for *in vitro* cell culture applications and are accepted by the FDA for certain biomedical applications. The thermoresponsive component, PDEGMA, was chosen as it is well-tolerated by cells, displays a lower critical solution temperature (LCST ~ 26 °C) just above ambient temperature but below human body temperature (Lutz et al., 2006, Lutz, 2008) and exhibits resistance to absorption of proteins (Hu et al., 2010) which would support weak, reversible cell attachment (Zhu et al., 2001). Moreover, this protein resistance property is importance for various surface-engineering applications including biomaterials, drug delivery, or biosensors (Heuberger et al., 2005). The thermoresponsive polymer was adsorbed on PS microspheres to generate thermo-switchable particle surfaces and subsequently produce thermoresponsive colloidal gels (figure 3.1).

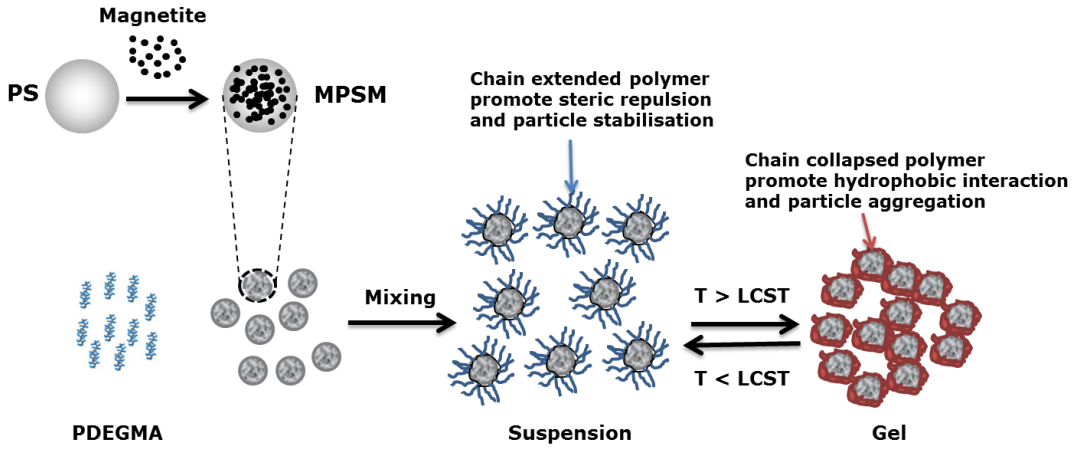


Figure 3.1: Schematic to show formation of reversibly gelling magnetic microspheres through physical adsorption of thermoresponsive polymer.

3.4.1. Synthesis and characterisations of polystyrene microspheres

Polystyrene microspheres were synthesised by dispersion polymerisation of styrene and divinylbenzene in ethanol/water. This method has been previously shown to be an effective route for producing micron-size monodisperse microspheres (Paine et al., 1990, Cho et al., 2016, Ha et al., 2010). The targeted particle size was from 1.5 to 3.5 μm to prevent potential internalisation of the particles when used with mammalian cells (Jiang et al., 2011, Rejman et al., 2004), while still keeping the microparticles in the colloidal range (Qin and Zaman, 2003).

Dispersion polymerization is a sensitive heterogeneous polymerization to the reaction conditions, such as the existence of oxygen during reaction or changing the ratios of the ingredients . Especially, a slight change in the concentration of an ingredient led to an obvious change in the particle size and properties. The effects of the concentration of monomer, stabiliser and cross-linker on the particle size and characteristics are summarized in table 3.1.

First, the concentration of DVB (crosslinker) were varied to obtain microspheres with suitable swelling properties, in chloroform. It can be seen that particles prepared without DVB or with high DVB content (> 5 g) couldn't be used for the next step application which is magnetic loading. The non-crosslinked particles were dissolved in chloroform instead of swelling but highly crosslinked particles were unable to swell at all.

Next,the concentration of PVP is reduced from 4 g to 3 g with stabilising the concentration of monomers. Consequently, the number average diameter of PS microspheres is increased from 1.3 to 1.5 μm. Higher stabilizer concentrations produced smaller PS particles. Because polymerization was initiated in the stabilizer micelles, more stabilizer allowed the formation of more micelles and thus, more particles. Subsequently, the monomer was distributed between more particles and thus, smaller latex particles were obtained. Considering that dispersion polymerization is sensitive to the reaction conditions, and monodisperse micron-sized polymer particles are usually obtained in a small window of the stabilizer concentration.

Finally, the concentration of styrene was increased from 5 g to 25 g with stabilising the concentration of PVP and DVB. Consequently, the number average diameter of PS microspheres is dramatically increased from 1.5 to 4.7 μm. Increasing monomer concentration produced larger particles. This was due to the fact that more monomer was available for polymerization and the critical chain length was greatly affected by the presence of Styrene monomer in the dispersion mixture. Styrene is a good solvent for PS. High concentrations of Styrene allowed the PS

chains to precipitate at higher chain lengths and induced the precipitation of fewer nuclei, thus forming larger particles.

Table 3.1: Experimental conditions and results for dispersion polymerisation of Styrene and DVB to produce PS microspheres. Different ratios of stabiliser : monomer composition were used.

Run no.	PVP K-30 (g)	Styrene (g)	DVB (g)	Yield (%)	Average diameter D_n (µm)	CV%	Swelling in $CHCl_3$
1	4	5	0	61	1.3±0.01	< 5	Dissolved
2	4	5	10	58	3.1±0.03	< 11	Not swell
3	4	5	5	60	2.7±0.02	< 9	Not swell
4	4	5	0.5	65	1.3±0.01	< 5	Swell
5	3	5	0.5	65	1.5±0.01	< 6	Swell
6	3	10	0.5	63	2.5±0.02	< 6	Swell
7	3	15	0.5	63	3.3±0.03	< 8	Swell
8	3	25	0.5	57	4.7±0.06	< 9	Swell

The particle size, size distribution and morphology of produced polystyrene microspheres were investigated using SEM (figure 3.2). It can be seen from SEM images, the shape and surface morphologies of produced microparticles were changed from smooth spherical shapes (figure 3.2 a) to 'chickpea' like (figure 3.2 b) then to 'cauliflower'-like (figure 3.2 c) shapes as the size of microparticles increased. However, irrespective of the morphologies, all these size ranges of microspheres were suitable for making responsive particulate suspension/gels. From this point onwards, PS microsphres which have average diameter 2.5 µm were used for all other characterisations and making magnetic

polystsyrene microspheres. This size was selected because microspheres still have spherical shapes, can be stabilised without too much efforts (as bigger particles needed), and reduced the risk of cells uptake by smaller particles.

ATR-FTIR (figure 3.3 b) and TGA analysis (figure 3.3 c) confirmed the structural composition and the purity of resultant particles. Water contact angle (WCA) measurements were performed to confirm that the hydrophobicity of the polystyrene particle surfaces was suitable to promote adsorption of the amphiphilic thermoresponsive PDEGMA. The results showed (figure 3.3 d) that the prepared polystyrene microparticles had a WCA value of 120° ± 3.

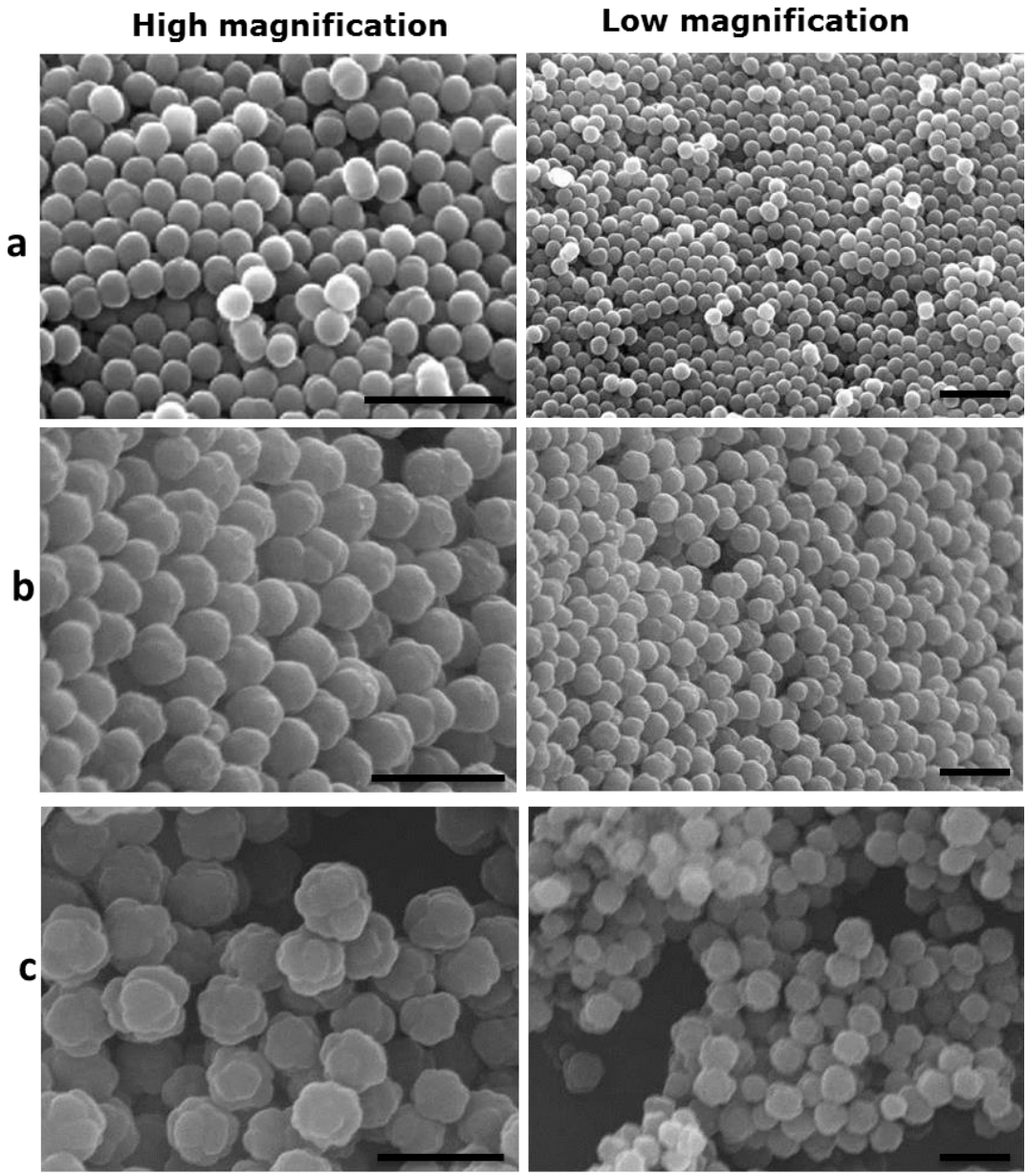


Figure 3.2: Scanning electron micrographs at low and high magnification of PS microspheres that shows (a) smooth spherical shapes (1.5 µm) and then particle morphology changes to (b) 'chickpea'-like at 2.5 µm and (c) 'cauliflower'-like at 3.3 µm. Scale bars 5 µm.

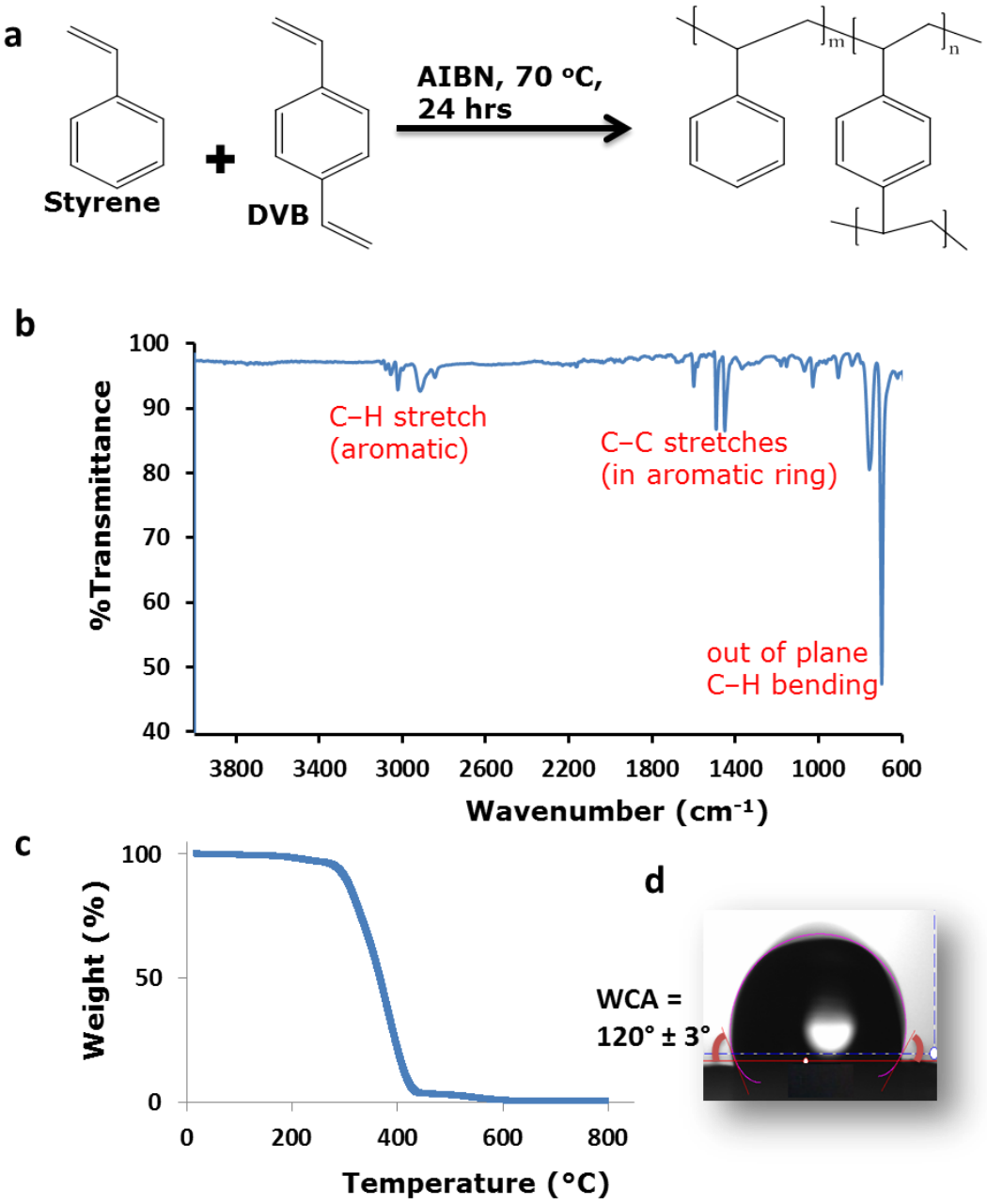


Figure 3.3: (a) reaction of styrene and divinylbenzene to produce lightly crosslinked polystyrene microspheres. (b) ATR-FTIR spectrum of PS microspheres. (c) TGA thermogram of polystyrene microspheres shows one step weight loss, thus confirming the purity of the particles. (d) WCA of PS particle film indicating hydrophobic surface.

3.4.2. Synthesis and characterization of magnetite nanoparticles

Magnetite (Fe_3O_4) nanoparticles were obtained by a chemical co-precipitation method as described elsewhere (Maity and Agrawal, 2007, Mascolo et al., 2013) with some modifications. Ferrous and ferric chloride were reacted in an alkaline medium under nitrogen purging. In order to avoid particle agglomeration, the magnetite particles were prepared in the presence of sodium oleate, which forms a stabilizing hydrophobic shell around the iron oxide nanoparticles. The prepared magnetite nanoparticles were of a black or dark brown colour, indicating the successful preparation of stable magnetite.

The size, size distribution and morphologies of prepared magnetite nanoparticles were determined by transmission electron microscopy. Figure 3.4 a shows TEM images of the prepared particles, confirming that the produced particles were of regular shape and acceptable particle size distribution, with an average particle size of ~10 nm. Previous research showed that particles in this size range exhibited superparamagnetic properties (Namanga et al., 2013, Wahajuddin and Arora, 2012). Furthermore, when external magnetic fields were applied to suspension of these particles (figure 3.4 b), they were strongly attracted by the magnetic field, but also easily re-dispersed by gentle shaking after removal of the applied field. ATR-FTIR (figure 3.5 a) and TGA analysis (figure 3.5 b) confirmed the presence of the stabilising oleate surface of the magnetite nanoparticles. ATR-FTIR showed absorption bands corresponding to the long chain alkyl carboxylate which covered the particles. TGA thermogram showed 50% weight loss from the particles

upon heating from 20-800 °C, corresponding to the decomposition of the oleate stabiliser that surrounded the magnetite nanoparticles.

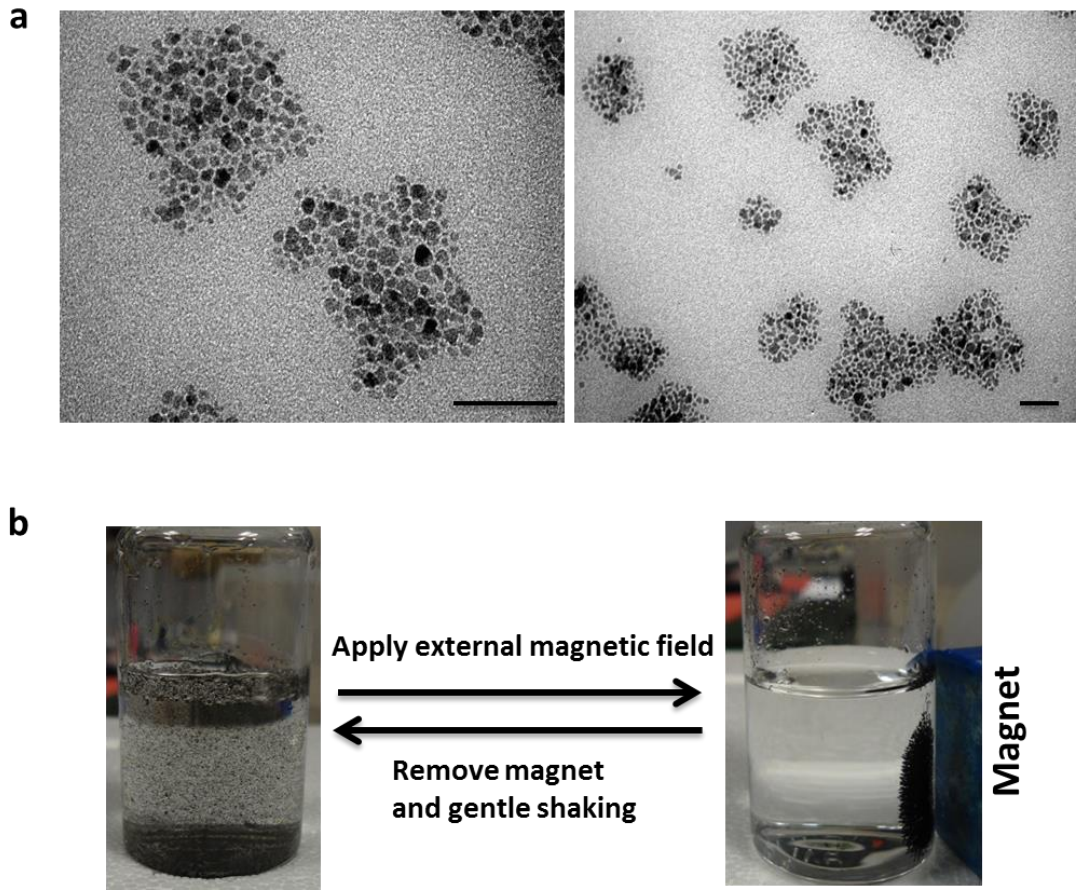


Figure 3.4: (a) TEM images of magnetite nanoparticles prepared by a modified chemical co-precipitation method, showing individual particles with average diameters of ~10 nm, scale bar 100 nm. (b) Photographic images of suspended magnetite nanoparticles, in the absence and presence of magnet. The strong magnetic response can be seen by the solution becoming clear upon application of the magnetic field, while upon removal of the field the particles were easily redispersed by gently shaking the vial.

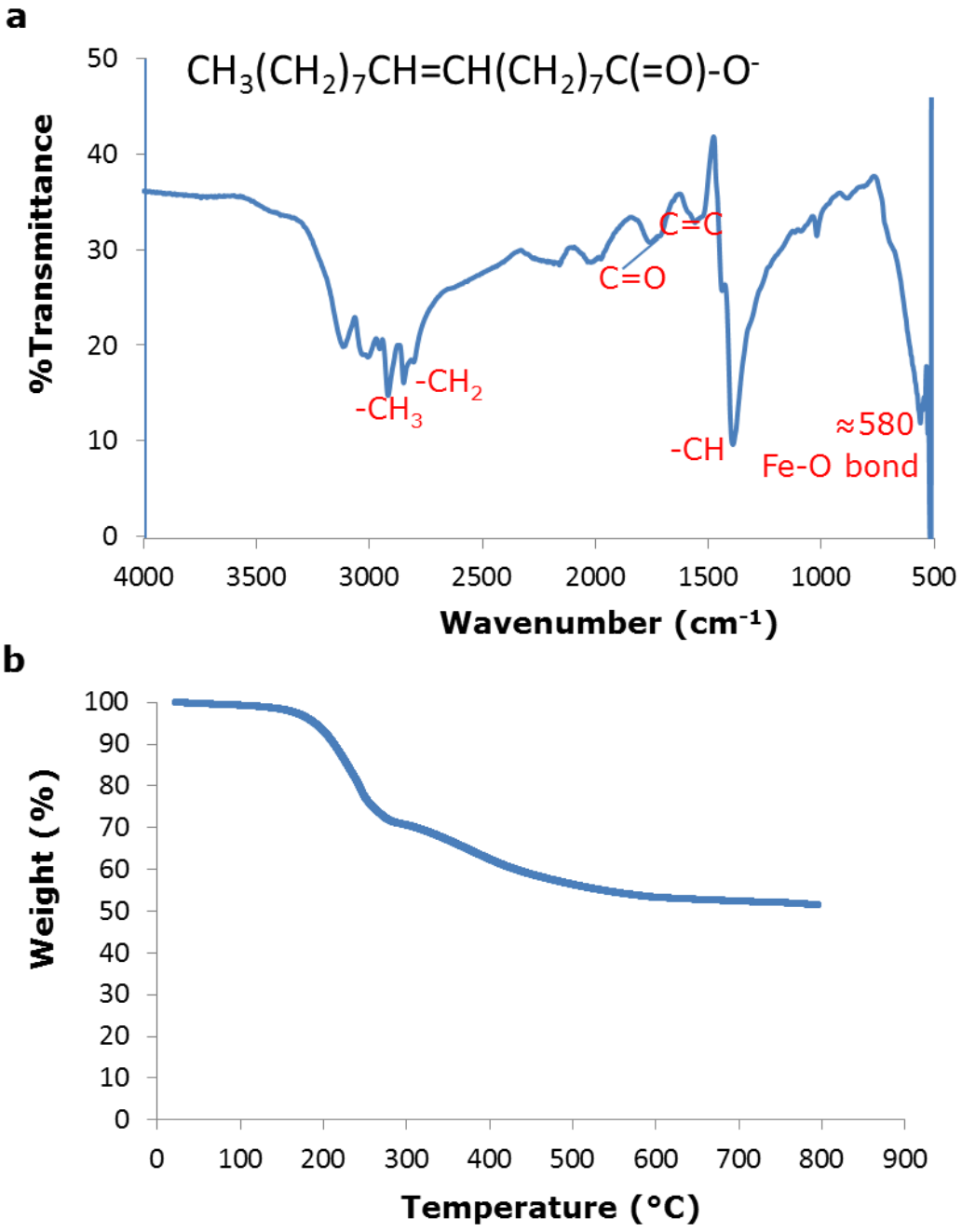


Figure 3.5: (a) ATR-FTIR spectrum of sodium oleate stabilised magnetite nanoparticles, showing peaks for aliphatic hydrocarbon corresponding to the oleate, confirming particle surface coverage by stabiliser. (b) TGA thermogram of stabilised magnetite nanoparticles, shows 50% weigh loss during heating from 20-800 °C, corresponding to the decomposition of oleate stabiliser that covered magnetite nanoparticles.

3.4.3. Loading magnetite nanoparticles to the microspheres

Magnetic polystyrene (MPS) microspheres were prepared by a swelling/de-swelling technique, through embedding magnetite nanoparticles into the lightly-cross-linked polystyrene microparticles (2.5 μm) suspended in chloroform (figure 3.6a). Magnetic polystyrene microspheres with 15% of magnetite content were prepared. TGA analysis (figure 3.6 b) of magnetic polystyrene microparticles showed that about 15% of the orgional weight remained at > 400 °C, this was attributed to the Fe_3O_4 content.Also, the SEM images (figure 3.6 c) of synthesised MPS microspheres shows no obvious change in particle size after magnetic loading (average diameter 2.5 μm) due to the high density and the small volume occupied by magnetite nanoparticles compared to PS microspheres.

The magnetic responsive properties were observed by applying an external magnetic field at room temperature (Figure 3.7 b). Typically magnetite-loaded microspheres showed strong magnetic responsive behaviour and most of the particles could be separated from the aqueous suspension under an externally applied magnetic field within 2 minutes, but were then easily redispersed by gentle shaking after removed of the external magnet.

SQUID magnetometry was used to confirm the paramagnetic properties of the prepared magnetic polystyrene particles. Figure 3.7 a a shows the temperature dependence of magnetization for the microspheres. Zero field cooling (ZFC) magnetization measurements showed the typical superparamagnetic behaviour of magnetite-based systems. The blocking temperature (TB), which is the critical temperature that magnetic

systems transfer from paramagnetic to ferromagnetic behaviour, can be seen in the magnetization curve as the ZFC trace exhibits a cusp. At room temperature, the microspheres displayed superparamagnetic behaviour, whereas with decreasing temperature they turned to the ferromagnetic state at the TB (around 170 K).

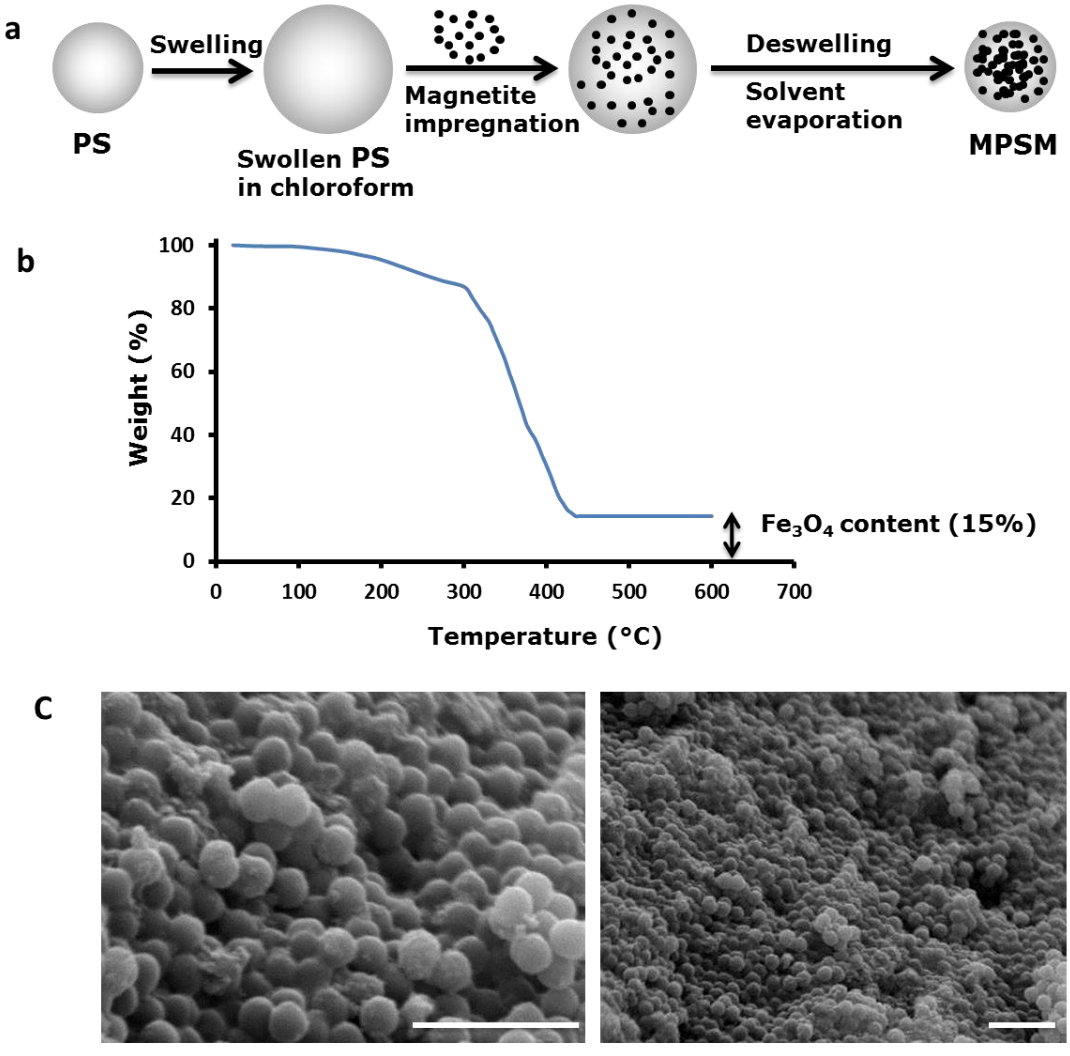


Figure 3.6: (a) Schematic of the preparation of magnetic polystyrene microspheres through loading magnetite into PS microspheres. (b) TGA thermogram of magnetic polystyrene microparticles showed that about 15% of the orgional weight remained at > 400 °C. (c) SEM images of magnetic polystyrene microspheres at low and high magnifications. Scale bars are 10 µm .

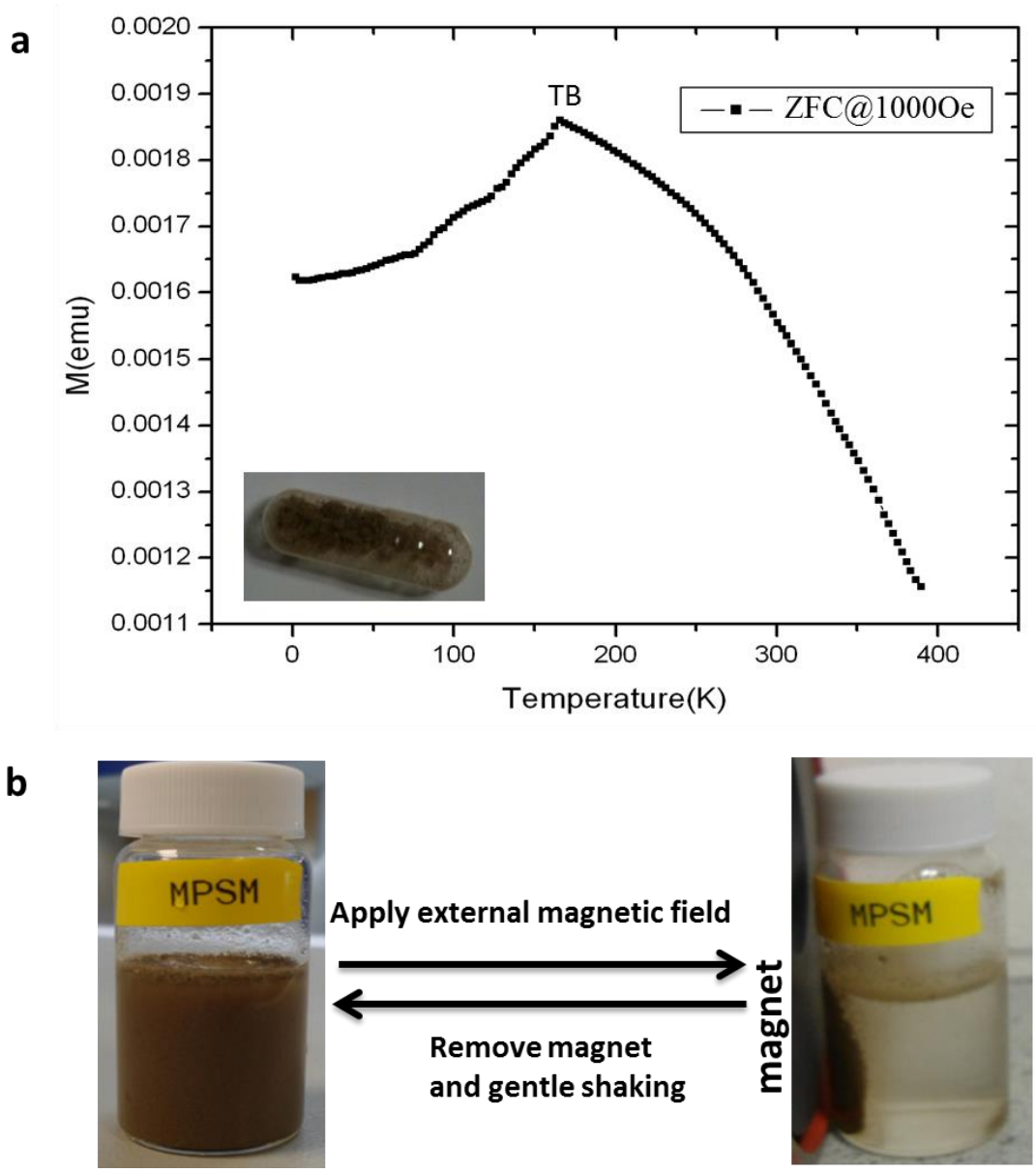


Figure 3.7: (a) Temperature dependence of the magnetization for magnetic polystyrene microspheres; zero field cooling shows a blocking temperature typical of paramagnetic behaviour. (b) Photographs of an aqueous dispersion of magnetic polystyrene microspheres in the absence and presence of magnet. It was observed that the particles were strongly attracted by external magnetic field and easily re-dispersed by removing this magnetic field and gentle shaking.

3.4.4. Synthesis and characterization of PDEGMA linear polymer

PDEGMA thermoresponsive polymers were synthesised by the conventional free radical polymerisation method using a thiol as a chain transfer agent to control molar mass (figure 3.8). Thiols have been effectively used for this purpose due to the weak S–H bond and the high reactivity of the thiyl radicals (Henriquez et al., 2003). 1-Dodecanethiol (DDT) was chosen to further enhance the overall amphiphilicity of the polymer and boost the hydrophobic adsorption onto the particles. The synthesized polymer was purified three times by solvent/ anti solvent techniques. The purity of the produced polymer and complete removal of monomer was confirmed by ^{1}H NMR spectra (figure 3.9); note the absence of peaks corresponding to the double bonds of monomer in the range between 5.5 - 6.5 ppm.

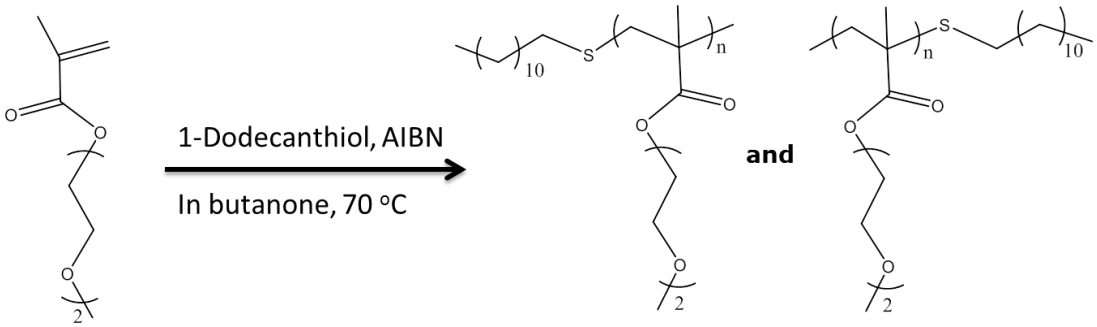


Figure 3.8: Synthesis of thermoresponsive polymer (PDEGMA-DDT) by conventional free radical polymerization.

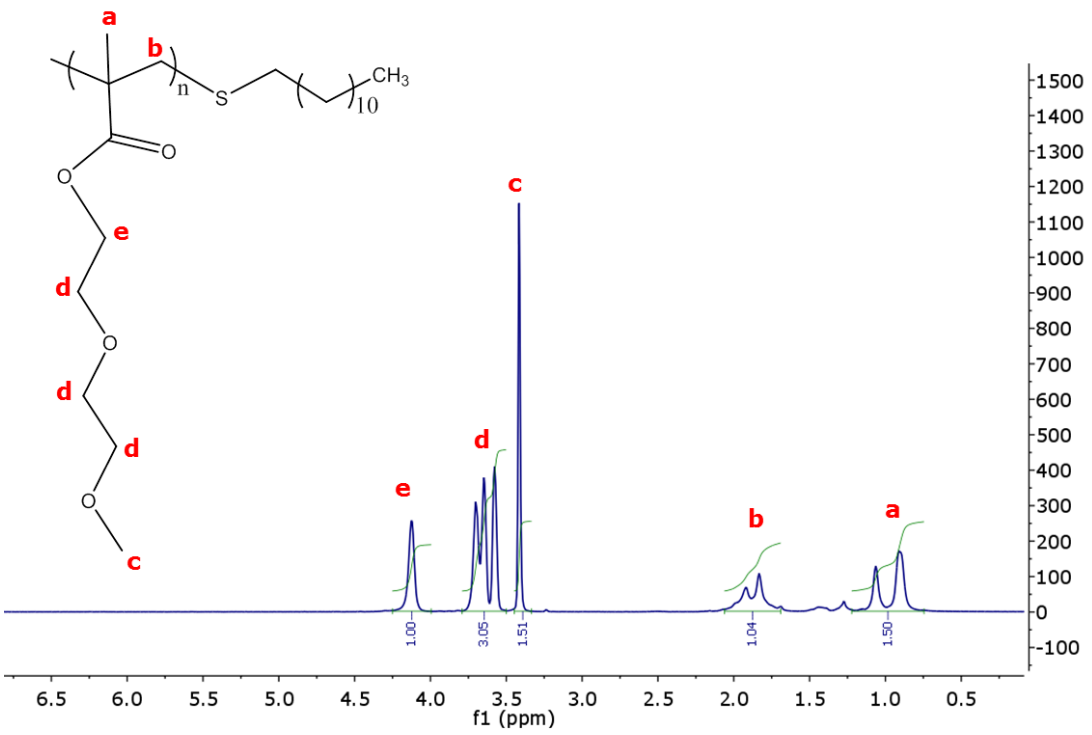


Figure 3.9: NMR spectrum of prepared PDEGMA which was used in the adsorption isotherm studies. The absence of monomer peaks (the range between 5.5 and 6.5) confirms the complete removal of monomer.

Moreover, number average molecular weight (M_n), weight average molecular weight (M_w), and polydispersity index (Đ) were determined using GPC , i.e. M_n= 50838, M_w= 28012, and Đ= 1.81487 were obtained. The synthesised polymers were polydisperse, as expected for polymers prepared by conventional free radical methods. Controlled free radical routes were not deemed necessary for these polymerisations owing to potential problems removing transition metal catalysts which may have been a source of toxicity when working with cells (Chen et al., 2006, Chang et al., 2009).

UV/visible spectroscopy was used to confirm the thermoresponsive properties of PDEGMA. Cloud point temperatures were measured as an approximation of the Lower Critical Solution Temperature (LCST) of the linear polymer (Alava and Saunders, 2006). The cloud point of PDEGMA

was measured in deionised water (Magnusson et al., 2008, Zhang et al., 2005b, Cho et al., 2008), using dilute solutions of PDEGMA (1% w/v), which were heated over a temperature range from 10 to 40^{o}C. Thermoresponsive polymers undergo a coil-to-globule transition at the LCST and become water insoluble (Liu et al., 2009d). When the polymers are in the collapsed state their solutions becomes turbid as a result of polymer chain aggregation. The solution turbidity starts at the cloud point temperature (CPT). The PDEGMA solution showed a marked increase in absorbance at 24 ^{o}C (Figure 3.10 a) indicating the cloud point (as an approximation of LCST) of the free polymer, resulting from pronounced chain collapse and aggregation of polymer chains.

The synthesized polymer was further characterized using thermal gravimetric analysis to further confirm the structural component compound and the purity of results. The PDEGMA thermogram showed a single step weight loss of 100% between 200 and 380 ^{o}C corresponding to decomposition of PDEGMA linear polymer. This indicated the high purity and lack of contamination such that the targeted compound had been synthesized (figure 3.10 b).

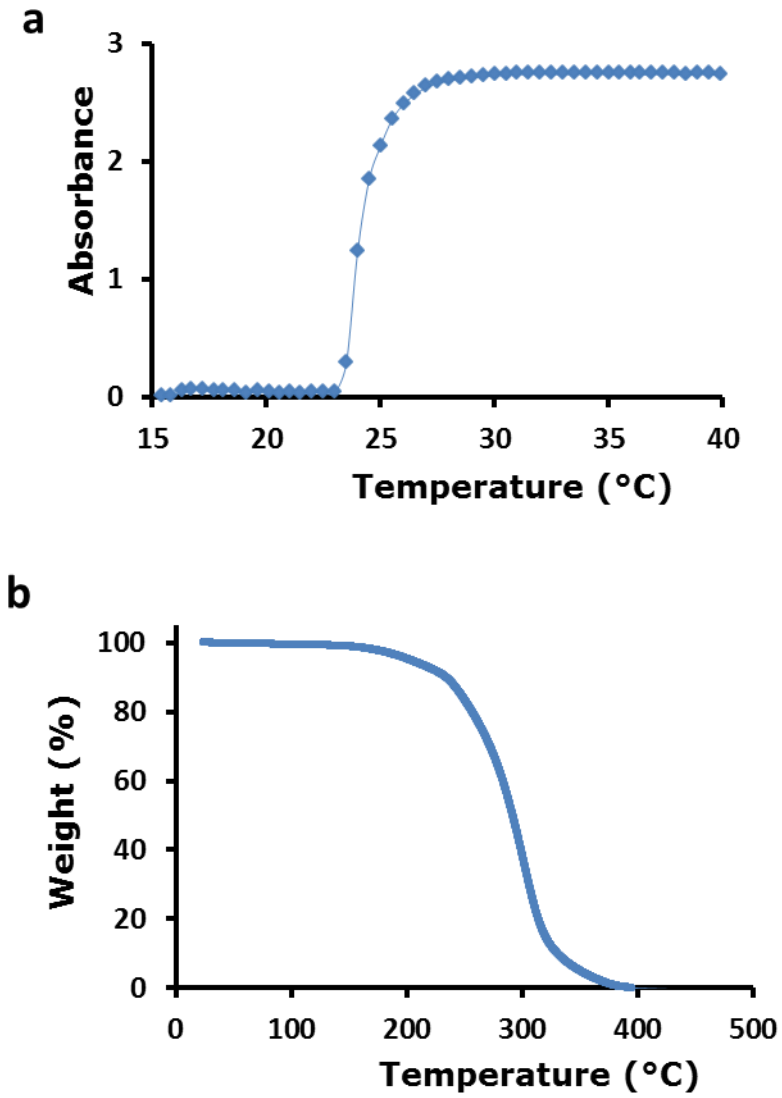


Figure 3.10: (a) Absorbance as a function of temperature for 1 % w/v PDEGMA solutions in deionized water, measured by UV-Visible spectroscopy. LCST behaviour observed at 24 °C. Absorbance of the samples was measured at a wavelength of 550 nm. (b) TGA thermogram shows one step of decomposition for PDEGMA polymer, indicating the high purity of results.

3.4.5. Colloidal gel evaluations

Thermoresponsive suspensions were obtained by mixing different percentage (weight/volume) of PS microspheres with PDEGMA solution, dissolved in complete DMEM medium or in deionised water.

The key requirements for effective steric stabilisation at the particle surface are strong adsorption of polymer chains to ensure high surface coverage, good solvency for the stabilising chains for effective repulsions, and low free polymer concentration to prevent depletion attraction through bombarding mciroparticles by the surrounding collapsed chain free polymer in the solution above the LCST (Marenduzzo et al., 2006). Thus, when the thermoresponsive polymer was adsorbed on microspheres below its LCST, it was able to act as a steric stabiliser and prevent interparticle association. However, above the LCST, particle destabilisation and flocculation can occur as the adsorbed polymer chains collapse. Particle interaction is important for gelation, aggregation of particles can lead to suspension gelation if a sufficiently high volume fractions of particles and strong inter-particle attractions are present. Space-filling networks of particle flocs, if present in sufficient strength and number, can give rise to space filling particle gels (Yanez et al., 1999).

Below its LCST, PDEGMA behaves as an amphiphile, due to its hydrophobic methacrylate backbone and hydrophilic ethylene glycol side chains. Consequently, the methacrylate backbone (as well as the dodecanethioether chain terminus) is adsorbed onto the surface of the PS microparticles in the suspension. Since the solvent quality for the steric stabiliser PDEGMA is largely dependent on temperature,

altering the temperature to above the LCST of PDEGMA causes marked changes in the associative behaviour of the coated particles in suspension. When water is a good solvent for PDEGMA (i.e. below the LCST) contacts with solvent molecules are enthalpically favoured which causes the polymer chains to swell and repel each other. However, these polymeric segments undergo a dimensional collapse, or a coil-to-globule transition, when water becomes a poor solvent (i.e. above the LCST) and these become mutually attractive. These mutual intermolecular attractions lead to intermolecular aggregation and the build-up of polymeric associations between the particles, giving rise to large 3D particle clusters.

The sterically stabilised PS particles with PDEGMA in a suspension were non-interacting below the LCST. Above the LCST, both the viscosity and the degree of shear thinning increased significantly as a result of structural build up from the aggregating particle networks. This suggests that the higher the temperature (above the LCST) the stronger the inter-particle attractions. On increasing the temperature to above the LCST, the PDEGMA chains shrunk into a globular conformation and their hydrophobic nature dominated the inter-particle interactions. The strong hydrophobic attractions between the collapsed layers drove the system into a gelled state.

Temperature-mediated colloidal fluid-gel transitions were investigated initially by simple tube inversion tests (figure 3.11 a). Several tube inversion assay experiments were performed using different weight combinations of PDEGMA and PS particles to determine the concentrations of PS and PDEGMA required to obtaining space-filling gels

at 37°C, since the gels would ultimately be used at this temperature. PDEGMA solutions were prepared in deionised water and cell culture medium (DMEM). The concentration of PDEGMA in the suspensions tested was varied between 1-4% to determine the relative lowest (critical) concentration of PS particles required to obtain gels at 37 °C. Gels were considered space-filling if they maintained their weight without syneresis upon tube inversion. Gels were only obtained above 10% (w/v)PS concentration combined with 4% w/v PDEGMA at 37 °C, while at PS concentrations below 10% w/v only particle aggregates were formed. When the PDEGMA content was reduced to below 3%, the amount of PS particles required for gelation increased to 15%.

The results presented in figure 3.11 b and table 3.2, confirm that the suspensions start to become gels when the minimum particle concentration was 10% PS with 3% or 4% PDEGMA. However, for suspensions containing 1% or 2% PDEGMA the gelation started only at 15% particle fraction. It was also observed that the maximum concentration of particles which could be loaded was 25%, as above this concentration the suspension became a paste and did not flow at any temperature.

Overall tube inversion results showed that the thermoreversible gelation in water and culture medium were compared and no obvious difference was found, so all experiments were subsequently carried out in culture medium. Also, it can be seen from the table 3.2 that the gelation is particle dependent because no thermoreversible gelation was found for the suspensions that were made from only PDEGMA without particles.

Table 3.2: Tube inversion test results of PS/ PDEGMA particulate suspensions in deionised water and/ or DMEM. The results show the reversible gelation (+) and flow (-) of suspensions at 37°C for different particle and PDEGMA concentrations. Suspensions made with either water or DMEM medium were compared and no difference was found.

		MPS microspheres%					
		0	10	15	20	25	30
PDEGMA %	1	-	-	+	+	+	paste
	2	-	-	+	+	+	paste
	3	-	+	+	+	+	paste
	4	-	+	+	+	+	paste

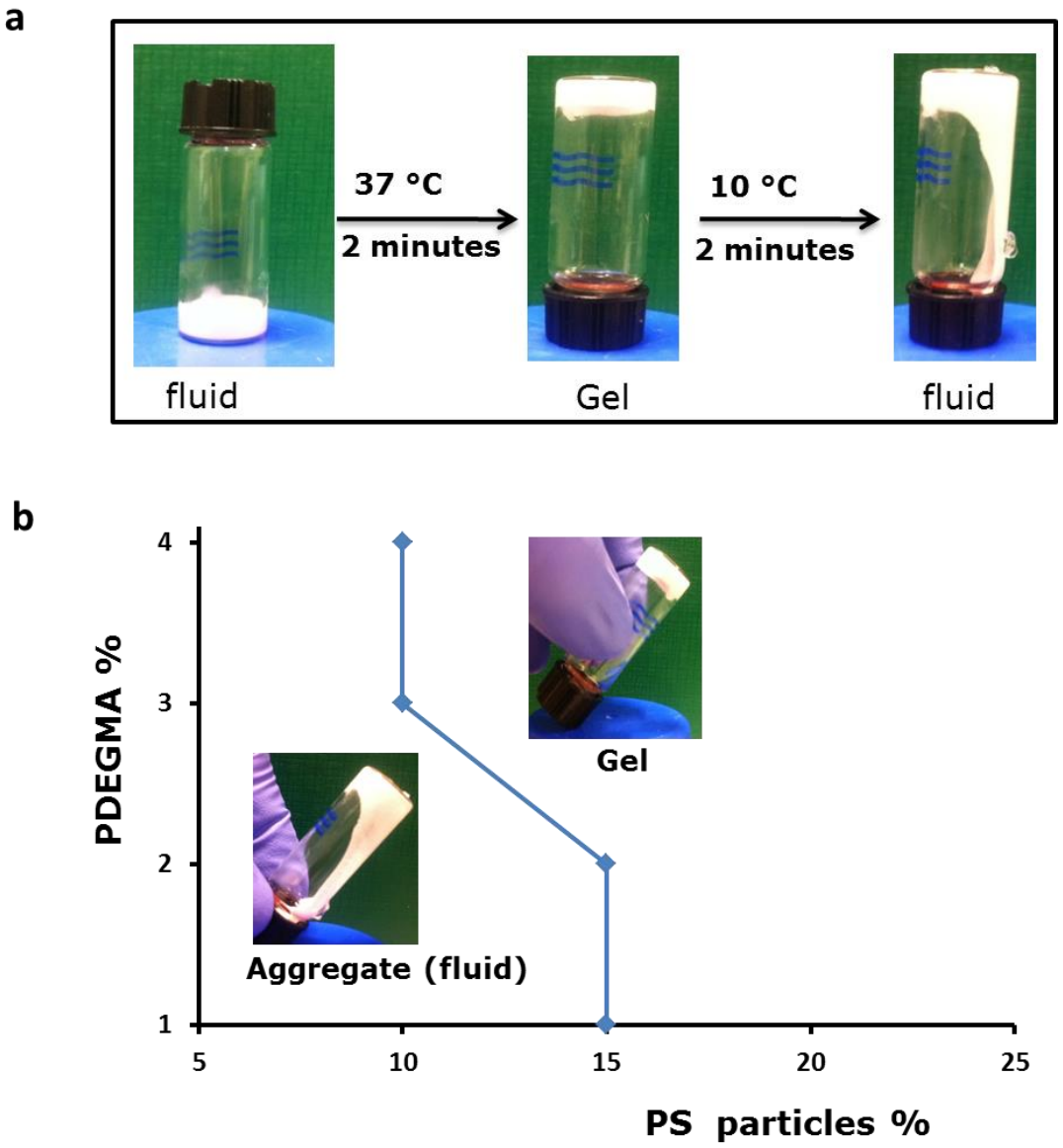


Figure 3.11: (a) Images of tube inversion test of suspension contain 25% of particles and 4% of PDEGMA. (b) Gel–fluid phase diagram for PS / PDEGMA suspensions at 37 °C, as determined by the tube inversion assay.

3.4.6. Rheological studies

Particle gels are viscoelastic materials because they show both viscous (flow) and elastic responses to an applied force (Tadros, 1996). Therefore, rheological measurements were performed to investigate the viscoelastic and mechanical properties of the thermoresponsive colloidal suspensions/ gels (Hsiao et al., 2014). MPS microspheres (2.5 μm) were used for all suspension/gels were used in rheological measurements. Although, the tube inversion results previously showed that there were no differences in thermoreversible gelation between suspensions made in DW and complete cell culture medium, but all the rheological experiments were performed with suspensions made in DMEM. This is because this medium had to be used during cell culture applications (chapter 5), not water.Temperature ramp tests were performed to investigate the temperature dependent viscoelastic properties of aqueous PS/PDEGMA suspensions/gels. Tests were performed for suspensions which contained varying concentrations of thermoresponsive polymer and/or no polymer, while maintaining the concentration of the PS particles at 25%. As can be seen from figure 3.12 a, all suspensions containing PDEGMA polymer displayed a temperature dependence of the storage modulus (G') above 20 °C and the order of this increase in G' values was proportional to the amount of PDEGMA in the suspension. In contrast, suspensions made from PS particles alone without any PDEGMA did not show any temperature dependent elastic modulus within the entire temperature range. At temperatures below 22 °C, both G' remained low and approximately constant, indicating that suspensions remained in the fluid (aggregated) state. At temperatures above 22 °C,

with increasing temperature there was a non-linear increase of G' values (by 2-3 orders of magnitude). The increase in G' with temperature indicates that inter-particle attraction also increased with temperature. Increased dehydration of the adsorbed PDEGMA layers with increasing temperatures resulted in stronger hydrophobic interactions, and hence increased interparticle associations.

Moreover, to show the influence of the particle concentration on the thermogelation behaviour of suspensions/gels, several temperature ramp tests for suspensions which contained different concentrations of MPS particles were performed, while the concentration of PDEGMA was maintained constant for all suspensions at 4% w/v. Figure 3.12 b shows that all suspensions displayed a temperature dependence of the storage modulus. However, suspensions which contained the higher particle concentrations showed higher G' values. Irrespective of thermoresponsive polymer concentration, increasing the MPS concentration yielded more elastic gels and increase of G' values, this feature widely reported for particle gels (Yanez et al., 1999). From figure 3.13 a, it is clearly seen that the tan δ values for all samples remained below 1, this is a critical behaviour of the gel state.

Thus in summation, by increasing the concentration of either thermoresponsive polymers and/or particles, the thermogelation behaviour and mechanical properties of the chosen suspensions were changed. The higher the temperature the lower the particle concentration required for gelation. The stronger inter-particle attractions at higher temperatures led to the formation of stronger particle networks, which formed more elastic gels that sustained their weights in a tube inversion

assay. However, when the inter-particle attraction was weaker at temperatures just above the LCST, more particles were required to form dense networks of sufficient elastic strength (Yanez et al., 1999, Shay et al., 2001).

Consecutive heating/cooling cycles of a suspension containing 20% particles (figure 3.13 b) confirmed the reversibility of their temperature response behaviour through multiple increase and decrease of G' values with raising and lowering the temperature, respectively.

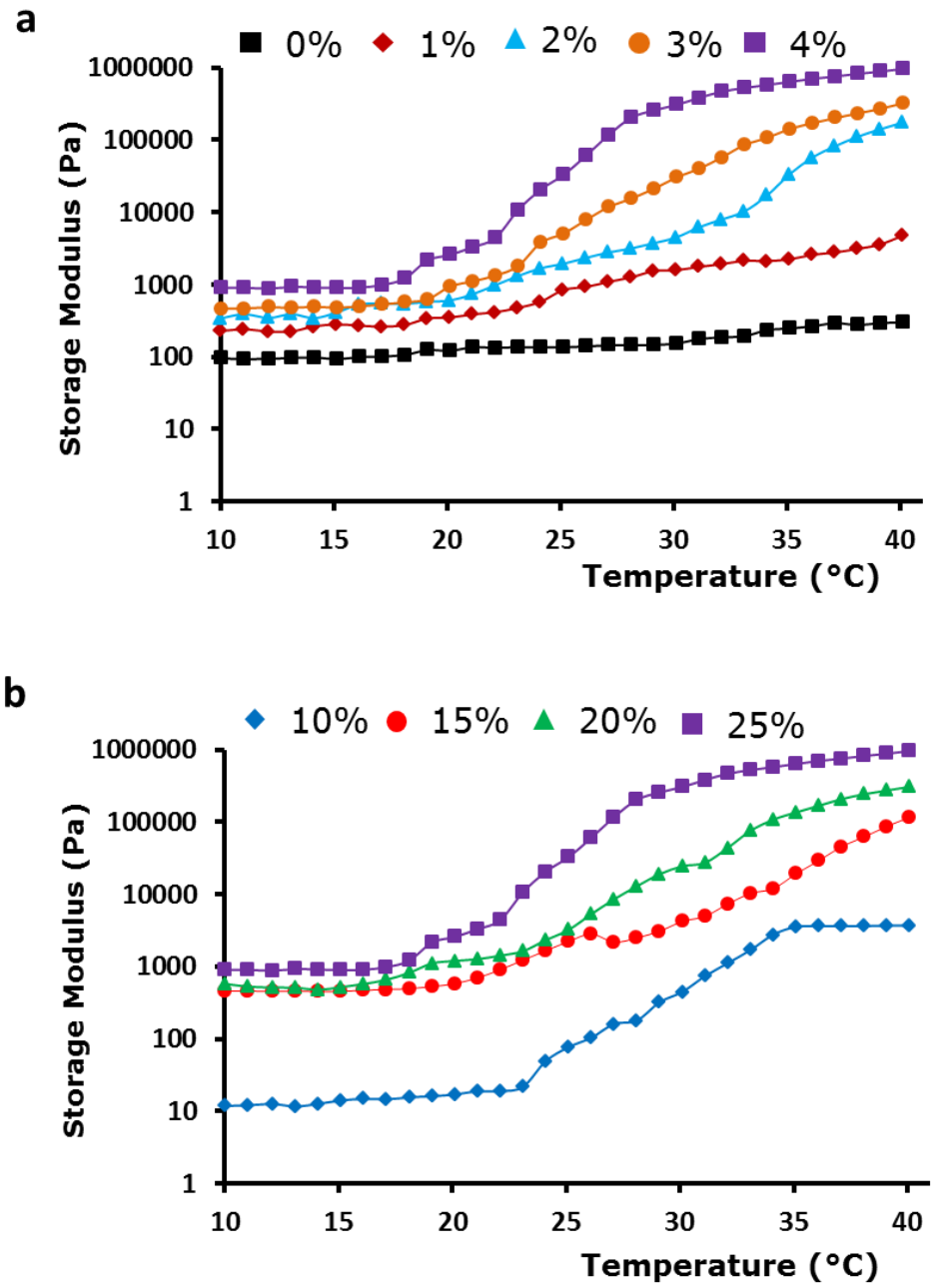


Figure 3.12: Temperature sweep tests show variation of G' with temperature for MPS/PDEGMA or MPS particulate suspensions at (a) Different PDEGMA concentrations and constant MPS particle concentrations of 25%;(b) different particle concentrations and PDEGMA concentration of 4%. For all experiments the frequency sweep was 1 rad sec^{-1} and strain 0.05% were used.

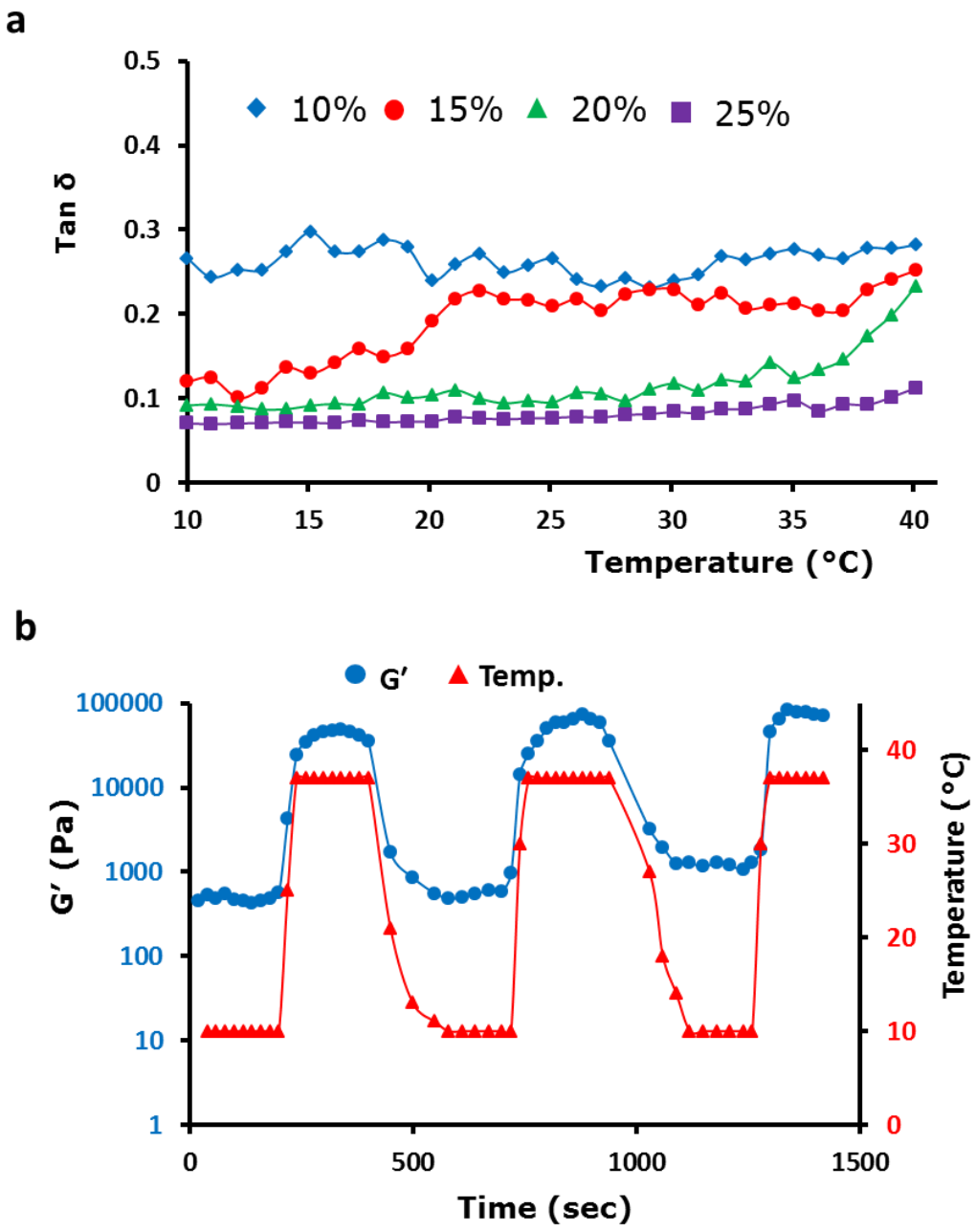


Figure 3.13: (a) Temperature sweep test shows the variation of tan δ with increase of temperature (b) Multiple heating-cooling cycles of a suspension containing 15% MPS particles and 4% PDEGMA which shows temperature driven Fluid-Gel-Fluid behaviour through variation of G′ values upon heating and cooling.

Strain sweep experiments were also conducted to investigate the mechanical properties and determine the linear viscoelastic region (LVR) of the prepared gel, which is the range where G’ is independent of strain. Beyond this region the breakdown of the gel structure was apparent from the rapid decline of *G’* at larger deformations. The gels transformed into liquid-like materials at the critical strain point (tan δ=1). It was observed that the LVR was dependent on the particle concentration. In a strain sweep test the elastic (G’) moduli are plotted against the deformation, the critical strain is usually taken as the strain at which tan δ=1 or a G’ and G’’ crossover occurs. Strain sweep for MPS/PDEGMA suspensions gelled at 37°C are shown in figure 3.14. All gels showed a small LVE, with critical strain values of around 1%. Since particles are less deformable than single chain polymer molecules and the strands of aggregated particles are much less flexible, particle gels tend to be more brittle than macromolecular gels and critical strain values less than 1% are common (Fraylich et al., 2010b). For all concentrations at low strains (less than 0.5%), *G’* was independent of the applied strain, suggesting the gels remained in the linear viscoelastic regime. It can be seen that the LVE region decreased (shortened) proportionally with increased particle concentrations, most likely due to increases in the solid particle content that made the gel more fragile and less viscous. Particle gels containing higher concentrations of MPS particles were found to be more elastic but also slightly more brittle. These networks of flocculated particles are not flexible and hence affected the overall flexibility of the gels (Yanez et al., 1999).

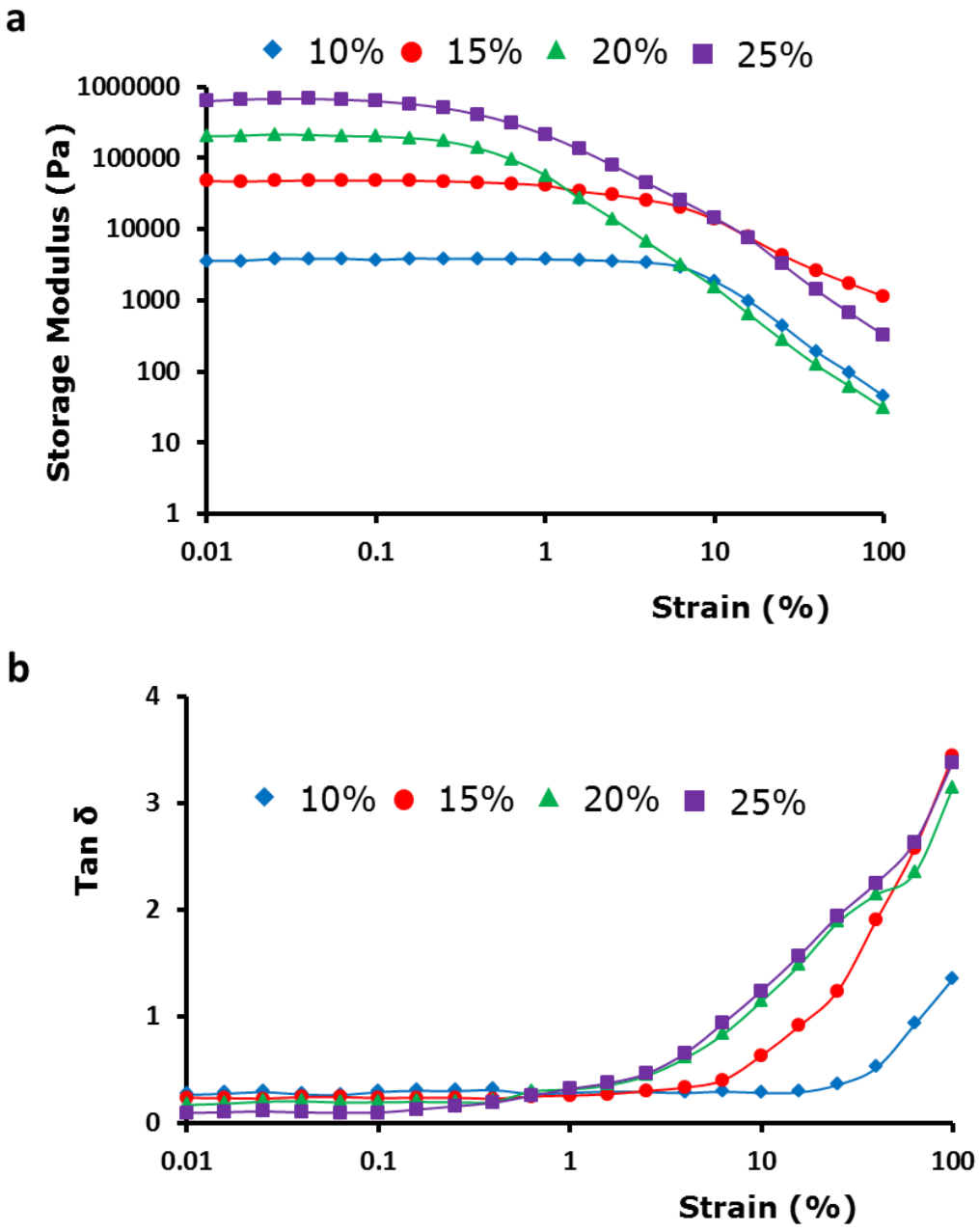
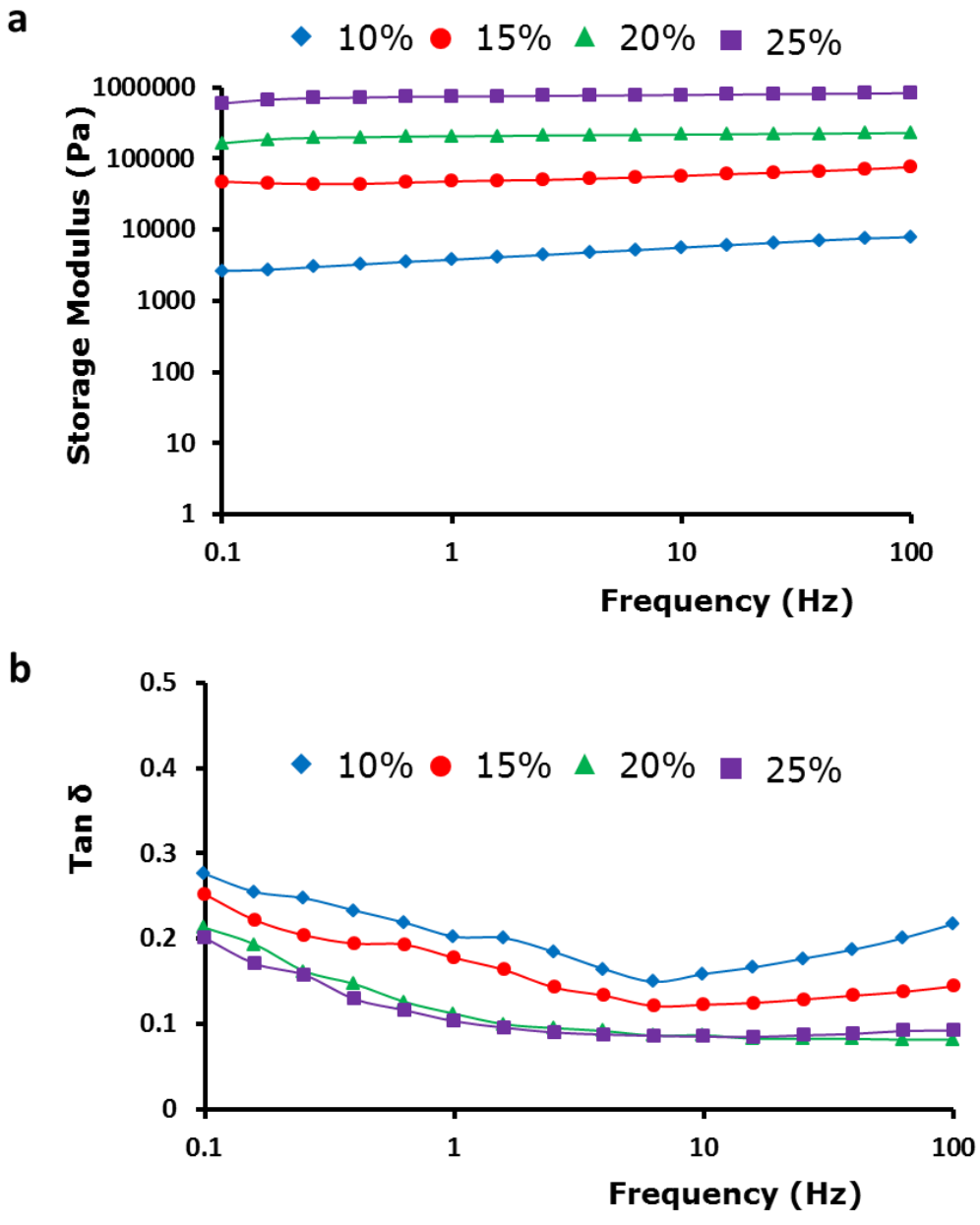


Figure 3.14: Strain sweep tests show the variation of (a) G′ and (b) tan δ with strain% for different MPS particle concentrations (same amount of PDEGMA 4%), measured at frequency 1 rad sec^{-1} and 37°C .

The frequency sweep analyses were also performed to investigate the mechanical properties of the prepared colloidal gels. The dynamic modulus measured as a function of frequency is a direct reflection of the interparticle forces because dynamic measurements do not disrupt the gel microstructure (Tadros, 1996). Particle gel elasticity depends on how strong the particle interconnections are (Fraylich et al., 2010b). Frequency sweep results indicated that the *G'* values were independent of frequency over the entire range for all particle concentrations that were studied (figure 3.15 a). The tan δ values of all examined samples were much lower than 1, meaning that storage modulus *G'* > loss modulus *G"*, typical of a gel state (figure 3.15 b). Increases in the particle concentration resulted in higher values of *G'*. Accordingly, each particle could be considered as a macro-crosslinker with weak chain-chain associative interactions via the collapsed PDEGMA layer above the polymer LCST. Attractive van der Waals interactions between the particles would also have been contributors to particle aggregation. As a consequence, the particle gel modulus increased as the number and density of linkages between the particles increased.

Overall rheometry results showed that the elasticity of the colloidal gel prepared here is much higher than previously reported (Al Ghanami et al., 2010, Fraylich et al., 2010b, Borzacchiello et al., 2011, Lapworth et al., 2012) including other hydrogels have been used for cell culture applications (Knapp et al., 1997, Arevalo et al., 2010, Yang et al., 2010). A possible explanation for this higher elasticity gel compared to other hydrogels may be due to the high solid (particles) content in the prepared colloidal gel that caused to increase the overall elasticity of the

gel. Since this high elasticity has not been found in previous colloidal gels it is probably due to the nature of the crosslinked and magnetic loaded particles that were used in this study, as well as the presence of high amount of aggregated polymer chain in the suspension which results in more elastic gels.



.

Figure 3.15: Frequency sweep tests show variation of (a) G′ and (b) tan δ with frequency for different concentration of MPS particle suspension (same amount of PDEGMA 4%); strain 0.05% and temperature 37 °C were used during measurements.

3.5. Conclusion

Dual thermo and magnetic responsive colloidal gel have been synthesised via physical adsorption of PDEGMA onto the surface of magnetic polystyrene microspheres. The advantage of the colloidal gel prepared here with previous thermally reversibly associated particles was coupling of the thermoresponsive entity to the magnetic responsive property in the same microspheres. This produced a system for the 3D culture and expansion of mammalian cells, and facilitated rapid and enzyme free recovery of the expanded cell population by simple magnetic separation. PDEGMA/ MPS microparticle suspensions in complete medium exhibited fast thermoreversible self-association combined with a simple magnetic separation stage. In this chapter, the results demonstrated the potential of these colloidal gels for use as a 3D scaffold in cell expansion. Finally, rheometry analysis demonstrated that prepared colloidal gels have a mechanical and viscoelastic properties suitable for use as scaffolds for cell culture applicatiosns.

The strategy described in this chapter (synthesis of thermoresponsive magnetic colloidal gel via physical adsorption) is rapid and can be adapted to many microparticle surfaces but has the drawback of possible desorption of polymer chains during extended or repeated use. The next chapter will describe synthesis of the responsive magnetic colloidal gel via a chemical grafting method, through the formation of covalent bonds between the polymer corona and the microparticle core to provide robust and better-defined materials despite being more complex and time-consuming.

4. Synthesis and characterisation of thermoresponsive magnetic PCMS- PDEGMA colloidal suspensions/ gels via surface-initiated polymerization from functional microspheres

The previous chapter concentrated on the synthesis of thermoresponsive magnetic colloidal gel via physical adsorption. This chapter now focused on conducting surface initiated atomic transfer radical polymerisation (SI-ATRP) to produce a novel magneto-thermally responsive colloidal gel. The new materials in this chapter will have the advantage over previous colloidal gel system in that the PDEGMA thermosensitive polymeric stabilizer is covalently grafted to the surface. Also, the synthetic method was easily adapted to incorporate magnetite nanoparticles into the thermoresponsive microparticles with retention of magnetic properties. This in turn will allows these materials to be used repeatedly for successive rounds of cell culture, without loss of the thermoresponsive polymer.

4.1. Introduction

Reversible gels which allow three dimensional cell proliferation and the recovery of cells after expansion would have considerable value in tissue engineering applications. Colloidal gels derived from reversibly associating microparticles are of increased recent research interest (Fraylich et al., 2008, Fraylich et al., 2010a, Vihola et al., 2007a, Pek et al., 2008) and of potential value in regenerative medicine. Over the last decade, temperature-responsive colloidal gels have been widely studied as scaffolds in tissue engineering, for example as building blocks to

support tissue growth (Al Ghanami et al., 2010, Wang et al., 2008), as microcarriers for delivery of therapeutic cells (Fraylich et al., 2010b, Wang et al., 2009), and for the 3D culture and expansion of stem cells and chondrocytes (Saeed et al., 2015, Lapworth et al., 2012, Pek et al., 2008). A desirable feature of these colloidal gels intended for cell culture applications is an ability to be dispersed into a mobile suspension below body temperature but also the capacity to form a supportive and stable gel at ≥ 37 °C.

Thermoresponsive polymers have been widely used as surface-modifiers of micro- and nano-particles to provide such reversibly-associative properties (Rimmer et al., 1996, Li and Ngai, 2010, Ramakrishnan and Zukoski, 2006, Elaissari, 2006b). At temperatures below their phase transition, thermoresponsive polymers attached to the surface of microparticles can provide steric stabilization, overcoming the tendency for interparticle aggregation. This enables the modified microparticles to be used in free-flowing suspensions with cells. Above the phase transition temperature of the attached thermoresponsive polymer, the outer 'corona' of the microparticles collapses, colloidal stability is lost and interparticle association occurs to form a heterogeneous gel. In addition, coupling of thermoresponsive polymers to magnetite-containing microspheres has recently been shown to enhance the culture and expansion of stem cells, and facilitate rapid recovery of the expanded cell population by simple magnetic separation (Saeed et al., 2015).

The 'switchable' component of reversibly associating colloidal microparticles can be generated by attaching the thermoresponsive polymer either by physical adsorption (Shahidan et al., 2013, Shakesheff

et al., 1997) or chemical grafting (Shay et al., 2001, Breed et al., 2009). The most simple method i.e. physical adsorption is rapid and can be adapted to many microparticle surfaces but has the drawback of possible desorption of polymer chains during extended application. The chemical grafting method i.e. the formation of covalent bonds between the polymer corona and the microparticle core, provides robust and better-defined materials but is more complex and time-consuming. Covalent links between surfaces and polymer can be generated either by growing polymers from initiator sites pre-attached at the surface ("grafting from") or by conjugating pre-formed polymers to reactive groups at the particle surface ("grafting to")(Seeber et al., 2011). While these approaches provide permanent attachment of responsive polymer to the microparticle surface, the "grafting from" technique generally provides denser surface polymer layers. This is because monomers have lower steric demands than polymers and can easily diffuse to initiator and propagation sites during polymerization reactions, thus producing a higher grafting density (Karagoz et al., 2010).

A number of controlled polymerization techniques have been used to graft polymer chains on the surface of particles. These include atom transfer radical polymerization (ATRP) (Zhao et al., 2014, Bicak et al., 2006, Mizutani et al., 2010b, Mizutani et al., 2010a), reversible addition fragmentation transfer (RAFT) (Kaupp et al., 2013) and nitroxide mediated polymerization (NMP) (Chevigny et al., 2009). Amongst these methods ATRP is of particular interest for grafting acrylic and methacrylic monomers. Surface-initiated atomic transfer radical polymerization (SI-ATRP) is one of the more useful techniques used to produce polymer

brushes on solid surfaces (Jhaveri et al., 2007) and good control over grafting density has been obtained when applied in dispersed media (Pyun et al., 2003).

SI-ATRP has been widely used to produce polymer brushes on the surfaces for many biomedical applications. It has been used to impart controlled cell adhesion and detachment (Dey et al., 2011, Xu et al., 2006, Chen et al., 2008, Xu et al., 2004, Mizutani et al., 2008, Zhang et al., 2006, Singh et al., 2008), biocompatibility (Jhaveri et al., 2007), antifouling (Ma et al., 2004, Xiao et al., 2004, Cringus-Fundeanu et al., 2007, Mei et al., 2005, Yoshikawa et al., 2006, Xu et al., 2007, Singh et al., 2007, Iwata et al., 2004, Gao et al., 2008), and antibacterial properties (Yao et al., 2008, Huang et al., 2007, Murata et al., 2007) to the surfaces. Moreover, it has been used to produce nanopatterns (Carter et al., 2003, Zhao et al., 2000) and stimuli-responsive surfaces (Boyes et al., 2002, Kong et al., 2001, Pyun et al., 2002, Zhao, 2003) and also for controlled drug delivery (Bai et al., 2006, Zhou et al., 2008).

4.2. Aims and Objectives

The aim of the work described in this chapter was the synthesis of thermo and magnetic responsive colloidal gels via chemical grafting of thermoresponsive polymer onto the surface of magnetic microsphere. To achieve this aim, the following hypotheses were proposed:

Monodisperse PCMS microspheres with the size range between 1-5 μm can be prepared via dispersion polymerisation.

PDEGMA can be grafted from the surface of PCMS microsparticles via SI-ATRP to produce thermoresponsive PCMS-PDEGMA microparticles.

These thermoresponsive microspheres can be magnetized by loading magnetite nanoparticles via swelling/deswelling techynique.

Thermoreversible magnertic colloidal suspensions/gels can be prepared via dispersing different concentration of magnetic PCMS-PDEGMA microspheres in cell culture medium (DMEM).

If successeful, the prepared colloidal gels would expected to have the viscoelastic properties suitable for use as a scaffold for *in vitro* 3D cell expansion. Colloidal gels with an elastic modulus ranging from 0.004 to 100 kPa were previously used for making 3D scaffolds, for mammalian cell culture (Al Ghanami et al., 2010, Fraylich et al., 2010b, Borzacchiello et al., 2011, Lapworth et al., 2012).

4.3. Materials and Methods

Chloromethylstyrene (CMS) and divinylbenzene (DVB) monomers were washed with 5% sodium hydroxide solution to remove inhibitors before being used. 2,2-Azobisisobutyronitrile (AIBN) was recrystallized from methanol. 2-Methoxyethanol, ethanol, polyacrylic acid (PAA-average molecular weight 3000 kDa), copper bromide (CuBr) N,N,N’,N’’,N’’-pentamethyldiethylenetriamine (PMDETA), diethyleneglycol methyl ether methacrylate and all other chemicals were bought from Sigma-Aldrich Company Ltd. UK and used as received.

4.3.1. Synthesis of poly(chloromethylstyrene) microspheres

Poly(chloromethylstyrene) microspheres were synthesised by dispersion polymerization. In a typical procedure, poly(acrylic acid) (0.30 g, 0. 1 µmol, MW= 3000 kDa) was dissolved in a mixture of ethanol (13 mL)

and 2-methoxyethanol (1 mL) and were placed in a polymerization reactor. Next, AIBN (0.02 g, 0.12 mmol), CMS monomer (1.52 g, 10 mmol), and DVB (0.076 g, 0.5 mmol) were added to the above solution. The resulting solution was sonicated for 1 minute within an ultrasonic water bath for the complete dissolution of AIBN in the polymerization medium. The solution was then degassed with nitrogen for 5 minutes. The reactor was sealed and placed into a shaking water bath (120 cycles per minute) at 70 °C and maintained at this temperature for 24 h to complete the polymerization. The reactor contents were cooled to room temperature and the obtained PCMS microspheres were separated by centrifugation (3000x g for 10 minutes) and repeatedly washed by re-suspension and centrifugation steps with with ethanol (3 x 100 mL) and water (2 x 100 mL). The resulting microspheres were dried in a freeze dryer

4.3.2. Preparation of magnetic PCMS-PDEGMA microspheres

Magnetic polymer microspheres were prepared by a swelling and solvent evaporation process. Polymer microspheres (1.0 g) were swollen by immersion in chloroform, and then dispersed magnetic nanoparticles (150 mg) in chloroform were added to the above suspension. The final mixture was shaken for 24 hours to allow the magnetite nanoparticles to enter the swollen polymer microspheres. After this time, the temperature of the solution was increased and the chloroform was evaporated slowly under reduced pressure, enabling the magnetite nanoparticles to be retained inside the microspheres. The resulting magnetite-impregnated microspheres were precipitated by addition of petroleum ether and separated by centrifugation (2000x g for 5 minutes). The final

microparticles were washed with ethanol then with distilled water before being lyophilised.

4.3.3. Surface initiated atomic transfer radical polymerization (SI-ATRP) for grafting of PDEGMA on PCMS microspheres.

A round-bottom flask was charged with poly(chloromethylstyrene) microparticles (1.2 g, 1.45 mmol), and DEGMA (13.6 g, 72.5 mmol, 27.3 g, 145 mmol or 41g, 217.5 mmol), dependent on the desired monomer: initiator ratio, CuBr (0.2 g, 1.45 mmol), PMDETA (0.25 g, 1.45 mmol) and cyclohexanone (5 mL). The flask was then degassed with argon for 30 minutes. The mmol ratios of initiator: CuBr: PMDETA: monomer were 1: 1: 1: 50 or 100 or 150, respectively. The solution was stirred as the temperature was increased to 80 °C and maintained at this temperature for 24 h to run the polymerisation. The produced PCMS-PDEGMA particles were separated by centrifugation and washed three times with THF to remove any non-surface-bound polymers produced during the polymerization reaction. The surface-grafted particles were washed repeatedly with EDTA solution to remove any residual copper. After two further water washes, the microparticles were lyophilised, pu it into a sealed plastic tube and stored in the fridge until further use.

4.3.4. Preparation of thermoresponsive suspensions

All suspensions studied were obtained by dispersing different concentrations (% w/v) of microspheres in cell culture medium (DMEM) or in distilled water, then the suspension were subjected to frequent vortex mixing.

4.3.5. Electronic Microscopy characterizations

Scanning electron microscopy (SEM) and transmission electron microscopy (TEM) characterizations were performed. The details of SEM and TEM procedures have been described in chapter two sections 2.2.1 and 2.2.2, respectively. Microparticle size measurements were made from three repeatable batches and these measurements were performed three times for each batch.

4.3.6. ATR- FTIR characterization

The details of ATR-FTIR characterization procedure are provided in chapter two, section 2.2.3.

4.3.7. Time-of-Flight Secondary Ion Mass Spectrometry (ToF-SIMS)

Analyses were performed using a ToF-SIMS IV instrument (ION-TOF GmbH, Münster, Germany) equipped with a bismuth liquid metal ion gun and a single-stage reflection analyser. Dry powder samples were adhered to double-sided tape to produce an immobile surface suitable for the instrument. Typical operating conditions utilized a Bi^{3+} primary ion energy of 25 kV and a pulsed target current of approximately 1.0 pA. Data in the negative and positive secondary ion polarities were collected and analysed using Surface Lab 6 (ION-TOF Gmbh, Münster, Germany).

4.3.8. X-Ray Photoelectron Spectroscopy

X-ray photoelectron spectroscopy analysis was performed using a Kratos Axis Ultra spectrometer (Kratos Analytic Ltd, UK) equipped with a monochromated X-ray source (1486.6 eV), at 15mA emission current and 10 kV anode potential. Dry powder samples were adhered to double

side tape. The instrument was operated at fixed transmission mode. Data analyses were carried out using CASAXPS software (version 2.3.16) (Casa software ltd, Teignmouth, United Kingdom). All scans were charge corrected to C 1s at 284 eV.

4.3.9. Temperature dependent turbidity measurement

A Beckman Coulter DU 800 UV spectrophotometer with a thermostat was used for measuring the change of absorption of dilute suspensions of particles over a temperature range of 10–50 °C. The temperature was controlled and measured using a Peltier plate heating system (Beckman) and was increased at a rate of 1 °C min^{-1}. Absorbances of the samples were measured at a wavelength of 550 nm.

4.3.10. Tube Inversion test

Typically 1 mL of aqueous polymer microparticle suspension was added to a 7mL glass vial. The sample was adjusted to the desired temperature (37 °C) for 2 minutes in a thermostat water bath. The mobility of the dispersions was assessed by inverting the vial. If the suspension had not flowed after 10 seconds it was considered to be a self-supporting gel.

4.3.11. Rheometry characterizations

The details of Rheometry characterization procedures have been provided in chapter 2, section 2.2.4.

4.4. Results and discussion

ATRP has been the most widely employed technique for the formation of polymer brushes onto the surfaces of microparticles via surface initiated polymerization (Zhang et al., 2006, Zhou et al., 2015). One particularly

interesting aspect of such surface-grown brushes is the possibility to achieve a high grafting density of polymer chains owing to the high curvature of the particle surfaces. SI-ATRP has been used to produce polymer brushes from functionalized particles serving as colloidal initiators (Pyun et al., 2003). Different kinds of brushes were grown by surface-initiated ATRP from organic latex particles/colloids (Pyun et al., 2003, Guerrini et al., 2000, Bontempo et al., 2002, Jayachandran et al., 2002, Senkal and Bicak, 2003, Zheng and Stover, 2002a, Zheng and Stover, 2002b). There have been previous literature reports on the surface functionalization of polymer-based latex particles with ATRP initiator groups, mainly alkyl halide, followed by SI-ATRP of polymer brushes (Bicak et al., 2006, Min et al., 2002, Hu et al., 2006, Sonmez et al., 2003, Jhaveri et al., 2007).

Here in this study, thermoresponsive PCMS-PDEGMA microparticles were synthesised by grafting of PDEGMA chains from the surface of PCMS microspheres using surface-initiated ATRP, as shown in figure 4.1. The reason was to generate thermo-switchable particle surfaces and subsequently to produce thermoresponsive colloidal gels for tissue engineering applications. PCMS microspheres were chosen as a core substrate because the chloromethyl groups on their surface are useful initiator sites for ATRP polymerization (Min et al., 2002) and they are well-established as supports for solid-phase chemistry (Bayraktar et al., 2012). The thermoresponsive component, PDEGMA, was chosen as it is well-tolerated by cells, displays a lower critical solution temperature (LCST ~ 26 °C) just above ambient temperature but below human body temperature (Lutz et al., 2006, Lutz, 2008) and displays resistance to

absorption of proteins which is importance for various surface-engineering applications including biomaterials, drug delivery, or biosensors (Heuberger et al., 2005, Hu et al., 2010). In addition, the applications properties of the microparticles were further enhanced by taking advantage of the swellable properties of the lightly-cross-linked polystyrene core to embed stabilized magnetite nanoparticles. This in turn allowed the preparation of a dual magneto-thermally responsive material. The reversible thermogelling behaviour allows formation of particulate gels, which have potential for 3D support structures for tissue culture, while the magnetic nanoparticle components enable simple and rapid separation of the colloidal particles following application.

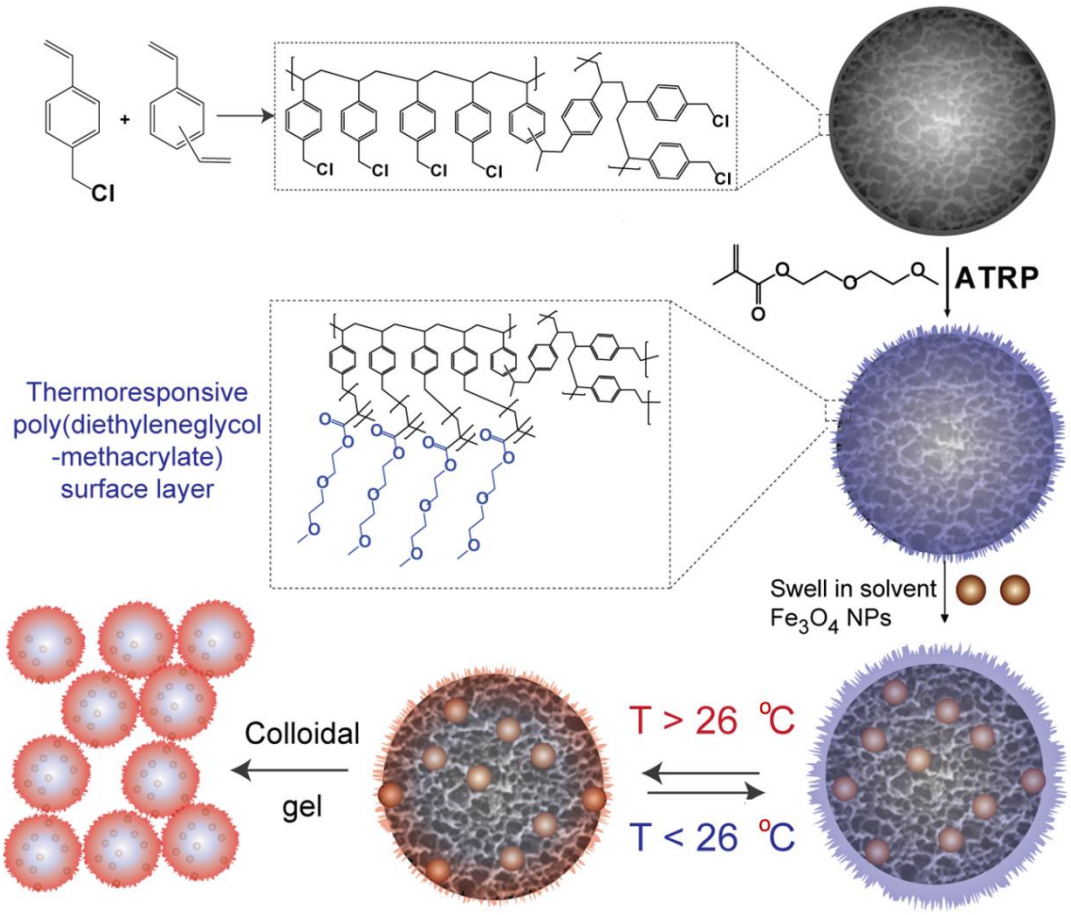


Figure 4.1: Schematic diagram shows synthesis of thermoresponsive magnetic microspheres.

4.4.1. Microscopy analysis

Dispersion polymerisation synthesis generated PCMS microspheres of uniform size (CV < 5%) and morphology as shown by Scanning Electron Microscopy (SEM) and Transmission Electron Microscopy (TEM). As apparent from the micrographs, PCMS microspheres (Figure 4.2, top row) were smooth and spherical, with a diameter of ~ 1.3 μm (Coefficient of Variance CV 5.4%). The surface ATRP procedure generated PCMS-PDEGMA microparticles with increasing size and surface roughness (Figure 4.2 rows 2-4). The average particle diameter of PCMS increased after grafting the PDEGMA from accessible chloromethyl residues. These diameters were 1.6 μm (CV < 7%), 1.8 μm (CV < 7%) and 2.1 μm (CV < 8%) for 1:50, 1:100 and 1:150 initiator:monomer ratios used during grafting process, respectively. Statistical analysis showed the significant increase ($P < 0.05$) in particle diameter after conducting polymerisation for all the above samples and P values are 0.0158, 0.007, and 0.001 for 1:50, 1:100 and 1:150 initiator:monomer ratios used, respectively. Also, there are asignificant differences between average diameters of grafted particles made from different concentration of initiator/monomer except in case of 1:50 and 1:110 comparison. Thus, the average particle diameters and surface roughness of the microspheres were increased as the initiator: monomer ratios were increased due to increase of the amount of grafted polymer from the surface via conduction SI-ATRP. Transmission electron microscopy (TEM) enabled visualisation of the grafted PDEGMA regions on the surface of microparticles, observed as lighter layer in the micrographs because the

brush layer was likely to be less compact compared to the core PCMS (Figure 4.3 rows 2-4).

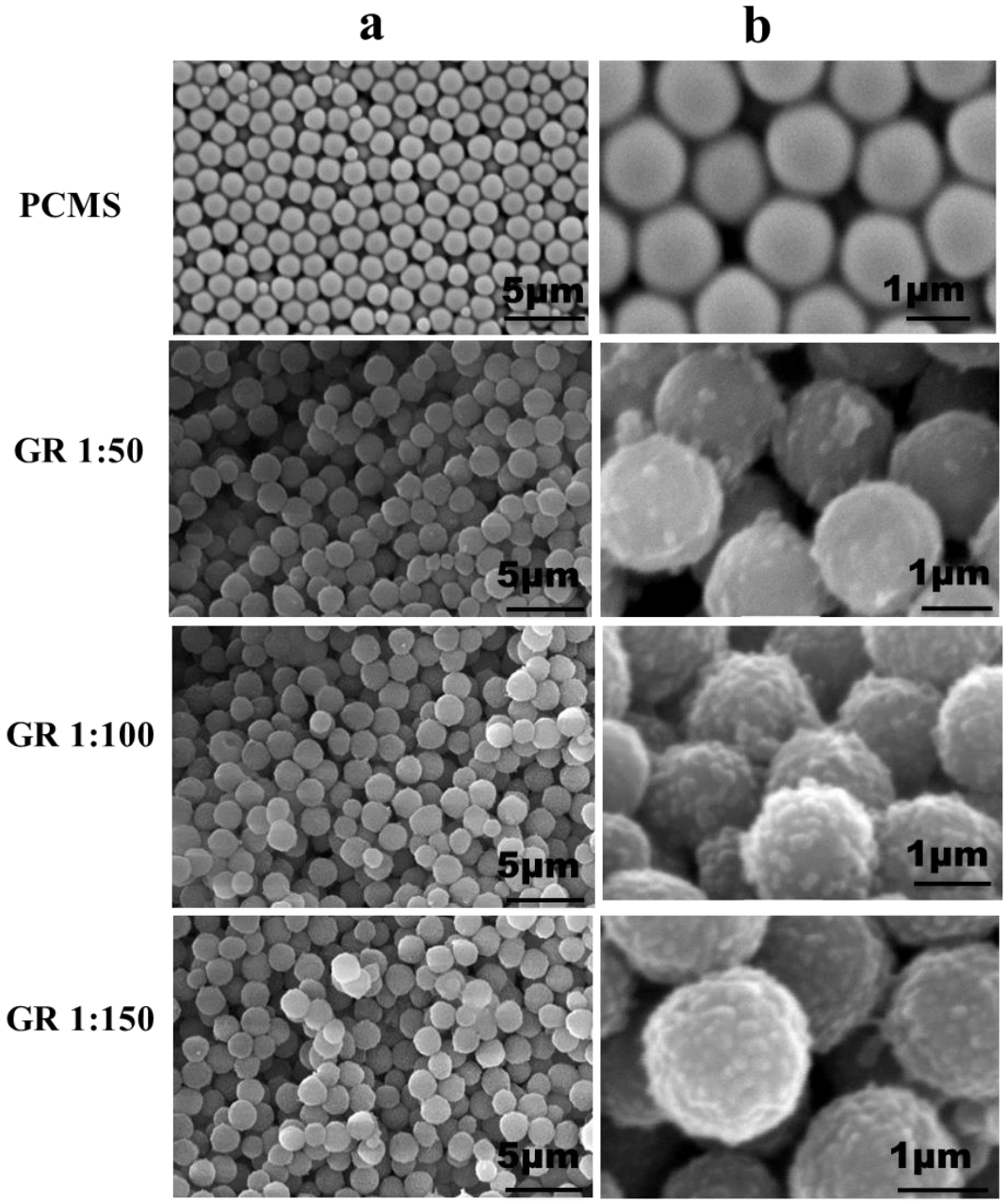


Figure 4.2: Representative scanning electron micrographs at low (a) and high (b) magnification of PCMS microparticles that shows smooth spherical shape and PCMS-PDEGMA microparticles produced with different initiator: monomer loading during grafting reaction (1:50, 1:100, and 1:150). After grafting, the particle diameter and surface roughness increased in line with monomer concentration during the surface ATRP reaction.

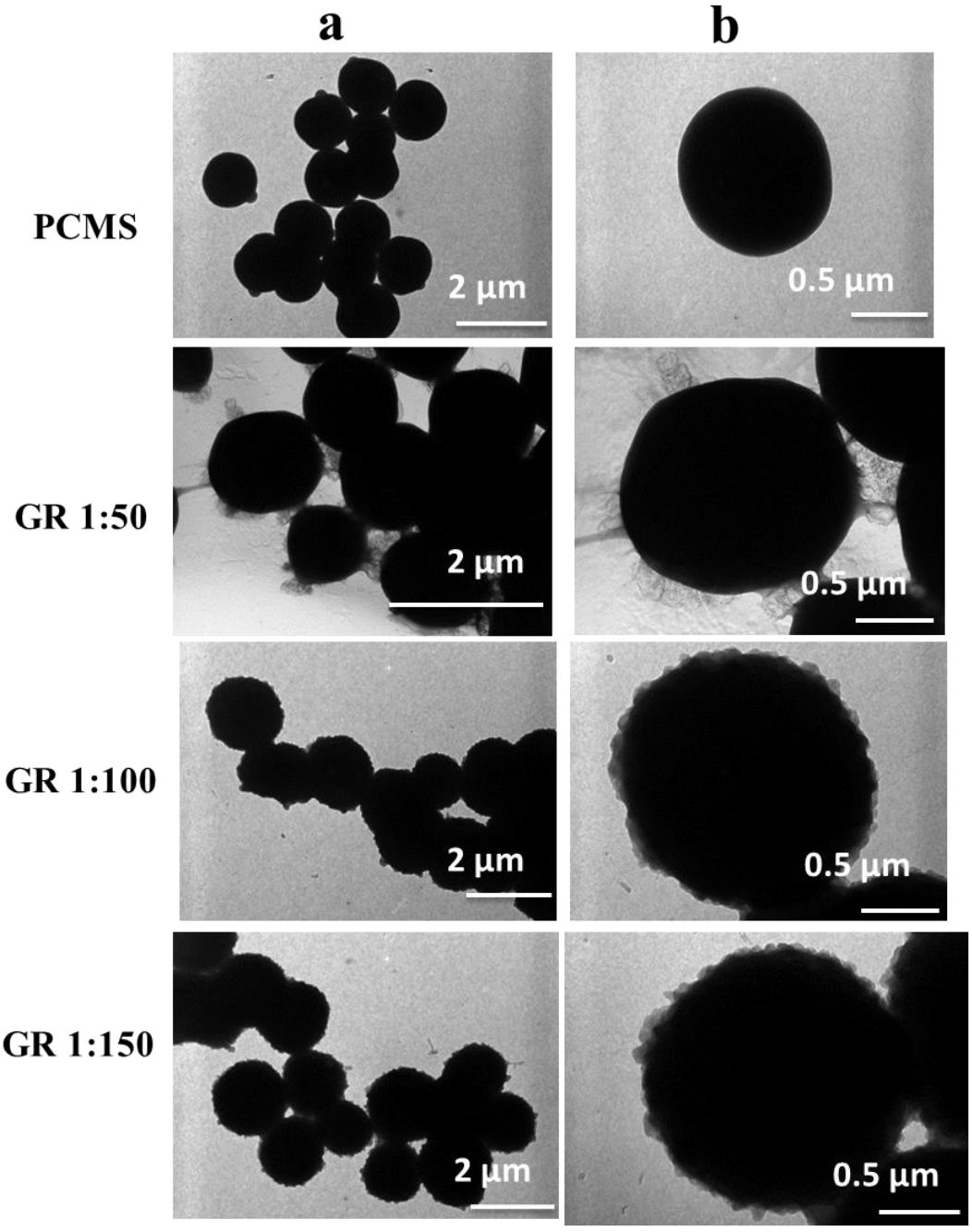


Figure 4.3: Representative Transmission electron micrographs at low (a) and high (b) magnification of the same samples. Images demonstrate that the grafted PDEGMA regions on and in the surface of microparticles, observed as diffuse regions because the brush layer was likely to be less compact compared to the core PCMS.

4.4.2. Surface characterisation

A number of surface sensitive characterization experiments (ATR-FTIR, XPS, ToF-SIMS) were performed to identify chloromethyl groups on the surface of PCMS, necessary for initiating ATRP reactions, and to confirm the presence of grafted PDEGMA. PDEGMA-PCMS microparticles which have been prepred from 1:150 initiator;monomer ratio were used in all of these charcaterisations and for subsequent applications. This is because these particles have highest amount of PDEGMA on ther surfaces, compared to other samples (1:50 and 1:100).

ATR-FTIR spectrum of PCMS (Figure 4.4 a) showed two characteristic absorption bands at 672 and 1263 cm^{-1}, attributed to the C-H bending vibrations in chloromethyl groups and stretching vibrations of C-Cl, respectively. However, the spectrum of PCMS-PDEGMA (Figure 4.4 b) showed two new distinct absorptions at 1105 cm^{-1} and 1725 cm^{-1} which could be attributed to C=O and C-O stretching vibrations from carboxylic groups of PDEGMA, respectively. It was also observed that the absorption bands for the chloromethyl group were reduced in intensity for the PCMS-PDEGMA beads.

Moreover, XPS spectra of PCMS (Figure 4.5 a) displayed emission peaks at 535, 284, and 200 eV, assigned to transitions of O1s, C1s, and Cl2p electrons, respectively. However, after grafting PDEGMA (Figure 4.5 b) the percentage of oxygen increased and percentage of C1s decreased and Cl2p disappeared. High resolution carbon spectra (Figure 4.5 c and d) showed a sharp increase in the proportion of methoxy groups corresponding to PDEGMA side-chain termini after grafting. However, it can be seen that the sample has adventitious carbonaceous over layers

and C1s spectrum for contamination typically has C-C, C-O-C and O-C=O components. Previous researches showed that most samples that have been exposed to the atmosphere when prepared in air or samples examined in less than optimal vacuum conditions will have a detectable quantity of adventitious carbon contamination (Evans, 1997, Mangolini et al., 2014, Castle and Baker, 1999, Miller et al., 2002).

Furthermore, Time-of-flight secondary ion mass spectroscopy (ToF-SIMS) was performed as a complementary characterisation technique to the XPS and ATR-FTIR analyses. ToF-SIMS overlaid spectra (Figure 4.6) indicated the presence of initiator groups in PCMS *via* the mass peaks at 35 m/z corresponding to the characteristic negative fragment ions of chlorine atoms. However, in the surface-grafted particles, the intensities of chlorine bands were decreased with increasing intensity of CH_3O^- (methoxy group in PDEGMA) components.

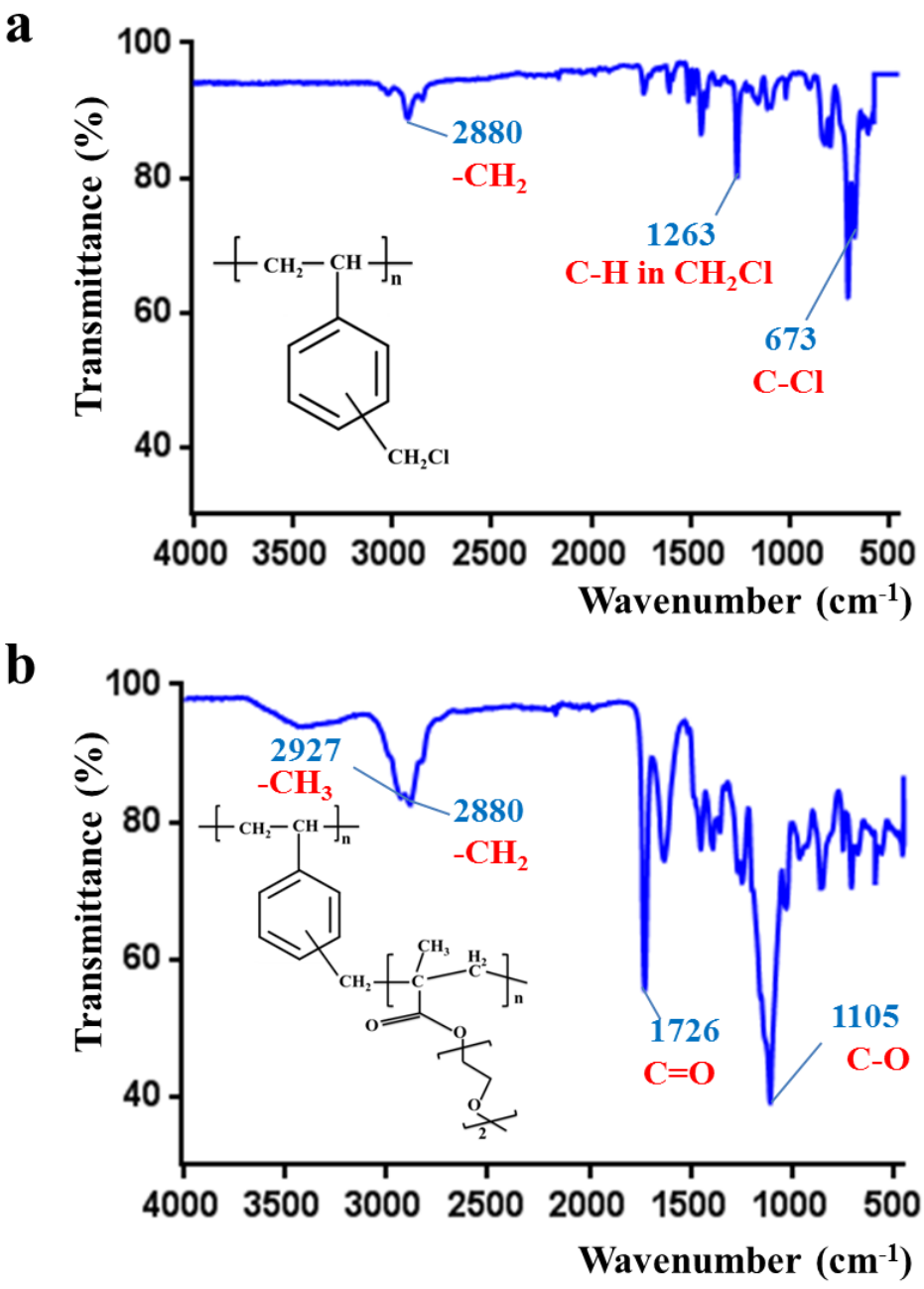


Figure 4.4: ATR-FTIR spectra of (a) PCMS and (b) PCMS- PDEGMA microspheres (2.1 µm) which have been prepared from 1:150 initiator;monomer ratio.

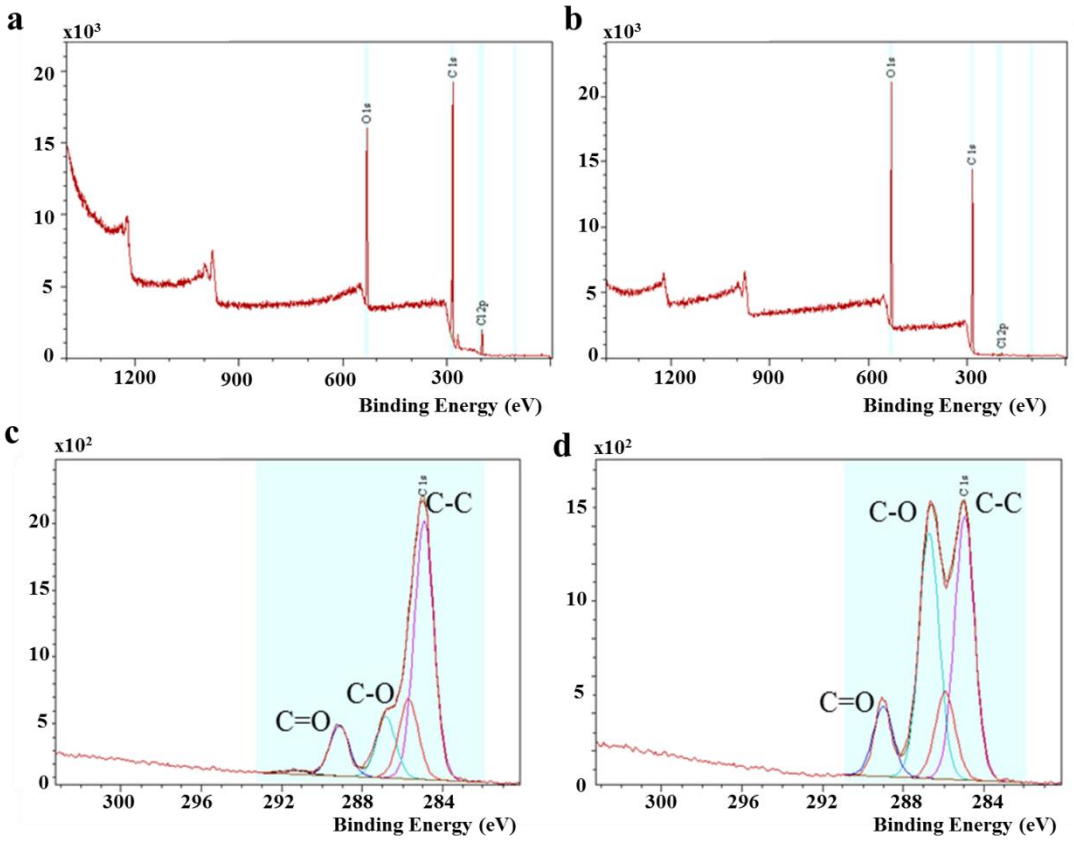


Figure 4.5: XPS survey spectra of (a) PCMS and (b) PCMS- PDEGMA microspheres (2.1 µm) which have been prepared from 1:150 initiator;monomer ratio. (c) and (d) are high resolution carbon spectra of PCMS and PCMS- PDEGMA (2.1 µm), respectively. The latter spectra show an increase in the proportion of methoxy groups corresponding to PDEGMA after grafting. Data analyses and curve fitting were carried out using CASAXPS software (version 2.3.16) (Casa software ltd, Teignmouth, United Kingdom). For high resolution carbon spectra all scans were charge corrected to C 1s at 284 eV.

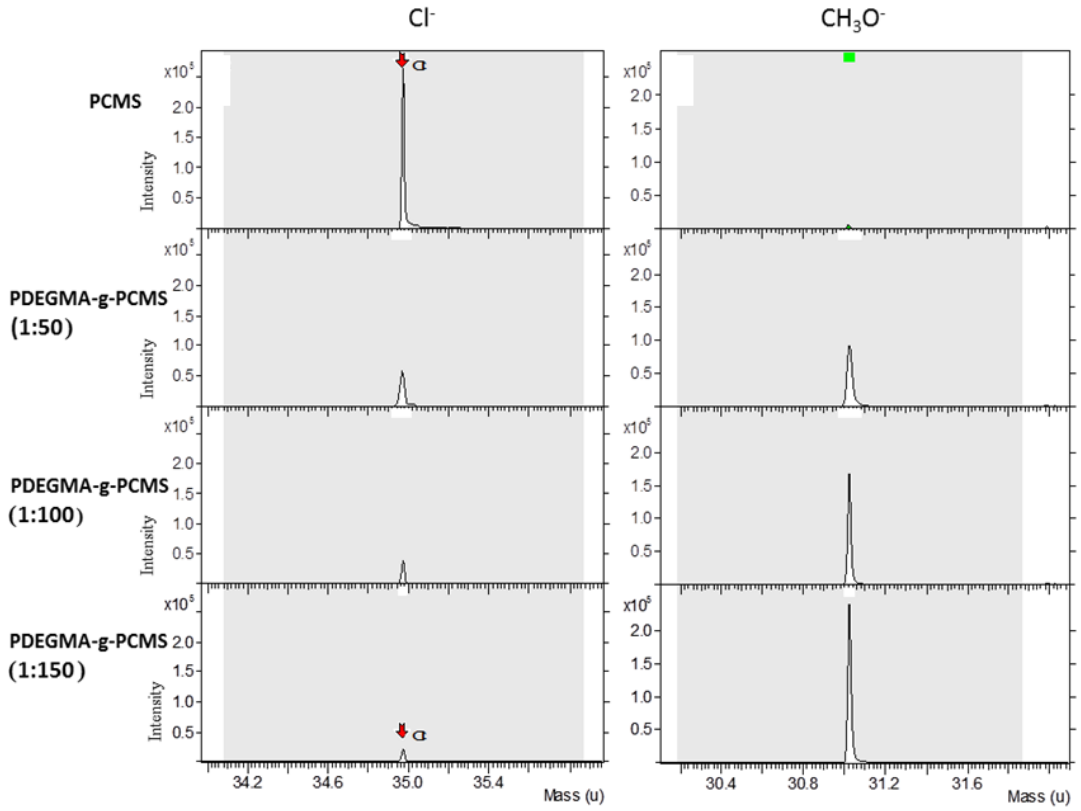


Figure 4.6: ToF-SIMS mass spectra of Cl^- and CH_3O^- present on the surface of PCMS and PCMS- PDEGMA (with different initiator: monomer ratio during grafting reactions). The spectra were obtained in the negative ion mode.

4.4.3. Thermal analysis

The extent of surface modification was quantified by thermo- gravimetric analysis (TGA) of linear PDEGMA polymer, PCMS particles and PCMS-PDEGMA particles (Figure 4.7). The PDEGMA thermogram showed a single step weight loss of 100% between 200 and 380°C. By comparison. PCMS particles exhibited two stages of decomposition, with the bulk of the polymer degraded between 400 and 500°C, with a second lower loss stage from ~800 to 1000°C. However, the PCMS-PDEGMA particles exhibited at least three transitions with temperature. A small weight loss occurring at ~ 100 °C was attributable to evaporation of water from the

partly hydrated PDEGMA chains, and a second loss stage between 200°C and 380°C which corresponded to decomposition of PDEGMA grafted on the surface of microspheres. The extent of weight loss for the second stage was ~ 15%, indicating the likely maximum of PDEGMA composition relative to the PCMS core. Further decomposition followed the same pattern observed for the PCMS microparticles, indicating also that the microparticles were composed of two distinct polymer types. However, at temperatures above 800°C no more weight loss occurred in the case of PCMS-PDEGMA and around 15wt% residue remained, which may be attributed to the mass of Fe_3O_4 nanoparticles loaded into the microspheres.

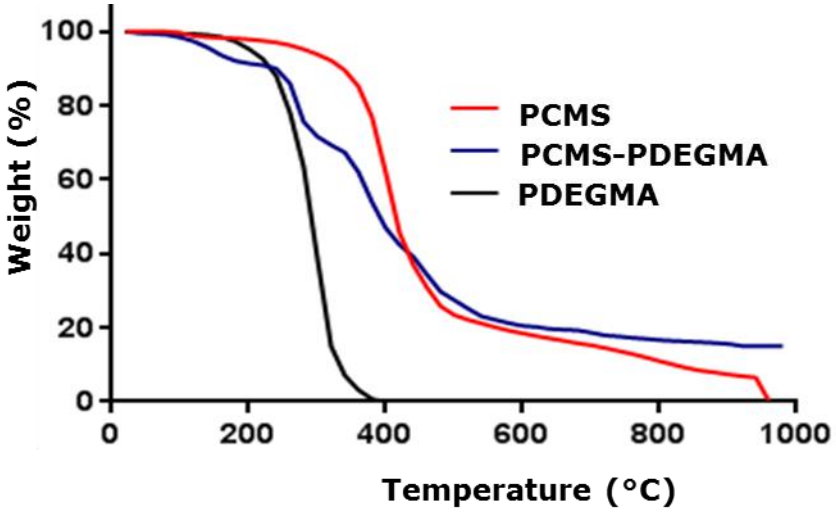


Figure 4.7: TGA thermogram showing the decomposition of PCMS microparticles, magnetic PCMS-PDEGMA microspheres (15% magnetite was loaded), and linear PDEGMA with temperature.

It was predicted that PDEGMA would grow from all accessible sites in the PCMS beads, as the microparticles were expected to be macroporous owing to their low degree of cross-linking and synthesis in polar solvents. The increase in overall size and roughness following grafting (Figure 24)

appeared to confirm this prediction. However, a surface layer of PDEGMA was also expected to be present, which would endow the microparticles with thermoresponsive properties in aqueous suspensions. Thus it was predicted that PCMS-PDEGMA microparticles would reversibly aggregate from water-based suspensions dependent on temperature whereas PCMS beads would not disperse irrespective of temperature. UV/ visible spectroscopy was used to confirm thermorespose particle aggregation by measuring the temperature dependent turbidity of dilute suspensions of PCMS and grafted particles over the temperature range from 10 to 60^{o}C. Suspensions of PDEGMA-grafted particles showed a marked decrease in turbidity from 20-40^{o}C whereas the ungrafted PCMS microsphere suspensions did not change in turbidity over this temperature range (Figure 4.8). A decrease in the absorbance with increase of temperature above the cloud point (as an approximation of the Lower Critical Solution temperature or LCST) of the free polymer is indicative of pronounced aggregation. The critical flocculation temperature (CFT) was taken as the onset of the decrease in absorbance as the temperature were increased, this was found to be ~ 22 °C for grafted particles which is very close to the cloud point of free PDEGMA polymer solution. Beyond this temperature the dispersions revealed intrinsic aggregation upon heating which was observed by a rapid decrease in absorbance. Below the phase transition temperature the PDEGMA brushes were chain extended on the surface of particles, thus stabilizing the particles but above the critical temperature the PDEGMA chains were collapsed leading to particle aggregation. These data indicated that growth of PDEGMA polymers from

the chloromethylstyrene residues was successful and resulted in an outer layer of thermoresponsive polymer on the microparticles.

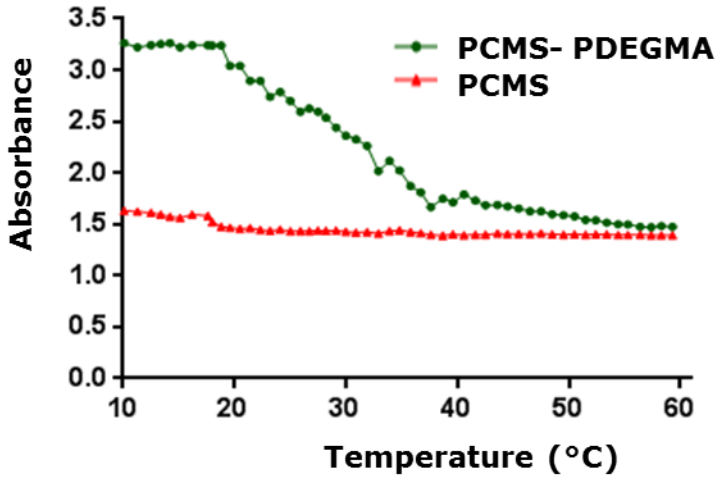


Figure 4.8: Temperature dependent turbidity measurements, showing the variation of absorbance as temperature increase of dilute suspensions of PCMS- PDEGMA and PCMS microspheres. Absorbances of the samples were measured at a wavelength of 550 nm.

Swelling of the microparticles in a good solvent for polystyrene ($CHCl_3$) enabled encapsulation of magnetite nanoparticles. The average sizes of the prepared magnetite nanoparticles were ~ 10 nm (Figure 4.9 a) Loading of the oleate coated magnetite nanoparticles was confirmed by TGA analysis (Figure 4.7) and magnetic response (Figure 4.9 c). Typically magnetite-loaded microspheres could be separated from suspensions within 2 minutes. Further TEM characterization (Figure 4.9 b) confirmed the penetration of magnetite nanoparticles into the microspheres.

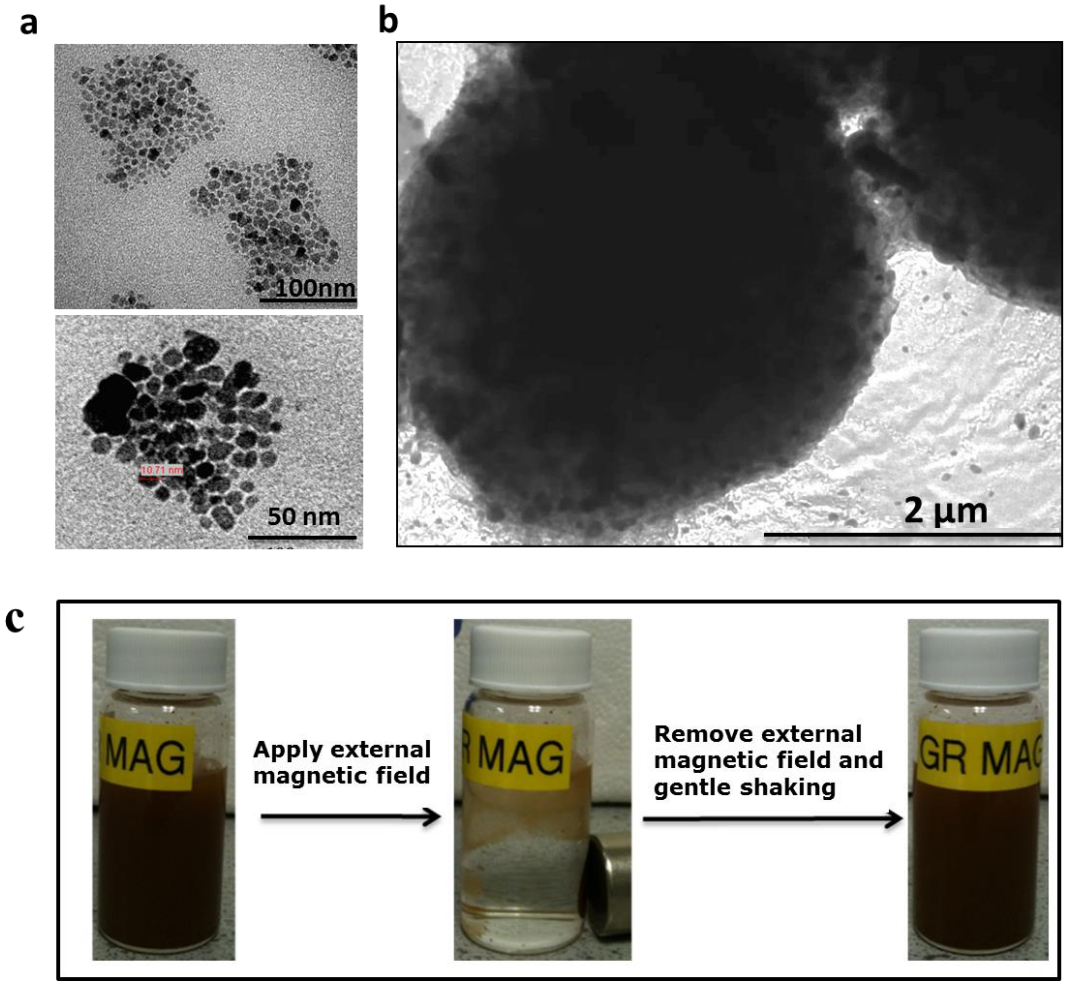


Figure 4.9: TEM images of (a) magnetite nanoparticles prepared by a co-precipitation method, showing individual particles with average diameters of ~10 nm. (b) Magnetic loaded microsphere showing the distribution of magnetite nanoparticles within the microsphere. (c) Photographic images of an aqueous suspension of magnetic magnetothermally responsive microspheres (magnetic PDEGMA-g-PCMS). It was observed that the particles were strongly attracted by an external magnetic field and easily re-dispersed by removing this magnetic field and with gentle shaking.

4.4.4. Colloidal gel evaluations

Temperature-mediated colloidal fluid-gel transitions were investigated initially by simple tube inversion tests. Images for these assays are presented in Figure 4.10 and a summary of the data are appended in Table 2. The suspensions showed thermoreversible association when the concentrations of particles were between 20-35% (weight/volume) for PCMS-PDEGMA, but magnetic PCMS-PDEGMA particles formed gels when the concentrations of particles were between 25-35%. It can be seen that magnetic PCMS-PDEGMA particles don't gel at 20, the reason should return to the higher density of magnetic microspheres and less volume occupied by these particles compared to the same weight of non magnetic ones. In contrast, suspensions prepared from PCMS particles did not show thermoreversible self-association over any range of concentrations. The suspensions made from 40% of magnetic and non magnetic PCMS-PDEGMA particles were like a paste at room temperature and were unable to due tube inversion tests for them.

Table 4.1: Tube inversion test results of particulate suspensions at different particle concentrations in DDW and/ or DMEM.

	Microspheres%						
	10	15	20	25	30	35	40
PCMS-PDEGMA in DW	-	-	+	+	+	+	paste
PCMS-PDEGMA in DMEM	-	-	+	+	+	+	paste
Magnetic PCMS-PDEGMA in DMEM	-	-	-	+	+	+	paste
PCMS in DMEM	-	-	-	-	-	-	-

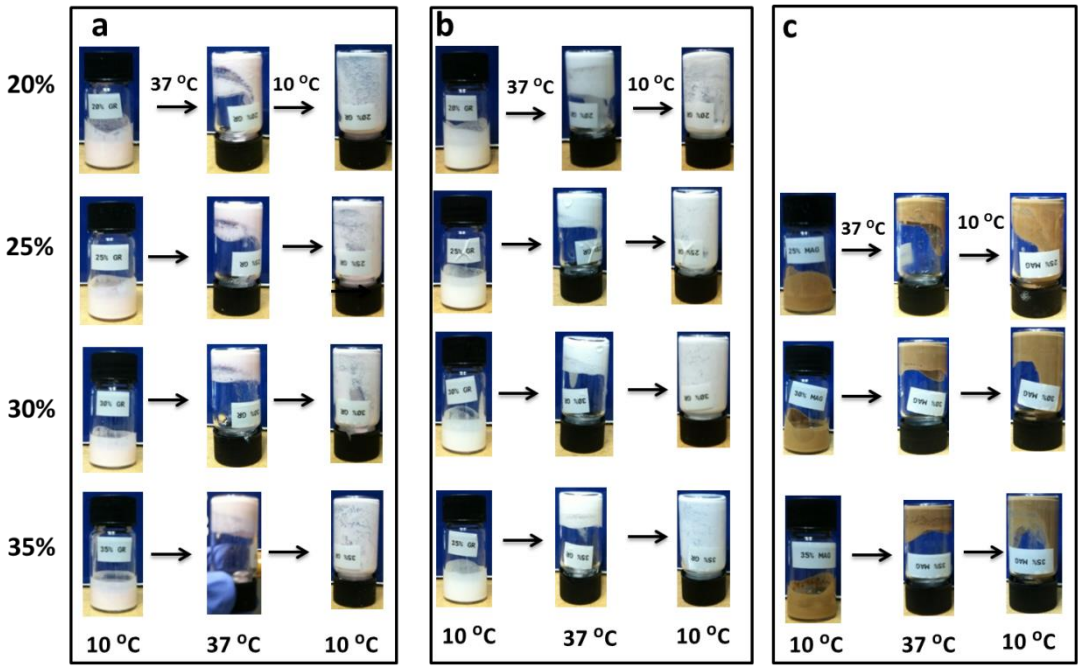


Figure 4.10: Images of tube inversion tests for different concentrations of particles. In (a) and (b) are shown PCMS-PDEGMA in cell culture medium and distilled water, respectively. In (c) magnetic PCMS-PDEGMA microparticles are shown in cell culture medium. Glass vial capacity 7 mL (Height 4.2 cm, Diameter 2 cm).

Overall tube inversion results showed that here (in this chapter) higher particle concentration were required to form thermoreversible colloidal gel Compared to the colloidal gels prepred via physical adsorption (chapter 3). This may return to the contribution of free chain collapsed polymers above their LCST to particle aggregation and gelation by depletion destabilisation and hydrophobic attraction.

4.4.5. Rheological studies

The mechanical and viscoelastic properties of magnetothermally responsive particulate suspensions/gels at different concentrations were investigated by rheometry. Magnetic PCMS-PDEGMA microspheres (2.1 μm) were have been used for making all suspensions/gels were used in

rheological measurments. Also, all the rheological measurements were have been performed for suspensions made in DMEDM because this medium has to be used in the future cell culture applications, not water.

Temperature ramp tests were performed to study the temperature dependent viscoelastic properties of aqueous suspensions made from PCMS and PCMS-PDEGMA. All the suspensions of the PCMS-PDEGMA particles displayed a temperature dependence of the storage modulus (G') above 20 °C. In contrast, suspensions prepared from PCMS particles did not show any temperature dependent elastic modulus within the same temperature range (figure 4.11 a). The elastic modulus was temperature-independent up to around 20 °C for suspensions prepared with a particle concentration of 25%, but a rapid increase in G' was observed above this temperature. This increase of G' appeared to shift to slightly higher temperatures as particle concentrations increased. The overall increase of G' for 35% particle suspensions was much lower than that of the sample at a concentration of 30%. This suggested that, at the higher concentration (35%), the network was formed of a larger number of elastically active links that resulted in larger maximum values. The gel-like structure thus became more persistent as the temperature increased, likely a consequence of increased (and stronger) contacts between 'crowded' microspheres, providing enhanced opportunity for attractive inter-particle associations. The PEGDMA-PEGDMA interactions at the surface changed from repulsive to attractive above the LCST which provided additional attraction to the interparticle bonds that were present. Also, temperature sweep tests (figure 4.11 c) showed reversible gelation and flow, as demonstrated through increased G' values upon

heating, and reduced G′ upon cooling. Furthermore, consecutive heating/cooling cycles of a suspension containing 30% particles (figure 4.11 d) confirmed their temperature responsive behaviour through multiple increases and decreases of G′ values with raising and lowering the temperature, respectively.

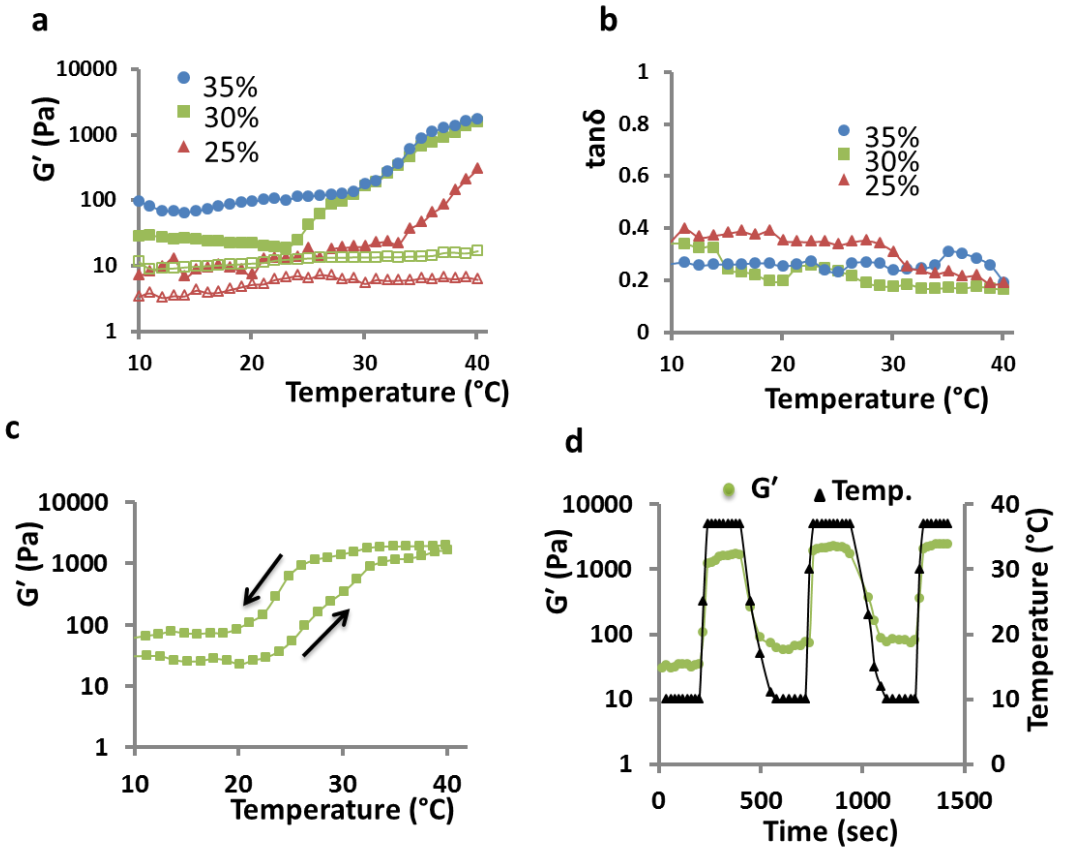


Figure 4.11: (a) and (b) Temperature ramp test showing variation of G′ and tan δ with temperature for magnetic PCMS-PDEGMA (filled marks) and magnetic PCMS particles (open marks) at different particle concentration, frequency 1 rad sec^{-1} and strain 0.05% were used. In (c) temperature sweep test shows reversible gelation and flow, and increased G′ values upon heating and reduced G′ upon cooling. In (d) is depicted multiple heating-cooling cycles of a suspension containing 30% particles which shows temperature driven Fluid-Gel-Fluid behaviour.

Temperature sweep test showed that the colloidal gel prepared via chemical grafting has lower elasticity moduli and the order of increase of G′ realtive to increase of temperature were lower too compared to the

colloidal gels prepred via physical adsorption (chapter 3). This may return to the contribution of free chain collapsed polymers above their LCST to increase overall elasticity of the gel.

Strain sweep tests were performed in order to identify the linear viscoelastic region (LVR), which is the range where G' is independent of strain. Beyond this region the breakdown of the gel structure was apparent from the rapid decline of *G'* at larger deformations. The gels transformed into liquid-like materials at the critical strain point (tan δ=1). It was observed that the LVR was dependent on the particle concentration. For all concentrations at low strains (less than 0.5%), *G'* was independent of the applied strain, suggesting the gels remained in the linear viscoelastic regime. For 25%, the linear viscoelastic region extended up to strain values around 1%. This value decreased proportionally with increased particle concentrations, most likely due to increases in the solid particle content that made the gel more fragile and less viscous (Figure 4.12 a). These results showed that chemical grafting produced more stable colloidal gel under strain compared to the colloidal gels prepred via physical adsorption (chapter 3). This may return to the permanent nature of attaching the thermoresponsive polymer to the surface of microspheres in this chapter.

The frequency sweep analysis indicated that the *G'* values were independent of frequency over the entire range for all particle concentrations that were studied (Figure 4.12 c). The tan δ values of all examined samples were much lower than 1 (i.e. storage modulus *G'* > loss modulus *G"*, typical of gel state). It was also observed that *G'* values increased, denoting a higher elasticity gel, at higher sweep frequencies.

Increases in the particle concentration resulted in higher values of G' while the value of tan δ did not show any marked change. The fact that the tan δ values were less than 1.0 at room temperature (Figure 4.12 d) shows that the dispersions were gels at this point but there were weak inter-particle bonds present and these become strengthened at higher temperature. The low *G'* values accounted for the flow observed in the tube inversion tests at room temperatures. Under these conditions the microparticle suspensions were weak gels, which became fluid particle suspensions on the application of shear. The low overall magnitude of the G' values, for these systems were postulated to arise from the particle network consisting of aggregated micrometre-sized particles. In effect, each particle could be considered as a macro-crosslinker with weak chain-chain associative interactions via the collapsed PDEGMA layer above the polymer LCST. Attractive van der Waals interactions between the particles would also have been contributors to particle aggregation. Accordingly, the particle gel modulus increased as the number and density of linkages between the particles increased, but for the micrometre-sized particles in this study the number of interparticle contacts was relatively low (compared to sub-micrometre particles) due to the lower surface area-to-volume ratio. Hence, G' values associated with weak gels (~ 1000 Pa) were not unexpected for these colloidal systems due to the lower number of (physical) crosslinks per unit volume, and were in agreement with prior reports of related colloidal gels (Shahidan et al., 2013). Overall rheological data revealed that the colloidal gels prepared in this chapter have elastic modulud much less than the ones Synthesised in previous chapter. The reason should return

to the contribution of chain collapsed free polymer in the solution to increase gel elasticity. The colloidal gels prepred here has softer mechanical properties and may be more interesting for making scaffolds for soft tissue construction.

The frequency sweep results showed that the produced gels here has lower elasticity compared to the gel prepared from physical adsorption. This may also return to the strong contribution of aggregated free polymer to increase overall gel elasticity.

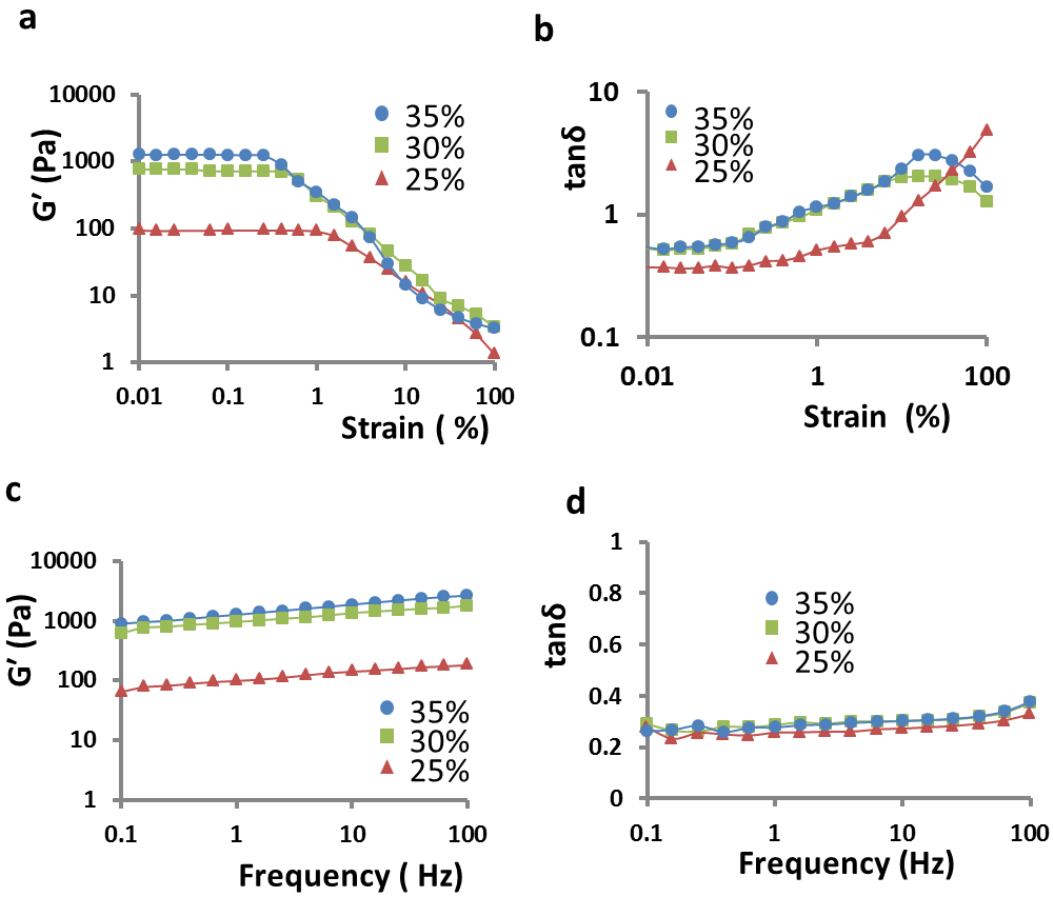


Figure 4.12: (a) and (b) strain sweep tests show the variation of G′ and tan δ with strain% for different magnetic PCMS-PDEGMA particle concentration, measured at frequency 1 rad sec^{-1} and 37°C . In (c) and (d) frequency sweep tests show variation of G′ and tan δ with frequency for different concentration of magnetic PCMS-PDEGMA particle suspension; strain 0.05% and temperature 37 °C were used during measurements.

Overall rheometric measurements showed that the produced gel in this chapter has the elasticity match to the soft gels which have low to moderate elasticities. These kind of colloidal gels have the potential in regenerative medicine applications, especially for non-load-bearing soft tissue repair (Shahidan et al., 2013).

4.5. Conclusions

Novel magnetothermally responsive core–shell microparticles have been synthesised. The aqueous suspensions of these particles exhibit fast thermoreversible fluid-to-gel transitions and retain good magnetic responsive properties. Rheological measurements demonstrated that the viscoelasticity of the prepared particle gels can be tuned, enabling these gels to have the mechanical properties that should facilitate their applications as 3D cell scaffolds for in vitro expansion of cells.

The new synthesised materials here in this chapter have the advantage over previous colloidal gel system in that the PDEGMA thermosensitive polymeric stabilizer is covalently grafted to the surface. This in turn will allows these materials to be used repeatedly for successive rounds of cell culture, without loss of the thermoresponsive polymer.

The next chapter will describe the applicability of the new developed thermoresponsive colloidal gels in this chaptes as scaffolds for *in vitro* cell expansion.

5. Study of the applicability of synthesised thermoresponsive magnetic colloidal gels for *in vitro* cell expansion

5.1. Introduction

Despite continuous development in tissue engineering and regenerative medicine, the exploitation of stem cells as therapeutic products remains challenging (Celiz et al., 2014). Recent studies and clinical trials have demonstrated the potential of these cells for the treatment of a range of conditions (Wei et al., 2013, Kim and Cho, 2013, Rodriguez et al., 2012, Farini et al., 2014, De Schauwer et al., 2013, Shekkeris et al., 2012). However, most stem cells are available only in rather limited numbers which are currently insufficient for widespread commercial or clinical use. Accordingly, primary cells must therefore be increased in number in a process termed 'expansion'. A variety of techniques have been used to help cells proliferate *in vitro* by either 2D or 3D cell culture models. There is now an increasing emphasis on 3D matrices due to significant problems associated with 2D culture (e.g. loss of phenotype) (Page et al., 2013) . In comparison to the traditional monolayer cell culture systems, 3D matrices provide higher surface areas to support growth to larger cell volumes and produce microenvironments which better mimic *in vivo* environments (Pampaloni et al., 2007, He et al., 2014).

Recently, several techniques have been developed to fabricate 3D scaffolds, consequently various kinds of polymeric scaffolds have been prepared for this purpose (Weigel et al., 2006, Li et al., 2014, Boffito et al., 2014). Although each method has certain advantages, none of the

existing techniques are able to solve all the fundamental problems linked to cell seeding, passaging, and harvesting. The essential requirements of an ideal scaffold for *in vitro* expansion are simplicity of cell seeding, mechanical stability and strength to support cell proliferation, and easy cell recovery after expansion.

Cell harvesting is still the main technical difficulty for most of the 3D cell culture methods. A particular problem is the requirement to use proteolytic enzymes such as trypsin to detach cells from support materials during passaging or after cell expansion. These enzymes can cause cleavage of membrane proteins and growth factor receptors thus altering the proteomic profile in mammalian cells (Umegaki et al., 2004, Garg et al., 2014, Steinber.Ms et al., 1973, Huang et al., 2010), which in turn might affect the ability of cells to adhere to further substrates and compromise their long term quality. Accordingly, there is a necessity for new materials that can support expansion of clinically relevant cell types and allow easy recovery of the cells after proliferation.

Stimuli-responsive polymers offer a means by which material properties can be switched (Liao et al., 2010, Nash et al., 2013, Rayatpisheh et al., 2012). Thermoresponsive polymers have been widely used as surface-modifiers to control cell adhesion and detachment (Dey et al., 2011, Xu et al., 2006, Chen et al., 2008, Xu et al., 2004, Mizutani et al., 2008, Zhang et al., 2006, Singh et al., 2008). Moreover, functionalised magnetic responsive microspheres have been widely used in biomedical separations (Bradbury et al., 2008, Widder et al., 1979, Zhang et al., 2016, Chung et al., 2009, Chen et al., 2010, Haik and Kanuri, 2008, Brandao et al., 2015).

Over the last decade, thermally reversibly-associating particles have been studied for growth and support of multiple cell types and for delivery of therapeutic cells (Al Ghanami et al., 2010, Wang et al., 2008, Fraylich et al., 2010b, Wang et al., 2009). In addition, coupling of thermoresponsive polymers to magnetite-containing microspheres has recently been shown to enhance the culture and expansion of stem cells, and facilitate rapid recovery of the expanded cell population by simple magnetic separation (Saeed et al., 2015).

In chapter 4 the preparation of reversible particulate suspension/gels that combine both thermo and magnetic responsive properties was shown. These materials might have considerable value in the expansion of therapeutically important cells for tissue engineering applications and have the advantage over previous colloidal gel systems (Al Ghanami et al., 2010, Wang et al., 2008, Fraylich et al., 2010b, Wang et al., 2009, Saeed et al., 2015) in that the PDEGMA thermosensitive polymeric stabilizer is covalently grafted to the surface.

5.2. Aims and objectives

The aim of the work described in this chapter was to investigate the applicability of prepared thermoresponsive magnetic colloidal gel from chapter 4, for *in vitro* expansion of mamalian cells. To achieve this aim, the following hypotheses were proposed:

Prepared dual responsive colloidal gels via chemical grafting can induce positive cellular response and good cytocompatibility to mammalian cells.

The new developed particle gel can be used as 3D cell scaffolds for *in vitro* expansion of mamalian cells. It can allow encapsulated cells to remain viable, adhere to the scaffold, and proliferate within the gel. Magnetic separation process can allow efficient and enzyme free cell recovery.

5.3. Materials and Methods

Mouse fibroblasts 3T3 and MSC cell lines were used in the following experiments. Cells were used within n+31 passages for 3T3 and n+4 passages for MSCs (from the initial passage at the cryopreservation). The particle gels used in the cell culture experiments were formulated to contain 30% w/v microparticles (see chapter 4).

5.3.1. Material sterilisation

All materials were sterilised before contact with cells through exposure to UV light at 280 nm for 60 minutes in a class II microbiology safety cabinet.

5.3.2. Cell culture and maintenance

All cell culture manipulations were performed using aseptic procedures in a Class II microbiology safety cabinet. 3T3 fibroblast cells and immortalised human mesenchymal stem cells (ihMSCs) were cultured in Complete Medium which consisted of Dulbecco's Modified Eagle Medium (DMEM)(Gibco, UK) supplemented with 10% foetal bovine serum (FBS), 1% antibiotic/antimycotic solution (contains 10,000 units/mL of penicillin, 10,000 µg/mL of streptomycin, and 25 µg/mL of amphotericin B), 1% L-glutamine (2 mM) and 1% non-essential amino acids (Sigma-

Aldrich, UK). Red fluorescent protein 3T3 cells (RFP-3T3) were derived and cultured as described elsewhere (Dixon et al., 2011).

All cells were maintained in T75 Nunc Flasks, in a humidified incubator at 37°C and with 5% CO_2. When they reached 70-90% confluence, they were passaged by rinsing once with PBS and incubation with 4 mL trypsin/EDTA solution (0.25%w/v trypsin, 2mM EDTA in PBS) for 5 minutes followed by addition of 6 mL of growth media to stop the activity of trypsin. The cells were collected by centrifugation at 180xg using a Sigma Laboratory centrifuge 3K15 (Scientific Laboratory Supplies, UK) for 5 minutes. The cell pellet was re-dispersed in fresh medium, and the cells were transferred to fresh tissue culture flasks.

Cell number standard curves were generated by measuring the fluorescence intensity of a seriouse of known numbers of both MSCs and 3T3 cells. The fluorescence intensity vs. the number of cells for each standard were plotted, and a regression line through the data points were determined using linear regression analysis. Cells were seeded and incubated for 4 hours to allow cell attachment prior to PrestoBlue conducted.

5.3.3. Cell culture on top of particle gels

The particle gels used in the cell experiments consisted of 30% w/v Magnetic PCMS-PDEGMA microspheres (2.1 μm) prepared as described in chapter 4. Typically, 300 μl of the particle suspension was added to each well in a 24 well-plate, and transformed into gels by incubating at 37 °C for 5 minutes. Unlabelled 3T3 and RFP-3T3 cells ($1x10^5$) dispersed in 300μl of media were seeded on top of the gels and maintained in

humidified incubator at 37°C. The cell nutrient medium (300µl Complete Medium) was changed every other day. The PrestoBlue viability assay was carried out on day 1, 3 and 6, following the manufacturer's instructions (Invitrogen, UK) with some modification to correct the background fluorescence. Individual samples were taken at each time point. The measurements were carried out in nine replicates. A standard calibration curve for 3T3 fibroblasts was used to determine the total number of viable cells.

5.3.4. Cell encapsulation and three dimensional cell cultures within the Colloidal Gels

The particle gels used in the cell culture experiments were formulated to contain 30% w/v microparticles. Aliquots of microparticle suspensions (300 µl) in Complete Medium were added to 24-well culture plates. While still fluid, Complete Medium (20 µl) containing approximately 1 x 10^5 3T3 or MSC cells was added with mixing. The plates were then placed in an incubator at 37 °C for 10 minutes to obtain individual particulate gels within which the cells were encapsulated. Further Complete Medium (300 µl) was added on top of the gelled suspensions and the plates were incubated at 37 °C until further experiments, imaging or viability assays were carried out. The cell nutrient medium was changed every 48 hr. The PrestoBlue assay was used to assess cell viability and proliferation. PrestoBlue viability assay was carried out on day 1, 3 and 6 for 3T3 cells and on day 1, 5 and 10 for MSCs, following the manufacturer's instructions (Invitrogen, UK) with some modification to correct the background fluorescence. Individual samples were taken for each time point. The measurements were carried out in nine replicates. The

standard calibration curve for 3T3 cells and MSCs were used to determine the total number of viable cells.

5.3.5. Trypsin-free cell recovery via magnetic cell separation and cell passages

Firstly, the cell-seeded colloidal gels were liquefied by cooling to 10 °C to release the cells, and the obtained suspensions were diluted in medium. Next, the mixtures were transferred to a glass tube and the colloidal particles were separated using a magnetic bar while the cells remained suspended in media. The cell suspension was mixed and the magnetic separation step was repeated three times in order to remove the magnetic particles. The separated suspension was then centrifuged (2000x g for 5 minutes), and the pellet was resuspended and seeded into tissue culture flasks. The cells were incubated at 37 °C for 3 hours in tissue culture flasks to permit cells to adhere. Finally, a PrestoBlue viability assay was performed to quantify the cell recovery.

5.3.6. Cell count and viability assessment for routine 2D cell culture

Cell counts and viability estimates were performed using a Trypan blue exclusion assay and a haemocytometer. Equal volumes of cell suspension and the Trypan blue solution (Invitrogen, UK) were mixed in an Eppendorf tube and left for 5 minutes at room temperature. The mixture was then placed in a Neubauer haemocytometer chamber viewed under a light microscope (10× objective). Dead cells, which lost membrane integrity, stained blue due to uptake of the dye, while live cells remained colourless. Cell number was calculated as follows: number of cells in 1

mm^3 x 10^4 multiplied by 2 to correct from 1:2 dlution from the trypan blue.

5.3.7. Statistical analysis

GraphPad Prism analysis software (Version 6) was used for statistical analysis. Differences among groups were determined by One-way ANOVA Multiple Comparisons Test and the differences were considered to be significant if $p < 0.05$.

5.3.8. Live/Dead cell viability assay

A Live/Dead cell viability/cytotoxicity assay (Molecular Probes) was used for evaluating the viability of encapsulated cells within the colloidal gels. The double colour fluorescent staining assay was performed following the manufacturer's instructions on days 5 and 10. Stained cells were imaged using a confocal laser scanning microscope (Leica TCS SPE Macro-Confocal) with appropriate filter sets. Live cells displayed bright green fluorescence (calcein AM), whereas dead cells fluoresced red (ethidium homodimer-1).

5.3.9. Confocal microscopy cell imaging

RFP -3T3 cells cultured within particle gels were imaged using Confocal Laser Scanning Microscopy (CLSM). A Zeiss LSM 510 Meta laser scanning confocal microscope, equipped with a 543 nm HeNe laser was used. Images were taken at 10x and 40x magnification. Also confocal laser scanning microscopy (Leica TCS SPE Macro-Confocal) with appropriate additional filters was used to perform Live/Dead cell viability/cytotoxicity assays.

5.3.10. Fluorescence microscopy

RFP-3T3 cells cultured on top and within the colloidal gels were imaged by fluorescence microscopy using a Nikon Eclipse TS 100 inverted microscope configured with an Epi-fluorescence attachment.

5.4. Results and discussion

This chapter comprises the investigations of prepared colloidal gels to promote positive cellular responses with regards to cell adhesion, viability and proliferation. The standard calibration curves for 3T3 cells and MSCs were used to quantify the total cell numbers throughout this chapter (figure 5.1) which show the linear response of PrestoBlue fluorescence to cell number between 0.1 x 10^6 and 1 x 10^6 cells.

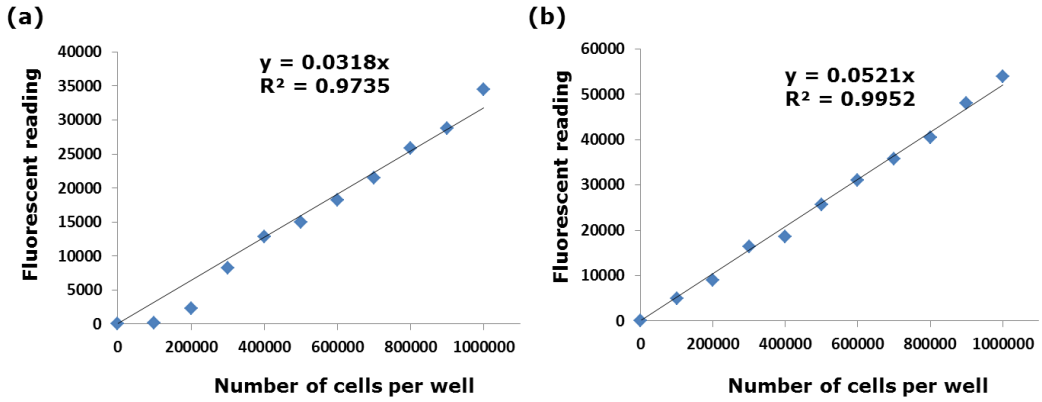


Figure 5.1: (a) 3T3 and (b) MSCs cell number standard curve determined using the PrestoBlue assay, cells were harvested from conventional 2D T75 culture flasks and counted using a haemocytometer and Trypan Blue dye exclusion. Serial dilutions were made to give appropriate cell, seeding numbers. (n = 3, average of three readings).

In the first stage, 3T3 fibroblasts cells were used as a model cell for investigating any possible cytotoxicity of newly developed materials because 3T3 cells are easily cultivated, are adhesion dependent, and widely used as a model cell in biocompatibility studies of polymeric

scaffolds (Bashur et al., 2006, Zhu et al., 2006). In the next stage, both 3T3 and human MSCs were used for investigation of the applicability of the developed material as 3D cell constructs for expansion and recovery of cells after proliferation. MSCs are the most widely investigated stem cells for therapy and have offered promise in the treatment of many diseases (Wei et al., 2013, Kim and Cho, 2013, Rodriguez et al., 2012, Larsen and Lewis, 2011, Chanda et al., 2010, Myers et al., 2010, Wang et al., 2012b, De Schauwer et al., 2013, Farini et al., 2014, Hanson et al., 2010a, Hanson et al., 2010b, Mariani and Facchini, 2012, Meirelles and Nardi, 2009, Shekkeris et al., 2012).

5.4.1. Evaluation of cell compatibility on the top of colloidal gels

Cytocompatibility was initially assessed with respect to two main criteria: cytotoxicity and cell adhesion, followed by prolonged culture of cells on colloidal gels surface while observing the adopted cellular morphology and cell proliferation patterns. A 3T3 fibroblastic cell line was selected for these studies, and *in vitro* methods were used. PCMS-PDEGMA particle gels were investigated initially by culturing cells on their surface. The gels selected consisted of 30% magnetic PCMS-PDEGMA particles suspended in complete medium. At this composition, the gels had sufficient mechanical strength to sustain the manipulations during cell culture. For any biomaterial, the surface structure in addition to composition can influence cell adhesion and proliferation (Jiao and Cui, 2007). Previous research has shown that the nano- and micro-structure of the surface affect various aspects of cell behaviours such as cell adhesion, cell spreading, cell orientation, mechanotransduction and gene

expression (Curtis and Dalby, 2009). This was taken into consideration when studying the cellular response to the particle gels.

One of the main advantages of prepared reversibly assembling colloidal gel is the ability to passage cells without using a trypsinization process or other biochemical cell detachment method, a required step to detach cells from most substrates including current 2D and 3D matrices. The surface properties of the microparticles were likely to be dominated by the presence of the PDEGMA corona, which exhibited temperature-induced changes in bound water. Consequently, above its coil-to-globule transition temperature the microparticle surfaces lost steric stabilisation from extended hydrated polymer chains and became more hydrophobic. In turn this reduced barriers to cell-particle attachment, allowing cells to adhere to the gel and proliferate. On reduction of the suspension temperature to below the expected lower critical solution temperature of PDEGMA (<25°C), the polymer chains became hydrated and chain-extended, resulting in cell detachment from the microparticle surfaces. This phenomenon of thermoreversible bioadhesion has been observed previously with grafted PEGMA polymers on various substrates (Dworak et al., 2013, Dey et al., 2011, Mertoglu et al., 2005, Brown et al., 2005, Wischerhoff et al., 2008b, Kessel et al., 2010).

The viability and proliferation of 3T3 cells cultured on the particle gels surface were quantified using the PrestoBlue viability assay (figure 5.2 a). The increase in cell metabolic activity with longer culture suggested that the cells were viable and proliferating. However, cell proliferation was slower on the particle gels than it was on conventional tissue culture plates used as a control (figure 5.2 b). This can be attributed

to the large differences in the surface properties between these two substrates. Previous research has shown that an increase of surface roughness and disorder can lead to increase of cell differentiation and synthesis of extracellular matrix with a corresponding decrease in cell proliferation (Wilson et al., 2005). It is possible that this is a plausible explanation for the slower cell proliferation on the colloidal gels. Statistical analysis showed significant increase of cell number (P value < 0.0001) over extended culture time, when they cultured either in 3D and 2D systems. However, the difference between these systems were not significant.

The opacity of the colloidal gels limited the range of imaging techniques that could be used to visualise the cells. RFP-3T3 cells were visualised by fluorescence microscopy to assess cell adhesion and growth on the top of the colloidal gels. Fluorescence microscopy images of RFP-3T3 cells cultured on the particle gels are shown in figure 5.3 a-d. After 1 day of seeding, single cells adhered to the gel surface, but with little increase in numbers. By day 3, the cells were well spread, and appeared to have proliferated in distinct cellular zones or islands. Cells were much more numerous and covered most of the sample surface on day 6 post seeding. However, more cell proliferation and spread single cells were seen on the tissue culture plate (figure 5.3 e-h), while the cells on the surface of PCMS-PDEGMA particle gels were mainly distributed in clusters/aggregates that became larger on longer culture. This could be attributed to the surface topography of the gels. Overall, fluorescence microscopy images indicated cell proliferation over longer culture times. This was also confirmed

using the PrestoBlue assay as described previously. (how does this assay confirming spreading of cell? Not evident from theseimages! Insufficient details)

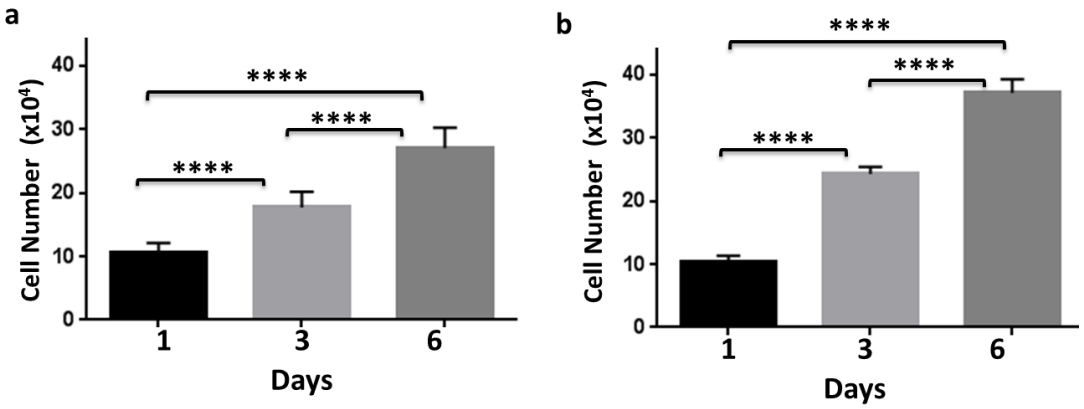


Figure 5.2: Proliferation of 3T3 cells cultured on the (a) colloidal gels and (b) tissue culture plates over 6 days, respectively. Cell numbers were measured by the PrestoBlue viability assay on day 1, 3 and 6. Error bars are ± standard deviations. (** represent P value < 0.0001). n= 9 (nine measurmentswere performed at each time point).**

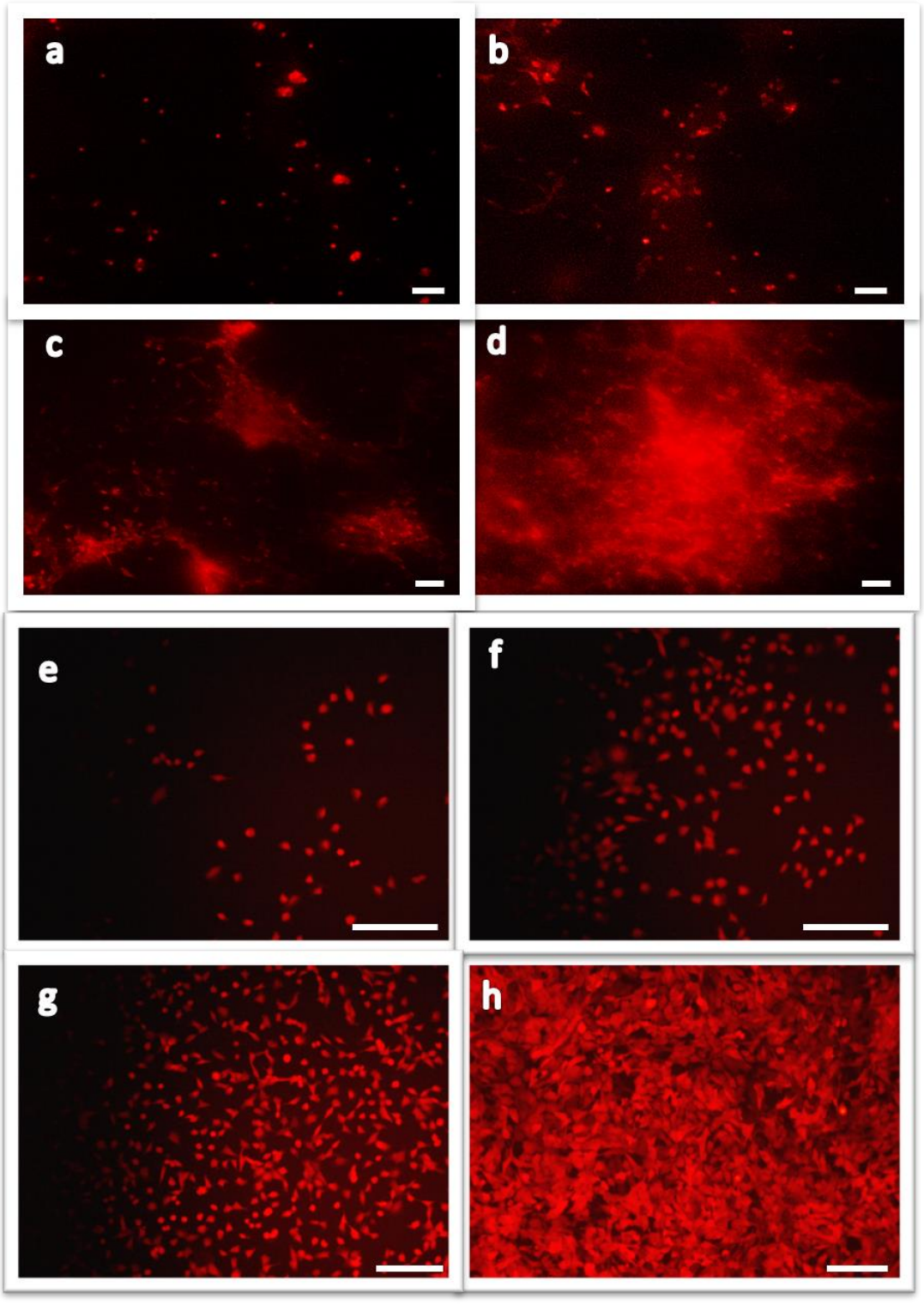


Figure 5.3: Fluorescence microscopy images of RFP-3T3 cells cultured over 6 days. (a) (b) (c) and (d) cells cultured on PCMS- PDEGMA magnetic colloidal gels on day 0, 1, 3 and 6, respectively. (e)(f)(g) and (h) cells cultured on tissue culture plate on day 0, 1, 3 and 6, respectively. *Scale bars - 100 µm.*

5.4.2. Application of thermoresponsive magnetic colloidal gels to 3D cell culture

The particle gels used as 3D scaffolds in this study contained 30% PCMS-PDEGMA particle suspensions. The temperature dependent fluid-to-gel transition of the particulate suspensions allowed for cell seeding by mixing the cells with the suspensions in their fluid state. Upon warming to 37°C, the rapid gelation locked the cells within the gel matrix, providing them with a 3D culture environment. A scaffold must maintain the viability of the encapsulated cells and support their proliferation and interaction to allow for neo-tissue formation. Cells at high density were seeded within the particle gels, to maintain sufficient cell interactions and communication. Figure 5.4 demonstrates the process of synthesis and application of thermoreversible PCMS-PDEGMA particle gel as 3D scaffolds for *in vitro* cell expansion.

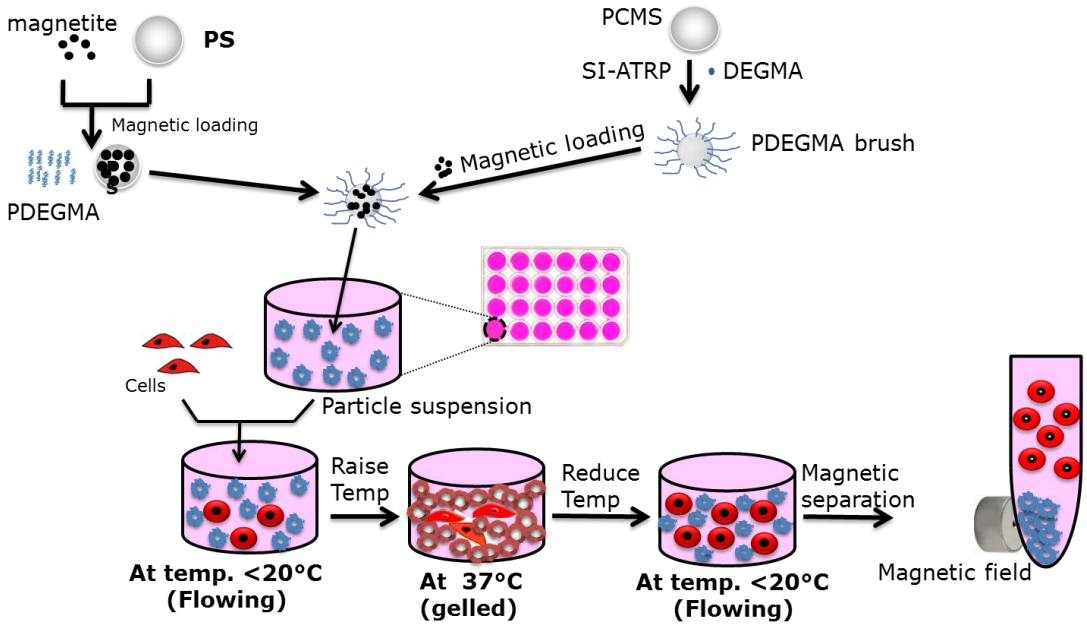


Figure 5.4: Schematic representation of the synthesis and application of thermoreversible PCMS-PDEGMA particle gel as 3D scaffolds for *in vitro* cell expansion. Reversible thermogelling behaviour allows easy cell seeding and encapsulation and the magnetic core allows cell harvesting after expansion.

A number of assays were carried out to evaluate the potential of the colloidal gels to be used in cell culture. Previous data had shown that PDEGMA adsorbed onto polystyrene-DVB microparticles with magnetic cores did not lead to any cytotoxicity in fibroblasts or stem cells (Saeed et al., 2015). Cell adhesion, distribution, viability and proliferation were thus evaluated. The thermoreversible fluid-to-gel transition of the colloidal gels allowed easy cell seeding when the gels were in their fluid state and good cell encapsulation within the colloidal gel matrix upon heating to 37°C. Incubation of cells within the colloidal gels proceeded without disruption of the gel structure. The surface properties of the microparticles were likely to be dominated by the presence of the PDEGMA corona, which exhibited temperature-induced changes in bound water. Consequently, above its coil-to-globule transition temperature the microparticle surfaces lost steric stabilisation from extended hydrated polymer chains and became more hydrophobic. In turn this reduced barriers to cell-particle attachment, allowing cells to adhere to the gel and proliferate. On reduction of the suspension temperature to below the expected lower critical solution temperature of PDEGMA (<25°C), the polymer chains became hydrated and chain-extended, resulting in cell detachment from the microparticle surfaces. This phenomenon of thermoreversible bioadhesion has been observed previously with grafted thermoresponsive polymers on various substrates (Dworak et al., 2013, Dey et al., 2011, Mertoglu et al., 2005, Brown et al., 2005, Wischerhoff et al., 2008b, Kessel et al., 2010).

PrestoBlue viability assays with 3T3 fibroblasts cultured within the prepared colloidal gel showed that the cells proliferated and remained viable with significant increases in cell number over time from 1.07×10^5 cells on day 1 to 2.9×10^5 on day 3 and 4.16×10^5 on day 6 of culture (figure 5.5 a). Significantly, mesenchymal stem cells (MSCs) also increased in number in the gels from 1.05×10^5 cells on day 1 to 2.5×10^5 on day 5 and 3.85×10^5 on day 10 (figure 5.5 b). From comparison of cells grown within the colloidal gel (3D) with cells grown in tissue culture plastic (2D), it was apparent (Figure 5.5 c and d) that the proliferation capacity on the 2D surface was lower than in the 3D gel. The total number of cells from the 3D matrices was higher compared to that for cells grown on the 2D wall plate surfaces. For instance, for the same cell seeding density on the 2D culture wall plate, the total numbers of 3T3 cells were 2.4×10^5 and 3.75×10^5 at day 3 and day 6, respectively, compared to 2.9×10^5 on day 3 and 4.16×10^5 for the 3D matrices. Similarly, the total MSC numbers were 2.1×10^5 and 3.41×10^5 at day 5 and day 10, respectively, again lower than those in the colloidal gels. Statistical analysis showed significant increase of cell number (P value < 0.0001) over extended culture time, when they cultured either in 3D and 2D systems. However, the difference between these systems were not significant. Overall, The encapsulated cells were viable over 6 days for 3T3 and 10 days for MSCs of culture, with evidence of proliferation from

the PrestoBlue quantification assays.

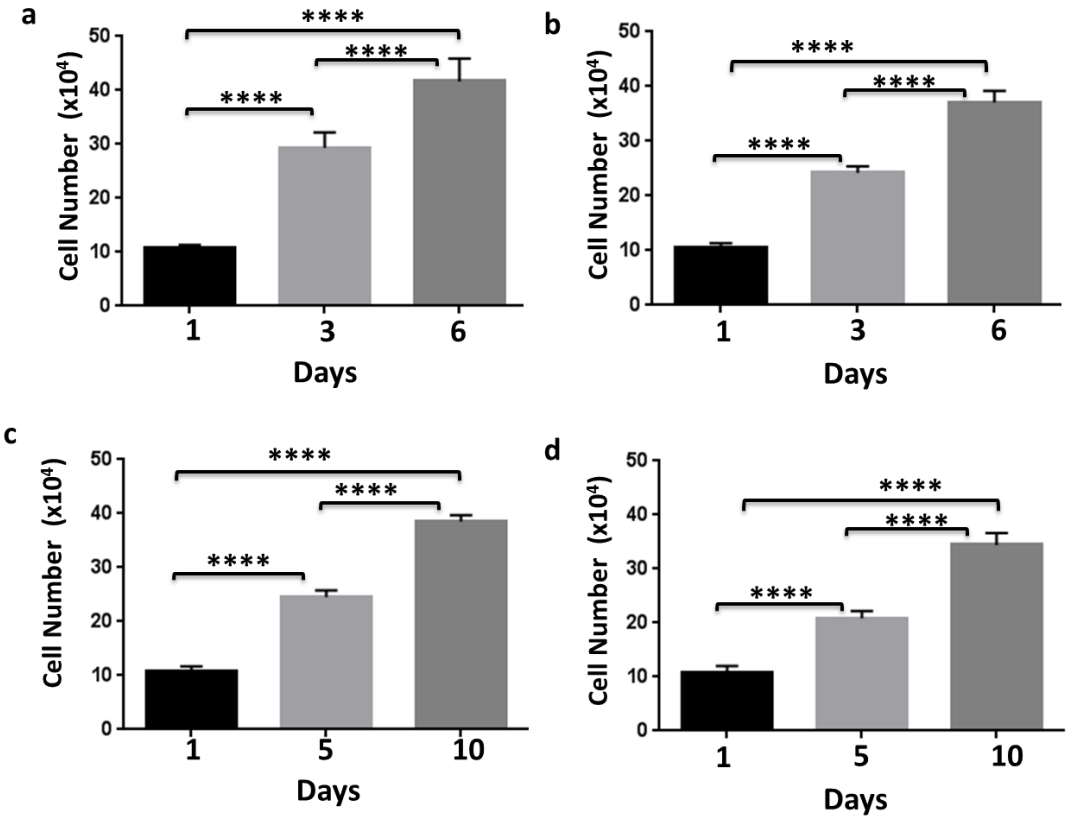


Figure 5.5: Proliferation of 3T3 cells cultured (a) within colloidal gel and (b) in tissue culture flask. (c) and (d) show proliferation of MSCs cultured within the particle gels and in tissue culture flasks, respectively. Cell numbers were measured by the PrestoBlue viability assay on day 1, 3 and 6 for 3T3 cells and on day 1, 5 and 10 for MSCs. Error bars are ± standard deviations. (** represent P value < 0.0001). n= 9 (nine measurmentswere performed at each time point).**

The assays described in the previous section are quantitative, but do not provide information on cell distribution within the gels. The opacity of the particle gels limited the range of imaging techniques that can be used to image the encapsulated cells. The common methods for imaging cells within 3D scaffolds include fluorescence or confocal microscopy. Fluorescence and confocal microscopy images (Figure 5.6 and 5.7, respectively) of 3T3 cells genetically modified to express red fluorescent protein (RFP-3T3) demonstrated that cells

adhered, remained viable, proliferated and retained normal similar morphology after repeat culture and release cycles, as seen in other studied (Cukierman et al., 2001, Ranella et al., 2010, Bhardwaj and Webster, 2015, Wang et al., 2014, Xie et al., 2012).

Live/Dead cell assays of MSC grown within the colloidal gel scaffold (Figure 5.8) in which viable and dead cells were stained with calcein AM (green) and ethidium homodimer-1 (red), respectively confirmed that cells grown within the colloidal gel were viable (green), with the number of dead cells (red).

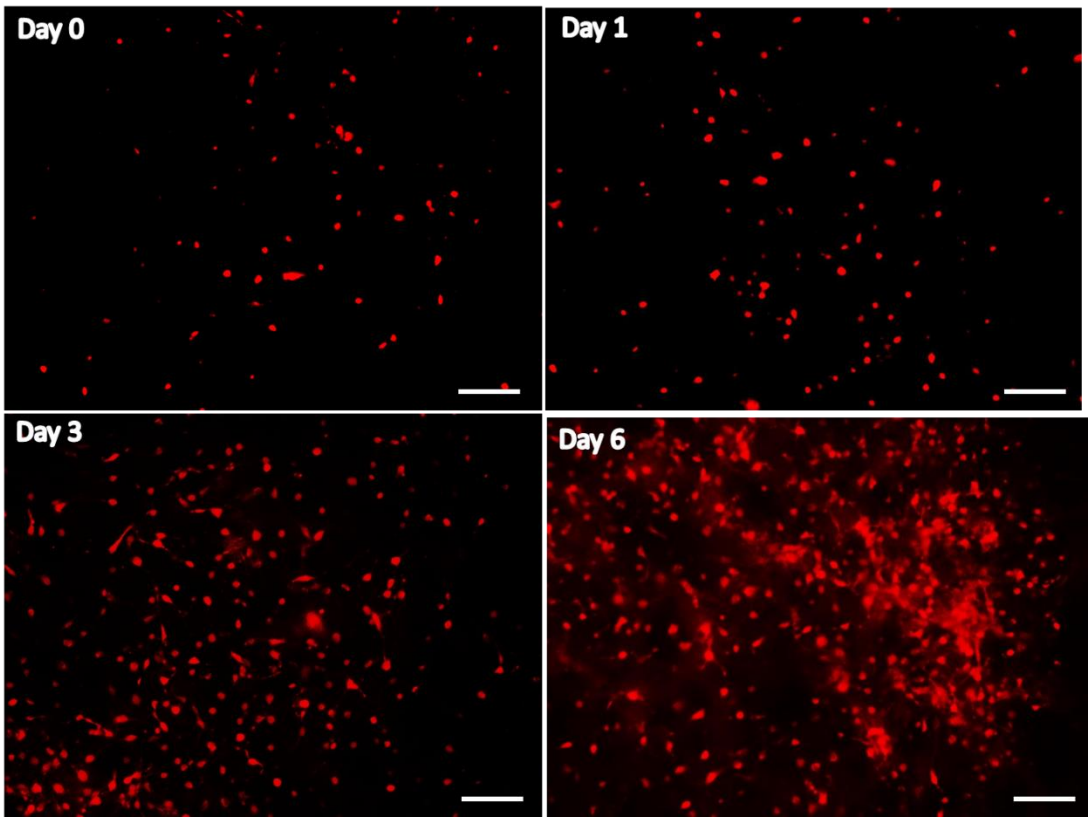


Figure 5.6: ***Fluorescence Microscopy Images of RFP-3T3 cells in 3D scaffold on day 0, 1, 3, and 6 post-seeding. Scale bars - 100 µm.***

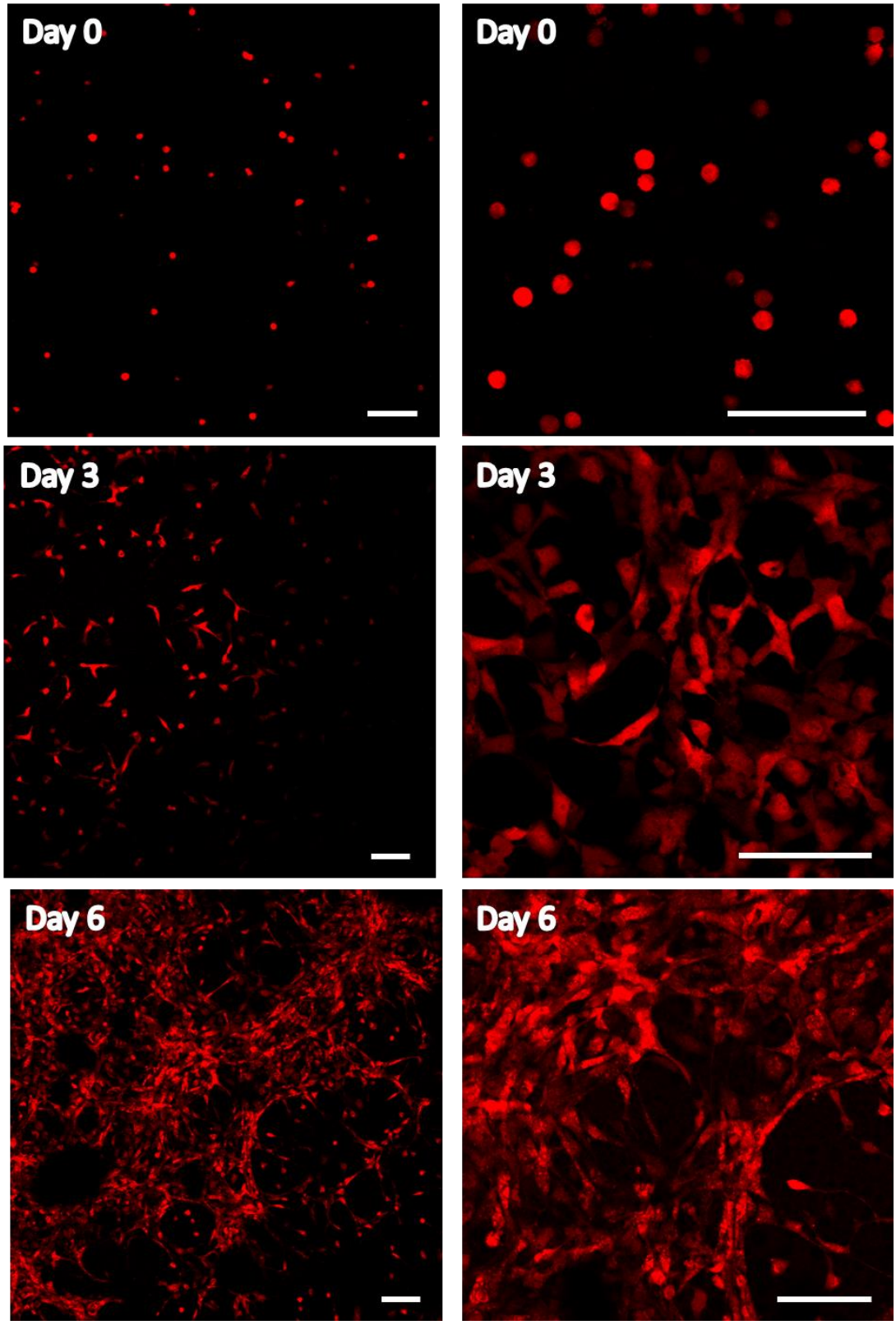


Figure 5.7: Confocal Microscopy Images of RFP-3T3 cells in 3D scaffold on day 0, 3, and 6 post-seeding. Images were taken at low (10X) and high (40X) magnification for the same samples. Scale bars - 100 µm.

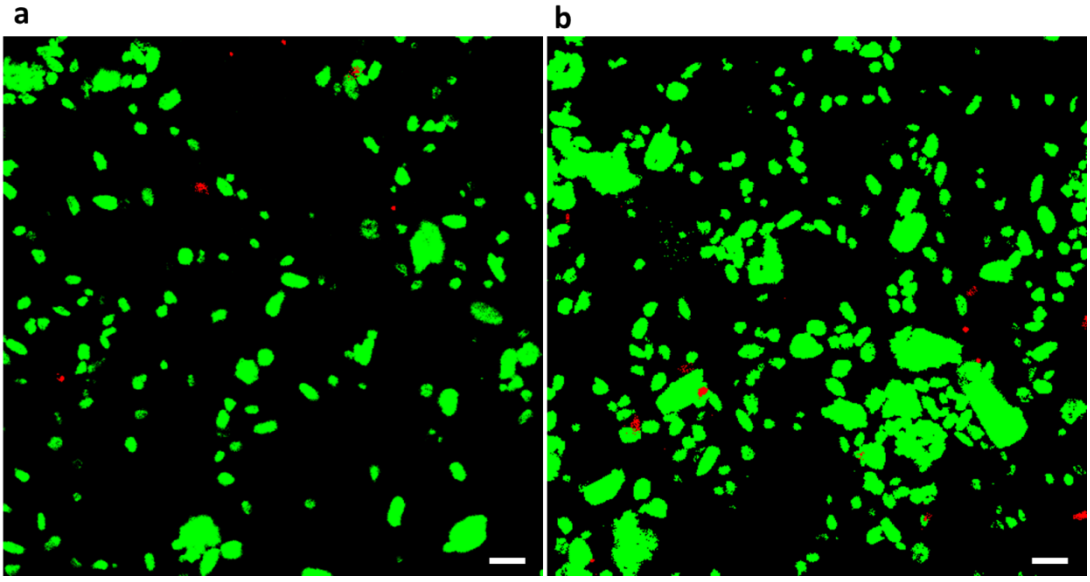


Figure 5.8: ***Confocal microscopic images represent Live/Dead assay of MSC grown within the colloidal gel scaffold at (a) 5 day and (b) 10 day. Green denotes cells staining positive for calcein AM (live) and red shows staining with ethidium homodimer (dead). Scale bars - 100 µm***

5.4.3. Cell recovery and passaging via Magnetic particle separation

Proof of principle experiments were performed to demonstrate the feasibility of cell recovery after expansion from magnetothermally responsive particulate suspension/gel. The cytocompatibility and applicability of the colloidal gels for *in vitro* cell proliferation were further explored in terms of the efficiency of cell recovery after expansion and to examine the possibility for multiple sequential cell passaging experiments without using trypsin.

Following three cycles of separation, the efficiency of cell recovery was quantified using the PrestoBlue viability assay and the total cell recoveries were recorded at days 3 and 6 for 3T3 cells and day 5 and 10 for MSC. The results showed a high recovery of 3T3 cells from the colloidal gel of 93.5% and 95.2% total cell content at day 3 and 6,

respectively. The recovery efficiencies for MSCs were 94.4% and 92.8% of cells at day 5 and 10, respectively as quantified by PrestoBlue assay (Figure 5.9 a and b).

The ability to support continuous cell proliferation and to carry out repeat passaging of cells with single batches of colloidal gel particles was also tested. Cells were grown in the gel matrices and magnetic separations were used as before to separate cells from the particles. The separated particles were then re-used to culture new batches of cells. The relevant data are shown in Figure 5.9 c and d; these results indicate that single batches of colloidal gel were suitable for multiple cycles of cell growth and separation. These experiments were performed with cooling cycles at 10 °C to effect the most rapid separations (typically 4 minutes per cycle). However, the same experiments could be performed with cooling cycles at room temperature with no loss in numbers of cells recovered. It should be noted that the overall numbers of separated and reloaded cells were less than when cells were continuously proliferated without separation. This was most likely due to incomplete separation of all cells at day 3 and 6 for 3T3 cells and at day 5 and 10 for MSC. The loss in number of cells was no more than 10 % after the third cycle, and it is likely that cell yields could be improved if slower processes of separation are performed or/and more diluted cell/particle suspension used. These steps would reduce the flow rates in the magnetic separation step and this might reduce co-aggregation of cells and particles. In addition, certain stages during the cell recovery procedure, specifically the heating/cooling or the wash/centrifugation steps, are likely to have contributed to the reduced efficiency of cell recovery from magnetic

thermoresponsive particle gels but the magnetic particles separation step did not appear to cause cell damage.

After performing the first separation cycle, a number of magnetic microparticles were found with the cells but after performing the second separation the numbers of these particles were reduced. After conducting the third separation cycle it was observed that no particles remained with the cells.

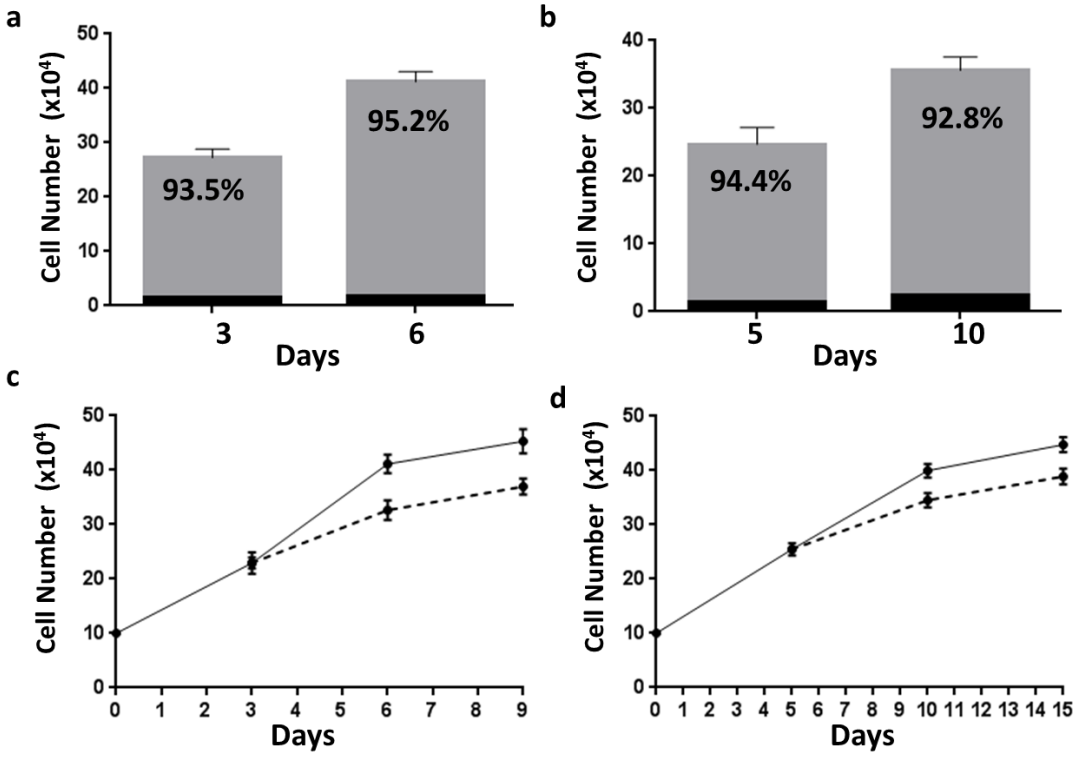


Figure 5.9: ***(a) and (b) the efficiency of the recovery of proliferated 3T3 and MSC within the colloidal gel by magnetic separation, respectively. The black region represent the number of unrecovered cells, after performed magnetic separation. (c) and (d) are 3T3 and MSC cell proliferation within the colloidal gel over time, respectively. Straight lines represent continuous cell proliferation without passage and dashed lines represent cell proliferation when passaged two times (on day 3 and 6 for 3T3 and on day 5 and 10 for MSC).*** **Error bars are ± standard deviations, n= 9.**

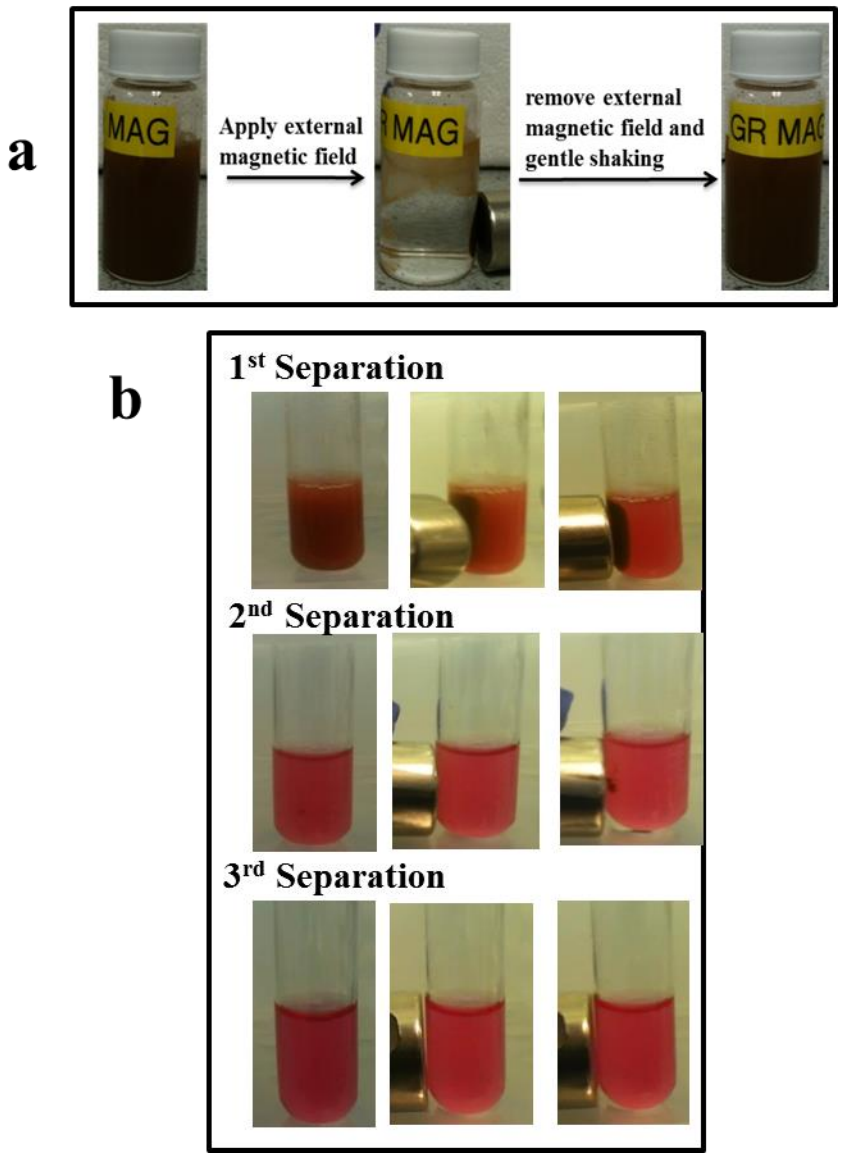


Figure 5.10: ***(a) Photographic images of aqueous suspension of magnetic and thermally responsive microspheres (magnetic PCMS-PDEGMA). It is observed that the particles are strongly attracted by external magnetic field and easily re-dispersed by removing this magnetic field and gentle shaking. In (b) images show magnetic separations over three separation cycles.***

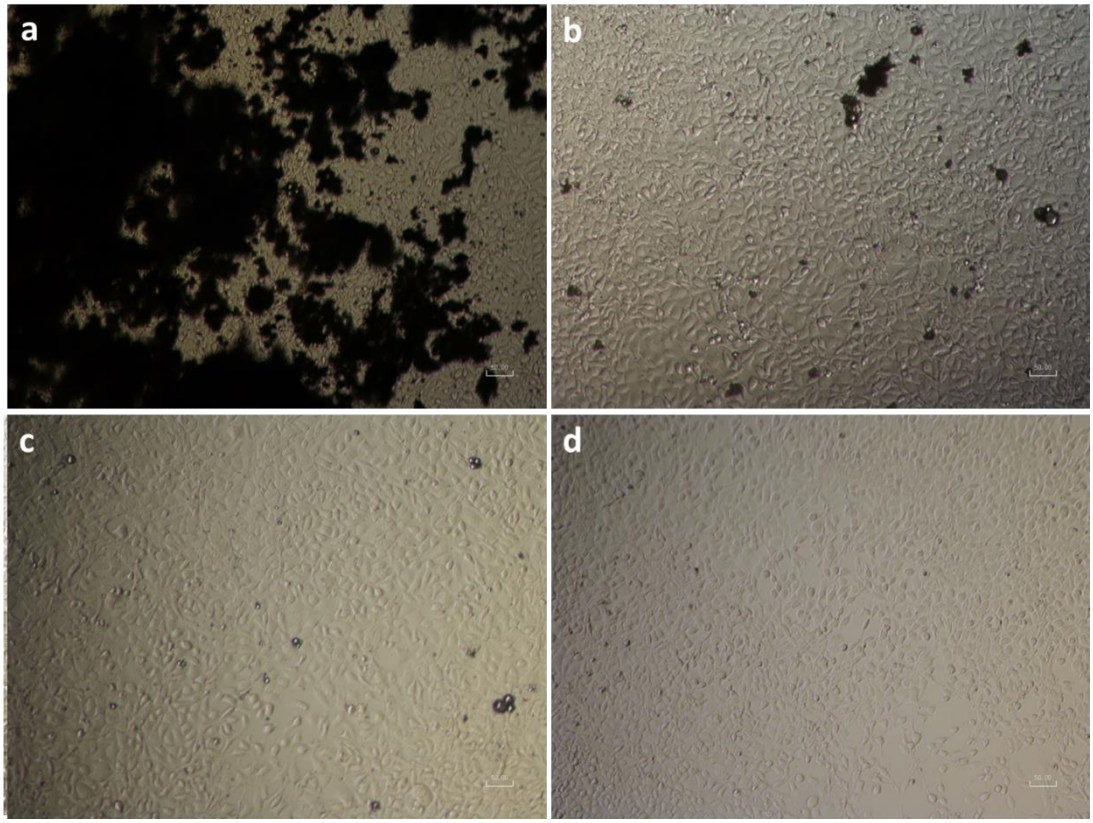


Figure 5.11: ***Representative light microscopy images of 3T3 cells recovered from the cell/particles mixture after successive magnetic separation process. The recovered cells were then cultured in TCP for 3 hours, then imaged. (a) without performing magnetic separation, many magnetic particles can be seen, (b) after performing first cycle separation, less particle are remaining, (c) after performing two susbsequent magnetic separation steps, few particle remaining with the cells, and (d) after three susbsequent magnetic separation steps, no further particles reman with the cells. Scale bar 100µm***

5.5. Conclusions

The overall results presented in this chapter revealed that the newly synthesised thermo and magnetic responsive colloidal gel were suitable for growth and support of cells for tissue culture applications. 3T3 cells adhered to the colloidal gel surface and were actively proliferating on the gel surface as confirmed by PrestoBlue assays and microscopy. These results confirm that the newly developed colloidal gels studied were biocompatible and didn't induce significant cell toxicity.

Moreover, PrestoBlue viability assays of 3T3 fibroblasts and MSCs cultured within the colloidal gel showed that the cells remained viable and proliferated, with significant increases in cell numbers over extended culture times. Furthermore, confocal microscopy images of 3T3 cells cultured within the colloidal gel demonstrated that cells adhered, spread and retained their normal morphologies during proliferation.

Finally, magnetic separation allowed efficient recovery of cells after their expansion *in vitro* without need for enzyme-mediated release steps. Trypsin-free cell passages were performed allowing multiple growths, separation and reloading of cells within the colloidal gels.

Overall, the results suggest this colloidal gel has potential as a 3D scaffold for *in vitro* expansion of a variety of cell types and for enzyme free cell harvesting.

6. Conclusions and future work

Over the last decade, thermally reversibly-associating particles have been studied for growth and support of multiple cell types and for delivery of therapeutic cells. Coupling of thermoresponsive properties to magnetic responsive properties in the same microspheres here in this thesis, would enhance the culture and expansion of stem cells, and facilitate rapid recovery of the expanded cell population by simple magnetic separation.

The work presented in this thesis describes the development of new types of colloidal gels that have dual thermo and magnetic responsive properties and their applicability as scaffolds for tissue engineering applications have been investigated. The newly developed materials can support expansion of clinically relevant cell types and allow enzyme free recovery of the cells after proliferation. The designed scaffolds possess most of the essential requirements of an ideal scaffold for *in vitro* cell expansion such as biocompatibility, simple cell seeding technique, mechanical strength and stability to support cell proliferation, and easy cell recovery after expansion. The superiority of these materials lies in the achievable level of control over their properties using mild stimuli such as temperature and/or magnetism, which opens up various avenues for applying these materials.

The designed colloidal gels have quick reversible thermogelling behaviour through using attached amphiphilic thermoresponsive polymer onto particle surfaces but also have strong magnetic responsive properties through embedding magnetite nanoparticles into the microsphere. Thermoresponsive properties allow easy cell seeding at temperatures

below the LCST of the polymer stabiliser and upon heating to above the LCST, cells were encapsulated and could be grown within the particle gels. The magnetic responsive property allowed easy and scaffold free cell recovery after expansion without the need for using trypsin or enzymatic treatment that can impact on the long term quality of the cultured cells.

The 'switchable' component of reversibly associating colloidal microparticles have been prepared either by physical adsorption of the thermoresponsive polymer which has been described in chapter 3 or by chemical grafting from particles which has been described in chapter 4. The most simple method i.e. physical adsorption is rapid and can be adapted to many microparticle surfaces but has the drawback of possible desorption of polymer chains during extended application. The chemical grafting method i.e. the formation of covalent bonds between the polymer corona and the microparticle core, provides robust and better-defined materials but is more complex and time-consuming. In both cases, particle aggregation in their suspensions occurred on increasing the temperature to above the LCST of PDEGMA, but could be reversed by cooling the suspensions back to below the LCST.

In chapter 3 thermoresponsive colloidal gel has been prepared by physical adsorption of PDEGMA onto PS microspheres. Polystyrene has been chosen to fabricate the microparticles, as this polymer is already widely used in cell culture assays. The thermoresponsive polymer selected was the biocompatible amphiphilic homopolymer PDEGMA, with its hydrophobic methacrylate backbone and hydrophilic PEG pendant side chains. This polymer previously has been used in tissue engineering to

control cell attachment/ detachment above and below its LCST temperature substrates (Dworak et al., 2013, Dey et al., 2011, Mertoglu et al., 2005, Brown et al., 2005, Wischerhoff et al., 2008b, Kessel et al., 2010). In addition, adsorbed thermoresponsive polymer has the ability to acts as a steric stabiliser below its LCST, and as flocculent above its LCST. PDEGMA could be synthesised by conventional FRP and its LCST was around 24 °C in deionised water.

Aqueous suspensions of magnetic PS/PDEGMA exhibited fast thermoreversible self-association behaviour combined with a simple magnetic separation stage. Rheological measurements to investigate the viscoelastic properties of PS/PDEGMA suspensions/ gels were observed that the gel elasticity and microstructure could be tuned by varying the temperature and the suspension compositions. The higher the temperature the higher the gel elasticity above the LCST due to the stronger interparticle attraction obtained. Also, increasing the concentration of both PDEGMA and/or PS microparticles in a range of concentration lead to increased gel elasticity. However, the effect of concentration of PS microspheres more obvious and were the most influential factor.

In chapter 4, a novel thermoresponsive magnetic colloidal gel has been prepared by chemical grafting from of PDEGMA onto functional PCMS microspheres. The newly developed colloidal gels have a key advantage over previous colloidal gel systems prepared by physical adsorption, in that the PDEGMA thermosensitive polymeric stabilizer is covalently grafted to the surface. This in turn allows these materials to be used repeatedly for successive rounds of cell culture without loss of the

thermoresponsive nature. The synthetic method was easily adaptable to incorporate magnetite nanoparticles into the thermoresponsive microparticles with retention of magnetic properties.

From comparison of colloidal suspensions/gels prepared by physical adsorption of PDEGMA (in chapter 3) with the one made by chemical grafting of PDEGMA (in chapter 4) it was observed that the first system showed gelation at lower concentration of particles and produced higher elasticity gels but less stable gels under applied strain. For example, in chapter 3 space filling gels were obtained when PS particle concentration was 10% w/v or higher for suspensions contain 4% of PDEGMA, while for grafted particles the gelation started at 25% particle concentration. This may return to the contribution of free chain collapsed polymers above their LCST to particle aggregation and gelation by depletion destabilisation and hydrophobic attraction. Moreover, the produced gels from physical adsorption have higher elasticity than those from chemical grafting. This may also return to the strong contribution of aggregated free polymer to increase gel elasticity. For example MPS/PDEGMA particle gels elasticity at 37 °C ranged between 3-700 kPa for gels containing 10-25% PS microparticles and 4% PDEGMA, while for grafted particles, colloidal gels elasticity at 37°C ranged between 0.1-1.5 kPa for gels containing 25-35% PCMS-PDEGMA microparticles.

In Chapter 5 the applicability of new developed particle gels (from chapter 4) as scaffolds for *in vitro* expansion of two types of mamalian cells has been studied. First the cytocompatibilty of this colloidal gel has been investigated by culturing 3T3 cells on the top of the prepared colloidal gels. PrestoBlue and microscopic imaging analysis results

showed that the gels supported the adhesion and proliferation of mouse NIH3T3 fibroblasts cultured on their surface over 9 days. In the next step, the ability to seed and culture cells within a 3D matrix formed by the self-assembling colloidal gel was evaluated. PrestoBlue viability assays of 3T3 fibroblasts and human mesenchymal stem cells cultured within the colloidal gel showed that the cells remained viable and proliferated, with significant increases in cell numbers over extended culture times. Confocal microscopy images of 3T3 cells cultured within the colloidal gel demonstrated that cells adhered, spread and retained their normal morphologies during proliferation. Furthermore, magnetic separation allowed efficient recovery of cells after their expansion *in vitro* without need for enzyme-mediated release steps. Trypsin-free cell passages were performed allowing multiple growth, separation and reloading of cells within the colloidal gels. Overall, the results suggest this colloidal gel has potential as a 3D scaffold for *in vitro* expansion of a variety of cell types and for enzyme free cell harvesting.

The uncertainty about homogeneous distribution of cells within the colloidal gels during extended culture time needs further investigations.

Future work

The materials developed and studied in this thesis may represent a significant contribution to the fields of biomaterials, tissue engineering, bio-separation and even drug delivery.

Although basic cellular responses such as cell adhesion, viability and proliferation have been investigated for the new developed colloidal

gelss. However, study of gene expression is still necessary to confirm the stemness maintenance in case of cultured MSCs.

The elasticity of the particle gels can be tuned over a wide range through changing the concentration of compositions. This property shows the importance of these colloidal gels for use in *in vitro* 3D differentiation of stem cells, as previous studies have shown that an obvious change in the adult stem cells niche can cause cell differentiation.

The colloidal gels can also be used for the *in vitro* construction of tissue models, as they offer an easily built three dimensional environment for cell culture. These tissues can be used in drug screening studies.

The developed particle gels would also have the potential in scalable cell culture for large scale production of therapeutic cells, thanks to their low cost, simple design, their 3D structure and physical associations, elasticity matching that of soft tissues, and combination of both thermo and magnetic responsive properties, which allow three dimensional cell proliferation and the scaffold free recovery of cells after expansion without the need for using enzymatic treatment, i.e. trypsin. This is a challenging area of research particularly with regards to stem cells.

References

ABBOTT, A. 2003. Cell culture: Biology's new dimension. *Nature,* 424**,** 870-872.

AHMED, F., ALEXANDRIDIS, P., SHANKARAN, H. & NEELAMEGHAM, S. 2001. The ability of poloxamers to inhibit platelet aggregation depends on their physicochemical properties. *Thrombosis and Haemostasis,* 86**,** 1532-1539.

AKBARZADEH, A., SAMIEI, M. & DAVARAN, S. 2012. Magnetic nanoparticles: preparation, physical properties, and applications in biomedicine. *Nanoscale Research Letters,* 7**,** 1-13.

AL GHANAMI, R. C., SAUNDERS, B. R., BOSQUILLON, C., SHAKESHEFF, K. M. & ALEXANDER, C. 2010. Responsive particulate dispersions for reversible building and deconstruction of 3D cell environments. *Soft Matter,* 6**,** 5037-5044.

ALAVA, C. & SAUNDERS, B. R. 2004. Effect of added surfactant on temperature-induced gelation of emulsions. *Langmuir,* 20**,** 3107-3113.

ALAVA, C. & SAUNDERS, B. R. 2005. Temperature-responsive emulsions: The effect of added surfactant. *Colloids and Surfaces a-Physicochemical and Engineering Aspects,* 270**,** 18-25.

ALAVA, C. & SAUNDERS, B. R. 2006. Polymer stabilisers for temperature-induced dispersion gelation: Versatility and control. *Journal of Colloid and Interface Science,* 293**,** 93-100.

ALBRECHT, D. R., UNDERHILL, G. H., WASSERMANN, T. B., SAH, R. L. & BHATIA, S. N. 2006. Probing the role of multicellular organization in three-dimensional microenvironments. *Nature Methods,* 3**,** 369-375.

ALEXANDRIDIS, P., HOLMQVIST, P. & LINDMAN, B. 1997. Poly(ethylene oxide)-containing amphiphilic block copolymers in ternary mixtures with water and organic solvent: effect of copolymer and solvent type on phase behavior and structure. *Colloids and Surfaces a-Physicochemical and Engineering Aspects,* 129**,** 3-21.

AMINI, A. A. & NAIR, L. S. 2012. Injectable hydrogels for bone and cartilage repair. *Biomedical Materials,* 7.

ARAKI, J., WADA, M. & KUGA, S. 2001. Steric stabilization of a cellulose microcrystal suspension by poly(ethylene glycol) grafting. *Langmuir,* 17**,** 21-27.

AREVALO, R. C., URBACH, J. S. & BLAIR, D. L. 2010. Size-Dependent Rheology of Type-I Collagen Networks. *Biophysical Journal,* 99**,** L65-L67.

ARMENTANO, I., DOTTORI, M., FORTUNATI, E., MATTIOLI, S. & KENNY, J. M. 2010. Biodegradable polymer matrix nanocomposites for tissue engineering: A review. *Polymer Degradation and Stability,* 95**,** 2126-2146.

BAI, Y. P., TENG, B., CHEN, S. H., CHANG, Y. & LI, Z. L. 2006. Preparation of magnetite nanoparticles coated with an amphiphilic block copolymer: A potential drug carrier with a core-shell-corona structure for hydrophobic drug delivery. *Macromolecular Rapid Communications,* 27**,** 2107-2112.

BASHUR, C. A., DAHLGREN, L. A. & GOLDSTEIN, A. S. 2006. Effect of fiber diameter and orientation on fibroblast morphology and proliferation on electrospun poly(D,L-lactic-co-glycolic acid) meshes. *Biomaterials,* 27**,** 5681-5688.

BAYRAKTAR, A., SARACOGLU, B., GOLGELIOGLU, C. & TUNCEL, A. 2012. Click-chemistry for surface modification of monodisperse-macroporous particles. *Journal of Colloid and Interface Science,* 365**,** 63-71.

BERENSMEIER, S. 2006. Magnetic particles for the separation and purification of nucleic acids. *Applied Microbiology and Biotechnology,* 73**,** 495-504.

BERTHIAUME, F., MAGUIRE, T. J. & YARMUSH, M. L. 2011. Tissue Engineering and Regenerative Medicine: History, Progress, and

Challenges. *Annual Review of Chemical and Biomolecular Engineering, Vol 2,* 2**,** 403-430.

BHARDWAJ, G. & WEBSTER, T. J. 2015. Increased NIH 3T3 fibroblast functions on cell culture dishes which mimic the nanometer fibers of natural tissues. *International Journal of Nanomedicine,* 10**,** 5293-9.

BICAK, N., GAZI, M., GALLI, G. & CHIELLINI, E. 2006. Polystyrene microspheres having epoxy functional dangling chains linked by hydrolytically stable bonds via ATRP. *Journal of Polymer Science Part a-Polymer Chemistry,* 44**,** 6708-6716.

BOFFITO, M., SARTORI, S. & CIARDELLI, G. 2014. Polymeric scaffolds for cardiac tissue engineering: requirements and fabrication technologies. *Polymer International,* 63**,** 2-11.

BONACCORSI, F., LEZZI, A., PREVEDELLO, A., LANZINI, L. & ROGGERO, A. 1993. Synthesis of Poly(4-Methylstyrene)-Graft-Poly(Ethylene Oxide)S and Application as Polymeric Dispersant in Coal Water Mixture. *Polymer International,* 30**,** 93-100.

BONTEMPO, D., TIRELLI, N., FELDMAN, K., MASCI, G., CRESCENZI, V. & HUBBELL, J. A. 2002. Atom transfer radical polymerization as a tool for surface functionalization. *Advanced Materials,* 14**,** 1239-+.

BORZACCHIELLO, A., GLORIA, A., MAYOL, L., DICKINSON, S., MIOT, S., MARTIN, I. & AMBROSIO, L. 2011. Natural/synthetic porous scaffold designs and properties for fibro-cartilaginous tissue engineering. *Journal of Bioactive and Compatible Polymers,* 26**,** 437-451.

BOYAN, B. D., LOHMANN, C. H., ROMERO, J. & SCHWARTZ, Z. 1999. Bone and cartilage tissue engineering. *Clinics in Plastic Surgery,* 26**,** 629-+.

BOYES, S. G., BRITTAIN, W. J., WENG, X. & CHENG, S. Z. D. 2002. Synthesis, characterization, and properties of ABA type triblock copolymer brushes of styrene and methyl acrylate prepared by atom transfer radical polymerization. *Macromolecules,* 35**,** 4960-4967.

BOYES, S. G., GRANVILLE, A. M., BAUM, M., AKGUN, B., MIROUS, B. K. & BRITTAIN, W. J. 2004. Polymer brushes - surface immobilized polymers. *Surface Science,* 570**,** 1-12.

BRADBURY, D., ANGLIN, E. J., BAILEY, S., MACARDLE, P. J., FENECH, M., THISSEN, H. & VOELCKER, N. H. 2008. Magnetic and Fluorescence Encoded Polystyrene Microparticles for Cell Separation. *Smart Materials V,* 7267.

BRADY, J. F. & VICIC, M. 1995. Normal Stresses in Colloidal Dispersions. *Journal of Rheology,* 39**,** 545-566.

BRANDAO, D., LIEBANA, S., CAMPOY, S., ALEGRET, S. & PIVIDORI, M. I. 2015. Immunomagnetic separation of Salmonella with tailored magnetic micro and nanocarriers. A comparative study. *Talanta,* 143**,** 198-204.

BREED, D. R., THIBAULT, R., XIE, F., WANG, Q., HAWKER, C. J. & PINE, D. J. 2009. Functionalization of Polymer Microspheres Using Click Chemistry. *Langmuir,* 25**,** 4370-4376.

BROMLEY, C. W. A. 1986. The Preparation of Sterically Stabilized Aqueous Lattices Using Polyethylene Oxide. *Colloids and Surfaces,* 17**,** 1-11.

BROWN, A. A., KHAN, N. S., STEINBOCK, L. & HUCK, W. T. S. 2005. Synthesis of oligo(ethylene glycol) methacrylate polymer brushes. *European Polymer Journal,* 41**,** 1757-1765.

BURDICK, J. A. 2012. Injectable gels for tissue/organ repair. *Biomedical Materials,* 7.

CARDENASVALERA, A. E., BAILEY, A. I. & DOROSZKOWSKI, A. 1995. Graft-Copolymers as Stabilizers for Oil-in-Water Emulsions .1. Synthesis of the Copolymers and Their Behavior as Monolayers Spread at the Air-Water and Oil-Water Interfaces. *Colloids and Surfaces a-Physicochemical and Engineering Aspects,* 96**,** 53-67.

CARTER, K. R., VON WERNE, T. A., GERMACK, D., HAGBERG, E. C., HAWKER, C. J. & BEINHOFF, M. 2003. Recent advances in contact molding for nanoscopic pattern transfer. *Abstracts of Papers of the American Chemical Society,* 225**,** U618-U618.

CASTLE, J. E. & BAKER, M. A. 1999. The feasibility of an XPS expert system demonstrated by a rule set for carbon contamination. *Journal of Electron Spectroscopy and Related Phenomena,* 105**,** 245-256.

CELIZ, A. D., SMITH, J. G. W., LANGER, R., ANDERSON, D. G., WINKLER, D. A., BARRETT, D. A., DAVIES, M. C., YOUNG, L. E., DENNING, C. & ALEXANDER, M. R. 2014. Materials for stem cell factories of the future. *Nature Materials,* 13**,** 570-579.

CHALMERS, J. J., XIONG, Y., JIN, X., SHAO, M., TONG, X., FARAG, S. & ZBOROWSKI, M. 2010. Quantification of Non-Specific Binding of Magnetic Micro- and Nanoparticles Using Cell Tracking Velocimetry: Implication for Magnetic Cell Separation and Detection. *Biotechnology and Bioengineering,* 105**,** 1078-1093.

CHANDA, D., KUMAR, S. & PONNAZHAGAN, S. 2010. Therapeutic Potential of Adult Bone Marrow-Derived Mesenchymal Stem Cells in Diseases of the Skeleton. *Journal of Cellular Biochemistry,* 111**,** 249-257.

CHANG, C. W., BAYS, E., TAO, L., ALCONCEL, S. N. S. & MAYNARD, H. D. 2009. Differences in cytotoxicity of poly(PEGA)s synthesized by reversible addition-fragmentation chain transfer polymerization. *Chemical Communications***,** 3580-3582.

CHANNELL, G. M. & ZUKOSKI, C. F. 1997. Shear and compressive rheology of aggregated alumina suspensions. *Aiche Journal,* 43**,** 1700-1708.

CHEN, B. Y., XU, F. J., FANG, N., NEOH, K. G., KANG, E. T., CHEN, W. N. & CHAN, V. 2008. Engineering cell de-adhesion dynamics on thermoresponsive poly(N-isopropylacrylamide). *Acta Biomaterialia,* 4**,** 218-229.

CHEN, F., SHI, R. B., XUE, Y., CHEN, L. & WAN, Q. H. 2010. Templated synthesis of monodisperse mesoporous maghemite/silica microspheres for magnetic separation of genomic DNA. *Journal of Magnetism and Magnetic Materials,* 322**,** 2439-2445.

CHEN, F. H. & TUAN, R. S. 2008. Mesenchymal stem cells in arthritic diseases. *Arthritis Research & Therapy,* 10.

CHEN, Z., MENG, H. A., XING, G. M., CHEN, C. Y., ZHAO, Y. L., JIA, G. A., WANG, T. C., YUAN, H., YE, C., ZHAO, F., CHAI, Z. F., ZHU, C. F., FANG, X. H., MA, B. C. & WAN, L. J. 2006. Acute toxicological

effects of copper nanoparticles in vivo. *Toxicology Letters,* 163**,** 109-120.
CHENG, N., BROWN, A. A., AZZARONI, O. & HUCK, W. T. S. 2008. Thickness-Dependent Properties of Polyzwitterionic Brushes (vol 41, pg 6317, 2008). *Macromolecules,* 41**,** 8288-8288.
CHEVIGNY, C., GIGMES, D., BERTIN, D., JESTIN, J. & BOUE, F. 2009. Polystyrene grafting from silica nanoparticles via nitroxide-mediated polymerization (NMP): synthesis and SANS analysis with the contrast variation method. *Soft Matter,* 5**,** 3741-3753.
CHO, Y. H., ZHANG, Y. J., CHRISTENSEN, T., SAGLE, L. B., CHILKOTI, A. & CREMER, P. S. 2008. Effects of Hofmeister Anions on the Phase Transition Temperature of Elastin-like Polypeptides. *Journal of Physical Chemistry B,* 112**,** 13765-13771.
CHO, Y. S., SHIN, C. H. & HAN, S. 2016. Dispersion Polymerization of Polystyrene Particles Using Alcohol as Reaction Medium. *Nanoscale Research Letters,* 11.
CHOI, C., CHAE, S. Y. & NAH, J. W. 2006. Thermosensitive poly(N-isopropylacrylamide)-b-poly(epsilon-caprolactone) nanoparticles for efficient drug delivery system. *Polymer,* 47**,** 4571-4580.
CHOI, G. N. & KRIEGER, I. M. 1986. Rheological Studies on Sterically Stabilized Model Dispersions of Uniform Colloidal Spheres .2. Steady-Shear Viscosity. *Journal of Colloid and Interface Science,* 113**,** 101-113.
CHUNG, H. J. & PARK, T. G. 2007. Surface engineered and drug releasing pre-fabricated scaffolds for tissue engineering. *Advanced Drug Delivery Reviews,* 59**,** 249-262.
CHUNG, T. H., CHANG, J. Y. & LEE, W. C. 2009. Application of magnetic poly(styrene-glycidyl methacrylate) microspheres for immunomagnetic separation of bone marrow cells. *Journal of Magnetism and Magnetic Materials,* 321**,** 1635-1638.
CLAYFIEL.EJ & LUMB, E. C. 1966. A Theoretical Approach for Polymeric Dispersant Action .1. Calculation of Entropic Repulsion Exerted by Random Polymer Chains Terminally Adsorbed on Plane Surfaces and Spherical Particles. *Journal of Colloid and Interface Science,* 22**,** 269-&.
CORNER, T. & GERRARD, J. J. 1982. Graft-Copolymers of Methyl-Methacrylate and Alpha-Methylstyrene Sulfonate - Preparation and Use as Stabilizers in Aqueous-Electrolyte Solutions. *Colloids and Surfaces,* 5**,** 187-195.
CRINGUS-FUNDEANU, I., LUIJTEN, J., VAN DER MEI, H. C., BUSSCHER, H. J. & SCHOUTEN, A. J. 2007. Synthesis and characterization of surface-grafted polyacrylamide brushes and their inhibition of microbial adhesion. *Langmuir,* 23**,** 5120-5126.
CROUCHER, M. D., LOK, K. P., WONG, R. W., DRAPPEL, S., DUFF, J. M., PUNDSACK, A. L. & HAIR, M. L. 1985. Use of Sterically Stabilized Polymer Colloids as Electrostatically-Based Liquid Developers. *Journal of Applied Polymer Science,* 30**,** 593-607.
CROWL, V. T. & MALATI, M. A. 1966. Adsorption of Polymers and Stability of Pigment Dispersions. *Discussions of the Faraday Society***,** 301-&.

CUKIERMAN, E., PANKOV, R., STEVENS, D. R. & YAMADA, K. M. 2001. Taking cell-matrix adhesions to the third dimension. *Science,* 294**,** 1708-12.
CURTIS, A. & DALBY, M. 2009. Cell response to nanofeatures in biomaterials. *Cellular Response to Biomaterials***,** 429-461.
DAS, B., GUO, X. & BALLAUFF, M. 2002. The osmotic coefficient of spherical polyelectrolyte brushes in aqueous salt-free solution. *Molecular Organisation on Interfaces,* 121**,** 34-38.
DAWKINS, J. V., MAGHAMI, G. G., SHAKIR, S. A. & HIGGINS, J. S. 1986. Nonaqueous Polymer Dispersions - Radical Dispersion Polymerization in the Presence of the Diblock Copolymer Poly(Styrene-B-[Ethylen-Co-Propylene]). *Colloid and Polymer Science,* 264**,** 616-618.
DAWKINS, J. V., NEEP, D. J. & SHAW, P. L. 1994. Nonaqueous Polystyrene Dispersions - Steric Stabilization by Partially Hydrolyzed Poly(Vinyl Alcohol) in Methanolic Media. *Polymer,* 35**,** 5366-5368.
DE SCHAUWER, C., MEYER, E., DE WALLE, G. V. & VAN SOOM, A. 2013. Current clinical applications of equine mesenchymal stem cells: update. *Vlaams Diergeneeskundig Tijdschrift,* 82**,** 327-336.
DELLINGER, J. G., CESARANO, J. & JAMISON, R. D. 2007. Robotic deposition of model hydroxyapatite scaffolds with multiple architectures and multiscale porosity for bone tissue engineering. *Journal of Biomedical Materials Research Part A,* 82A**,** 383-394.
DERUBEIS, A. R. & CANCEDDA, R. 2004. Bone marrow stromal cells (BMSCs) in bone engineering: Limitations and recent advances. *Annals of Biomedical Engineering,* 32**,** 160-165.
DEY, S., KELLAM, B., ALEXANDER, M. R., ALEXANDER, C. & ROSE, F. R. A. J. 2011. Enzyme-passage free culture of mouse embryonic stem cells on thermo-responsive polymer surfaces. *Journal of Materials Chemistry,* 21**,** 6883-6890.
DHANDAYUTHAPANI, B., YOSHIDA, Y., MAEKAWA, T. & KUMAR, D. S. 2011a. Fabrication and Characterization of Nanofibrous Scaffold Developed by Electrospinning. *Materials Research-Ibero-American Journal of Materials,* 14**,** 317-325.
DHANDAYUTHAPANI, B., YOSHIDA, Y., MAEKAWA, T. & KUMAR, D. S. 2011b. Polymeric Scaffolds in Tissue Engineering Application: A Review. *International Journal of Polymer Science*.
DICKINSON, E. 1995. Simulated Structure of Mixed Particle Gels. *Journal of the Chemical Society-Faraday Transactions,* 91**,** 51-58.
DICKINSON, E. 2000. Structure and rheology of simulated gels formed from aggregated colloidal particles. *Journal of Colloid and Interface Science,* 225**,** 2-15.
DIEDWARDO, C. A., PETROSKO, P., ACARTURK, T. O., DIMILLA, P. A., LAFRAMBOISE, W. A. & JOHNSON, P. C. 1999. Muscle tissue engineering. *Clinics in Plastic Surgery,* 26**,** 647-+.
DIMITROV, I., TRZEBICKA, B., MULLER, A. H. E., DWORAK, A. & TSVETANOV, C. B. 2007. Thermosensitive water-soluble copolymers with doubly responsive reversibly interacting entities. *Progress in Polymer Science,* 32**,** 1275-1343.
DIXON, J. E., DICK, E., RAJAMOHAN, D., SHAKESHEFF, K. M. & DENNING, C. 2011. Directed differentiation of human embryonic

stem cells to interrogate the cardiac gene regulatory network. *Mol Ther,* 19**,** 1695-703.

DRURY, J. L. & MOONEY, D. J. 2003. Hydrogels for tissue engineering: scaffold design variables and applications. *Biomaterials,* 24**,** 4337-4351.

DURAND, D., GIMEL, J. C. & NICOLAI, T. 2002. Aggregation, gelation and phase separation of heat denatured globular proteins. *Physica a-Statistical Mechanics and Its Applications,* 304**,** 253-265.

DWORAK, A., UTRATA-WESOLEK, A., SZWEDA, D., KOWALCZUK, A., TRZEBICKA, B., ANIOL, J., SIERON, A. L., KLAMA-BARYLA, A. & KAWECKI, M. 2013. Poly[tri(ethylene glycol) ethyl ether methacrylate]-Coated Surfaces for Controlled Fibroblasts Culturing. *Acs Applied Materials & Interfaces,* 5**,** 2197-2207.

EAGLSTEIN, W. H. & FALANGA, V. 1998. Tissue engineering for skin: An update. *Journal of the American Academy of Dermatology,* 39**,** 1007-1010.

EDERLE, J., DOBSON, J., FEATHERSTONE, R. L., BONATI, L. H., VAN DER WORP, H. B., DE BORST, G. J., LO, T. H., GAINES, P., DORMAN, P. J., MACDONALD, S., LYRER, P. A., HENDRIKS, J. M., MCCOLLUM, C., NEDERKOORN, P. J., BROWN, M. M., ALGRA, A., BAMFORD, J., BEARD, J., BLAND, M., BRADBURY, A. W., BROWN, M. M., CLIFTON, A., GAINES, P., HACKE, W., HALLIDAY, A., MALIK, I., MAS, J. L., MCGUIRE, A. J., SIDHU, P., VENABLES, G., BRADBURY, A., BROWN, M. M., CLIFTON, A., GAINES, P., COLLINS, R., MOLYNEWC, A., NAYLOR, R., WARLOW, C., FERRO, J. M., THOMAS, D., BONATI, L. H., COWARD, L., DOBSON, J., EDERLE, J., FEATHERSTONE, R. F., TINDALL, H., MCCABE, D. J. H., WALLIS, A., BROOKS, M., CHAMBERS, B., CHAN, A., CHU, P., CLARK, D., DEWEY, H., DONNAN, G., FELL, G., HOARE, M., MOLAN, M., ROBERTS, A., ROBERTS, N., BEILES, B., BLADIN, C., CLIFFORD, C., FELL, G., GRIGG, M., NEW, G., BELL, R., BOWER, S., CHONG, W., HOLT, M., SAUNDER, A., THAN, P. G., GETT, S., LEGGETT, D., MCGAHAN, T., QUINN, J., RAY, M., WONG, A., WOODRUFF, P., FOREMAN, R., SCHULTZ, D., SCROOP, R., STANLEY, B., ALLARD, B., ATKINSON, N., CAMBELL, W., DAVIES, S., FIELD, P., MILNE, P., MITCHELL, P., TRESS, B., YAN, B., BEASLEY, A., DUNBABIN, D., STARY, D., WALKER, S., CRAS, P., D'ARCHAMBEAU, O., HENDRIKS, J. M. H., VAN SCHIL, P., et al. 2010. Carotid artery stenting compared with endarterectomy in patients with symptomatic carotid stenosis (International Carotid Stenting Study): an interim analysis of a randomised controlled trial. *Lancet,* 375**,** 985-997.

ELAISSARI, A. 2006a. Thermally sensitive colloidal particles: From preparation to biomedical applications. *PROGRESS IN COLLOID AND POLYMER SCIENCE.*

ELAISSARI, A. 2006b. Thermally sensitive colloidal particles: From preparation to biomedical applications. *Smart Colloidal Materials,* 133**,** 9-14.

ELSTAD, N. L. & FOWERS, K. D. 2009. OncoGel (ReGel/paclitaxel) -- Clinical applications for a novel paclitaxel delivery system. *Advanced Drug Delivery Reviews,* 61**,** 785-794.

EVANS, S. 1997. Correction for the effects of adventitious carbon overlayers in quantitative XPS analysis. *Surface and Interface Analysis,* 25**,** 924-930.
FARAJI, M., YAMINI, Y. & REZAEE, M. 2010. Magnetic Nanoparticles: Synthesis, Stabilization, Functionalization, Characterization, and Applications. *Journal of the Iranian Chemical Society,* 7**,** 1-37.
FARINI, A., SITZIA, C., ERRATICO, S., MEREGALLI, M. & TORRENTE, Y. 2014. Clinical Applications of Mesenchymal Stem Cells in Chronic Diseases. *Stem Cells International*.
FEIGIN, R. I. & NAPPER, D. H. 1980. Depletion Stabilization and Depletion Flocculation. *Journal of Colloid and Interface Science,* 75**,** 525-541.
FEIL, H., BAE, Y. H., FEIJEN, J. & KIM, S. W. 1993. Effect of Polyelectrolytes on the Lower Critical Solution Temperature of Ionizable, Thermosensitive Polymers. *Makromolekulare Chemie-Rapid Communications,* 14**,** 465-470.
FILIPCSEI, G. 2008. Smart polymers for biomedical application and environmental protection. *Express Polymer Letters,* 2**,** 77-77.
FISCHBACH, C., CHEN, R., MATSUMOTO, T., SCHMELZLE, T., BRUGGE, J. S., POLVERINI, P. J. & MOONEY, D. J. 2007. Engineering tumors with 3D scaffolds. *Nat Methods,* 4**,** 855-60.
FOX, J. R., KOKOROPOULOS, P. C., WISEMAN, G. H. & BOWEN, H. K. 1987. Steric Stabilization of Stober Silica Dispersions Using Organosilanes. *Journal of Materials Science,* 22**,** 4528-4531.
FRANKS, G. V. 2005. Innovative applications of controlled particle interactions *Chemical Engineering Research and Design,* 83**,** 937–945.
FRANKS, G. V., YAN, Y. D., BIGGS, S. & JAMESON, G. J. 2004. *Stimulant sensitive flocculation and consolidation*.
FRAYLICH, M., WANG, W. X., SHAKESHEFF, K., ALEXANDER, C. & SAUNDERS, B. 2008. Poly(D,L-lactide-co-glycolide) dispersions containing pluronics: from particle preparation to temperature-triggered aggregation. *Langmuir,* 24**,** 7761-7768.
FRAYLICH, M. R., LIU, R., RICHARDSON, S. M., BAIRD, P., HOYLAND, J., FREEMONT, A. J., ALEXANDER, C., SHAKESHEFF, K., CELLESI, F. & SAUNDERS, B. R. 2010a. Thermally-triggered gelation of PLGA dispersions: towards an injectable colloidal cell delivery system. *J Colloid Interface Sci,* 344**,** 61-9.
FRAYLICH, M. R., LIU, R. X., RICHARDSON, S. M., BAIRD, P., HOYLAND, J., FREEMONT, A. J., ALEXANDER, C., SHAKESHEFF, K., CELLESI, F. & SAUNDERS, B. R. 2010b. Thermally-triggered gelation of PLGA dispersions: Towards an injectable colloidal cell delivery system. *Journal of Colloid and Interface Science,* 344**,** 61-69.
FRITZ, G., SCHADLER, V., WILLENBACHER, N. & WAGNER, N. J. 2002. Electrosteric stabilization of colloidal dispersions. *Langmuir,* 18**,** 6381-6390.
GALAEV, I. Y. & MATTIASSON, B. 1999. 'Smart' polymers and what they could do in biotechnology and medicine. *Trends in Biotechnology,* 17**,** 335-340.
GAO, X., FENG, W., ZHU, S. P., SHEARDOWN, H. & BRASH, J. L. 2008. A facile method of forming nanoscale patterns on poly(ethylene

glycol)-based surfaces by self-assembly of randomly grafted block copolymer brushes. *Langmuir,* 24**,** 8303-8308.
GARG, A., HOULIHAN, D. D., ALDRIDGE, V., SURESH, S., LI, K. K., KING, A. L., SUTARIA, R., FEAR, J., BHOGAL, R. H., LALOR, P. F. & NEWSOME, P. N. 2014. Non-enzymatic dissociation of human mesenchymal stromal cells improves chemokine-dependent migration and maintains immunosuppressive function. *Cytotherapy,* 16**,** 545-559.
GARTI, N., ROSSANO, A. & AVNI, Y. 1993. Graft-Copolymers as Emulsifiers .1. Grafted Polyethyleneglycol on Polymethylmetacrylate. *Journal of Dispersion Science and Technology,* 14**,** 47-70.
GENOVESE, D. B. 2012. Shear rheology of hard-sphere, dispersed, and aggregated suspensions, and filler-matrix composites. *Advances in Colloid and Interface Science,* 171**,** 1-16.
GERMAIN, L., AUGER, F. A., GRANDBOIS, E., GUIGNARD, E., GIASSON, M., BOISJOLY, H. & GUERIN, S. L. 1999. Reconstructed human cornea produced in vitro by tissue engineering. *Pathobiology,* 67**,** 140-147.
GIBAUD, T., FRELAT, D. & MANNEVILLE, S. 2010. Heterogeneous yielding dynamics in a colloidal gel. *Soft Matter,* 6**,** 3482-3488.
GIL, E. S. & HUDSON, S. M. 2004. Stimuli-reponsive polymers and their bioconjugates. *Progress in Polymer Science,* 29**,** 1173-1222.
GREGORIO-JAUREGUI, K. M., PINEDA, M. G., RIVERA-SALINAS, J. E., HURTADO, G., SAADE, H., MARTINEZ, J. L., ILYINA, A. & LOPEZ, R. G. 2012. One-Step Method for Preparation of Magnetic Nanoparticles Coated with Chitosan. *Journal of Nanomaterials*.
GRIFFITH, L. G. & NAUGHTON, G. 2002. Tissue engineering - Current challenges and expanding opportunities. *Science,* 295**,** 1009-+.
GRIFFITH, L. G. & SWARTZ, M. A. 2006. Capturing complex 3D tissue physiology in vitro. *Nature Reviews Molecular Cell Biology,* 7**,** 211-224.
GUARDIA, P., LABARTA, A. & BATLLE, X. 2011. Tuning the Size, the Shape, and the Magnetic Properties of Iron Oxide Nanoparticles. *Journal of Physical Chemistry C,* 115**,** 390-396.
GUERRINI, M. M., CHARLEUX, B. & VAIRON, J. P. 2000. Functionalized latexes as substrates for atom transfer radical polymerization. *Macromolecular Rapid Communications,* 21**,** 669-674.
GUILLAME-GENTIL, O., SEMENOV, O., ROCA, A. S., GROTH, T., ZAHN, R., VOROS, J. & ZENOBI-WONG, M. 2010. Engineering the Extracellular Environment: Strategies for Building 2D and 3D Cellular Structures. *Advanced Materials,* 22**,** 5443-5462.
GUO, X. & BALLAUFF, M. 2000. Spatial dimensions of colloidal polyelectrolyte brushes as determined by dynamic light scattering. *Langmuir,* 16**,** 8719-8726.
GUO, X. & BALLAUFF, M. 2001. Spherical polyelectrolyte brushes: Comparison between annealed and quenched brushes. *Physical Review E,* 64.
GUO, X., WEISS, A. & BALLAUFF, M. 1999. Synthesis of spherical polyelectrolyte brushes by photoemulsion polymerization. *Macromolecules,* 32**,** 6043-6046.

GUTOWSKA, A., JEONG, B. & JASIONOWSKI, M. 2001. Injectable gels for tissue engineering. *Anatomical Record,* 263**,** 342-349.
HA, S. T., PARK, O. O. & IM, S. H. 2010. Size control of highly monodisperse polystyrene particles by modified dispersion polymerization. *Macromolecular Research,* 18**,** 935-943.
HAI, N. H., LUONG, N. H., CHAU, N. & TAI, N. Q. 2009. Preparation of magnetic nanoparticles embedded in polystyrene microspheres. *Apctp-Asean Workshop on Advanced Materials Science and Nanotechnology (Amsn08),* 187.
HAIK, Y. & KANURI, S. 2008. Mixing Efficiency of Red Blood Cells With Magnetic Microspheres for a Hybrid Separation System. *Journal of Medical Devices-Transactions of the Asme,* 2.
HANSON, S. E., GUTOWSKI, K. A. & HEMATTI, P. 2010a. Clinical Applications of Mesenchymal Stem Cells in Soft Tissue Augmentation. *Aesthetic Surgery Journal,* 30**,** 838-842.
HANSON, S. E., THIBEAULT, S. L. & HEMATTI, P. 2010b. Clinical Applications of Mesenchymal Stem Cells in Laryngotracheal Reconstruction. *Current Stem Cell Research & Therapy,* 5**,** 268-272.
HAO, R., XING, R. J., XU, Z. C., HOU, Y. L., GAO, S. & SUN, S. H. 2010. Synthesis, Functionalization, and Biomedical Applications of Multifunctional Magnetic Nanoparticles. *Advanced Materials,* 22**,** 2729-2742.
HAYCOCK, J. W. 2011. 3D Cell Culture: A Review of Current Approaches and Techniques. *3d Cell Culture: Methods and Protocols,* 695**,** 1-15.
HE, C., KIM, S. W. & LEE, D. S. 2008. In situ gelling stimuli-sensitive block copolymer hydrogels for drug delivery. *J Control Release,* 127**,** 189-207.
HE, W. Q., KUANG, Y. Q., XING, X. M., SIMPSON, R. J., HUANG, H. D., YANG, T., CHEN, J. M., YANG, L. B., LIU, E. Y., HE, W. F. & GU, J. W. 2014. Proteomic Comparison of 3D and 2D Glioma Models Reveals Increased HLA-E Expression in 3D Models is Associated with Resistance to NK Cell-Mediated Cytotoxicity. *Journal of Proteome Research,* 13**,** 2272-2281.
HENCH, L. L. & POLAK, J. M. 2002. Third-generation biomedical materials. *Science,* 295**,** 1014-+.
HENRIQUEZ, C., BUENO, C., LISSI, E. A. & ENCINAS, M. V. 2003. Thiols as chain transfer agents in free radical polymerization in aqueous solution. *Polymer,* 44**,** 5559-5561.
HEUBERGER, M., DROBEK, T. & SPENCER, N. D. 2005. Interaction forces and morphology of a protein-resistant poly(ethylene glycol) layer. *Biophysical Journal,* 88**,** 495-504.
HOFFMAN, A. S. 2002. Hydrogels for biomedical applications. *Advanced Drug Delivery Reviews,* 54**,** 3-12.
HOFFMAN, A. S. 2013. Stimuli-responsive polymers: Biomedical applications and challenges for clinical translation. *Advanced Drug Delivery Reviews,* 65**,** 10-16.
HOFFMAN, A. S. & STAYTON, P. S. 2004. Bioconjugates of smart polymers and proteins: Synthesis and applications. *Macromolecular Symposia,* 207**,** 139-151.

HOFMANN, A., THIERBACH, S., SEMISCH, A., HARTWIG, A., TAUPITZ, M., RUHL, E. & GRAF, C. 2010. Highly monodisperse water-dispersable iron oxide nanoparticles for biomedical applications. *Journal of Materials Chemistry,* 20**,** 7842-7853.

HOU, Q. P., DE BANK, P. A. & SHAKESHEFF, K. M. 2004. Injectable scaffolds for tissue regeneration. *Journal of Materials Chemistry,* 14**,** 1915-1923.

HSIAO, L. C., SOLOMON, M. J., WHITAKER, K. A. & FURST, E. M. 2014. A model colloidal gel for coordinated measurements of force, structure, and rheology. *Journal of Rheology,* 58**,** 1485-1504.

HU, F. X., NEOH, K. G., CEN, L. & KANG, E. T. 2006. Cellular response to magnetic nanoparticles "PEGylated" via surface-initiated atom transfer radical polymerization. *Biomacromolecules,* 7**,** 809-816.

HU, J. M., QIAN, Y. F., WANG, X. F., LIU, T. & LIU, S. Y. 2012. Drug-Loaded and Superparamagnetic Iron Oxide Nanoparticle Surface-Embedded Amphiphilic Block Copolymer Micelles for Integrated Chemotherapeutic Drug Delivery and MR Imaging. *Langmuir,* 28**,** 2073-2082.

HU, Z. B., CAI, T. & CHI, C. L. 2010. Thermoresponsive oligo(ethylene glycol)-methacrylate- based polymers and microgels. *Soft Matter,* 6**,** 2115-2123.

HUANG, H. L., HSING, H. W., LAI, T. C., CHEN, Y. W., LEE, T. R., CHAN, H. T., LYU, P. C., WU, C. L., LU, Y. C., LIN, S. T., LIN, C. W., LAI, C. H., CHANG, H. T., CHOU, H. C. & CHAN, H. L. 2010. Trypsin-induced proteome alteration during cell subculture in mammalian cells. *Journal of Biomedical Science,* 17.

HUANG, J. Y., MURATA, H., KOEPSEL, R. R., RUSSELL, A. J. & MATYJASZEWSKI, K. 2007. Antibacterial polypropylene via surface-initiated atom transfer radical polymerization. *Biomacromolecules,* 8**,** 1396-1399.

HUH, D., HAMILTON, G. A. & INGBER, D. E. 2011. From 3D cell culture to organs-on-chips. *Trends in Cell Biology,* 21**,** 745-754.

HUTMACHER, D. W. 2000. Scaffolds in tissue engineering bone and cartilage. *Biomaterials,* 21**,** 2529-2543.

IFKOVITS, J. L. & BURDICK, J. A. 2007. Review: Photopolymerizable and degradable biomaterials for tissue engineering applications. *Tissue Engineering,* 13**,** 2369-2385.

ISHIDA, N. & BIGGS, S. 2010. Effect of Grafting Density on Phase Transition Behavior for Poly(N-isopropylacryamide) Brushes in Aqueous Solutions Studied by AFM and QCM-D. *Macromolecules,* 43**,** 7269-7276.

ITO, K., YOKOYAMA, S. & ARAKAWA, F. 1986. Poly(Ethylene Oxide) Macromonomers .5. Dodecyloxy Poly(Ethylene Glycol) Methacrylate as an Amphiphilic Macromonomer for Dispersion Polymerization. *Polymer Bulletin,* 16**,** 345-349.

IWATA, R., SUK-IN, P., HOVEN, V. P., TAKAHARA, A., AKIYOSHI, K. & IWASAKI, Y. 2004. Control of nanobiointerfaces generated from well-defined biomimetic polymer brushes for protein and cell manipulations. *Biomacromolecules,* 5**,** 2308-2314.

JAGUR-GRODZINSKI, J. 2006. Polymers for tissue engineering, medical devices, and regenerative medicine. Concise general review of recent studies. *Polymers for Advanced Technologies,* 17**,** 395-418.

JAISWAL, N., HAYNESWORTH, S. E., CAPLAN, A. I. & BRUDER, S. P. 1997. Osteogenic differentiation of purified, culture-expanded human mesenchymal stem cells in vitro. *Journal of Cellular Biochemistry,* 64**,** 295-312.

JAYACHANDRAN, K. N., TAKACS-COX, A. & BROOKS, D. E. 2002. Synthesis and characterization of polymer brushes of poly(N,N-dimethylacrylamide) from polystyrene latex by aqueous atom transfer radical polymerization. (vol 35, pg 4247, 2002). *Macromolecules,* 35**,** 6070-6070.

JEONG, B., BAE, Y. H. & KIM, S. W. 1999. Thermoreversible gelation of PEG-PLGA-PEG triblock copolymer aqueous solutions. *Macromolecules,* 32**,** 7064-7069.

JEONG, B., BAE, Y. H., LEE, D. S. & KIM, S. W. 1997. Biodegradable block copolymers as injectable drug-delivery systems. *Nature,* 388**,** 860-862.

JEONG, B. & GUTOWSKA, A. 2002. Lessons from nature: stimuli-responsive polymers and their biomedical applications (vol 20, pg 305, 2002). *Trends in Biotechnology,* 20**,** 360-360.

JHAVERI, S. B., KOYLU, D., MASCHKE, D. & CARTER, K. R. 2007. Synthesis of polymeric core-shell particles using surface-initiated living free-radical polymerization. *Journal of Polymer Science Part a-Polymer Chemistry,* 45**,** 1575-1584.

JI, Y., GHOSH, K., SHU, X. Z., LI, B. Q., SOKOLOV, J. C., PRESTWICH, G. D., CLARK, R. A. F. & RAFAILOVICH, M. H. 2006. Electrospun three-dimensional hyaluronic acid nanofibrous scaffolds. *Biomaterials,* 27**,** 3782-3792.

JIANG, T., KUMBAR, S. G., NAIR, L. S. & LAURENCIN, C. T. 2008. Biologically active chitosan systems for tissue engineering and regenerative medicine. *Current Topics in Medicinal Chemistry,* 8**,** 354-364.

JIANG, X. E., MUSYANOVYCH, A., ROCKER, C., LANDFESTER, K., MAILANDER, V. & NIENHAUS, G. U. 2011. Specific effects of surface carboxyl groups on anionic polystyrene particles in their interactions with mesenchymal stem cells. *Nanoscale,* 3**,** 2028-2035.

JIAO, Y. P. & CUI, F. Z. 2007. Surface modification of polyester biomaterials for tissue engineering. *Biomedical Materials,* 2**,** R24-R37.

JONAS, A. M., GLINEL, K., OREN, R., NYSTEN, B. & HUCK, W. T. S. 2007. Thermo-responsive polymer brushes with tunable collapse temperatures in the physiological range. *Macromolecules,* 40**,** 4403-4405.

KAAKI, K., HERVE-AUBERT, K., CHIPER, M., SHKILNYY, A., SOUCE, M., BENOIT, R., PAILLARD, A., DUBOIS, P., SABOUNGI, M. L. & CHOURPA, I. 2012. Magnetic Nanocarriers of Doxorubicin Coated with Poly(ethylene glycol) and Folic Acid: Relation between Coating Structure, Surface Properties, Colloidal Stability, and Cancer Cell Targeting. *Langmuir,* 28**,** 1496-1505.

KABANOV, A. V., BATRAKOVA, E. V. & ALAKHOV, V. Y. 2002. Pluronic (R) Block Copolymers as Novel Polymer Therapeutics for Drug and Gene Delivery. *Journal of Controlled Release,* 82**,** 189-212.

KAPPLER, T. E., HICKSTEIN, B., PEUKER, U. A. & POSTEN, C. 2008. Characterization of magnetic ion-exchange composites for protein separation from biosuspensions. *Journal of Bioscience and Bioengineering,* 105**,** 579-585.

KARAGOZ, B., BAYRAMOGLU, G., ALTINTAS, B., BICAK, N. & ARICA, M. Y. 2010. Poly(glycidyl methacrylate)-Polystyrene Diblocks Copolymer Grafted Nanocomposite Microspheres from Surface-Initiated Atom Transfer Radical Polymerization for Lipase Immobilization: Application in Flavor Ester Synthesis. *Industrial & Engineering Chemistry Research,* 49**,** 9655-9665.

KARUMANCHI, R. S. M. S., DODDAMANE, S. N., SAMPANGI, C. & TODD, P. W. 2002. Field-assisted extraction of cells, particles and macromolecules. *Trends in Biotechnology,* 20**,** 72-78.

KAUPP, M., TISCHER, T., HIRSCHBIEL, A. F., VOGT, A. P., GECKLE, U., TROUILLET, V., HOFE, T., STENZEL, M. H. & BARNER-KOWOLLIK, C. 2013. Photo-Sensitive RAFT-Agents for Advanced Microparticle Design. *Macromolecules,* 46**,** 6858-6872.

KEDZIOREK, D. A. & KRAITCHMAN, D. L. 2010. Superparamagnetic Iron Oxide Labeling of Stem Cells for MRI Tracking and Delivery in Cardiovascular Disease. *Stem Cells for Myocardial Regeneration: Methods and Protocols,* 660**,** 171-183.

KESSEL, S., SCHMIDT, S., MULLER, R., WISCHERHOFF, E., LASCHEWSKY, A., LUTZ, J. F., UHLIG, K., LANKENAU, A., DUSCHL, C. & FERY, A. 2010. Thermoresponsive PEG-Based Polymer Layers: Surface Characterization with AFM Force Measurements. *Langmuir,* 26**,** 3462-3467.

KHADEMHOSSEINI, A. & LANGER, R. 2007. Microengineered hydrogels for tissue engineering. *Biomaterials,* 28**,** 5087-5092.

KIEVIT, F. M. & ZHANG, M. Q. 2011. Surface Engineering of Iron Oxide Nanoparticies for Targeted Cancer Therapy. *Accounts of Chemical Research,* 44**,** 853-862.

KIM, D. K., ZHANG, Y., VOIT, W., RAO, K. V. & MUHAMMED, M. 2001. Synthesis and characterization of surfactant-coated superparamagnetic monodispersed iron oxide nanoparticles. *Journal of Magnetism and Magnetic Materials,* 225**,** 30-36.

KIM, J. B. 2005. Three-dimensional tissue culture models in cancer biology. *Seminars in Cancer Biology,* 15**,** 365-377.

KIM, M. H., HONG, H. N., HONG, J. P., PARK, C. J., KWON, S. W., KIM, S. H., KANG, G. & KIM, M. 2010. The effect of VEGF on the myogenic differentiation of adipose tissue derived stem cells within thermosensitive hydrogel matrices. *Biomaterials,* 31**,** 1213-1218.

KIM, M. S., PARK, S. J., CHUN, H. J. & KIM, C. H. 2011. Thermosensitive Hydrogels for Tissue Engineering. *Tissue Engineering and Regenerative Medicine,* 8**,** 117-123.

KIM, N. & CHO, S. G. 2013. Clinical applications of mesenchymal stem cells. *Korean Journal of Internal Medicine,* 28**,** 387-402.

KIM, S., HYUN, K., MOON, J. Y., CLASEN, C. & AHN, K. H. 2015. Depletion Stabilization in Nanoparticle-Polymer Suspensions: Multi-Length-Scale Analysis of Microstructure. *Langmuir,* 31**,** 1892-1900.

KNAPP, D. M., BAROCAS, V. H., MOON, A. G., YOO, K., PETZOLD, L. R. & TRANQUILLO, R. T. 1997. Rheology of reconstituted type I

collagen gel in confined compression. *Journal of Rheology,* 41**,** 971-993.
KOH, A. Y. C. & SAUNDERS, B. R. 2005. Small-angle neutron scattering study of temperature-induced emulsion gelation: the role of sticky microgel particles. *Langmuir,* 21**,** 6734-6741.
KONG, X. X., KAWAI, T., ABE, J. & IYODA, T. 2001. Amphiphilic polymer brushes grown from the silicon surface by atom transfer radical polymerization. *Macromolecules,* 34**,** 1837-1844.
KRISHNAMOORTHY, M., HAKOBYAN, S., RAMSTEDT, M. & GAUTROT, J. E. 2014. Surface-Initiated Polymer Brushes in the Biomedical Field: Applications in Membrane Science, Biosensing, Cell Culture, Regenerative Medicine and Antibacterial Coatings. *Chemical Reviews,* 114**,** 10976-11026.
KUMASHIRO, Y., YAMATO, M. & OKANO, T. 2010. Cell Attachment-Detachment Control on Temperature-Responsive Thin Surfaces for Novel Tissue Engineering. *Annals of Biomedical Engineering,* 38**,** 1977-1988.
LANGER, R. 2009. Perspectives and Challenges in Tissue Engineering and Regenerative Medicine. *Advanced Materials,* 21**,** 3235-3236.
LANGER, R. & TIRRELL, D. A. 2004. Designing materials for biology and medicine. *Nature,* 428**,** 487-492.
LANGER, R. & VACANTI, J. P. 1993. Tissue Engineering. *Science,* 260**,** 920-926.
LAPWORTH, J. W., HATTON, P. V., GOODCHILD, R. L. & RIMMER, S. 2012. Thermally reversible colloidal gels for three-dimensional chondrocyte culture. *Journal of the Royal Society Interface,* 9**,** 362-375.
LARSEN, S. & LEWIS, I. D. 2011. Potential therapeutic applications of mesenchymal stromal cells. *Pathology,* 43**,** 592-604.
LEE, B. H., LEE, Y. M., SOHN, Y. S. & SONG, S. C. 2002. A thermosensitive poly(organophosphazene) gel. *Macromolecules,* 35**,** 3876-3879.
LEE, B. H. & SONG, S. C. 2004. Synthesis and characterization of biodegradable thermosensitive poly(organophosphazene) gels. *Macromolecules,* 37**,** 4533-4537.
LEE, J., CUDDIHY, M. J. & KOTOV, N. A. 2008. Three-dimensional cell culture matrices: State of the art. *Tissue Engineering Part B-Reviews,* 14**,** 61-86.
LEE, K., SILVA, E. A. & MOONEY, D. J. 2011. Growth factor delivery-based tissue engineering: general approaches and a review of recent developments. *Journal of the Royal Society Interface,* 8**,** 153-170.
LEE, M., DUNN, J. C. Y. & WU, B. M. 2005. Scaffold fabrication by indirect three-dimensional printing. *Biomaterials,* 26**,** 4281-4289.
LEE, P. Y., COBAIN, E., HUARD, J. & HUANG, L. 2007. Thermosensitive hydrogel PEG-PLGA-PEG enhances engraftment of muscle-derived stem cells and promotes healing in diabetic wound. *Molecular Therapy,* 15**,** 1189-1194.
LEE, S. B., SONG, S. C., JIN, J. I. & SOHN, Y. S. 1999. A new class of biodegradable thermosensitive polymers. 2. Hydrolytic properties and salt effect on the lower critical solution temperature of

poly(organophosphazenes) with methoxypoly(ethylene glycol) and amino acid esters as side groups. *Macromolecules,* 32**,** 7820-7827.
LEVENBERG, S., HUANG, N. F., LAVIK, E., ROGERS, A. B., ITSKOVITZ-ELDOR, J. & LANGER, R. 2003. Differentiation of human embryonic stem cells on three-dimensional polymer scaffolds. *Proceedings of the National Academy of Sciences of the United States of America,* 100**,** 12741-12746.
LI, L., SHAN, H., YUE, C. Y., LAM, Y. C., TAM, K. C. & HU, X. 2002. Thermally induced association and dissociation of methylcellulose in aqueous solutions. *Langmuir,* 18**,** 7291-7298.
LI, X. M., AKASAKA, T. & DUNNE, N. 2014. Polymeric Scaffolds for Tissue Engineering. *International Journal of Polymer Science*.
LI, Z. F. & NGAI, T. 2010. Macroporous Polymer from Core-Shell Particle-Stabilized Pickering Emulsions. *Langmuir,* 26**,** 5088-5092.
LIANG, W., TADROS, T. F. & LUCKHAM, P. F. 1992. Rheological Studies on Concentrated Polystyrene Latex Sterically Stabilized by Poly(Ethylene Oxide) Chains. *Journal of Colloid and Interface Science,* 153**,** 131-139.
LIAO, T. Q., MOUSSALLEM, M. D., KIM, J., SCHLENOFF, J. B. & MA, T. 2010. N-Isopropylacrylamide-Based Thermoresponsive Polyelectrolyte Multilayer Films for Human Mesenchymal Stem Cell Expansion. *Biotechnology Progress,* 26**,** 1705-1713.
LIU, R., CELLESI, F., TIRELLI, N. & SAUNDERS, B. R. 2009a. A study of thermoassociative gelation of aqueous cationic poly(N-isopropyl acrylamide) graft copolymer solutions. *Polymer,* 50**,** 1456-1462.
LIU, R., DE LEONARDIS, P., CELLESI, F., TIRELLI, N. & SAUNDERS, B. R. 2008. Cationic temperature-responsive poly(N-isopropyl acrylamide) graft copolymers: from triggered association to gelation. *Langmuir,* 24**,** 7099-7106.
LIU, R., DE LEONARDIS, P., TIRELLI, N. & SAUNDERS, B. R. 2009b. Thermally-responsive surfaces comprising grafted poly(N-isopropylacrylamide) chains: Surface characterisation and reversible capture of dispersed polymer particles. *Journal of Colloid and Interface Science,* 340**,** 166-175.
LIU, R., TIRELLI, N., CELLESI, F. & SAUNDERS, B. R. 2009c. Temperature-Triggered Gelation of Aqueous Laponite Dispersions Containing a Cationic Poly(N-isopropyl acrylamide) Graft Copolymer. *Langmuir,* 25**,** 490-496.
LIU, R. X., FRAYLICH, M. & SAUNDERS, B. R. 2009d. Thermoresponsive copolymers: from fundamental studies to applications. *Colloid and Polymer Science,* 287**,** 627-643.
LIU, R. X., TIRELLI, N., CELLESI, F. & SAUNDERS, B. R. 2010. Colloidal thermoresponsive gel forming hybrids. *Journal of Colloid and Interface Science,* 349**,** 527-536.
LIU, Y. Q., ZHANG, Y. & WANG, J. 2014. Mesocrystals as a class of multifunctional materials. *Crystengcomm,* 16**,** 5948-5967.
LUTOLF, M. P. & BLAU, H. M. 2009. Artificial Stem Cell Niches. *Advanced Materials,* 21**,** 1-14.
LUTOLF, M. P. & HUBBELL, J. A. 2005a. Synthetic biomaterials as instructive extracellular microenvironments for morphogenesis in tissue engineering. *Nat Biotechnol,* 23**,** 47-55.

LUTOLF, M. P. & HUBBELL, J. A. 2005b. Synthetic biomaterials as instructive extracellular microenvironments for morphogenesis in tissue engineering. *Nature Biotechnology,* 23**,** 47-55.
LUTZ, J. F. 2006. Solution self-assembly of tailor-made macromolecular building blocks prepared by controlled radical polymerization techniques. *Polymer International,* 55**,** 979-993.
LUTZ, J. F. 2008. Polymerization of oligo(ethylene glycol) (meth)acrylates: Toward new generations of smart biocompatible materials. *Journal of Polymer Science Part a-Polymer Chemistry,* 46**,** 3459-3470.
LUTZ, J. F., AKDEMIR, O. & HOTH, A. 2006. Point by point comparison of two thermosensitive polymers exhibiting a similar LCST: Is the age of poly(NIPAM) over? *Journal of the American Chemical Society,* 128**,** 13046-13047.
MA, H. W., HYUN, J. H., STILLER, P. & CHILKOTI, A. 2004. "Non-fouling" oligo(ethylene glycol)-functionalized polymer brushes synthesized by surface-initiated atom transfer radical polymerization. *Advanced Materials,* 16**,** 338-+.
MA, Z. W., KOTAKI, M., INAI, R. & RAMAKRISHNA, S. 2005. Potential of nanofiber matrix as tissue-engineering scaffolds. *Tissue Engineering,* 11**,** 101-109.
MA, Z. Y. & LIU, H. Z. 2007. Synthesis and surface modification of magnetic particles for application in biotechnology and biomedicine. *China Particuology,* 5**,** 1-10.
MACAYA, D. & SPECTOR, M. 2012. Injectable hydrogel materials for spinal cord regeneration: a review. *Biomedical Materials,* 7.
MACKOR, E. L. 1951. A Theoretical Approach of the Colloid-Chemical Stability of Dispersions in Hydrocarbons. *Journal of Colloid Science,* 6**,** 492-495.
MACKOR, E. L. & VANDERWAALS, J. H. 1952. The Statistics of the Adsorption of Rod-Shaped Molecules in Connection with the Stability of Certain Colloidal Dispersions. *Journal of Colloid Science,* 7**,** 535-550.
MAGNUSSON, J. P., KHAN, A., PASPARAKIS, G., SAEED, A. O., WANG, W. X. & ALEXANDER, C. 2008. Ion-sensitive "isothermal" responsive polymers prepared in water. *Journal of the American Chemical Society,* 130**,** 10852-+.
MAITY, D. & AGRAWAL, D. C. 2007. Synthesis of iron oxide nanoparticles under oxidizing environment and their stabilization in aqueous and non-aqueous media. *Journal of Magnetism and Magnetic Materials,* 308**,** 46-55.
MANGOLINI, F., MCCLIMON, J. B., ROSE, F. & CARPICK, R. W. 2014. Accounting for Nanometer-Thick Adventitious Carbon Contamination in X-ray Absorption Spectra of Carbon-Based Materials. *Analytical Chemistry,* 86**,** 12258-12265.
MARENDUZZO, D., FINAN, K. & COOK, P. R. 2006. The depletion attraction: an underappreciated force driving cellular organization. *Journal of Cell Biology,* 175**,** 681-686.
MARIANI, E. & FACCHINI, A. 2012. Clinical Applications and Biosafety of Human Adult Mesenchymal Stem Cells. *Current Pharmaceutical Design,* 18**,** 1821-1845.

MASCOLO, M. C., PEI, Y. B. & RING, T. A. 2013. Room Temperature Co-Precipitation Synthesis of Magnetite Nanoparticles in a Large pH Window with Different Bases. *Materials,* 6**,** 5549-5567.

MATSUDA, N., SHIMIZU, T., YAMATO, M. & OKANO, T. 2007. Tissue engineering based on cell sheet technology. *Advanced Materials,* 19**,** 3089-3099.

MAYER, J., KARAMUK, E., AKAIKE, T. & WINTERMANTEL, E. 2000. Matrices for tissue engineering-scaffold structure for a bioartificial liver support system. *Journal of Controlled Release,* 64**,** 81-90.

MCGUIGAN, A. P. & SEFTON, M. V. 2006. Vascularized organoid engineered by modular assembly enables blood perfusion. *Proceedings of the National Academy of Sciences of the United States of America,* 103**,** 11461-11466.

MEI, Y., WU, T., XU, C., LANGENBACH, K. J., ELLIOTT, J. T., VOGT, B. D., BEERS, K. L., AMIS, E. J. & WASHBURN, N. R. 2005. Tuning cell adhesion on gradient poly(2-hydroxyethyl methacrylate)-grafted surfaces. *Langmuir,* 21**,** 12309-12314.

MEIRELLES, L. D. & NARDI, N. B. 2009. Methodology, biology and clinical applications of mesenchymal stem cells. *Frontiers in Bioscience,* 14**,** 4281-4298.

MELERO-MARTIN, J., SANTHALINGAM, S. & AL-RUBEAI, M. 2007. Large-scale expansion of cells for use as therapeutic agents. *Cell Technology for Cell Products***,** 335-338.

MERTOGLU, M., GARNIER, S., LASCHEWSKY, A., SKRABANIA, K. & STORSBERG, J. 2005. Stimuli responsive amphiphilic block copolymers for aqueous media synthesised via reversible addition fragmentation chain transfer polymerisation (RAFT). *Polymer,* 46**,** 7726-7740.

MEWIS, J., FRITH, W. J., STRIVENS, T. A. & RUSSEL, W. B. 1989. The Rheology of Suspensions Containing Polymerically Stabilized Particles. *Aiche Journal,* 35**,** 415-422.

MIANO, F., BAILEY, A., LUCKHAM, P. F. & TADROS, T. F. 1992a. Adsorption of Nonyl Phenol Propylene-Oxide Ethylene-Oxide Surfactants on Carbon-Black and the Rheology of the Resulting Dispersions. *Colloids and Surfaces,* 62**,** 111-118.

MIANO, F., BAILEY, A., LUCKHAM, P. F. & TADROS, T. F. 1992b. Adsorption of Poly(Ethylene Oxide) Poly(Propylene Oxide) Aba Block Copolymers on Carbon-Black and the Rheology of the Resulting Dispersions. *Colloids and Surfaces,* 68**,** 9-16.

MIKOS, A. G., THORSEN, A. J., CZERWONKA, L. A., BAO, Y., LANGER, R., WINSLOW, D. N. & VACANTI, J. P. 1994. Preparation and Characterization of Poly(L-Lactic Acid) Foams. *Polymer,* 35**,** 1068-1077.

MILLER, D. J., BIESINGER, M. C. & MCINTYRE, N. S. 2002. Interactions of CO2 and CO at fractional atmosphere pressures with iron and iron oxide surfaces: one possible mechanism for surface contamination? *Surface and Interface Analysis,* 33**,** 299-305.

MIN, K., HU, J. H., WANG, C. C. & ELAISSARI, A. 2002. Surface modification of polystyrene latex particles via atom transfer radical polymerization. *Journal of Polymer Science Part a-Polymer Chemistry,* 40**,** 892-900.

MIYAZAKI, S., SUISHA, F., KAWASAKI, N., SHIRAKAWA, M., YAMATOYA, K. & ATTWOOD, D. 1998. Thermally reversible xyloglucan gels as vehicles for rectal drug delivery. *Journal Of Controlled Release,* 56**,** 75-83.

MIZUTANI, A., KIKUCHI, A., YAMATO, M., KANAZAWA, H. & OKANO, T. 2008. Preparation of thermoresponsive polymer brush surfaces and their interaction with cells. *Biomaterials,* 29**,** 2073-2081.

MIZUTANI, A., NAGASE, K., KIKUCHI, A., KANAZAWA, H., AKIYAMA, Y., KOBAYASHI, J., ANNAKA, M. & OKANO, T. 2010a. Preparation of thermo-responsive polymer brushes on hydrophilic polymeric beads by surface-initiated atom transfer radical polymerization for a highly resolutive separation of peptides. *Journal of Chromatography A,* 1217**,** 5978-5985.

MIZUTANI, A., NAGASE, K., KIKUCHI, A., KANAZAWA, H., AKIYAMA, Y., KOBAYASHI, J., ANNAKA, M. & OKANO, T. 2010b. Thermo-responsive polymer brush-grafted porous polystyrene beads for all-aqueous chromatography. *Journal of Chromatography A,* 1217**,** 522-529.

MOHAMMAD, J., SHENAQ, J., RABINOVSKY, E. & SHENAQ, S. 2000. Modulation of peripheral nerve regeneration: A tissue-engineering approach. The role of amnion tube nerve conduit across a 1-centimeter nerve gap. *Plastic and Reconstructive Surgery,* 105**,** 660-666.

MOLINA-BOLIVAR, J. A. & ORTEGA-VINUESA, J. L. 1999. How proteins stabilize colloidal particles by means of hydration forces. *Langmuir,* 15**,** 2644-2653.

MURATA, H., KOEPSEL, R. R., MATYJASZEWSKI, K. & RUSSELL, A. J. 2007. Permanent, non-leaching antibacterial surfaces - 2: How high density cationic surfaces kill bacterial cells. *Biomaterials,* 28**,** 4870-4879.

MYERS, T. J., GRANERO-MOLTO, F., LONGOBARDI, L., LI, T. S., YAN, Y. & SPAGNOLI, A. 2010. Mesenchymal stem cells at the intersection of cell and gene therapy. *Expert Opinion on Biological Therapy,* 10**,** 1663-1679.

NA, K., PARK, J. H., KIM, S. W., SUN, B. K., WOO, D. G., CHUNG, H. M. & PARK, K. H. 2006. Delivery of dexamethasone, ascorbate, and growth factor (TGF beta-3) in thermo-reversible hydrogel constructs embedded with rabbit chondrocytes. *Biomaterials,* 27**,** 5951-5957.

NALBANDIAN, R. M., HENRY, R. L., BALKO, K. W., ADAMS, D. V. & NEUMAN, N. R. 1987. Pluronic F-127 Gel Preparation as an Artificial Skin in the Treatment of 3rd-Degree Burns in Pigs. *Journal of Biomedical Materials Research,* 21**,** 1135-1148.

NAM, Y. S., YOON, J. J. & PARK, T. G. 2000. A novel fabrication method of macroporous biodegradable polymer scaffolds using gas foaming salt as a porogen additive. *Journal of Biomedical Materials Research,* 53**,** 1-7.

NAMANGA, J., FOBA, J., NDINTEH, D. T., YUFANYI, D. M. & KRAUSE, R. W. M. 2013. Synthesis and Magnetic Properties of a Superparamagnetic Nanocomposite "Pectin-Magnetite Nanocomposite". *Journal of Nanomaterials*.

NAPPER, D. H. 1970. Flocculation Studies of Sterically Stabilized Dispersions. *Journal of Colloid and Interface Science,* 32**,** 106-&.
NAPPER, D. H. 1977. Steric Stabilization. *Journal of Colloid and Interface Science,* 58**,** 390-407.
NAPPER, D. H. 1983. *Polymeric stabilisation of colloidal dispersions* Academic Press.
NASH, M. E., FAN, X. L., CARROLL, W. M., GORELOV, A. V., BARRY, F. P., SHAW, G. & ROCHEV, Y. A. 2013. Thermoresponsive Substrates used for the Expansion of Human Mesenchymal Stem Cells and the Preservation of Immunophenotype. *Stem Cell Reviews and Reports,* 9**,** 148-157.
NETTLES, D. L., CHILKOTI, A. & SETTON, L. A. 2010. Applications of elastin-like polypeptides in tissue engineering. *Adv Drug Deliv Rev,* 62**,** 1479-85.
NG, C. P., SHARIF, A. R. M., HEATH, D. E., CHOW, J. W., ZHANG, C. B. Y., CHAN-PARK, M. B., HAMMOND, P. T., CHAN, J. K. Y. & GRIFFITH, L. G. 2014. Enhanced ex vivo expansion of adult mesenchymal stem cells by fetal mesenchymal stem cell ECM. *Biomaterials,* 35**,** 4046-4057.
NISBET, D. R., CROMPTON, K. E., HAMILTON, S. D., SHIRAKAWA, S., PRANKERD, R. J., FINKELSTEIN, D. I., HORNE, M. K. & FORSYTHE, J. S. 2006. Morphology and gelation of thermosensitive xyloglucan hydrogels. *Biophysical Chemistry,* 121**,** 14-20.
NISBET, D. R., PATTANAWONG, S., RITCHIE, N. E., SHEN, W., FINKELSTEIN, D. I., HORNE, M. K. & FORSYTHE, J. S. 2007. Interaction of embryonic cortical neurons on nanofibrous scaffolds for neural tissue engineering. *Journal of Neural Engineering,* 4**,** 35-41.
NISBET, D. R., RODDA, A. E., HORNE, M. K., FORSYTHE, J. S. & FINKELSTEIN, D. I. 2010. Implantation of Functionalized Thermally Gelling Xyloglucan Hydrogel Within the Brain: Associated Neurite Infiltration and Inflammatory Response. *Tissue Engineering Part A,* 16**,** 2833-2842.
NITSCHKE, M., GRAMM, S., GOTZE, T., VALTINK, M., DRICHEL, J., VOIT, B., ENGELMANN, K. & WERNER, C. 2007. Thermo-responsive poly(NiPAAm-co-DEGMA) substrates for gentle harvest of human corneal endothelial cell sheets. *Journal of Biomedical Materials Research Part A,* 80A**,** 1003-1010.
NOMBELA-ARRIETA, C., RITZ, J. & SILBERSTEIN, L. E. 2011. The elusive nature and function of mesenchymal stem cells. *Nature Reviews Molecular Cell Biology,* 12**,** 126-131.
OBERPENNING, F., MENG, J., YOO, J. J. & ATALA, A. 1999. De novo reconstitution of a functional mammalian urinary bladder by tissue engineering. *Nature Biotechnology,* 17**,** 149-155.
ORTEGA-VINUESA, J. L. & BASTOS-GONZALEZ, D. 2001. A review of factors affecting the performances of latex agglutination tests. *Journal of Biomaterials Science-Polymer Edition,* 12**,** 379-408.
ORTEGA-VINUESA, J. L., HIDALGO-ALVAREZ, R., DE LAS NIEVES, F. J., DAVEY, C. L., NEWMAN, D. J. & PRICE, C. P. 1998. Characterization of immunoglobulin G bound to latex particles using surface plasmon resonance and electrophoretic mobility. *Journal of Colloid and Interface Science,* 204**,** 300-311.

OSUNA, Y., GREGORIO-JAUREGUI, K. M., GAONA-LOZANO, J. G., DE LA GARZA-RODRIGUEZ, I. M., ILYNA, A., BARRIGA-CASTRO, E. D., SAADE, H. & LOPEZ, R. G. 2012. Chitosan-Coated Magnetic Nanoparticles with Low Chitosan Content Prepared in One-Step. *Journal of Nanomaterials*.

OTTEWILL, R. H. & SATGURUNATHAN, R. 1988. Nonionic Lattices in Aqueous-Media .2. Stability to Added Electrolytes. *Colloid and Polymer Science,* 266**,** 547-553.

PAGE, H., FLOOD, P. & REYNAUD, E. G. 2013. Three-dimensional tissue cultures: current trends and beyond. *Cell and Tissue Research,* 352**,** 123-131.

PAINE, A. J., LUYMES, W. & MCNULTY, J. 1990. Dispersion Polymerization of Styrene in Polar-Solvents .6. Influence of Reaction Parameters on Particle-Size and Molecular-Weight in Poly(N-Vinylpyrrolidone)-Stabilized Reactions. *Macromolecules,* 23**,** 3104-3109.

PAMPALONI, F., REYNAUD, E. G. & STELZER, E. H. K. 2007. The third dimension bridges the gap between cell culture and live tissue. *Nature Reviews Molecular Cell Biology,* 8**,** 839-845.

PARK, M. R., CHUN, C., CHO, C. S. & SONG, S. C. 2010a. Enhancement of sustained and controlled protein release using polyelectrolyte complex-loaded injectable and thermosensitive hydrogel. *European Journal of Pharmaceutics and Biopharmaceutics,* 76**,** 179-188.

PARK, M. R., CHUN, C. J., AHN, S. W., KI, M. H., CHO, C. S. & SONG, S. C. 2010b. Sustained delivery of human growth hormone using a polyelectrolyte complex-loaded thermosensitive polyphosphazene hydrogel. *Journal of Controlled Release,* 147**,** 359-367.

PEK, Y. S., WAN, A. C. A., SHEKARAN, A., ZHUO, L. & YING, J. Y. 2008. A thixotropic nanocomposite gel for three-dimensional cell culture. *Nature Nanotechnology,* 3**,** 671-675.

PENG, Z. G., HIDAJAT, K. & UDDIN, M. S. 2004. Adsorption and desorption of lysozyme on nano-sized magnetic particles and its conformational changes. *Colloids and Surfaces B-Biointerfaces,* 35**,** 169-174.

PETER, S. J., MILLER, M. J., YASKO, A. W., YASZEMSKI, M. J. & MIKOS, A. G. 1998. Polymer concepts in tissue engineering. *Journal of Biomedical Materials Research,* 43**,** 422-427.

PHILLIPS, D. J. & GIBSON, M. I. 2015. Towards being genuinely smart: 'isothermally-responsive' polymers as versatile, programmable scaffolds for biologically-adaptable materials. *Polymer Chemistry,* 6**,** 1033-1043.

POLAK, J. M. & BISHOP, A. E. 2006. Stem cells and tissue engineering: past, present, and future. *Ann N Y Acad Sci,* 1068**,** 352-66.

PRABAHARAN, M. & MANO, J. F. 2006. Stimuli-responsive hydrogels based on polysaccharides incorporated with thermo-responsive polymers as novel biomaterials. *Macromolecular Bioscience,* 6**,** 991-1008.

PRESTIDGE, C. & TADROS, T. F. 1988. Viscoelastic Properties of Aqueous Concentrated Polystyrene Latex Dispersions Containing Grafted Poly(Ethylene Oxide) Chains. *Journal of Colloid and Interface Science,* 124**,** 660-665.

PRIJIC, S., SCANCAR, J., ROMIH, R., CEMAZAR, M., BREGAR, V. B., ZNIDARSIC, A. & SERSA, G. 2010. Increased Cellular Uptake of

Biocompatible Superparamagnetic Iron Oxide Nanoparticles into Malignant Cells by an External Magnetic Field. *Journal of Membrane Biology,* 236**,** 167-179.

PYUN, J., JIA, S. J., KOWALEWSKI, T., SAVIN, D. A., PATTERSON, G. D., LIU, T. Q. & MATYJASZEWSKI, K. 2002. Synthesis of nanostructured organic/inorganic hybrid materials using controlled/living radical polymerization: Spherical brushes, core-shell colloids and block copolymer brushes. *Abstracts of Papers of the American Chemical Society,* 224**,** U360-U360.

PYUN, J., KOWALEWSKI, T. & MATYJASZEWSKI, K. 2003. Synthesis of polymer brushes using atom transfer radical polymerization. *Macromolecular Rapid Communications,* 24**,** 1043-1059.

QIN, K. D. & ZAMAN, A. A. 2003. Viscosity of concentrated colloidal suspensions: comparison of bidisperse models. *Journal of Colloid and Interface Science,* 266**,** 461-467.

QUEMADA, D. & BERLI, C. 2002. Energy of interaction in colloids and its implications in rheological modeling. *Advances in Colloid and Interface Science,* 98**,** 51-85.

RAMAKRISHNAN, S. & ZUKOSKI, C. F. 2006. Microstructure and rheology of thermoreversible nanoparticle gels. *Langmuir,* 22**,** 7833-7842.

RANELLA, A., BARBEROGLOU, M., BAKOGIANNI, S., FOTAKIS, C. & STRATAKIS, E. 2010. Tuning cell adhesion by controlling the roughness and wettability of 3D micro/nano silicon structures. *Acta Biomater,* 6**,** 2711-20.

RATNER, B. D. & BRYANT, S. J. 2004. Biomaterials: where we have been and where we are going. *Annu Rev Biomed Eng,* 6**,** 41-75.

RAYATPISHEH, S., LI, P. & CHAN-PARK, M. B. 2012. Argon-Plasma-Induced Ultrathin Thermal Grafting of Thermoresponsive pNIPAm Coating for Contractile Patterned Human SMC Sheet Engineering. *Macromolecular Bioscience,* 12**,** 937-945.

REED, J. A., LUCERO, A. E., HU, S., ISTA, L. K., BORE, M. T., LOPEZ, G. P. & CANAVAN, H. E. 2010. A Low-Cost, Rapid Deposition Method for "Smart" Films: Applications in Mammalian Cell Release. *Acs Applied Materials & Interfaces,* 2**,** 1048-1051.

REINOUT, S. 2008. Smart biomaterials for tissue engineering of cartilage. *Injury,* 39**,** 77-87.

REJMAN, J., OBERLE, V., ZUHORN, I. S. & HOEKSTRA, D. 2004. Size-dependent internalization of particles via the pathways of clathrin- and caveolae-mediated endocytosis. *Biochemical Journal,* 377**,** 159-169.

RIMMER, S., RAMLI, A. N. M. & LEFEVRE, S. 1996. Preparation of polystyrene-poly(styrene-g-N-isopropylacrylamide) core-shell particles: Copolymerization of oligo(N-isopropylacrylamide) macromonomers and styrene onto polystyrene seed particles and stability of the resultant particles. *Polymer,* 37**,** 4135-4139.

ROBINSON, I., ALEXANDER, C., LU, L. T., TUNG, L. D., FERNIG, D. G. & THANH, N. T. K. 2007. One-step synthesis of monodisperse water-soluble 'dual-responsive' magnetic nanoparticles. *Chemical Communications***,** 4602-4604.

RODRIGUEZ, R., GARCIA-CASTRO, J., TRIGUEROS, C., ARRANZ, M. G. & MENENDEZ, P. 2012. Multipotent Mesenchymal Stromal Cells:

Clinical Applications and Cancer Modeling. *Stem Cell Transplantation,* 741**,** 187-205.
RUEB, C. J. & ZUKOSKI, C. F. 1992. Effect of Attractive Interactions on the Flow Properties and Microstructure of a Flocculated Suspension. *Theoretical and Applied Rheology, Vols 1 and 2***,** 657-657.
RUEB, C. J. & ZUKOSKI, C. F. 1998. Rheology of suspensions of weakly attractive particles: Approach to gelation. *Journal of Rheology,* 42**,** 1451-1476.
RUSSEL, W. B. 1980. Review of the Role of Colloidal Forces in the Rheology of Suspensions. *Journal of Rheology,* 24**,** 287-317.
SAEED, A., FRANCINI, N., WHITE, L., DIXON, J., GOULD, T., RASHIDI, H., AL GHANAMI, R. C., HRUSCHKA, V., REDL, H., SAUNDERS, B. R., ALEXANDER, C. & SHAKESHEFF, K. M. 2015. A Thermoresponsive and Magnetic Colloid for 3D Cell Expansion and Reconfiguration. *Advanced Materials,* 27**,** 662-668.
SALVAY, D. M. & SHEA, L. D. 2006. Inductive tissue engineering with protein and DNA-releasing scaffolds. *Molecular Biosystems,* 2**,** 36-48.
SASAKI, J. I., ASOH, T. A., MATSUMOTO, T., EGUSA, H., SOHMURA, T., ALSBERG, E., AKASHI, M. & YATANI, H. 2010. Fabrication of Three-Dimensional Cell Constructs Using Temperature-Responsive Hydrogel. *Tissue Engineering Part A,* 16**,** 2497-2504.
SAUNDERS, J. M., ALAVA, C. & SAUNDERS, B. R. 2007. Temperature-triggered modification of polymer-solvent interactions: From fluid-to-gel transitions to particle capture. *Macromolecular Symposia,* 251**,** 63-71.
SCHILD, H. G. 1992. Poly (N-Isopropylacrylamide) - Experiment, Theory and Application. *Progress in Polymer Science,* 17**,** 163-249.
SCHMOLKA, I. R. 1972. Artificial Skin .1. Preparation and Properties of Pluronic F-127 Gels for Treatment of Burns. *Journal of Biomedical Materials Research,* 6**,** 571-&.
SCHNAPER, H. W., KLEINMAN, H. K. & GRANT, D. S. 1993. Role of Laminin in Endothelial-Cell Recognition and Differentiation. *Kidney International,* 43**,** 20-25.
SEEBER, M., ZDYRKO, B., BURTOVVY, R., ANDRUKH, T., TSAI, C. C., OWENS, J. R., KORNEV, K. G. & LUZINOV, I. 2011. Surface grafting of thermoresponsive microgel nanoparticles. *Soft Matter,* 7**,** 9962-9971.
SENKAL, B. F. & BICAK, N. 2003. Grafting on crosslinked polymer beads by ATRP from polymer supported N-chlorosulfonamides. *European Polymer Journal,* 39**,** 327-331.
SERBO, J. V. & GERECHT, S. 2013. Vascular tissue engineering: biodegradable scaffold platforms to promote angiogenesis. *Stem Cell Research & Therapy,* 4.
SHAHIDAN, N. N., ALEXANDER, C., SHAKESHEFF, K. M. & SAUNDERS, B. R. 2013. Gelation of microsphere dispersions using a thermally-responsive graft polymer. *Journal of Colloid and Interface Science,* 396**,** 187-196.
SHAKESHEFF, K. M., EVORA, C., SORIANO, I. & LANGER, R. 1997. The adsorption of poly(vinyl alcohol) to biodegradable microparticles

studied by x-ray photoelectron spectroscopy (XPS). *Journal Of Colloid And Interface Science,* 185**,** 538-547.
SHAY, J. S., RAGHAVAN, S. R. & KHAN, S. A. 2001. Thermoreversible gelation in aqueous dispersions of colloidal particles bearing grafted poly(ethylene oxide) chains. *Journal of Rheology,* 45**,** 913-927.
SHEKKERIS, A. S., JAISWAL, P. K. & KHAN, W. S. 2012. Clinical Applications of Mesenchymal Stem Cells in the Treatment of Fracture Non-Union and Bone Defects. *Current Stem Cell Research & Therapy,* 7**,** 127-133.
SHIMIZU, K., ITO, A., YOSHIDA, T., YAMADA, Y., UEDA, M. & HONDA, H. 2007. Bone tissue engineering with human mesenchymal stem cell sheets constructed using magnetite nanoparticles and magnetic force. *Journal of Biomedical Materials Research Part B-Applied Biomaterials,* 82B**,** 471-480.
SHIMIZU, T., YAMATO, M., KIKUCHI, A. & OKANO, T. 2003. Cell sheet engineering for myocardial tissue reconstruction. *Biomaterials,* 24**,** 2309-2316.
SHIRAKAWA, M., YAMATOYA, K. & NISHINARI, K. 1998. Tailoring of xyloglucan properties using an enzyme. *Food Hydrocolloids,* 12**,** 25-28.
SINGH, N., CUI, X. F., BOLAND, T. & HUSSON, S. M. 2007. The role of independently variable grafting density and layer thickness of polymer nanolayers on peptide adsorption and cell adhesion. *Biomaterials,* 28**,** 763-771.
SINGH, N., WANG, J., ULBRICHT, M., WICKRAMASINGHE, S. R. & HUSSON, S. M. 2008. Surface-initiated atom transfer radical polymerization: A new method for preparation of polymeric membrane adsorbers. *Journal of Membrane Science,* 309**,** 64-72.
SMITH, T. L. & BRUCE, C. A. 1979. Intrinsic Viscosities and Other Rheological Properties of Flocculated Suspensions of Nonmagnetic and Magnetic Ferric Oxides. *Journal of Colloid and Interface Science,* 72**,** 13-26.
SODIAN, R., SPERLING, J. S., MARTIN, D. P., STOCK, U., MAYER, J. E. & VACANTI, J. P. 1999. Tissue engineering of a trileaflet heart valve - Early in vitro experiences with a combined polymer. *Tissue Engineering,* 5**,** 489-493.
SONMEZ, H. B., SENKAL, B. F., SHERRINGTON, D. C. & BICAK, N. 2003. Atom transfer radical graft polymerization of acrylamide from N-chlorosulfonamidated polystyrene resin, and use of the resin in selective mercury removal. *Reactive & Functional Polymers,* 55**,** 1-8.
SPECTOR, M. 2006. Biomaterials-based tissue engineering and regenerative medicine solutions to musculoskeletal problems. *Swiss Medical Weekly,* 136**,** 293-301.
STANCIU, L., WON, Y. H., GANESANA, M. & ANDREESCU, S. 2009. Magnetic Particle-Based Hybrid Platforms for Bioanalytical Sensors. *Sensors,* 9**,** 2976-2999.
STEINBER.MS, ARMSTRON.PB & GRANGER, R. E. 1973. Recovery of Adhesiveness by Trypsin-Dissociated Cells. *Journal of Membrane Biology,* 13**,** 97-128.

STEINLEITNER, A., LAMBERT, H., KAZENSKY, C. & CANTOR, B. 1991. Poloxamer 407 as an Intraperitoneal Barrier Material for the Prevention of Postsurgical Adhesion Formation and Reformation in Rodent Models for Reproductive Surgery. *Obstetrics and Gynecology,* 77**,** 48-52.

STEPHEN, Z. R., KIEVIT, F. M. & ZHANG, M. Q. 2011. Magnetite nanoparticles for medical MR imaging. *Materials Today,* 14**,** 330-338.

STILE, R. A. & HEALY, K. E. 2002. Poly(N-isopropylacrylamide)-based semi-interpenetrating polymer networks for tissue engineering applications. 1. Effects of linear poly(acrylic acid) chains on phase behavior. *Biomacromolecules,* 3**,** 591-600.

STUART, M. A., HUCK, W. T., GENZER, J., MULLER, M., OBER, C., STAMM, M., SUKHORUKOV, G. B., SZLEIFER, I., TSUKRUK, V. V., URBAN, M., WINNIK, F., ZAUSCHER, S., LUZINOV, I. & MINKO, S. 2010. Emerging applications of stimuli-responsive polymer materials. *Nat Mater,* 9**,** 101-13.

TABATA, Y. 2001. Recent progress in tissue engineering. *Drug Discovery Today,* 6**,** 483-487.

TADROS, T. 2011. Interparticle interactions in concentrated suspensions and their bulk (Rheological) properties. *Advances in Colloid and Interface Science,* 168**,** 263-277.

TADROS, T. F. 1996. Correlation of viscoelastic properties of stable and flocculated suspensions with their interparticle interactions. *Advances in Colloid and Interface Science,* 68**,** 97-200.

TAKAHASHI, M., SHIMAZAKI, M. & YAMAMOTO, J. 2001. Thermoreversible gelation and phase separation in aqueous methyl cellulose solutions. *Journal of Polymer Science Part B-Polymer Physics,* 39**,** 91-100.

TANG, Z. L., AKIYAMA, Y. & OKANO, T. 2014. Recent Development of Temperature-Responsive Cell Culture Surface Using Poly(N-isopropylacrylamide). *Journal of Polymer Science Part B-Polymer Physics,* 52**,** 917-926.

TATE, M. C., SHEAR, D. A., HOFFMAN, S. W., STEIN, D. G. & LAPLACA, M. C. 2001. Biocompatibility of methylcellulose-based constructs designed for intracerebral gelation following experimental traumatic brain injury. *Biomaterials,* 22**,** 1113-1123.

TAUER, K., GAU, D., SCHULZE, S., VOLKEL, A. & DIMOVA, R. 2009. Thermal property changes of poly(N-isopropylacrylamide) microgel particles and block copolymers. *Colloid and Polymer Science,* 287**,** 299-312.

TIBBITT, M. W. & ANSETH, K. S. 2009. Hydrogels as Extracellular Matrix Mimics for 3D Cell Culture. *Biotechnology and Bioengineering,* 103**,** 655-663.

TZIAMPAZIS, E. & SAMBANIS, A. 1995. Tissue Engineering Of A Bioartificial Pancreas - Modeling The Cell Environment And Device Function. *Biotechnology Progress,* 11**,** 115-126.

UCCELLI, A., MORETTA, L. & PISTOIA, V. 2008. Mesenchymal stem cells in health and disease. *Nature Reviews Immunology,* 8**,** 726-736.

UHRICH, K. E., CANNIZZARO, S. M., LANGER, R. S. & SHAKESHEFF, K. M. 1999. Polymeric systems for controlled drug release. *Chemical Reviews,* 99**,** 3181-3198.

UMEGAKI, R., KINO-OKA, M. & TAYA, M. 2004. Assessment of cell detachment and growth potential of human keratinocyte based on observed changes in individual cell area during trypsinization. *Biochemical Engineering Journal,* 17**,** 49-55.

VACANTI, J. P. & LANGER, R. 1999. Tissue engineering: the design and fabrication of living replacement devices for surgical reconstruction and transplantation. *Lancet,* 354**,** Si32-Si34.

VASITA, R. & KATTI, D. S. 2006. Nanofibers and their applications in tissue engineering. *International Journal of Nanomedicine,* 1**,** 15-30.

VERNON, B., SUNG, W. K. & YOU, H. B. 1999. Insulin release from islets of Langerhans entrapped in a poly(N-isopropylacrylamide-co-acrylic acid) polymer gel. *Journal of Biomaterials Science, Polymer Edition,* 10**,** 183-198.

VIHOLA, H., LAUKKANEN, A., VALTOLA, L., TENHU, H. & HIRVONEN, J. 2005. Cytotoxicity of thermosensitive polymers poly(N-isopropylacrylamide), poly(N-vinylcaprolactam) and amphiphilically modified poly(N-vinylcaprolactam). *Biomaterials,* 26**,** 3055-3064.

VIHOLA, H., MARTTILA, A. K., PAKKANEN, J. S., ANDERSSON, M., LAUKKANEN, A., KAUKONEN, A. M., TENHU, H. & HIRVONEN, J. 2007a. Cell-polymer interactions of fluorescent polystyrene latex particles coated with thermosensitive poly (N-isopropylacrylamide) and poly (N-vinylcaprolactam) or grafted with poly(ethylene oxide)-macromonomer. *International Journal of Pharmaceutics,* 343**,** 238-246.

VIHOLA, H., MARTTILA, A. K., PAKKANEN, J. S., ANDERSSON, M., LAUKKANEN, A., KAUKONEN, A. M., TENHU, H. & HIRVONEN, J. 2007b. Cell-polymer interactions of fluorescent polystyrene latex particles coated with thermosensitive poly(N-isopropylacrylamide) and poly(N-vinylcaprolactam) or grafted with poly(ethylene oxide)-macromonomer. *Int J Pharm,* 343**,** 238-46.

WAHAJUDDIN & ARORA, S. 2012. Superparamagnetic iron oxide nanoparticles: magnetic nanoplatforms as drug carriers. *International Journal of Nanomedicine,* 7**,** 3445-3471.

WAN, J., CAI, W., MENG, X. & LIU, E. 2007. Monodisperse water-soluble magnetite nanoparticles prepared by polyol process for high-performance magnetic resonance imaging. *Chemical Communications***,** 5004-5006.

WANG, F., LI, D. C., ZHANG, M. & ZHANG, Z. L. 2012a. Experimental Study of Property of Magnetic Nanoparticle Prepared in Different Temperatures. *Chinese Ceramics Communications Ii,* 412**,** 155-158.

WANG, Q., WANG, L. M., DETAMORE, M. S. & BERKLAND, C. 2008. Biodegradable colloidal gels as moldable tissue engineering scaffolds. *Advanced Materials,* 20**,** 236-+.

WANG, S. F., LU, L. C., WANG, C., GAO, C. Y. & WANG, X. S. 2011. Polymeric Biomaterials for Tissue Engineering Applications 2011. *International Journal of Polymer Science*.

WANG, S. H., QU, X. B. & ZHAO, R. C. 2012b. Clinical applications of mesenchymal stem cells. *Journal of Hematology & Oncology,* 5.

WANG, W. W., LI, G. P., ZHANG, W. G., GAO, J., ZHANG, J. M., LI, C., DING, D. & KONG, D. L. 2014. Reduction-triggered formation of

EFK8 molecular hydrogel for 3D cell culture. *Rsc Advances,* 4**,** 30168-30171.

WANG, W. X., LIANG, H., AL GHANAMI, R. C., HAMILTON, L., FRAYLICH, M., SHAKESHEFF, K. M., SAUNDERS, B. & ALEXANDER, C. 2009. Biodegradable Thermoresponsive Microparticle Dispersions for Injectable Cell Delivery Prepared Using a Single-Step Process. *Advanced Materials,* 21**,** 1809-+.

WARD, M. A. & GEORGIOU, T. K. 2010. Thermoresponsive Terpolymers Based on Methacrylate Monomers: Effect of Architecture and Composition. *Journal of Polymer Science Part a-Polymer Chemistry,* 48**,** 775-783.

WARD, M. A. & GEORGIOU, T. K. 2011. Thermoresponsive Polymers for Biomedical Applications. *Polymers,* 3**,** 1215-1242.

WEI, X., YANG, X., HAN, Z. P., QU, F. F., SHAO, L. & SHI, Y. F. 2013. Mesenchymal stem cells: a new trend for cell therapy. *Acta Pharmacologica Sinica,* 34**,** 747-754.

WEIGEL, T., SCHINKEL, G. & LENDLEIN, A. 2006. Design and preparation of polymeric scaffolds for tissue engineering. *Expert Review of Medical Devices,* 3**,** 835-851.

WESSLEN, B. & WESSLEN, K. B. 1989. Preparation and Properties of Some Water-Soluble, Comb-Shaped, Amphiphilic Polymers. *Journal of Polymer Science Part a-Polymer Chemistry,* 27**,** 3915-3926.

WIDDER, K. J., SENYEI, A. E., OVADIA, H. & PATERSON, P. Y. 1979. Magnetic Protein-a Microspheres - Rapid Method for Cell-Separation. *Clinical Immunology and Immunopathology,* 14**,** 395-400.

WILSON, C. J., CLEGG, R. E., LEAVESLEY, D. I. & PEARCY, M. J. 2005. Mediation of biomaterial-cell interactions by adsorbed proteins: A review. *Tissue Engineering,* 11**,** 1-18.

WISCHERHOFF, E., UHLIG, K., LANKENAU, A., BORNER, H. G., LASCHEWSKY, A., DUSCHL, C. & LUTZ, J. F. 2008a. Controlled cell adhesion on PEG-based switchable surfaces. *Angew Chem Int Ed Engl,* 47**,** 5666-8.

WISCHERHOFF, E., UHLIG, K., LANKENAU, A., BORNER, H. G., LASCHEWSKY, A., DUSCHL, C. & LUTZ, J. F. 2008b. Controlled cell adhesion on PEG-based switchable surfaces. *Angewandte Chemie-International Edition,* 47**,** 5666-5668.

WONG, R., HAIR, M. L. & CROUCHER, M. D. 1988. Sterically Stabilized Polymer Colloids and Their Use as Ink-Jet Inks. *Journal of Imaging Technology,* 14**,** 129-131.

XIAO, D. Q., VAN LE, T. & WIRTH, M. J. 2004. Surface modification of the channels of poly(dimethylsiloxane) microfluidic chips with polyacrylamide for fast electrophoretic separations of proteins. *Analytical Chemistry,* 76**,** 2055-2061.

XIE, B. J., PARKHILL, R. L., WARREN, W. L. & SMAY, J. E. 2006. Direct writing of three-dimensional polymer scaffolds using colloidal gels. *Advanced Functional Materials,* 16**,** 1685-1693.

XIE, J. W., MICHAEL, P. L., ZHONG, S. P., MA, B., MACEWAN, M. R. & LIM, C. T. 2012. Mussel inspired protein-mediated surface modification to electrospun fibers and their potential biomedical applications. *Journal of Biomedical Materials Research Part A,* 100a**,** 929-938.

XU, F. J., ZHAO, J. P., KANG, E. T., NEOH, K. G. & LI, J. 2007. Functionalization of nylon membranes via surface-initiated atom-transfer radical polymerization. *Langmuir,* 23**,** 8585-8592.

XU, F. J., ZHONG, S. P., YUNG, L. Y. L., KANG, E. T. & NEOH, K. G. 2004. Surface-active and stimuli-responsive polymer-Si(100) hybrids from surface-initiated atom transfer radical polymerization for control of cell adhesion. *Biomacromolecules,* 5**,** 2392-2403.

XU, F. J., ZHONG, S. P., YUNG, L. Y. L., TONG, Y. W., KANG, E. T. & NEOH, K. G. 2006. Thermoresponsive comb-shaped copolymer-Si(100) hybrids for accelerated temperature-dependent cell detachment. *Biomaterials,* 27**,** 1236-1245.

YALLAPU, M. M., OTHMAN, S. F., CURTIS, E. T., GUPTA, B. K., JAGGI, M. & CHAUHAN, S. C. 2011. Multi-functional magnetic nanoparticles for magnetic resonance imaging and cancer therapy. *Biomaterials,* 32**,** 1890-1905.

YAMATO, M., SHIMIZU, T., HARIMOTO, M., HIROSE, M., KUSHIDA, A., KWON, O. H., KIKUCHI, A. & OKANO, T. 2001. Cell sheet engineering: toward the next generation tissue engineering. *Tissue Engineering for Therapeutic Use 5,* 1222**,** 93-100.

YANEZ, J. A., LAARZ, E. & BERGSTROM, L. 1999. Viscoelastic properties of particle gels. *Journal of Colloid and Interface Science,* 209**,** 162-172.

YANG, J., YAMATO, M., SEKINE, H., SEKIYA, S., TSUDA, Y., OHASHI, K., SHIMIZU, T. & OKANO, T. 2009. Tissue Engineering Using Laminar Cellular Assemblies. *Advanced Materials,* 21**,** 3404-3409.

YANG, Y. L., MOTTE, S. & KAUFMAN, L. J. 2010. Pore size variable type I collagen gels and their interaction with glioma cells. *Biomaterials,* 31**,** 5678-5688.

YAO, F., FU, G. D., ZHAO, J. P., KANG, E. T. & NEOH, K. G. 2008. Antibacterial effect of surface-functionalized polypropylene hollow fiber membrane from surface-initiated atom transfer radical polymerization. *Journal of Membrane Science,* 319**,** 149-157.

YOSHIKAWA, C., GOTO, A., TSUJII, Y., FUKUDA, T., KIMURA, T., YAMAMOTO, K. & KISHIDA, A. 2006. Protein repellency of well-defined, concentrated poly(2-hydroxyethyl methacrylate) brushes by the size-exclusion effect. *Macromolecules,* 39**,** 2284-2290.

YU, F. Q. & YANG, V. C. 2010. Size-tunable synthesis of stable superparamagnetic iron oxide nanoparticles for potential biomedical applications. *Journal of Biomedical Materials Research Part A,* 92A**,** 1468-1475.

YUAN, Q. C. & WILLIAMS, R. A. 2007. Large scale manufacture of magnetic polymer particles using membranes and microfluidic devices. *China Particuology,* 5**,** 26-42.

ZACCARELLI, E. 2007. Colloidal gels: equilibrium and non-equilibrium routes. *Journal of Physics-Condensed Matter,* 19.

ZENTNER, G. M., RATHI, R., SHIH, C., MCREA, J. C., SEO, M. H., OH, H., RHEE, B. G., MESTECKY, J., MOLDOVEANU, Z., MORGAN, M. & WEITMAN, S. 2001. Biodegradable block copolymers for delivery of proteins and water-insoluble drugs. *Journal of Controlled Release,* 72**,** 203-215.

ZHANG, M. M., LIU, L., ZHAO, H. Y., YANG, Y., FU, G. Q. & HE, B. L. 2006. Double-responsive polymer brushes on the surface of colloid particles. *Journal of Colloid and Interface Science,* 301**,** 85-91.
ZHANG, N. L. & KOHN, D. H. 2012. Using Polymeric Materials to Control Stem Cell Behavior for Tissue Regeneration. *Birth Defects Research Part C-Embryo Today-Reviews,* 96**,** 63-81.
ZHANG, S. G. 2004. Beyond the Petri dish. *Nature Biotechnology,* 22**,** 151-152.
ZHANG, S. G., GELAIN, F. & ZHAO, X. J. 2005a. Designer self-assembling peptide nanofiber scaffolds for 3D tissue cell cultures. *Seminars in Cancer Biology,* 15**,** 413-420.
ZHANG, X. Z., YANG, Y. Y., CHUNG, T. S. & MA, K. X. 2001. Preparation and characterization of fast response macroporous poly(N-isopropylacrylamide) hydrogels. *Langmuir,* 17**,** 6094-6099.
ZHANG, Y., DONG, C. H., SU, L., WANG, H. J., GONG, X. Q., WANG, H. Q., LIU, J. Q. & CHANG, J. 2016. Multifunctional Microspheres Encoded with Upconverting Nanocrystals and Magnetic Nanoparticles for Rapid Separation and Immunoassays. *Acs Applied Materials & Interfaces,* 8**,** 745-753.
ZHANG, Y. J., FURYK, S., BERGBREITER, D. E. & CREMER, P. S. 2005b. Specific ion effects on the water solubility of macromolecules: PNIPAM and the Hofmeister series. *Journal of the American Chemical Society,* 127**,** 14505-14510.
ZHAO, B. 2003. Synthesis of binary mixed homopolymer brushes by combining atom transfer radical polymerization and nitroxide-mediated radical polymerization. *Polymer,* 44**,** 4079-4083.
ZHAO, B. & BRITTAIN, W. J. 2000. Polymer brushes: surface-immobilized macromolecules. *Progress in Polymer Science,* 25**,** 677-710.
ZHAO, B., BRITTAIN, W. J., ZHOU, W. S. & CHENG, S. Z. D. 2000. Nanopattern formation from tethered PS-b-PMMA brushes upon treatment with selective solvents. *Journal of the American Chemical Society,* 122**,** 2407-2408.
ZHAO, M. N., ZHOU, G. W., ZHANG, L., LI, X. Y., LI, T. D. & LIU, F. F. 2014. Fabrication and photoactivity of a tunable-void SiO2-TiO2 core-shell structure on modified SiO2 nanospheres by grafting an amphiphilic diblock copolymer using ARGET ATRP. *Soft Matter,* 10**,** 1110-1120.
ZHENG, G. D. & STOVER, H. D. H. 2002a. Grafting of poly(alkyl (meth)acrylates) from swellable poly(DVB80-co-HEMA) microspheres by atom transfer radical polymerization. *Macromolecules,* 35**,** 7612-7619.
ZHENG, G. D. & STOVER, H. D. H. 2002b. Grafting of polystyrene from narrow disperse polymer particles by surface-initiated atom transfer radical polymerization. *Macromolecules,* 35**,** 6828-6834.
ZHOU, J., LIU, X. N., ZHONG, Y., WEI, R. Q., CHEN, Y. L. & ZHENG, T. 2015. Research progress in functionalization on polystyrene-divinylbenzene based microsphere. *Asia-Pacific Journal of Chemical Engineering,* 10**,** 15-21.
ZHOU, Y., WANG, S. X., DING, B. J. & YANG, Z. M. 2008. Modification of magnetite nanoparticles via surface-initiated atom transfer radical polymerization (ATRP). *Chemical Engineering Journal,* 138**,** 578-585.

ZHOU, Z. W., SCALES, P. J. & BOGER, D. V. 2001. Chemical and physical control of the theology of concentrated metal oxide suspensions. *Chemical Engineering Science,* 56**,** 2901-2920.

ZHU, A. P., FANG, N., CHAN-PARK, M. B. & CHAN, V. 2006. Adhesion contact dynamics of 3T3 fibroblasts on poly (lactide-co-glycolide acid) surface modified by photochemical immobilization of biomacromolecules. *Biomaterials,* 27**,** 2566-2576.

ZHU, B., EURELL, T., GUNAWAN, R. & LECKBAND, D. 2001. Chain-length dependence of the protein and cell resistance of oligo(ethylene glycol)-terminated self-assembled monolayers on gold. *Journal of Biomedical Materials Research,* 56**,** 406-416.